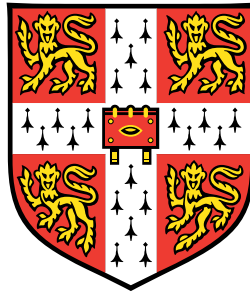


Extracellular regulation of TGF- β
superfamily signalling in early
Xenopus laevis development

Samantha Morris



Clare College, University of Cambridge
5th September 2006

This dissertation is submitted for the degree of Doctor of Philosophy

Declaration

This dissertation is the result of my own work and includes nothing which is the outcome of work done in collaboration except where specifically indicated in the text. This dissertation does not exceed 300 pages of double spaced text.



Stans

Abstract

TGF- β superfamily members are involved in critical processes such as cell differentiation, migration, death and cell cycle regulation. In early *Xenopus laevis* embryogenesis TGF- β signalling is important for regulation of mesoderm and endoderm formation and thus crucial for establishment of the germ layers. In addition to this, FGF signalling has also been shown to play an important role in mesoderm and endoderm specification.

Here we describe a novel secreted regulator of pathways involved in germ layer establishment, Tsukushi (TSK). *TSK* is expressed during germ layer formation and gastrulation, with highest expression levels detected in the ectoderm, dorsal mesoderm and endoderm. Overexpression of *TSK* in the mesoderm, where expression levels are lowest, results in inhibition of mesoderm marker (*Xbra*) expression. In contrast to this, ectopic expression of endoderm markers (*Sox17 α* , *GATA4*) is induced at the site of *TSK* overexpression and expression of the dorsal mesoderm marker, *goosecoid* is expanded. In addition to this, loss of function analysis with morpholino against TSK produces an expansion of mesoderm whilst inhibiting endoderm formation.

To look at the mechanism by which loss and gain of TSK function affects germ layer formation, we studied interactions with pathways important for mesoderm and endoderm formation. Activity of Xnr2, a member of the TGF- β superfamily is required for mesoderm and endoderm induction whilst FGF signal activation is required for mesoderm, whereas inhibition may be required for endoderm formation, in addition to inhibition of BMP signalling. TSK has previously been shown to interact with and inhibit BMP signalling. Here we show TSK also interacts with Xnr2, potentiating its activity, and its EGF-CFC co-receptor, FRL1. TSK can also inhibit FGF signalling where this combined regulation of Xnr2, BMP and FGF by TSK results in segregation between mesoderm and endoderm in the *Xenopus* embryo. In addition to this, I will also present a smaller functional analysis of the activin inhibitor, follistatin.

Contents

List of Abbreviations	xv
I Introduction	1
1 Introduction	2
1.1 The First Embryologist	2
1.2 Overview of <i>Xenopus laevis</i> development	3
1.2.1 Early <i>Xenopus laevis</i> embryogenesis	4
1.3 The molecular mechanics of early <i>Xenopus</i> embryogenesis	7
1.3.1 The role of TGF- β superfamily members in early embryogenesis	8
1.3.2 TGF- β superfamily signalling	9
1.3.3 TGF- β superfamily members functioning in early <i>Xenopus</i> development	10
1.3.4 EGF-CFCs; coreceptors for nodal and Vg1 signalling	15
1.4 Regulation of the TGF- β superfamily	18
1.4.1 Extracellular regulation	18
1.4.2 SLRPs and modulation of TGF- β signalling	26
1.5 Tsukushi, a novel BMP inhibitor	26
1.5.1 Functional analysis of TSK in chick embryogenesis	27
1.5.2 Confirmation of BMP inhibition by TSK; <i>Xenopus laevis</i> as a model system	30
1.5.3 Role of TSK in <i>Xenopus</i> ectoderm patterning	32

1.5.4	In <i>Xenopus</i> embryogenesis, TSK regulates ectoderm patterning and neural crest specification	32
1.5.5	Further questions on the role of TSK in early <i>Xenopus laevis</i> embryogenesis	33
2	Aims of this study	34
II	Materials and Methods	35
3	Materials and Methods	36
3.1	Developmental Biology	36
3.1.1	<i>Xenopus laevis</i> embryos and animal cap assay	36
3.1.2	mRNA extraction	36
3.1.3	Agarose gel electrophoresis	37
3.1.4	Semi-quantitative reverse transcriptase PCR analysis	37
3.1.5	Structural models	37
3.1.6	Multiple sequence alignments and phylogenetic trees	37
3.1.7	DNA constructs used in this study	38
3.1.8	Synthesis and microinjection of capped mRNA into <i>Xenopus</i> embryos	38
3.1.9	Extraction of protein	39
3.1.10	Quantification of protein	39
3.1.11	PNGaseF treatment of embryo lysates	39
3.1.12	SDS-Polyacrylamide Gel Electrophoresis (PAGE)	40
3.1.13	Western blotting	40
3.1.14	Cell signalling assays	40
3.1.15	Regulated homodimerization	41
3.1.16	Fixing and bleaching of embryos	41
3.1.17	<i>In situ</i> hybridisation probe synthesis reaction	42
3.1.18	Whole mount <i>in situ</i> hybridisation	42
3.1.19	β -Galactosidase staining	43
3.1.20	<i>In situ</i> hybridisation on sectioned embryos	43

3.1.21 Pulldown of tagged proteins 43
3.1.22 Loss of function with morpholino 44

III Results I: Activin-follistatin structure and function 45

4 Activin-Follistatin: structure-function 46

4.1 Follistatin inhibition of activin 46
4.1.1 Structure and function of activin A 47
4.1.2 Domain structure of follistatin 49
4.1.3 Activin function is inhibited by Fs12, Fs2 and Fs123 frag-
ments 49
4.2 Crystal structure of the activin-Fs12 complex 51
4.2.1 Formation of activin-follistatin complexes 52
4.2.2 Activin A-Fs12 structure 52
4.3 Mutational analysis of the follistatin Fs12 domain, importance
of R192 55

**IV Results II: TSK, a novel regulator of the TGF- β super-
family 56**

5 TSK features and expression 57

5.1 Features of Tsukushi, a novel secreted protein 57
5.1.1 TSK sequence analysis and orthologues 57
5.1.2 TSK is a new member of the Small Leucine Rich Repeat
Proteoglycan family 59
5.1.3 TSK is post-translationally modified with addition of N-
linked carbohydrates 61
5.1.4 Chick TSK and *Xenopus* TSK have some functional dif-
ferences and differ in their C-termini compositions 63
5.1.5 Primary structure of TSK may be directly comparable to
that of decorin 63
5.2 *TSK* expression pattern 65

5.2.1	<i>TSK</i> is expressed zygotically in the dorsal mesoderm and endoderm, in addition to maternal and zygotic expression in the ectoderm.	65
5.2.2	<i>TSK</i> expression pattern in sectioned embryos, <i>TSK</i> is expressed in endoderm from early gastrula stages	67
5.2.3	<i>TSK</i> mRNA expression levels peak during blastula and gastrula stages of development	70
5.3	Gain-of-function analysis of <i>TSK</i> in early <i>Xenopus laevis</i> embryogenesis.	71
6	<i>TSK</i> gain-of-function analysis	72
6.1	Analysis of <i>TSK</i> function in <i>Xenopus laevis</i>	72
6.1.1	<i>TSK</i> overexpression in the ventral marginal zone does not result in secondary axis formation	72
6.1.2	Overexpression of <i>X-TSK</i> in <i>Xenopus</i> marginal zone inhibits pan-mesoderm marker expression whilst expanding expression of dorsal mesoderm and endoderm markers	74
6.1.3	<i>TSK</i> inhibition of the muscle marker, <i>MyoD</i> , is evident during gastrula and neurula stages	76
6.2	Is the <i>TSK</i> gain-of-function phenotype explained by BMP inhibition?	78
6.2.1	BMP inhibition by chordin and truncated BMP receptor (tBR); effect on mesoderm and endoderm marker expression	78
6.2.2	Induction of endoderm markers are partially blocked and expansion of dorsal mesoderm markers is blocked by BMP signal activation	82
7	<i>TSK</i> loss of function analysis	84
7.1	Loss of <i>TSK</i> function results in expansion of the mesoderm marker, <i>MyoD</i>	84
7.2	Loss of <i>TSK</i> function results in expansion of the organizer-specific marker, <i>goosecoid</i>	85

7.3	Loss of TSK function results in diminished expression of the endoderm markers, <i>Sox17α</i> and <i>GATA4</i>	86
7.4	Loss of TSK function in late-stage embryos	89
7.5	Rescue of gastrula stage TSK-depletion phenotype with expression human TSK in endoderm	91
7.6	Effect of TSK depletion in neurula stage embryos	93
8	Mechanism of TSK action	96
8.1	Major signalling pathways in the <i>Xenopus</i> embryos	96
8.2	Intracellular signalling downstream of TSK	97
8.3	Consequence of MAPK inhibition by TSK in the <i>Xenopus</i> marginal zone	100
8.4	TSK inhibits the activity of FGF8 in the <i>Xenopus</i> embryo	101
8.5	Rescue of TSK mediated <i>Xbra</i> expression inhibition by vras	103
8.6	Dimerisation of a caFGF Receptor may be inhibited by TSK	105
8.7	TSK function in mesoderm is blocked by chemically activated homodimerisation of a synthetic FGF receptor	107
8.8	Is TSK functioning to induce endoderm through inhibition of FGF signalling?	109
9	TSK mechanism II; TGF-β signals	111
9.1	TGF- β signal candidates for TSK function in germ layer formation	111
9.2	TGF- β candidate for TSK mechanism: Nodal	111
9.3	Endoderm marker expression induction by TSK is blocked by inhibition of nodal signalling	113
9.4	Rescue of TSK depletion phenotype with <i>Xnr2</i>	115
9.5	Complex formation between TSK and <i>Xnr2</i> : Nickel bead pull-down assay	115
9.6	Signalling downstream of the TSK- <i>Xnr2</i> interaction	118
9.7	<i>Xbra</i> expression in <i>TSK</i> and <i>Xnr2</i> injected embryos	120
9.8	<i>Gsc</i> expression in <i>TSK</i> and <i>Xnr2</i> injected embryos	120
9.9	<i>Sox17α</i> expression in <i>TSK</i> and <i>Xnr2</i> injected embryos	123

9.10	<i>GATA4</i> expression in <i>TSK</i> and <i>Xnr2</i> injected embryos	123
9.11	Interaction between nodal, BMP and FGF signalling in endo- derm formation	127
10	Regulation of TSK expression	128
10.1	TSK expression is regulated by FGF-MAPK, Vg1 and Notch signalling activities in the embryo	128
V	Discussion	131
11	Discussion	132
11.1	TSK features and expression pattern	132
11.1.1	TSK is a secreted proteoglycan belonging to the SLRP family	132
11.2	Expression and function of TSK in early <i>Xenopus</i> development .	134
11.2.1	<i>TSK</i> is expressed maternally and zygotically in the ecto- derm	134
11.2.2	<i>TSK</i> is expressed in dorsal mesoderm and may play a role in dorsal patterning	136
11.2.3	Expression levels of <i>TSK</i> are diminished in ventro-lateral mesoderm where TSK functions to inhibit mesoderm for- mation	138
11.2.4	<i>TSK</i> is expressed in the endoderm and has a role in in- duction of endoderm tissue	139
11.2.5	<i>TSK</i> functions in germ layer formation and patterning in <i>Xenopus</i>	142
11.3	TSK function in germ layer patterning cannot be explained by BMP inhibition alone	143
11.4	Signalling in early <i>Xenopus</i> development	145
11.4.1	FGF signalling and mesoderm formation	145
11.4.2	Regulation of FGF-MAPK signalling by TSK functions to inhibit mesoderm formation	146

11.4.3 Akt signalling	148
11.4.4 The role of nodal signalling in mesoderm and endoderm formation	149
11.5 TSK functionally interacts with nodal signalling to pattern the germ layers	149
11.5.1 Regulation and gradients of nodal signalling	151
11.5.2 TSK and nodal interaction	151
11.6 Model of TSK function in early <i>Xenopus</i> embryogenesis	154
11.7 Multiple pathway regulation	155
11.7.1 Morphogen gradients and border formation	156
11.7.2 Future directions: formation of an extracellular network hypothesis	159
Acknowledgments	161
Appendix: Original publication	202

List of Figures

1.1	Early patterning of the <i>Xenopus</i> embryo	4
1.2	Dorsoventral patterning of the <i>Xenopus</i> embryo	6
1.3	Selected TGF- β superfamily members and regulators involved in patterning the <i>Xenopus</i> embryo	25
1.4	Overview of chick embryonic structures	28
1.5	The role of TSK in induction of the node by the middle primitive streak.	30
4.1	Activin A dose response in <i>Xenopus</i> animal caps.	48
4.2	Inhibition of activin A by follistatin fragments in <i>Xenopus</i> animal cap explants	50
4.3	Overall architecture of the activin-Fs12 complex	53
4.4	Activity of R192A Fs12 mutant to inhibit activin A in <i>Xenopus</i> animal cap explants	54
5.1	Features of C-TSK-A identified from the amino acid sequence	58
5.2	Multiple sequence alignment of TSKs and SLRPs	60
5.3	Phylogenetic trees of SLRPs and TSKs	61
5.4	Removal of N-linked carbohydrates from C-TSK-A and X-TSK-B1	62
5.5	Primary structure of TSK and SLRP family member, Decorin	64
5.6	Endogenous <i>TSK</i> mRNA expression in <i>Xenopus laevis</i> embryos	66

5.7	Endogenous TSK mRNA expression in sectioned <i>Xenopus laevis</i> embryos	69
5.8	<i>TSK</i> mRNA expression in <i>Xenopus laevis</i> as measured by RT-PCR	71
6.1	Secondary axis formation by TSK orthologues in <i>Xenopus laevis</i>	73
6.2	Overexpression of <i>TSK</i> in the marginal zone; analysis of mesoderm and endoderm marker expression	75
6.3	Overexpression of <i>TSK</i> with analysis of the muscle marker, <i>MyoD</i> In neurula stages of development	77
6.4	Overexpression of <i>X-TSK</i> with analysis of the muscle marker, <i>MyoD</i> In gastrula stages of development	78
6.5	Titration of BMP inhibition by <i>chordin</i> or <i>tBR</i> mRNA levels required for secondary axis formation	79
6.6	Effect of BMP inhibition by <i>chordin</i> and <i>tBR</i> upon mesoderm and endoderm marker expression	81
6.7	Mesoderm and endoderm marker expression in <i>TSK</i> and <i>caALK3</i> injected embryos	83
7.1	<i>MyoD</i> expression in <i>TSK</i> morpholino injected embryos	85
7.2	<i>Xbra</i> expression in <i>TSK</i> morpholino injected embryos	86
7.3	<i>Gsc</i> and <i>MyoD</i> expression in <i>TSK</i> MO injected embryos	87
7.4	<i>Sox17α</i>, <i>GATA4</i> and <i>Xbra</i> expression in <i>TSK</i> MO injected embryos	88
7.5	Measurement of gut dimensions in late stage <i>TSK</i> morpholino injected embryos	90
7.6	Rescue of gastrula stage TSK-depletion phenotype with expression human TSK in endoderm	92
7.7	Shift of neural markers in response to <i>TSK</i> overexpression or morpholino injection	94

8.1	Intracellular signalling downstream of TSK; MAPK, Smad 2 and Smad1	97
8.2	Cell signalling downstream of <i>TSK</i> morpholino	98
8.3	Intracellular signalling downstream of Chd, tBR; MAPK, Smad2 and Smad1	99
8.4	Expression of <i>Xbra</i> is inhibited by the dominant negative FGF receptor, XFD	101
8.5	TSK partially blocks FGF8b expansion of <i>Xbra</i> expression	102
8.6	TSK Inhibition of <i>Xbra</i> expression is rescued by <i>vras</i> . . .	104
8.7	<i>TSK</i> blocks caFGFR activation of MAPK phosphorylation and expansion of <i>Xbra</i> expression	106
8.8	TSK inhibition of <i>Xbra</i> expression is rescued by chemical activation of FGF Receptor dimerisation	108
8.9	<i>Sox17α</i> expression in <i>TSK</i> and <i>vras</i> injected embryos . . .	110
9.1	Partial rescue of <i>TSK</i> morpholino mediated endoderm depletion by <i>Xnr2</i>	114
9.2	Rescue of <i>TSK</i> mediated endoderm expansion by nodal signal inhibition	116
9.3	<i>Xnr2</i> is pulled down in complex with TSK	117
9.4	FRL1/CR1 is pulled down in complex with X-TSK . . .	118
9.5	MAPK and Smad2 signals downstream of TSK and <i>Xnr2</i>	119
9.6	<i>Xbra</i> expression in <i>TSK</i> and <i>Xnr2</i> injected embryos	121
9.7	<i>Gsc</i> expression in <i>TSK</i> and <i>Xnr2</i> injected embryos	122
9.8	<i>Sox17α</i> expression in <i>TSK</i> and <i>Xnr2</i> injected embryos . . .	124
9.9	<i>GATA4</i> expression in <i>TSK</i> and <i>Xnr2</i> injected embryos . . .	125
9.10	<i>Xbra</i> expression in <i>FRL1/CR1</i> and <i>CR3s</i> injected embryos	126
9.11	<i>Sox17α</i> expression in <i>Xnr2</i>, <i>tBR</i> and <i>XFD</i> injected embryos	127
10.1	<i>TSK</i> expression is regulated by MAPK activity	129
10.2	<i>TSK</i> expression is regulated by Vg1 and Notch activity .	130
11.1	Regulation of <i>TSK</i> expression in <i>Xenopus</i>	143

11.2 Model of TSK function mechanism in <i>Xenopus</i> endoderm formation	156
11.3 Model of TSK function in <i>Xenopus</i> mesoderm formation .	157
11.4 Model of TSK function in <i>Xenopus</i> ectoderm formation .	158
11.5 Model of the extracellular network in <i>Xenopus laevis</i> . . .	160

List of Abbreviations

ALK	Activin Like Kinase
Bgn	Biglycan
BMP	Bone Morphogenetic Protein
ca	Constitutively Active
Cer-S	Cerberus Short
Chd	Chordin
cm	Cleavage mutant
C-TSK	chick Tsukushi
CR	Cripto Related
CR3s	Cripto Related 3 Short
DMZ	Dorsal Marginal Zone
dn	Dominant Negative
EGF-CFC	Epidermal Growth Factor-Cripto FRL-1 Cryptic
En2	Engrailed2
ERK	Extracellular signal-Regulated Kinase
FGF	Fibroblast Growth Factor
Fs	Follistatin
FRL1	FGF Receptor Ligand
GDF	Growth and differentiation factor
Gsc	Gooseoid
H-TSK	Human Tsukushi
LMZ	Lateral Marginal Zone
LRR	Leucine Rich Repeat
MAPK	Mitogen Activated Protein Kinase
N_{ICD}	Notch Intracellular Domain
ODC	Ornithine Decarboxylase
P	Phosphorylation
PCR	Polymerase Chain Reaction
PI3K	Phosphatidylinositol-3-Kinase
PLC- γ	Phospholipase C- γ
RT	Reverse Transcriptase
SH2	Src Homology 2
SLRP	Small Leucine Rich Proteoglycan
tBR	Truncated BMP Receptor
TGF- β	Transforming Growth Factor- β
TMEFF1	Tomoregulin

Tsg	Twisted gastrulation
TSK	Tsukushi
UTR	Untranslated Region
VMZ	Ventral Marginal Zone
vras	Constitutively active ras
WB	Western blot
WOC	Water Only Control
Xbra	<i>Xenopus</i> brachyury
XFD	Dominant negative <i>Xenopus</i> FGF Receptor
Tsg	Twisted gastrulation
Xatv	<i>Xenopus</i> Antivin
xTld	<i>Xenopus</i> Tolloid
X-TSK	<i>Xenopus</i> Tsukushi
Xnr	<i>Xenopus</i> Nodal Related
Z-TSK	Zebrafish Tsukushi
<i>Italicised</i>	Reference to gene or RNA
Standard	Reference to protein

Part I

Introduction

Chapter 1

Introduction

1.1 The First Embryologist

“Change in all things is sweet.”

Aristotle (384BC-322BC)

Aristotle was the first documented embryologist, describing the embryological development of the chick in the 4th century BC. Aristotle performed the classic experiment of simultaneously starting over 20 eggs incubating and opening one each successive day to document chick development. Although it can be argued that Aristotle had some misunderstandings in his account of biology (*Historia Animalium*), his study of chick development is remarkably accurate given the absence of microscopy at this time.

The dramatic changes in the developing chick embryo as recorded by Aristotle are paralleled by the changes in the study of embryology over the past two millennia. For example, the advent of molecular biology has provided developmental biologists with the apparatus to vastly further the description of development. This of course is not restricted to *Gallus gallus*, the organism of choice for Aristotle. In the scope of this study, i.e. the TGF- β superfamily and germ layer specification, *Xenopus laevis* (African Clawed Frog) is a preferred model organism.

1.2 Overview of *Xenopus laevis* development

The frog life cycle covers development from the gametes to the sexually mature adult. A brief overview can be found in *Principles of Development* [Gilbert, 2003]. During the process of gametogenesis in the mature female, oocytes develop with their yolk rich vegetal hemisphere contrasting with the relatively yolk-deficient animal hemisphere, a region of faster cell division. Following external fertilisation, the oocyte completes a second round of meiotic division, resulting in formation of a second haploid pronucleus. The pronuclei from both gametes combine to form the zygote nucleus and accompanying this is a cortical rotation of the cytoplasm and activation of cell cleavage and development.

As a result of cell cleavage, the embryo is divided into tens of thousands of cells with no accompanying increase in volume. After a period of division, a fluid-filled cavity, the blastocoel, forms in the animal hemisphere to facilitate cell movements within the embryo¹. These cell movements are dramatic and signify the end of the rapid cleavage stage into the gastrulation² stages. Gastrulation functions to rearrange cells of the three germ layers of the embryo; the ectoderm (precursor of epidermis and nerves), mesoderm (precursor of blood, kidney, gonad, bone and connective tissue) and endoderm (precursor of the gut lining) see Figure 1.1. As a result, gastrulation moves the endoderm to the inside of the embryo, with the ectoderm at the external surface and the mesoderm lying in between.

After completion of gastrulation, organogenesis commences with inductive interactions from the mesoderm instructing the ectoderm to form neural tissue. Following neurogenesis is the generation of back muscles, spinal vertebrae and dermis, collectively termed somatogenesis. The embryo begins to elongate and progresses to the larval stages. In later stages of the life cycle, the tadpole undergoes metamorphosis to form the terrestrial adult organism. The scope of this study is mainly concerned with the earlier stages of embryogenesis during germ layers specification and the commencement of gastrulation.

¹The blastocoel also functions to physically prevent premature cell interactions.

²From the Latin: *gaster*, meaning belly.

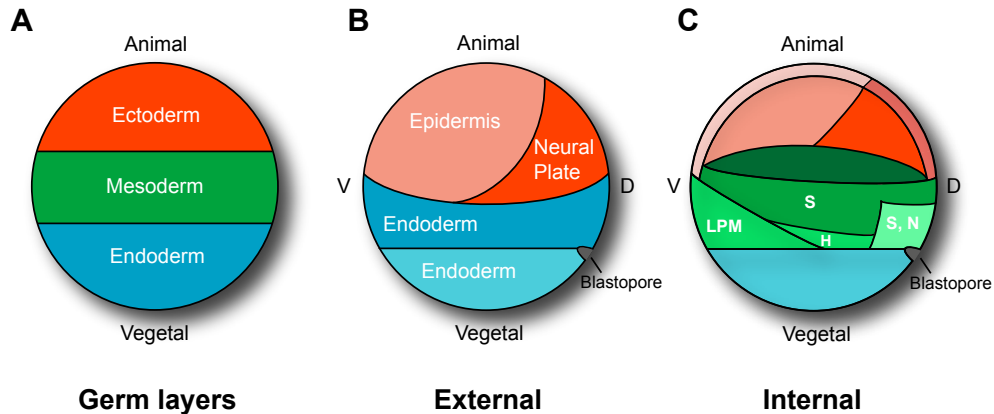


Figure 1.1: **Early patterning of the *Xenopus* embryo**
 Fate maps adapted from Gilbert [2003]. **(A)** Position of the three germ layers; ectoderm, mesoderm and endoderm in the *Xenopus* embryo. **(B)** External fate map relating to the ectoderm (Epidermis and neural plate) and endoderm. **(C)** Internal fate map relating to mesoderm fate; LPM (Lateral plate mesoderm), S (Somites), H (Heart), N (Notochord).

1.2.1 Early *Xenopus laevis* embryogenesis

Germ layer formation and animal vegetal polarity

Up until gastrulation, cell cleavage is the main process to be visualised in the *Xenopus* embryo. From the 16-64 cell stage (stage 4 to 6.5), the embryo is referred to as a *morula*³ Formation of the blastocoel is evident from the first cleavage [Kalt, 1971] although it is only at the 128 cell stage (Stage 7) where it visibly appears and the embryo is referred to as a *blastula*⁴

It is in these blastula stages (stages 7-9) that the embryo undergoes a dramatic change in cell cycle, the mid-blastula transition (MBT). Up until this point, the blastomeres have been progressing through a two-step cell cycle, consisting of only mitosis and DNA synthesis. The cell divisions are rapid and independent of the nuclear genome. At the point of MBT, gap phases, G₁ and G₂ are added to the cell cycle, this being shortly after the twelfth cleavage.⁵ Cell division, having been synchronised up until this point, is lost, and new mRNAs are transcribed [Newport and Kirschner, 1982a,b]. Thus before

³From '*Morus*', Latin translation for 'Mulberry', which the embryo resembles.

⁴From Greek '*Blastos*', meaning 'bud'.

⁵The twelfth cleavage corresponds to stage 8 of development.

MBT, only maternal genes are transcribed, whereas post-MBT, transcription of zygotic genes commences. It is the transcription of these zygotic genes that permits the commencement of gastrulation.

Prior to MBT, only a few zygotic genes are transcribed [Yang et al., 2002] although these are essential for establishment of the germ layers. It is at the point of contact between the vegetal cells and animal cells where mesoderm is induced. The vegetal cells are an active signalling centre in driving this mesoderm induction, as shown in the classic experiments by Pieter Nieuwkoop where vegetal and animal cap explants were combined to form mesoderm tissue [Nieuwkoop, 1977, 1973, 1967a,b]. It was also shown that cells removed from the mid-blastula embryo can form mesoderm in culture. It is considered that these inductive signals arise early in development before MBT (Reviewed in Heasman [1997]) and thus are dependent on pre-localized maternal cytoplasmic factors. This only results in animal-vegetal (ectoderm, mesoderm and endoderm) polarity however, with additional determinants required for dorsal-ventral patterning.

Establishment of the dorsal-ventral axis

Germ layer specification pre-MBT as described above produces tissue of only ventral character, thus requiring further instruction to specify dorsal tissue. In addition, also before zygotic transcription commences, the animal cells receive differential inducing signals from the vegetal cell mass. The vegetal hemisphere is itself pre-divided into ventral and dorsal halves, and is able to form mesoderm with the respective characters [Darras et al., 1997] (Figure 1.2). Thus the dorsoventral and anteroposterior axes are specified already at this early stage, with the addition of later signals refining the pattern. The establishment of the dorsal-ventral axes has been covered in the reviews; Robertis and Kuroda [2004] and Robertis et al. [2000],

Initial establishment of the three germ layers is a UV-insensitive event, whereas production of dorsal-type tissue is UV-sensitive [Grant and Wacaster, 1972, Malacinski, 1974]. The ability of UV irradiation to obliterate dorsoventral

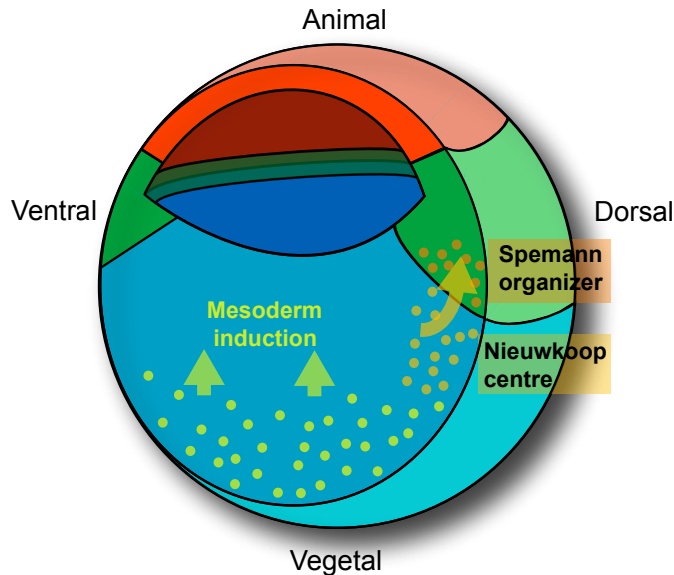


Figure 1.2: **Dorsoventral patterning of the *Xenopus* embryo**

(A) Formation of the Nieuwkoop centre is induced in dorsal endoderm. The Nieuwkoop centre is then responsible for inducing formation of the Spemann organizer in overlying dorsal mesoderm. The Spemann organizer functions to define further pattern in the embryo.

polarity can be explained by the failure of a determinant (or determinants) to localise differentially in the vegetal hemisphere, by a cortical cytoplasmic rotation that occurs during fertilisation⁶. This area in the vegetal hemisphere is referred to as ‘the Nieuwkoop centre’, the position of which is determined by the point of sperm entry.

The fate of the cells composing the Nieuwkoop centre will remain endodermal. The cells overlying are induced to form mesoderm, and destined to become the ‘Spemann-Mangold organizer’ with dorsal character (Reviewed in Robertis et al. [2000] and Harland and Gerhart [1997]). This organizer is responsible for induction of dorsal ectoderm into neural tissue, formation of the anteroposterior body axis from the surrounding mesoderm, initiation of gastrulation movements, whilst itself differentiates into dorsal mesoderm derivatives [Harland and Gerhart, 1997]. In addition to formation of the organizer, a re-

⁶The cortical rotation is inhibited by a UV mediated disorganisation of microtubules required for localisation of cytoplasmic determinants.

gion referred to as the BCNE⁷ centre is also formed in the dorsal region in cells above the Nieuwkoop centre [Wessely et al., 2001, Kuroda et al., 2004].

Gastrulation

Formation of the organizer signifies specification of dorsoventral polarity in the mesoderm. Full development of the dorsoventral, anteroposterior and left-right axes commences during gastrulation. The future dorsal side of the embryo is the site of gastrulation, the start of which is marked by the appearance of the blastopore lip (The embryo is now at stage 10, marking the beginning of the gastrula phase).

During gastrulation, the cells from the surface of the embryo invaginate through the blastopore and move internally. Mesodermal precursors migrate underneath the ectoderm to induce neural tissue in overlying ectoderm cells. The end result of gastrulation is to create an embryo surrounded by ectoderm, with endoderm internalised and mesoderm situated in between. This is signified by the disappearance of the blastocoel. The dramatic cell movements of gastrulation, essential for patterning the embryo are in turn dependent on germ layer formation specified by much earlier events. These critical processes in early *Xenopus* embryogenesis have been extensively studied, and it still remains a goal to identify the exact nature of the molecular events regulating such processes. Many molecules have been identified in playing specific roles in each of the stages described above, although some key events are yet to have their ‘molecular code’ cracked.

1.3 The molecular mechanics of early *Xenopus* embryogenesis

Molecules of the TGF- β , FGF and Wnt signalling pathways play important roles in the embryo. For example, Wnt signalling pathway derivatives have been identified as playing a role in early polarity determination in the vegetal hemisphere. The main events in early embryogenesis such as germ layer for-

⁷BCNE; Blastula Chordin and Noggin expression centre. Previously referred to as the ‘preorganizer’.

mation, formation of the Nieuwkoop centre and Spemann organizer and neural induction rely upon inductive events from neighbouring cells. Such induction is achieved by secretion of signalling molecules. In deciphering the mechanism of early events in the embryo, the TGF- β superfamily of signalling molecules has been focused upon.

1.3.1 The role of TGF- β superfamily members in early embryogenesis

The TGF- β superfamily is a large group of around 30 secreted proteins. Members of the family have been shown to be involved in a wide range cell processes such as differentiation, migration, apoptosis, and cell cycle regulation. A summary of TGF- β superfamily members and their associated functions can be found in the table below. This table (adapted from Massagué [1998]) broadly covers roles in human and mouse with important *Xenopus* orthologues highlighted. The following paragraphs discuss each member in further detail specifically in the context of *Xenopus*.

Subfamily	Activities	References
BMP2 Subfamily BMP2 (dpp in <i>Drosophila</i>) BMP4	Mesoderm formation and patterning, neural patterning, somite patterning, chondrogenesis, apoptosis in limb patterning. Organogenesis (Kidney, tooth, lung, gut).	[Hogan, 1996] [Mehler et al., 1997] [Harland, 1994]
BMP5 Subfamily BMP5 BMP6/Vgr1 BMP7/OP1 BMP8/OP2	Similar activities to the BMP2 subfamily BMP7: roles in kidney, eye and limb development.	[Hogan, 1996] [Mehler et al., 1997]
GDF5 Subfamily GDF5/CDMP1 GDF6/CDMP2 GDF7	Chondrogenesis in developing limbs. GDF6: epidermis induction, neural inhibition.	[Kingsley, 1994]

Vg1 Subfamily GDF1 (Vg1 in <i>Xenopus</i>) GDF3/Vgr2	Vg1: mesoderm induction in <i>Xenopus</i>	[Kingsley, 1994]
BMP3 Subfamily BMP3/osteogenin GDF10	Endochondral bone formation. Monocyte chemotaxis. Stimulation of TGF- β production.	[Cunningham et al., 1992]
Intermediate Members Nodal GDF8	Nodal: mesoderm and endoderm induction. Establishment of left-right axis. GDF8: negative regulator of skeletal muscle growth.	[Beddington, 1996] [Hogan, 1996] [McPherron et al., 1997]
Activin Subfamily Activin β A, B, C and E	Mesoderm induction in <i>Xenopus</i> . Stimulation of Follicle Stimulating Hormone production. Erythrocyte differentiation.	[Harland, 1994] [Gaddy-Kurten et al., 1995]
TGF-β Subfamily TGF- β 1 TGF- β 2 TGF- β 3	Cell cycle arrest, mediation of mesenchymal cell proliferation differentiation, wound healing, extracellular matrix production, immunosuppression.	[Massagué, 1990]

1.3.2 TGF- β superfamily signalling

Members of the TGF- β superfamily are bioactive in their dimeric form, the protomers held together by hydrophobic interactions and an intersubunit disulphide bond [Sun and Davies, 1995]. The different TGF- β members are also capable of exerting their biological effects by forming heterodimers, as is the case with GDF6 and BMP2 [Chang and Hemmati-Brivanlou, 1999]. Signalling is ini-

tiated by TGF- β ligand bringing together two types of receptor serine/threonine protein kinases (type II and type I receptors). This results in formation of a oligomeric complex, consisting of two molecules each of type II and type I receptors in addition to growth factor [Kirsch et al., 2000]. In the receptor complex, the constitutively active type II receptors transphosphorylate the type I receptors. As a result of phosphorylation the type I receptors are activated and phosphorylate intracellular substrates (Reviewed in Miyazawa et al. [2002]).

The major intracellular substrates downstream of the serine/threonine kinase receptors are the Smad proteins. Three subclasses of Smads exist; the receptor-activated Smads (R- Smads: Smads1, 2, 3, 5 and 8) common mediator Smads (Co-Smads: Smad4) and inhibitory Smads (I-Smads: Smads 6 and 7 [Moustakas et al., 2001]. Different Smads are responsible for transducing signals from different TGF- β superfamily members. For example, BMP subfamily signals are transduced by Smad1, 5 and 8 whereas TGF- β and activin-like signals are generally transduced by Smad2 and Smad3 (Reviewed in Massagué [1998], Whitman [1998], Hill [2001]).

1.3.3 TGF- β superfamily members functioning in early *Xenopus* development

Activin

- Activin has mesoderm inducing activity, acting in a concentration dependent manner. At high concentrations, activin induces dorsal mesoderm.

During mesoderm induction, signals from the vegetal region induce the overlying animal hemisphere cells to become mesoderm in the earliest inductive interaction during blastula stages [Gurdon et al., 1985, Smith, 1989]. Numerous candidates have been proposed as 'Mesoderm Inducing Factors' (MIFs), including TGF- β superfamily member, activin [Smith et al., 1990]. Mesodermal tissues are induced by activin in a concentration-dependent manner; a high concentration induces dorsal tissues, a medium concentration induces intermediate tissues and a low concentration induces ventral tissues [Green and Smith, 1990, Ariizumi et al., 1991]. In addition to this, overexpression of activin can

result in partial secondary axis induction [Thomsen et al., 1990]. Activin can exert long range effects in tissue [Gurdon et al., 1994, 1995, Jones et al., 1996, McDowell et al., 1997], which in combination with its concentration dependent effects suggests that activin acts as a morphogen in the *Xenopus* embryo.

Experiments in which activin signals are blocked in the *Xenopus* embryo by a dominant negative activin receptor have shown that activin is required for mesoderm formation [Dyson and Gurdon, 1997, Hemmati-Brivanlou and Melton, 1992, New et al., 1997]. This interpretation is complicated though by the fact that the dominant negative receptor used in these studies may interfere with other pathways. In addition to this, overexpression of the activin inhibitor, follistatin, cannot block mesoderm formation [Schulte-Merker et al., 1994], and thus the importance of activin in mesoderm formation remains unclear. In addition to this, mesoderm induction occurs in during the morula and blastula stages, and thus a maternal MIF candidate may seem more likely. Although this is further complicated by contradictory findings that follistatin can inhibit mesoderm formation [Marchant et al., 1998b]. Although this aspect of activin function is unclear, it is clear that activin is important for patterning of the embryo [Piepenburg et al., 2004].

Vg1

- Vg1 is a mesoderm and endoderm inducer, also involved in left-right axis patterning.

Another candidate mesoderm inducing factor is Vg1. Vg1 was originally identified in a screen for vegetally localised maternal transcripts, proposed to act as an axial mesoderm inducer [Kessler and Melton, 1995, Melton, 1987, Thomsen and Melton, 1993, Weeks and Melton, 1987]. Vg1 signals through an identical pathway to nodal signalling and also has roles in left/right axis formation [Schier, 2003, Hoodless et al., 1999] where response to this activin-like signalling is restricted until after MBT [Lee et al., 2001]. It has thus far been difficult to confirm an essential role for Vg1 in mesoderm formation as Vg1 mutants disrupt only dorsal mesoderm formation [Joseph and Melton, 1998], although

these experiments do demonstrate a role for Vg1 in endoderm formation.

Derrière

- Derrière is a mesoderm and endoderm inducer, related to Vg1

Derrière is closely related to Vg1 and required for correct mesoderm patterning in the *Xenopus* embryo. Derrière is expressed zygotically in the future endoderm and mesoderm of the blastula stage embryo and can potently induce mesoderm and endoderm, whereas a cleavage mutant of Derrière prevents posterior development [Sun et al., 1999]. In addition, it has been shown that Derrière can form heterodimers with Nodal proteins and a cleavage mutant can block all mesoderm formation [Eimon and Harland, 2002].

Nodals

- Nodals induce and pattern mesoderm in addition to inducing endoderm.

Nodals are also involved in left-right pattern formation.

A total of 6 *Nodal* genes have been identified in *Xenopus* (*Xnr1-6*, *Xenopus nodal related*). Activin induces *Xnr* transcription, suggesting Xnrs relay or maintain induction processes initiated by activin-like molecules [Jones et al., 1995]. Therefore nodal signalling is strongly implicated in mesoderm formation and patterning.

Xnr-1/2

Xnr1 and *Xnr2* are first expressed in the vegetal region of late blastulae, and later in marginal zone with enrichment in the dorsal blastopore lip. These Xnr family members function as dose dependent dorsoanterior and ventral mesoderm inducers, and can dorsalise ventral marginal zone explants, in addition to rescue of a complete embryonic axis in UV-ventralised embryos [Jones et al., 1995]. *Xnr1* together with *noggin* induces notochord formation in ectodermal explants and complete secondary axes in whole embryos, suggesting they work together to induce axial pattern in gastrulation and may play role in left-right patterning [Lustig et al., 1996]. *Xnr1* expression correlates with orientation of

cardiac looping, suggesting Xnr1 is a component of the left-right specification pathway [Lohr et al., 1997]. Of Xnr1-4, only *Xnr1* is re-expressed unilaterally in the left lateral plate mesoderm at neurula/tailbud stages [Sampath et al., 1997].

Expression of a non-cleavable form of Xnr2, *cmXnr2* (cleavage mutant) results in delayed dorsal blastopore lip formation and anterior truncations associated with delayed or suppressed expression of markers for dorsoanterior endoderm, associated with the head organiser region. Xnr2 induces dorsoanterior endoderm markers (*Cerberus*, *Xhex-1*, *Frzb*) in animal cap ectoderm, indicating Xnrs have a role in initiation of gastrulation, leading to dorsal mesendodermal specification, including the head organiser [Osada and Wright, 1999]. *Xnr1* and *Xnr2* are expressed in a dorsal to ventral gradient in endodermal cells and are responsible for mesoderm induction at the blastula stage [Agius et al., 2000]. Xnr1 and 2 also play a role in endoderm formation where activation of early endodermal genes by maternal VegT is relayed by zygotic Xnr1 and Xnr2 [Yasuo and Lemaire, 1999].

Xnr-3

Functional screening for gene products that rescue dorsal development in ventralised *Xenopus* embryos yielded *Xnr3*, found to be expressed in the Spemann organizer, in the epithelial layer just prior to and through gastrulation. *Xnr3* was also isolated in differential screening by Ecochard et al. [1995] *Xnr3* is the only nodal family member that is a direct target of the maternal Wnt/ β catenin pathway [McKendry et al., 1997]. Xnr3 also differs in that it cannot induce a full secondary axis like other family members [Smith et al., 1995]. Also, Xnr3 differs structurally in that it lacks the last seven conserved cysteine residues involved in intrachain disulphide bonding [Ezal et al., 2000].

Xnr3 can induce muscle in ventral mesoderm explants. [Smith et al., 1995] and there is also cooperation between Xnr3 and XWnt 11 to induce secondary axes and dorsalisation of ventral mesoderm [Glinka et al., 1996]. In contrast to other nodal family members, Xnr3 lacks mesoderm inducing activity but can

directly induce neural markers in animal caps. In addition to this, *Xnr3* overexpression inhibits mesoderm induction by BMP4, and also partially blocks mesoderm induction by activin, setting it apart from noggin and chordin [Hansen et al., 1997]. Finally, *Xnr3* is unique in the nodal family of proteins in that it regulates convergent extension movement by activating FGF signalling [Yokota et al., 2003].

Xnr-4

Xnr4, is expressed at gastrula stages in the Spemann organizer, and later in notochord and neural tube. Ectopic expression of *Xnr4* can induce and dorsalise mesoderm [Joseph and Melton, 1997] and can also rescue mesoderm formation in VegT depleted embryos [Kofron et al., 1999].

During blastula stages, *Xnr1*, *Xnr2* and *Xnr4* are expressed in a dorsal to ventral gradient in endodermal cells. The carboxy-terminal fragment of Cerberus (Cer-S) does not inhibit activity of any mesoderm inducers other than Xnrs⁸. Expression of Cer-S blocks induction of dorsal and ventral mesoderm in animal-vegetal Nieukoop-type recombinants. This work revealed an endogenous activity gradient of Xnrs and supports a model in which a gradient of multiple nodal-related signals induce mesoderm from the endoderm of the blastula stage embryo [Agius et al., 2000].

Xnr-5/6

Xnr5 and *Xnr6* are expressed zygotically in the blastula stage embryo in the dorsal vegetal region. Both these nodal family members are potent inducers of mesoderm and endoderm, and can also induce expression of *Xnr1* and *Xnr2*. Interestingly, expression of *Xnr5* and *Xnr6* is regulated by VegT and β catenin, and unlike other nodal family members, do not require TGF β signalling for their expression [Takahashi et al., 2000].

⁸Cer-S (Cerberus-Short) cannot inhibit neural induction by *Xnr3*.

BMPs

- BMP signalling ventralises mesoderm tissue and induces epidermis in opposition to the activity of the organiser to dorsalise mesoderm and induce neural tissue.

The BMP family comprises a large branch of the TGF- β superfamily and members include BMP2, BMP4 and BMP7 (Reviewed in Hogan [1996]), where there is a large body of work on BMP4 in particular in *Xenopus*. *BMP4* is maternally expressed and localised uniformly in the ectoderm and mesoderm upon initiation of zygotic transcription in the late blastula stages [Hemmati-Brivanlou and Thomsen, 1995]. At the onset of gastrulation, *BMP4* expression remains localised to the animal cap and subsequently to the ventral and lateral marginal zone [Fainsod et al., 1994]. BMP4 has the ability to induce mesoderm in animal caps [Köster et al., 1991], although upon loss of function using dominant negative receptors or BMP4 depletion, mesoderm becomes dorsalised rather than diminished [Suzuki et al., 1994, Maéno et al., 1994, Steinbeisser et al., 1995]. Conversely, overexpression of *BMP4* strongly ventralises mesoderm, even in the presence of high concentrations of activin which produce dorsalisation [Dale et al., 1992, Jones et al., 1992, Köster et al., 1991].

1.3.4 EGF-CFCs; coreceptors for nodal and Vg1 signalling

The first EGF-CFC⁹ protein, related to epidermal growth factor, was identified in human as ‘cripto’ in undifferentiated human teratocarcinoma cells [Ciccodicola et al., 1989]. The EGF-CFC family members, ranging from 171 to 202 amino acids in length, have a potential N-terminal signal peptide, a modified EGF-like motif, a conserved cysteine-rich motif and a short hydrophobic region at the C-terminus which contains consensus sequences for potential GPI attachment [Ciccodicola et al., 1989, Kinoshita et al., 1995, Shen et al., 1997, Zhang et al., 1998, Gritsman et al., 1999]. Cripto may be structurally related

⁹EGF-CFC; denoted as such due to a) similarity with epidermal growth factor, hence ‘EGF’, and b) the orthologues in human (cripto), *Xenopus* (FRL1/CR1) and mouse (cryptic), hence ‘CFC’

to FGFs, as found in a search for Cripto remote homologues by Minchiotti et al. [2001].

The first identified EGF-CFC in *Xenopus* was FRL1/CR1, found in a functional screen for ligands for receptor tyrosine kinases [Kinoshita et al., 1995]. FRL1/CR1 activates the FGF receptor and overexpression induces mesoderm and neural-specific genes in explants which can be blocked by a dominant negative inhibitor of the FGF receptor. *FRL1/CR1* is expressed during gastrulation and rapidly declines during early neurula stages. Overexpression results in head defects, suggesting FRL1/CR1 might cause posteriorisation of anterior tissue or loss of anteriorisation.

Zhang et al. [1998] identified *One-eyed pinhead (oep)* as encoding a novel EGF-CFC protein in Zebrafish. *Oep* is expressed both maternally and zygotically, with the highest levels found in the gastrula margin and in axail structures and forebrain. Interestingly, *Oep* was found to be membrane-associated via a GPI anchor [Minchiotti et al., 2000]. It was then later found, also in zebrafish, that *Oep* is essential for nodal signalling [Gritsman et al., 1999]. This study showed that embryos lacking maternal and zygotic *Oep* activity are defective in germ layer, organizer and anterior-posterior axis development, an identical phenotype to double mutants for the Zebrafish *nodal*-related genes, *squint* and *cyclops*. Mutations in *Oep* block response to *Squint* and *Cyclops* overexpression but this can be rescued by expression of activin and activation of *Smad2*, supporting a role for *Oep* in nodal signalling. Models of function are reviewed in Shen and Schier [2000] and Saloman et al. [2000]. Schiffer et al. [2001] and Yan et al. [2002] have shown that in the case of human cripto, O-linked fucose modification within the EGF-link domain is functionally important for cripto facilitation of nodal signalling. The consensus sequence for the fucose modification is conserved through all the EGF-CFC family members. Yan et al. [2002] have also shown, using cell coculture assays that cripto can act as both a coreceptor and a secreted coligand in nodal signalling. In addition to a requirement of nodal signalling for EGF-CFCs, *Vg1* and *GDF1* have also been shown to require EGF-CFC cofactors for signalling through the activin receptor in the

zebrafish embryo [Cheng et al., 2003]. Interestingly, activin does not require EGF-CFCs for its signalling [Massagué and Chen, 2000, Schier and Shen, 2000, Yeo and Whitman, 2001]. Yeo and Whitman [2001] uncovered more on the mechanism of nodals requirement of cripto. Cripto interacts with the ALK4 type I receptor via its CFC motif in cripto, where this interaction is required for nodal receptor binding and nodal mediated Smad2 activation.

A role for EGF-CFCs in *Xenopus* development beyond the initial work by Kinoshita et al. [1995] is now clear. Yabe et al. [2003] showed that FRL1/CR1 is essential for neural differentiation in *Xenopus* though suppression of BMP signalling. FRL1/CR1 is expressed in presumptive neuroectoderm of the late gastrula stage embryo and overexpression of FRL1/CR1 in animal caps induces neural markers and suppresses expression of BMP-responsive genes in the animal cap. Depletion of endogenous FRL1/CR1 with antisense morpholino resulted in embryos lacking neural structures, but no differences in mesoderm tissue were reported, thus suggesting FRL1/CR1 alone is not essential for nodal signalling. Yabe et al. [2003] suggested that FRL1/CR1 enables the response to neural inducing signals in the ectoderm, and MAPK activation by FRL1/CR1 (in blastula stage embryos) is required for BMP inhibition and neural induction.

Two EGF-CFC genes in addition to *FRL1/CR1* have been identified in *Xenopus*. *XCR2* is the only EGF-CFC expressed in post-gastrula embryos and depletion with antisense morpholino affects left-right patterning of the heart and gut, and thus is linked to nodal signalling [Onuma et al., 2006, Dorey and Hill, 2006]. A third EGF-CFC has also been identified in *Xenopus*, as *XCR3* [Dorey and Hill, 2006, Onuma et al., 2006]. Dorey and Hill [2006] have shown that *XCR3* is expressed ubiquitously. Both XCR1 (FRL1/CR1) and XCR3 are required for signalling by nodal related ligands in the embryo, and dual depletion of XCR1 and XCR3 results in dramatically impaired Smad2 activation with a resulting block of gastrulation and mesendoderm formation.

1.4 Regulation of the TGF- β superfamily

TGF- β signalling is regulated at many levels. Regulation can be at the intracellular level at which inhibitory molecules, such as Smads 6 and 7 prevent other Smads propagating the signal to the nucleus [Itoh et al., 2001]. Other intracellular regulation is mediated by pseudoreceptors, such as BAMBI. BAMBI has been found to inhibit activin and TGF- β signalling in *Xenopus* [Onichtchouk et al., 1999, Grotewold et al., 2001]. In addition to intracellular mechanisms of regulation, TGF- β signals are also modulated at the extracellular level

1.4.1 Extracellular regulation

Extracellular regulation controls functional cytokine concentration. This is important as signalling output is dependent on the concentration of TGF- β cytokines [Hama and Weinstein, 2001]. BMP signalling provides a good example in this instance as at least 7 extracellular inhibitors have already been described, including noggin, chordin and follistatin. For example, noggin functions as a BMP inhibitor by physically blocking BMP dimers from binding to type I and type II receptors [Groppe et al., 2002]. The following sections describe selected regulators of TGF- β superfamily signalling in greater detail.

Chordin

- Chordin antagonises BMP signalling.

Chordin was identified in a differential screen as a gene activated by the homeobox genes, *Gooseoid* and *Xnot2*. Chordin is a novel 941 amino acid protein, and microinjection of its mRNA produces axis duplication in *Xenopus*. Expression of *chordin* is detected in the Spemann organizer, and it was proposed that it acts as a potent dorsalising factor [Sasai et al., 1994]. *Chordin* was found to be the *Xenopus* homologue of *Drosophila Short gastrulation (Sog)* which also functions in dorsal-ventral axis formation [Francois and Bier, 1995].

This gave further clues to the mechanism of chordin action as in *Drosophila*, Sog was known to antagonise dpp signalling [Francois et al., 1994], of which *BMP* is the homologue of in *Xenopus*. Chordin was shown to have neutralising

activity in animal caps that could be antagonised by BMP-4 [Sasai et al., 1995]. This mechanism was apparently conserved in *Drosophila* [Schmidt et al., 1995]. Piccolo et al. [1996] then went on to show that chordin inhibits ventral signals by direct binding to BMP-4 to block binding to its receptor. Interestingly, the BMP-4 activity gradient is not established by diffusion of BMP-4 protein in the *Xenopus* embryo. It was suggested that the long range effects of chordin, and another BMP inhibitor, noggin, are responsible for establishment of the BMP-4 morphogen gradient [Jones and Smith, 1998]. This was later challenged though by Blitz et al. [2000] with the proposal that chordin actually acts as a short-range factor as low levels of chordin can still induce secondary axes.

More detailed study of chordin showed that expression of chordin in the organizer requires Wnt and VegT activity to be expressed [Xanthos et al., 2002], unveiling greater complexities of the molecular nature of the organizer. The importance of chordin in this context was demonstrated by Oelgeschläger et al. [2003a] where the depletion of chordin with morpholinos against both pseudoalles resulted in embryos with reduced dorsoanterior and expanded ventroposterior tissues. Strong evidence came from the findings that chordin morpholinos block dorsalisation by lithium chloride, elongation and muscle differentiation in animal cap explants induced by activin, and induction of the central nervous system, somites and notochord by organizer transplanted to the ventral region. The elimination of chordin in the whole embryo produces a modest effect, most likely due to redundancy with similarly functioning molecules in the organizer. Khokha et al. [2005] simultaneously depleted chordin, noggin and follistatin in *Xenopus tropicalis*, resulting in a much more dramatic loss of dorsal structures. Further analysis of the role of chordin in *Xenopus* embryogenesis revealed chordin to act as an endoderm inducer. This induction of endoderm by chordin is blocked by BMP-4 but potentiated by inhibition of FGF signalling with a dominant-negative FGF receptor [Sasai et al., 1996].

As chordin plays such a pivotal role in early *Xenopus* embryogenesis, it is crucial for its activity to be regulated. One such mechanism is achieved by cleavage of chordin by the metalloprotease, Xolloid [Piccolo et al., 1997]. Xolloid

is capable of cleaving chordin, in addition to chordin-BMP complexes, leading to inhibition of chordin function, as demonstrated in terms of secondary axis formation. Interestingly, another level of complexity is added in the form of Sizzled, a Frizzled-related protein which competes with chordin for binding to a Xolloid related protease, and thus protecting chordin from cleavage [Lee et al., 2006]. In addition to cleavage by Xolloid, chordin is also subject to regulation through cleavage by a closely-related metalloprotease, BMP1 [Wardle et al., 1999].

Noggin

- Noggin antagonises BMP signalling.

Noggin¹⁰ was identified by Smith and Harland [1992] as a novel polypeptide of 26 kDa with the ability to induce dorsal development in *Xenopus*. *Noggin* is expressed maternally and zygotically, where it is localised to the presumptive dorsal mesoderm in the zygote and becomes enriched in the dorsal blastopore lip. It is also expressed in neurula stages in the notochord and prechordal mesoderm. Injection of *noggin* mRNA can rescue ventralised embryos and this suggested that *noggin* plays a role in normal dorsal development. It was later shown by Smith et al. [1993] that soluble *noggin* protein added to ventral marginal zone in gastrulation induces muscle, leading to the proposal that *noggin* is the dorsalising signal patterning the mesoderm in *Xenopus*. This was supported by Cunliffe and Smith [1994], showing that *noggin* can indeed dorsalise ventral mesoderm.

In addition to dorsalisation of mesoderm, *noggin* was also found to directly induce neural tissue in animal cap explants [Lamb et al., 1993]. *Noggin* induces expression of *XIPOU2*, a gene with direct neuralising activity [Witta et al., 1995]. Closer inspection of *noggin*-induced neural tissue shows defined differentiation and organisation, leading to the possibility that *noggin* also plays a role in dorsal-ventral patterning of the forebrain. *XWnt3a* synergises with *noggin* to increase expression of posterior neural genes [McGrew et al., 1995].

¹⁰Noggin was named as such due to its ability to induce excessive head development

The first evidence that noggin functions through interaction with BMP-4 came from Re'em-Kalma et al. [1995]; endogenous BMP-4 transcripts are downregulated in noggin-dorsalised ventral marginal zone explants. Further evidence came that noggin binds to BMP-4 and thus blocks signalling by inhibiting BMP-4 binding to its receptors [Zimmerman et al., 1996].

Follistatin

- Follistatin antagonises BMP and activin signalling.

Follistatin was first identified as a specific activin-binding protein [Tashiro et al., 1991]. Fukui et al. [1993] then went onto show that the activity of purified activin in *Xenopus* explants is inhibited by purified follistatin. Follistatin was shown not to interact with Vg1, and as part of these experiments where follistatin overexpression does not perturb mesoderm formation, the importance of activin in mesoderm induction was questioned [Schulte-Merker et al., 1994]. This study used human follistatin though and toxic effects were produced by its overexpression. Subsequent analysis by [Marchant et al., 1998a] with *Xenopus* follistatin overexpression showed inhibition of mesoderm formation, thus re-igniting the debate on the role of activin in mesoderm induction. The crystal structure of activin in complex with follistatin reveals that follistatin inhibits activin function by blocking receptor binding [Thompson et al., 2005]. Work presented here from Harrington et al. [2006] identifies the region of follistatin-mediated activin inhibition in a combinatorial approach of structural biology and functional analysis in *Xenopus* (See chapter 4).

Follistatin is expressed maternally [Fukui et al., 1994, Uchiyama et al., 1994]. In addition to this, zygotic expression is detected in the organizer and notocord, locations associated with its ability to directly induce neural tissue [Hemmati-Brivanlou et al., 1994]. Further evidence of a role for follistatin in neural induction and patterning came from McGrew et al. [1995], showing that follistatin synergises with Wnt signalling to enhance the expression of posterior neural genes. The mechanism for neural induction by follistatin is mediated by the ability of follistatin to bind BMP4, inhibiting its activity to block neural induc-

tion [Fainsod et al., 1997]. Follistatin can in fact interact with multiple BMPs, inhibiting all aspects of their activities in the *Xenopus* embryo [Iemura et al., 1998].

Twisted gastrulation

- Twisted gastrulation can enhance/antagonise BMP signalling.

Xenopus Twisted gastrulation (xTsg) is a BMP agonist expressed ventrally in the embryo. xTsg promotes BMP signalling by dislodging latent BMPs bound to chordin, thus creating high levels of BMP signalling in the embryo [Oelgeschläger et al., 2000]. In support of this, Tsg functions to promote BMP signalling during head development in the mouse [Zakin and Robertis, 2004]. Interestingly, xTsg can also act as a cofactor in BMP antagonism by chordin by increasing chordin binding to BMP [Scott et al., 2001] and in support of this Ross et al. [2001] showed that xTsg functions with chordin to antagonize BMP signalling. Tsg binds directly to and forms a ternary complex with chordin and BMPs [Chang et al., 2001]. Tsg also functions in *Xenopus tropicalis* to inhibit BMP in cooperation with chordin [Wills et al., 2006]. Further detail was uncovered on the dual activity of Tsg by Larrain et al. [2001]. Tsg primarily enhances BMP antagonism by chordin by forming a ternary complex and prevents BMP binding to its receptor. Then, after cleavage of chordin by Xolloid, Tsg facilitates their degradation, and thus Xolloid acts as the switch for Tsg from anti-BMP to pro-BMP signalling factor. This second pro-BMP activity of Tsg is independent of binding to BMP [Oelgeschläger et al., 2003b]. Loss of Tsg function in *Xenopus* results in moderate head defects which can be rescued by chordin and dorsal marker gene expression in reduced with expanded ventral marker gene expression. Blitz et al. [2003] showed that antisense depletion of Tsg and chordin cooperates to repress head formation and loss of Tsg results in diminished BMP inhibition by chordin. This suggests that Tsg is acting as a BMP inhibitor in cooperation with chordin in early embryogenesis. A second *Tsg* gene, *xTsg-2* has been found in *Xenopus*, expression of which is restricted to later stages of development [Oelgeschläger et al., 2004].

Cerberus

- Cerberus antagonises BMP, nodal and Wnt signalling.

Isolated by differential screening, cerberus is enriched in the anterior endoderm of Spemann's organizer. Microinjection of *cerberus* mRNA into *Xenopus* induces ectopic heads [Bouwmeester et al., 1996]. Glinka et al. [1997] reported that cerberus is a potent antagonist of Wnt signalling. Cerberus also antagonises BMP signalling [Hsu et al., 1998] and was proposed by this group to also block signalling by activin- and nodal-like members of the TGF- β superfamily. Piccolo et al. [1999] showed that cerberus binds to and inhibits nodal, BMP and Wnt signals via independent sites of the secreted protein, thus leading to the hypothesis that all three signals must be inhibited during head formation. The BMP antagonists, noggin and chordin are important for maintaining cerberus expression [Zorn et al., 1999].

Schneider and Mercola [1999] showed that ablation of cerberus-expressing endoderm in *Xenopus* decreased the incidence of heart, but not head formation whereas removal of prechordal mesoderm caused defects in anterior head structures. In addition to this, they showed that although cerberus induces ectopic heads, it cannot induce genes thought to be involved in head induction. In support of this, Silva et al. [2003] showed that depletion of cerberus with morpholino did not impair head formation in the embryo, but they went on to show that endogenous cerberus is in fact required for anterior head specification. In the case of simultaneous knockdown of cerberus with increasing levels of BMP4, Xnr1 and XWnt8, a more severe head phenotype was produced than with the three signalling agonists alone, indicating that inhibition by endogenous cerberus is important for head formation. Cerberus is also required in prospective endomesoderm in combination with chordin in prospective neuroectoderm for CNS formation [Kuroda et al., 2004]. In chick, cerberus regulates left-right symmetry of the head and the heart [Zhu et al., 1999].

Gremlin

- Gremlin antagonises BMP signalling.

Gremlin (belonging to same family as cerberus) is expressed in *Xenopus* neural crest and inhibits BMP signalling [Hsu et al., 1998]. In contrast to cerberus, gremlin does not abolish mesoderm induction when misexpressed during early development [Eimon and Harland, 1999]. *Gremlin* is a marker of pronephric ducts [Osafune et al., 2002] and may play a role in renal development in *Xenopus* [Hensey et al., 2002].

DAN

- DAN antagonises BMP signalling.

Also a BMP inhibitor in same family as cerberus, Hsu et al. [1998] showed that cerberus, gremlin and DAN bind to BMPs and prevent them from interacting with their receptors. DAN is a secreted glycoprotein, a member of the cystine knot superfamily¹¹ [Stanley et al., 1998]. *xDan* is maternally expressed and also at later stages in cells associated with cranial and trunk neural crest [Eimon and Harland, 2001].

Coco

- Coco antagonises BMP, nodal, activin and Wnt signalling.

Coco¹² is also a member of the Cerberus/DAN family. Bell et al. [2003] showed that *coco* is expressed maternally in an animal to vegetal gradient with expression levels declining following gastrulation. Coco binds to and inhibits Xnr1, BMP4, Activin and Wnt8 and is proposed to play a role in the regulation of ectodermal competence by preventing fate specification in the ectoderm and thus maintains the stem-cell like properties of the ectoderm. In addition to this, coco may lower overall levels of BMP signalling in the ectoderm, allowing additional BMP inhibitors in the organizer to induce neural tissue. This is supported by the fact that coco can act as a neural inducer.

Lefty/Xantivin

- Lefty/Xantavin antagonises nodal and Vg1 signalling.

¹¹The cystine knot superfamily includes TGF- β s and BMPs

¹²'Coco', meaning 'head' in Spanish

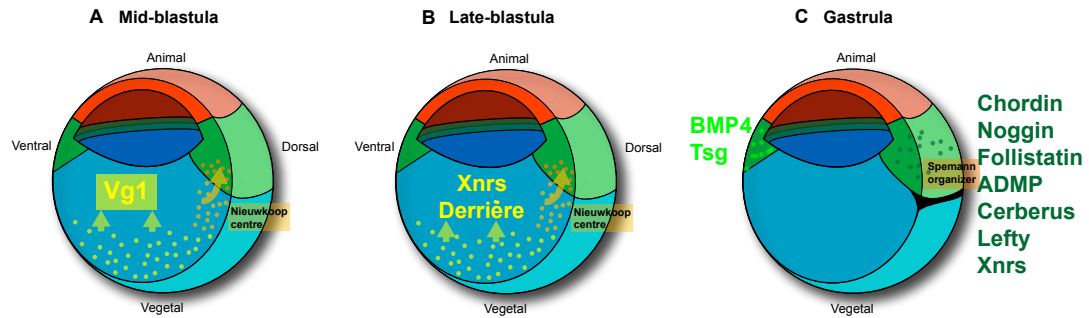


Figure 1.3: **Selected TGF- β superfamily members and regulators involved in patterning the *Xenopus* embryo**

(A) Early-blastula embryo, mesoderm (green) induction by Vg1 signals from the vegetal region (blue). (B) Late-blastula embryo, mesoderm induction and patterning by Xnrs and Derrière. (C) Gastrula-stage embryo, dorsal-ventral patterning by BMP, BMP inhibitors, and Xnrs.

Mouse genes, *Lefty-1* and *Lefty-2* can directly induce neural tissue in animal cap explants, suggesting they are capable of antagonising BMP signalling [Meno et al., 1997]. Cheng et al. [2000] identified a lefty-related factor in *Xenopus*, called antivin (*Xatv*). *Xatv* is first expressed in the marginal zone of early gastrula embryos and later becomes restricted to axial tissues. During tailbud stages, *Xatv* is expressed in the left lateral plate mesoderm and left dorsal endoderm in addition to other areas. *Xatv* expression is induced by mesoderm inducers such as Xnr2 and activin, and is capable of antagonizing their activities to provide a ‘left’ signal in the embryo, and in gastrulation provide a negative feedback loop to regulate mesoderm formation. Further work by Tanegashima et al. [2000] showed that overexpression of *Xatv* in the *Xenopus* marginal zone suppressed mesoderm formation, giving rise to gastrulation defects and inhibited secondary axis formation in response to Xnr1 and activin, suggesting feedback inhibition by *Xatv*. In contrast to this, Xnr1 and activin could not be antagonised by *Xatv* in the animal cap, suggesting that *Xatv* has differential behaviour in the marginal zone and animal region. Antisense depletion of *Xatv* results in gastrulation defects (exogastrulation) and both nodal and Wnt responsive organizer gene expression was expanded. This suggested that *Xatv* is essential for normal organizer patterning and gastrulation through negative feedback of

nodal and Wnt signalling [Branford and Yost, 2002]. Xatv blocks nodal and Vg1 signals by antagonism of EGF-CFC coreceptors required for signalling [Cheng et al., 2004, Tanegashima et al., 2004, Cha et al., 2006].

Tomoregulin

Tomoregulin (TMEFF1) is a membrane protein containing two follistatin modules in addition to an epidermal growth factor (EGF) domain. In *Xenopus*, TMEFF1 inhibits nodal but not activin signalling, and must be attached to the membrane for inhibition of nodal signalling. TMEFF1 is also capable of blocking mesodermal but not epidermal induction by BMP2, requiring TMEFF1s cytoplasmic tail [Chang et al., 2003].

1.4.2 SLRPs and modulation of TGF- β signalling

The small leucine rich repeat proteoglycans (SLRPs) are a family of over a dozen secreted proteoglycans. SLRP family members include decorin, biglycan and asporin. Decorin binds to and inhibits the activity of TGF- β 1 in cell culture systems [Kolb et al., 2001]. More interestingly in the context of development, work by Moreno et al. [2005] demonstrated a role for the SLRP family member, biglycan (Bgn), during early *Xenopus* embryogenesis. They showed that *Bgn* is expressed uniformly in the ectoderm and mesoderm and microinjection of *Bgn* mRNA induces secondary axis formation, dorsalises mesoderm and inhibits BMP4 activity. In addition to this, they demonstrated Bgn binding to both BMP4 and chordin, increasing BMP4 binding to chordin thus enhancing BMP inhibition. Furthermore, they showed that Bgn is able to inhibit BMP4 by enhancing the efficiency of chordin-Tsg complexes and that secondary axis formation by Bgn requires chordin.

1.5 Tsukushi, a novel BMP inhibitor

Tsukushi, (TSK) was identified during a signal trap screen¹³ of a chick lens library [Klein et al., 1996], several years ago by Kunimasa Ohta. TSK is a unique

¹³The signal trap screen specifically identifies genes encoding secreted proteins by virtue of their secretion signal sequence.

secreted protein belonging to the Small Leucine Rich Proteoglycan (SLRP) family of extracellular matrix proteins, with TSK itself containing 12 Leucine Rich Repeats (LRRs). The SLRP family and primary structure will be discussed in more detail in the results section. The initial work on TSK is described in Ohta et al. [2004] and will be summarised here.

1.5.1 Functional analysis of TSK in chick embryogenesis

Alternate splicing of *C-TSK*

Two forms of TSK generated by alternate splicing have been identified in chick. These isoforms, designated C-TSK-A and C-TSK-B differ in their C-terminal regions. The originally described TSK [Ohta et al., 2004] corresponds to the C-TSK-A form, a strong BMP antagonist whose expression in the chick is mainly localised to Hensen's node and the anterior primitive streak during gastrulation. Interestingly, C-TSK-B is a weaker antagonist of BMP signalling and is enriched in the middle primitive streak [Ohta et al., 2006].

The sequences of TSK orthologues identified thus far are generally well conserved with the exception of the C-TSK-A C-terminal region. Searching on the Ensembl chick genome database shows that the chick *TSK* gene is located on chromosome 1. The *C-TSK-B* cDNA sequence is identical to the sequence of *C-TSK* genomic DNA. In *C-TSK-A*, 319nt section of sequence is deleted from the gene by alternate 5' splicing, yielding the *C-TSK-A* isoform.

Expression pattern

The presence of the Nieuwkoop centre and Spemann organizer, discussed above, is generally conserved in the vertebrates. The chick embryo is no exception where the middle of the primitive streak corresponds to the Nieuwkoop centre, whilst Hensen's node corresponds to the organizer [Joubin and Stern, 1999]. Expression of *BMP* is excluded from the node [Joubin and Stern, 1999], whereas expression of the BMP inhibitor, chordin is localised to the node [Streit et al., 1998, Skromne and Stern, 2002]. Misexpression of BMP prevents node formation, and conversely, misexpression of Chordin generates an ectopic primitive streak with node [Streit et al., 1998]. Thus formation of the primitive streak

and Hensen's node requires BMP inhibition [Joubin and Stern, 1999]. *TSK* expression is detected by *in situ* hybridisation in the primitive streak, appearing strongly shortly after in Hensen's node. Later, *TSK* expression is detected in the newly forming somites, as summarised in Figure 1.4¹⁴

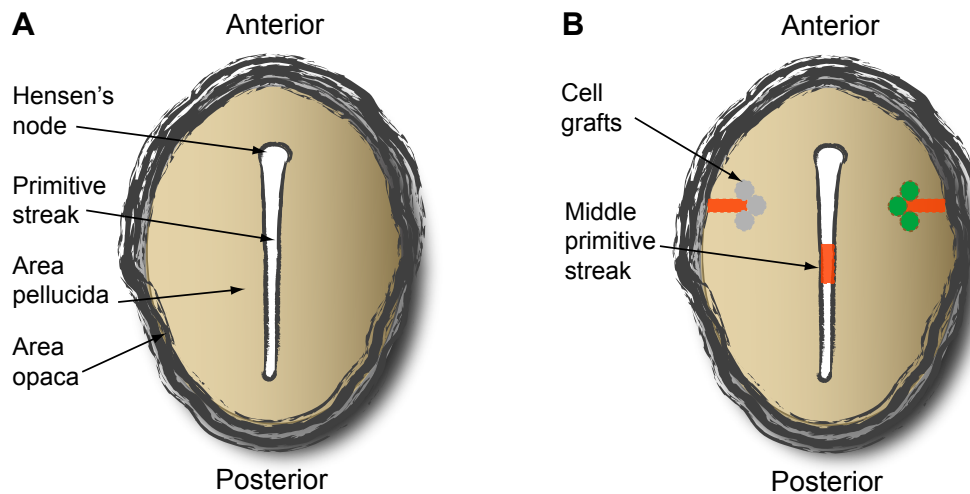


Figure 1.4: **Overview of chick embryonic structures**

(A) Nieuwkoop centre (primitive streak) and organizer (Hensen's node) in the chick embryo. (B) *TSK* gain and loss of function experiments where middle primitive streak (red) is transplanted with aggregates of COS-7 cells.

Misexpression of *TSK* induces ectopic node formation in chick

Expression of *TSK* in the primitive streak and node, in comparison to *chordin* expression in the node only, suggested a specific role for *TSK* in node induction. To determine if *TSK* can induce node formation, aggregates of *TSK*-expressing COS-7 cells were grafted in areas external to the site of normal primitive streak formation (Figure 1.4B). The embryos were screened for expression of node, primitive streak and neural plate markers; *chordin*, *brachyury*, and *Sox3* respectively. Misexpression of *TSK* alone was unable to induce expression of these markers.

Earlier research by Joubin and Stern [1999] reported that signals from the middle primitive streak had to be integrated with BMP inhibition (in their case,

¹⁴It is from this expression pattern in chick from where *TSK* derives its name, due to the resemblance with the Horsetail plant, *Tsukushi*.

with noggin) in order to facilitate node induction. When aggregates of TSK secreting COS-7 cells were transplanted together with middle primitive streak, ectopic expression of *chordin* was induced in 59% of the embryos. Since the middle primitive streak is known to express *cVg1* and *Wnt8C* [Joubin and Stern, 1999], the experiment was repeated with a stable fibroblast line secreting Wnt1 (known to mimic Wnt8C activity [Shimizu et al., 1997]) and cVg1 expressing cells. In this case, the combination of TSK, cVg1 and Wnt1 produced ectopic chordin expression in 40% of embryos as opposed to 13% in the case of cVg1 and Wnt1 expression alone, suggesting TSK induces ectopic node in cooperation with Vg1 and Wnt signals.

Loss of TSK function analysis in the chick embryo

To support a role for TSK in node/organizer induction in the chick embryo, loss of function was performed by electroporation of *TSK* siRNA into the node. *TSK* siRNA nodes were transplanted into host embryos where the endogenous node had been removed (Figure 1.4B). Two middle primitive streaks were then taken from other donor embryos and transplanted adjacent to the transplant node and induction of *chordin* nearby analysed. Ablation of TSK in the node resulted in ectopic expression of *chordin* in 25% of embryos, compared to 44% in the presence of control siRNA electroporated nodes, supporting a role for TSK in node formation in chick development.

The role of TSK in chick embryogenesis

As stated above, BMP inhibition is essential for primitive streak formation and node induction in the chick embryo [Joubin and Stern, 1999, Streit et al., 1998]. However, known BMP antagonists such as *chordin*, *noggin*, *folliculin* and *cerberus* are only expressed in the node, and remain absent from the primitive streak [Chapman et al., 2002]. TSK differs in that it is expressed in the middle primitive streak in addition to the node. It was hypothesised that TSK is acting as a BMP inhibitor to induce node formation. In addition to this, it was found that Vg1 is pulled down in complex with TSK, suggesting links with TGF- β superfamily signalling.

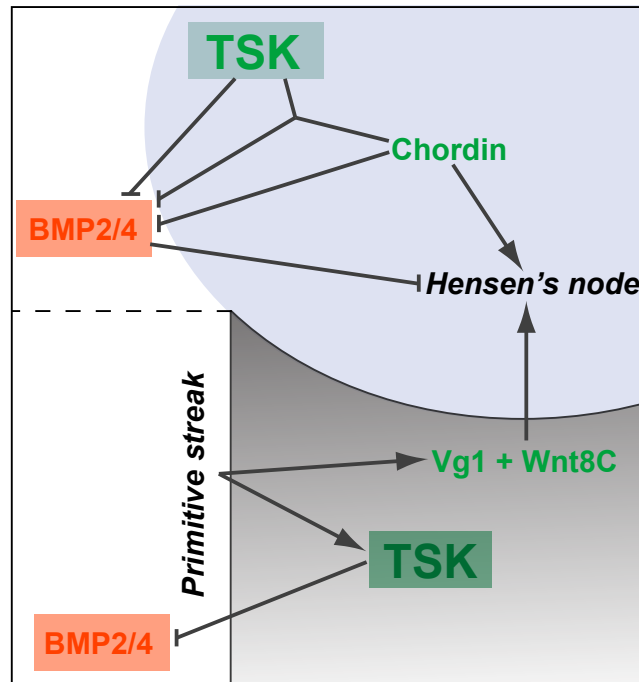


Figure 1.5: **The role of TSK in induction of the node by the middle primitive streak.**

Adapted from [Ohta et al., 2004]. *TSK* is expressed in primitive streak in addition to node. Inhibition of BMP signalling by TSK in cooperation with chordin facilitates node induction. In addition to this, TSK enhances node induction by cooperation with Vg1 and Wnt8C signalling in the primitive streak.

1.5.2 Confirmation of BMP inhibition by TSK; *Xenopus laevis* as a model system

To analyse the function of TSK in further detail, *Xenopus laevis* was used as a model system in which C-TSK-A was expressed. In *Xenopus*, *TSK* is expressed in the dorsal blastopore lip of the early gastrula stage embryo, suggesting a role in organizer formation similar to the chick. In support of this, expression of *C-TSK-A* mRNA in the ventral marginal zone of *Xenopus* results in secondary axis formation in 55% of embryos. When C-TSK-A is expressed in ventral marginal zone explants, when grown to stage 25, the explants demonstrate convergent extension movements and expression of muscle actin, consistent with induction of tissue of a dorsal type. In addition, expression of *C-TSK-A* in *Xenopus* animal caps activates expression of the neural markers, *XAG-1*, *Sox2* and *Xotx2*,

suggesting C-TSK-A is an inducer of neural tissue. This neural induction by TSK is direct since no induction of the dorsal mesoderm marker, *muscle actin* is detected in the animal caps.

The dorsalising activity and direct neural induction by TSK, in combination with the above chick analysis suggested that TSK was acting as a BMP inhibitor. In support of this, when C-TSK-A is universally expressed, embryos with a dorsalisated phenotype are produced. In contrast to this, when the same experiment is performed with BMP4, ventralised embryos are produced. However, upon coexpression of *C-TSK-A* and *BMP4*, relatively normal embryos develop, suggesting antagonism between TSK and BMP4. This antagonism is produced upstream of the BMP receptor level, as TSK in the presence of a constitutively active BMP type I Receptor, caALK3 [Onichtchouk et al., 1999], completely blocks the ability of TSK to induce neural markers in animal caps.

Activity of TSK upstream of receptor level raised the possibility of TSK binding to BMP. Indeed, BMP2, 4 and 7 is pulled down in complex with TSK, and in addition to this, Vg1. No interaction with the TGF- β superfamily members, activin or ADMP has been found. In addition to interactions with TGF- β superfamily members, chordin can also be pulled down in complex with TSK. This raised the possibility of ternary complex formation between TSK, BMP and chordin, as it has been reported that chordin and twisted gastrulation form a ternary complex with BMPs [Chang et al., 2001, Oelgeschläger et al., 2000]. Indeed, chordin is pulled down in complex with TSK¹⁵ and chemical cross-linking experiments with DTSSP demonstrate ternary complex formation. This interaction is of functional significance as low doses of *C-TSK-A* and *chordin* injected separately, result in weak secondary axis formation, whereas coinjection of *C-TSK-A* and *chordin* results in strong secondary axis induction in 50% of embryos¹⁶.

Whilst the functional analysis of C-TSK-A in *Xenopus laevis* provided an insight into the function of TSK during chick embryogenesis; further interesting questions on the role of X-TSK in *Xenopus* itself were generated.

¹⁵The BMP inhibitors, noggin and follistatin are not pulled down in complex with TSK

¹⁶This effect is shown to be cooperative, rather than additive

1.5.3 Role of TSK in *Xenopus* ectoderm patterning

The *Xenopus* orthologue of TSK, in common with C-TSK, possesses 12 LRRs. Overexpression of X-TSK in a similar manner to the expression experiments performed in *Xenopus*, results in dorsalisation of mesoderm and direct neural induction, although no secondary axial structures are induced upon X-TSK overexpression¹⁷. This will be discussed in more detail later within an analysis of TSK primary structure.

BMP inhibition by TSK also plays a role during patterning of the *Xenopus* ectoderm. Neural crest tissue arises at the border between the neural plate and epidermis, ultimately giving rise to the peripheral nervous system, melanocytes and craniofacial skeleton [Hall, 1999, Le Douarin and Kalcheim, 1999]. Specifically, ectodermal patterning is specified by a mediolateral gradient of BMP signalling, higher in the epidermis and lower in the neuroectoderm. At a specific threshold of BMP signalling, neural crest is specified [LaBonne and Bronner-Fraser, 1998, Marchant et al., 1998b, Nguyen et al., 1998]. Additional signals such as Wnts, Fibroblast Growth Factors (FGFs) and Retinoic Acid (RA) restrict neural crest to the posterior neural plate border [Hopwood et al., 1989a, Mayor et al., 1995, Villanueva et al., 2002]. In addition, the Notch pathway is involved in neural crest specification through regulation of *BMP* expression [Glavic et al., 2004].

X-TSK is strongly expressed during the period of neural crest specification at the border between epidermis and neural plate, in the area of presumptive neural crest. With this spatial and temporal overlap of *X-TSK* with neural crest and known BMP inhibition, the role of TSK in neural crest formation was examined.

1.5.4 In *Xenopus* embryogenesis, TSK regulates ectoderm patterning and neural crest specification

The work by Ohta et al. [2004] focused upon the A form of C-TSK which has additional amino acids in the C-terminal cysteine cluster. A shorter B form

¹⁷BMPs are also pulled down in complex with X-TSK.

of C-TSK is present in chick, and its orthologue was also identified in *Xenopus laevis*. Kuriyama et al. [2006] showed that *Xenopus* TSK¹⁸ is expressed in presumptive neural crest in *Xenopus* and gain of function results in enhanced neural crest specification whereas depletion of TSK impairs neural crest formation. The function of TSK in neural crest is explained by inhibition of BMP to achieve intermediate levels of signalling required to form neural crest. TSK also indirectly regulates *BMP4* mRNA expression at the neural plate border through interaction with Notch-Delta signalling. TSK in fact physically interacts with the extracellular region of X-Delta-1, to modulate Delta-Notch signalling activity.

1.5.5 Further questions on the role of TSK in early *Xenopus laevis* embryogenesis

Previous functional analyses of TSK function as summarised above, focused upon chick organizer induction and *Xenopus* neural crest formation. Expression of chick TSK in *Xenopus* ventral marginal zone results in secondary axis formation and dorsalisation. This in combination with the function of C-TSK in organizer induction in the chick suggested that there may be a function of X-TSK in *Xenopus* development, earlier than the point of neural crest induction. This analysis of X-TSK presented here is based upon the function of TSK during *Xenopus* germ layer formation and gastrulation.

¹⁸Of the two TSK genes identified in *Xenopus*, both of B form, X-TSK-B1 was used in this neural crest study

Chapter 2

Aims of this study

Part 1: Functional analysis of follistatin inhibition of activin

The aim of this part of the study was to use *Xenopus* as a model system to determine the minimum functional unit of follistatin. This was part of, and complementary to a larger study in which the structure of activin A in complex with follistatin was solved, the publication of which is summarised in chapter 4 and included in the appendix [Harrington et al., 2006].

Part 2: Role of TSK in early *Xenopus laevis* embryogenesis

This study was concerned with the functional analysis of the small leucine rich proteoglycan, Tsukushi. The main aims involved analysis of expression pattern in early *Xenopus* development, functional analysis during germ layer formation and patterning, and analysis of the mechanism of TSK function with known cell signalling pathways acting during these processes. This analysis is covered from chapters 5 to 11.

Part II

Materials and Methods

Chapter 3

Materials and Methods

3.1 Developmental Biology

3.1.1 *Xenopus laevis* embryos and animal cap assay

Xenopus embryos were obtained by *in vitro* fertilisation [Smith and Slack, 1983], dejellied with 2% cysteine, pH 8.0, maintained in 0.1 X Modified Barths Solution (MBS) and staged according to Nieuwkoop and Faber (1967). After fertilisation, embryos were maintained at 14°C and cultured until stage 8. Animal caps were dissected from stage 8/8.5 embryos. They were incubated at room temperature in 0.7 X MBS containing 0.1% BSA in the presence or absence of activin +/- follistatin until control embryos had reached the desired stage. For phenotypic analysis, caps were cultured until control embryos reached stage 25, and imaged. For RT-PCR analysis, caps were cultured until stage 10.5, and then snap-frozen prior to RNA isolation. A total of 30 units of activin were added (final concentration 150pM), while follistatin fragments were used at a concentration of 100nM. Full length follistatin used as a positive control was obtained from Peprotech (Rock Hill, NJ, USA).

3.1.2 mRNA extraction

Embryos or animal caps at the indicated stages (5 and 10 per stage, respectively) were snap-frozen, followed by RNA isolation according to the manufacturers protocol (RNeasy, Qiagen). Extracted RNA was stored in RNase-free water at -80°C.

3.1.3 Agarose gel electrophoresis

For DNA analysis, samples were loaded in DNA loading buffer (20 % Glycerol, 40mM EDTA pH8, 20mM Tris pH8, 1% Bromophenol blue, 0.25% Xylene cyanol) and separated on a 0.8% agarose gel with 1% Ethidium Bromide (Sigma), at 50 Volts. After electrophoresis, bands were imaged under UV light (302nm) using the GelDoc analysis software (Alpha Innotech).

3.1.4 Semi-quantitative reverse transcriptase PCR analysis

cDNAs were generated from the extracted mRNA according to the manufacturer's instructions (Applied Biosystems). Primers used were;

<i>Chordin</i> fwd	5'-CCT CCA ATC CAA GAC TCC AGC AG-3'	[Cho et al., 1991]
<i>Chordin</i> rev.	5'-GGA GGA GGA GGA GCT TTG GGA CAA G-3'	
<i>Goosecoid</i> fwd	5'-CAC ACA AAG TCG CAG AGT CTC-3'	[Sasai et al., 1994]
<i>Goosecoid</i> rev.	5'-GGA GAG CAG AAG TTG GGG CCA-3'	
<i>ODC</i> fwd	5'-CAG CTA GCT GTG GTG TGG-3'	[Agius et al., 2000]
<i>ODC</i> rev.	5'-CAA CAT GGA AAC TCA CAC C-3'	
<i>X-TSK-B1</i> fwd	5'-CTA ACA ATG GCT CTT TCT TCT T-3'	[Kuriyama et al., 2006]
<i>X-TSK-B1</i> rev.	5'-GTT TCC AGA AGG TTG TGA CTC A-3'	

Quantitative ranges were determined before the final analysis. All reactions were normalised against the *ODC* gene product. PCR primers were synthesised by Sigma Genosys, Europe.

3.1.5 Structural models

Published structure coordinates for activin, follistatin and decorin were downloaded from the Protein Quaternary Structure database (PQS, www.pqs.ebi.ac.uk). Structures were then manipulated using the Pymol program (<http://pymol.sourceforge.net>).

3.1.6 Multiple sequence alignments and phylogenetic trees

Sequences of TSK from the indicted species and identified *H.sapiens* SLRPs were obtained from the Ensembl website (www.ensembl.org). Multiple sequence alignment was performed using the ClustalX program (EMBL). Construction of phylogenetic trees was performed using the NJ Plot program (University of Lyon, France).

3.1.7 DNA constructs used in this study

Insert	Vector	Source
<i>constitutively active ALK3</i>	pCS2	Dr. Giuseppe Lupo
<i>dominant negative ALK4</i>	pCS2	Dr. Giuseppe Lupo
<i>Cerberus Short</i>	pCS2	Dr. Giuseppe Lupo
<i>C-TSK-A</i>	pCS2	Dr. Kunimasa Ohta
<i>C-TSK-B</i>	pCS2	Dr. Kunimasa Ohta
<i>H-TSK</i>	pCS2	Dr. Kunimasa Ohta
<i>X-TSK-B1</i>	pCS2	Dr. Kunimasa Ohta
<i>X-TSK-B2</i>	pCS2	Dr. Kunimasa Ohta
<i>X-TSK-B1</i>	pBSK	Dr. Kunimasa Ohta
<i>C-TSK-A-Myc-His</i>	pCS2	Dr. Kunimasa Ohta
<i>X-TSK-B1-Myc-His</i>	pCS2	Dr. Kunimasa Ohta
<i>nuclear β-Gal</i>	pSP64TS	Dr. Anna Philpott
<i>tBR</i>	pSP64T	Dr. Giuseppe Lupo
<i>chordin</i>	pCS2	Dr. Kunimasa Ohta
<i>Xbra</i>	pSP73	Dr. Anna Philpott
<i>Sox17α</i>	pBSK(-)	Dr. Aaron Zorn
<i>gooseoid</i>	pBSK	Dr. Toshiaki Mochizuki
<i>GATA4</i>	pSP64T	Prof. Roger Patient
<i>MyoD</i>	pSP64T	Dr. Anna Philpott
<i>Xnr2</i>	pSP64T	Dr. Giuseppe Lupo
<i>Krox20</i>	pBSK	Dr. Anna Philpott
<i>Otx2</i>	pBSK	Dr. Anna Philpott
<i>En2</i>	pBSK	Dr. Anna Philpott
<i>FGF8</i>	pCS2	Dr. Giuseppe Lupo
<i>vras</i>	pSP64T	Dr. Carol LaBonne
<i>XFD</i>	pCS2	Dr. Kevin Dingwell
<i>caFGFR-C249Y</i>	pCS2	Dr. Kevin Dingwell
<i>iFGFR</i>	pCS2	Dr. Giuseppe Lupo
<i>Xnr2-Myc</i>	pCS2	Dr. Chris Wright
<i>FRL1-3Flag</i>	pCS2	Prof. Makoto Asashima
<i>FRL1</i>	pCS2	Prof. Makoto Asashima
<i>CR3-Short</i>	pCS2	Dr. Malcolm Whitman
<i>CR3-Long</i>	pCS2	Dr. Malcolm Whitman
<i>NotchICD</i>	pCS2	Dr. Anna Philpott
<i>Vg1(Ser)</i>	pCS2	Prof. Janet Heasman
<i>VegT</i>	pCS2	Prof. Janet Heasman

3.1.8 Synthesis and microinjection of capped mRNA into *Xenopus* embryos

Capped mRNAs were synthesised from linearised DNA, as according to the manufacturer's protocol (mMessage Machine, Ambion). RNA solutions were

stored in nuclease-free water at -80°C . Embryos were obtained, dejellied and cultured as described above. Microinjections of mRNAs ranging at concentrations of 1pg to 1ng were microinjected in 10nl volumes into the indicated blastomeres of stage 1 to 32 stage embryos using a Picoinjector microinjector (Harvard Apparatus). Microinjection of embryos was performed in 4% Ficoll, 0.2% MBS with (0.1 $\mu\text{g}/\text{ml}$) Gentamycin. Embryos were then cultured at 14°C until the desired stage.

3.1.9 Extraction of protein

Stage 10.5 embryos or animal caps were lysed in lysis buffer (recipe 150mM NaCl, 100mM Tris-HCl pH7.5, 0.1% NP-40 with protease inhibitors, 10 $\mu\text{g}/\text{ml}$ Leupeptin, 1 $\mu\text{g}/\text{ml}$ Pepstatin and 10 $\mu\text{g}/\text{ml}$ Chymostatin (Sigma)). 5 μl lysis buffer per embryo or 20 μl per 10 animal caps was used with vortexing, followed by centrifugation at 13,500 rpm at 4°C for 5 minutes. The soluble fraction was carefully removed by pipette for SDS-PAGE and Western blot analysis.

3.1.10 Quantification of protein

Protein content of embryo lysates was quantified using the Bradford assay. 2 μl of embryo lysate was mixed and incubated at room temperature for 5 minutes with a 20% solution of Bradford reagent (Biorad). The mixture was subsequently analysed for protein content using the Eppendorf spectrophotometer (Eppendorf) at a wavelength of 515nm.

3.1.11 PNGaseF treatment of embryo lysates

25 μl Embryo lysates expressing the proteins of interest were denatured in Glycoprotein Denaturing Buffer (0.5%SDS, 1% Beta-mercaptoethanol) at 100°C for 10 minutes. After the addition of 10% NP-40 and G7 Reaction buffer (50 mM Sodium Phosphate, pH7.5), 1 unit PNGaseF (New England Biolabs) was added and the reaction mixture incubated for 1 hour at 37°C . Products were then analysed by SDS-PAGE and Western blotting.

3.1.12 SDS-Polyacrylamide Gel Electrophoresis (PAGE)

Proteins contained within embryo and animal cap lysates were separated on 10 to 15% polyacrylamide gels. Gels consisted of an upper stacking portion (Tris-HCl, pH6.8) and a lower resolving portion (Tris-HCl, pH8.8). All gels contained 1% Sodium Dodecyl Sulphate (SDS). Prior to loading, lysates were boiled at 95°C for 5 min in 2 X loading buffer with the addition of β -mercaptoethanol and 20 μ l of sample loaded per lane. 5 μ l protein ladder (Seeblue, Invitrogen) was also loaded to distinguish sizes of the separated proteins. Electrophoresis was performed with the Mini-Protean III system (Biorad), at 60 Volts (Stacking gel) followed by 100 Volts (resolving gel) in 1 X Running Buffer (100mM Glycine, 100mM Tris Base, 1% SDS). The gels were subsequently prepared for Western blotting.

3.1.13 Western blotting

Proteins separated by SDS-PAGE were transferred onto a nitrocellulose membrane using a wet transfer system (Biorad) at 100 V for 1 hour at 4°C. After transfer, membranes were blocked in 5% nonfat milk in Phosphate Buffered Saline (PBS) + 0.1% Tween or Tris Buffered Saline (TBS) + 0.1% Tween for 1 hour at room temperature with gentle agitation. Membranes were then incubated with primary antibody in the appropriate blocking solution or 5% BSA in PBS+ 0.1% Tween at room temperature for 1 hour or overnight at 4°C. Following 3 washes in PBS or TBS + 0.1% Tween, the membrane was incubated with secondary antibody, donkey-anti-mouse or goat-anti-rabbit Horseradish Peroxidase (HRP) (Amersham) at a 1/5000 dilution in blocking solution for 1 hour at room temperature. After a further 3 washes in PBS + 0.1% Tween, chemiluminescence substrate (Supersignal, Pierce) was applied to the membrane, followed by visualisation on x-ray film (Fuji film).

3.1.14 Cell signalling assays

Xenopus embryos were injected into the indicated blastomeres at the indicated stage and cultured until stage 8. Animal caps were dissected in 1 X MBS and

cultured in 0.7 X MBS until stage 10. Explants were lysed in lysis buffer (LPC, 150mM NaCl, 1% NP-40, 0.5% PMSF, 0.1% SDS, 50mM Tris, pH 8.0, 1mM sodium fluoride and 1mM sodium orthovanadate). The Bradford assay was carried out on cell lysates to ensure equal loading of protein onto SDS-PAGE gels.

Antibody	Dilution	Source
Activated clone MAPK-YT ERK (pan ERK)	1/1000	Sigma
Phospho Smad2	1/500	BD Biosciences
Smad2	1/1000	Cell Signalling Technology
Phospho Smad1	1/1000	BD Biosciences
Smad1	1/1000	Cell Signalling Technology
		Santa Cruz

3.1.15 Regulated homodimerization

The Argent Regulated Homodimerization kit (ARIAD Pharmaceuticals) was used according to [Pownall et al., 2003]. mRNA for a mutant form of the FGF receptor (iFGFR) was microinjected into *Xenopus* embryos at the two cell stage in the range of 0.5 to 50pg. After incubation until stage 9, animal caps were cut as described above and incubated in 0.7 X MBS with the addition of 5nM homodimerization reagent (AP1510) or an ethanol vehicle control until caps reached stage 10. Caps were subsequently lysed and analysed by Western blotting. Whole embryos were incubated in 5nM AP1510 from late-blastula stages to early gastrula stages where they were fixed and subject to analysis by *in situ* hybridisation.

3.1.16 Fixing and bleaching of embryos

Prior to *in situ* hybridisation, embryos at the indicated stages were fixed in MEMFA (100mM MOPS, 2mM EGTA, 1mM MgSO₄, 3.7% formaldehyde) for 1 hour at room temperature. Following fixation, embryos were washed with 1 X PBS and stored in methanol at -20°C . Subsequent re-hydration of methanol-dehydrated embryos was performed by incubation in 50% Methanol/PBS followed by 100% PBS. The embryos were then incubated in bleaching solution (3% H₂O₂, 5% Formamide and 0.1% SSC) at room temperature on a light box

until the pigment had bleached.

3.1.17 *In situ* hybridisation probe synthesis reaction

Adapted from Harland [1991]. Indicated probes for *in situ* hybridisation were labeled with Digoxigenin. Purified linearised DNA was incubated in 10 X Transcription buffer (Boehringer Mannheim), Dig labelling mix (Roche) and T7, T3 or SP6 polymerase as required (Roche). The reaction mixture was incubated at 37°C for 2 hours, followed by a 15 minute incubation with 1 unit DNaseI (Sigma) in order to digest the DNA template. The mixture was then precipitated overnight at -20°C with LiCl₂ and ethanol. After centrifugation at 13,500 rpm at 4°C for 30 minutes and washing with 70% ethanol, the pellet was air-dried and resuspended in hybridisation buffer (50% Formamide, 0.75M NaCl, 1XPE, 100μ/μl tRNA, 0.05% heparin, 0.1% Tween). Quantification of probe concentration was performed using a Nanodrop spectrophotometer, ND-1000 (Labtech).

3.1.18 Whole mount *in situ* hybridisation

Bleached, rehydrated embryos were incubated at room temperature for 2 minutes with 3μg/ml ProteinaseK (Sigma) in 1 X PBS + 0.1% Tween. After refixation in 4% paraformaldehyde, samples were washed and prehybridised in hybridisation buffer for 1 hour at 60°C. Hybridisation with the indicated probes at a concentration of 2ng/ul was carried out overnight at 60°C.

Following washing, the samples were incubated at 37°C for one hour in 10μg/ml RNase A (Sigma) and 1U/ml RNase T1(Roche), in order to digest unbound probe. Subsequent washing in formamide containing buffers inactivated any remaining enzyme activity. Following washing of the formamide from the embryos, blocking in 2%) BMBR (Boeringer Mannheim Blocking Reagent, Boeringer Mannheim), 5%) heat-inactivated goat serum, and 2mM Levamisole (Sigma) in MABT (Maleic Acid Buffer (0.1M maleic acid, 0.15M NaCl) with 0.1%) Tween) was performed for 1 hour at room temperature. Incubation of the alkaline phosphatase conjugated anti-digoxigenin antibody (Roche) was carried out in blocking buffer at 4°C overnight.

Unbound antibody was washed from the embryos in several changes of MABT with 2mM levamisole. Equilibration in NTMT (100mM Tris pH 9.5, 100mM NaCl, 50mM MgCl₂) with 2mM levamisole was followed by the colouring reaction overnight at room temperature with BM Purple alkaline phosphate substrate (Roche) with 2mM Levamisole. Once colour had suitable developed, the colouring reaction was stopped with PBS + 0.1% Tween + 2mM EDTA. Embryos were then refixed in MEMFA, washed and imaged using a dissection microscope (Leica) connected to the Openlab software (Openlab) via a CCD camera (Hamamatsu Ocra).

3.1.19 β -Galactosidase staining

For identification of microinjection targeting, embryos were injected with nuclear or cytoplasmic β -Galactosidase as indicated, at a concentration of 500pg per blastomere. After incubation to the stages indicated, embryos were fixed for 1 hour at room temperature in MEMFA. After washing and equilibration in 1 X PBS + 2nM MgCl₂, the colouring reaction was developed at 37°C in X-Gal mixer (25mM K₃Fe(CN₆), 25mMK₄Fe(CN₆)·3H₂O, 2mM MgCl₂, 0.01% Sodium deoxycholate, 0.02% NP40 in PBS, pH 7.4) with 2.5 μ g/ml X-Gal in DMF (Dimethyl Formamide). The reaction was stopped with washing and the embryos were stored in methanol at -20°C.

3.1.20 *In situ* hybridisation on sectioned embryos

In situ hybridisation on sectioned embryos was performed as according to Butler et al. [2001]. Embryos at the indicated were fixed and microtome (Leica) sectioned to a 15 μ M thickness. Microinjected embryos were coinjected with β -Galactosidase and developed to identify the location of injection in the case of endoderm targeting.

3.1.21 Pulldown of tagged proteins

Cell lysates of embryos injected with *X-TSK-Myc-His*, *Xnr2-Myc* or *FRL1-3 Flag* and incubated for 12 hours at 4°C in 1 ml of buffer containing 150mM NaCl, 20mM Tris-HCl pH 7.5, 1.5mM CaCl₂, 1.5mM MgCl₂, 0.1% Triton X-

100, 0.1% CHAPS, 5% Glycerol and 0.1% BSA (As according to Larrain et al. [2000]). This was followed by incubation with 25 μ l ProBond resin (Invitrogen) for 2 hours at 4°C. After washing in 5-fold concentrated buffer without BSA, the bound proteins were precipitated by heating the beads to 95°C for 5 minutes, followed by Western blotting analysis.

3.1.22 Loss of function with morpholino

X-TSK morpholino *X-TSK MO*, 5'-TCTAACAATGGCTCTTTCTTCTTGG-3' (Gene Tools, LLC) was designed against the 5'UTR of X-TSK-B1. As a control morpholino, Zebrafish *chordin* morpholino (*Control MO*) was used, (Gene Tools, LLC). Both morpholinos have been characterised previously [Ohta et al., 2004, Kuriyama et al., 2006].

Part III

Results I: Activin-follistatin structure and function

Chapter 4

Activin-Follistatin: structure-function

The work presented in this chapter is as a result of a collaboration with the group of Dr. Marko Hyvönen, Department of Biochemistry, University of Cambridge. The resulting publication, [Harrington et al., 2006], is included in Appendix A.

4.1 Follistatin inhibition of activin

In the *Xenopus* embryo, the TGF- β superfamily member activin is capable of inducing mesoderm. The role of activin in early *Xenopus* development still remains unclear though as follistatin inhibition of activin may or may not inhibit mesoderm formation [Marchant et al., 1998b, Schulte-Merker et al., 1994] respectively. It is clear though that activin acts as a morphogen, exerting long range effects in the embryo [Gurdon et al., 1994, 1995, Jones et al., 1996, McDowell et al., 1997]. It is also evident that activin has an important biological function in mesoderm patterning, and can modulate expression of other mesoderm inducing agents [Piepenburg et al., 2004]. Thus correct regulation of activin signalling in the embryo is essential for normal development.

Several inhibitors of BMP signalling have been identified, and include noggin, gremlin and chordin [Esch et al., 1987, Hemmati-Brivanlou et al., 1994, Piccolo et al., 1996, Zimmerman et al., 1996, Fainsod et al., 1997, Hsu et al., 1998]. In addition to this, follistatin, is known to inhibit BMP signalling and activin

in addition [Iemura et al., 1998, Amthor et al., 2002, 2004, Glister et al., 2004]. BMP inhibition by follistatin is biologically important in the organiser region of the *Xenopus* embryo for normal development [Hemmati-Brivanlou et al., 1994, McGrew et al., 1995, Fainsod et al., 1997]. The importance of activin inhibition by follistatin in early development may be associated with the interpretation of activin signalling gradients. Repression of activin signalling is essential for proper expression of the activin responsive genes, *gooseoid* (*Gsc*), *chordin* (*Chd*) and *Xbrachyury* (*Xbra*) [Kurth et al., 2005]. Extracellular inhibition of activin by follistatin and other inhibitors could be one possible mechanism for this repression.

However, it has not previously been described as to the minimum functional unit of follistatin required for inhibition of activin A activity. This chapter covers the findings of a study performed to identify the region of follistatin important for activin inhibition, using a combinatorial approach of structural, biochemical and *Xenopus* biological analyses.

4.1.1 Structure and function of activin A

Activin A is one of four activin genes identified in humans. Dimeric activin activates signalling through binding to its type II receptor, ActRIIB, followed by recruitment of the type I receptor (Reviewed in Massagué [1998]). ActRIIB binds to the knuckle epitope at the back of the of the activin ‘fingers’ and brings the receptors into close proximity [Thompson et al., 2003].

In *Xenopus* animal caps, activin is a potent mesoderm inducer, resulting in extensive morphogenetic movement and tissue elongation [Symes KR, 1987, Green et al., 1992]. This makes it a useful system to examine the effects of inhibitors on activin function [Schulte-Merker et al., 1994]. In this study, we used novel recombinant activin A, the titration of which in *Xenopus* animal caps is shown in Figure 4.1.

The titrated human activin A in figure 4.1 was expressed in *Escherichia coli*. To confirm the activity of recombinant activin A used in the structural determination, animal caps were dissected from stage 8 - 8.5 embryos, and treated with

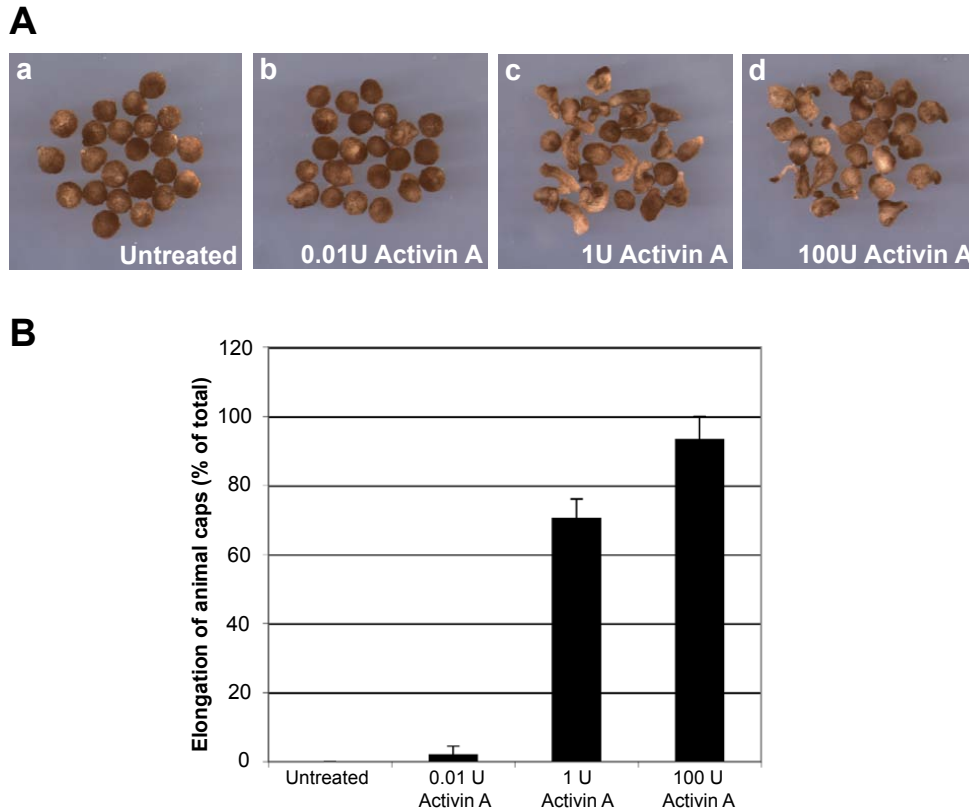


Figure 4.1: **Activin A dose response in *Xenopus* animal caps.** (A) Treatment of *Xenopus* animal cap explants with human recombinant activin A, at a concentration range from 0.01 to 100Units/ml. (B) Graphical representation of animal cap elongation, represented as the percentage of total caps treated. n is in the range of 60-70 for each data set.

0.01Units (U) to 100U activin A. 1U of activin A has previously been specified as the minimum concentration of activin required to observe elongation of the animal caps [Symes KR, 1987]. This corresponds to a concentration of 5pM activin A.

Untreated caps do not demonstrate elongation, as the tissue is of ectodermal fate. Very little elongation, in less than 5% of the total caps treated, is observed with treatment of the caps with 0.01U activin A. At a 100-fold increase in activin concentration to 1U, elongation of the caps is evident in 70% of the total treated. This figure rises to 90% of caps treated exhibiting elongation when 100U activin A is applied. This data demonstrates that the activin used

in this study is functionally active, comparable to previously published data [Symes KR, 1987].

4.1.2 Domain structure of follistatin

Three major isoforms of follistatin can be identified by virtue of differences in their C-terminal sequences, arising from a combination of alternative splicing and proteolytic processing. The functional difference in these isoforms is associated with their ability to bind heparan sulphates. The commonality between the isoforms lies in the four distinct domains of mature follistatin, represented in figure 4.2A. Follistatin is composed of an N-terminal unique domain, Fs0 (residues 1-63), and three follistatin domains; Fs1 (residues 64-135), Fs2 (residues 136-212), and Fs3 (215-288) [Shimasaki et al., 1989, Ullman and Perkins, 1997]. The long isoform of follistatin also includes an acidic tail, bringing the total length of the protein to 315 residues [Sumitomo et al., 1995].

4.1.3 Activin function is inhibited by Fs12, Fs2 and Fs123 fragments

Each Fs domain in follistatin consists of an EGF-like and Kazal-type subdomain. It has previously been suggested that the Kazal-type subdomains of Fs1 and Fs2 contain sequences required for follistatin binding to activin [Keutmann et al., 2004]. It has also been reported that synthetic polypeptides akin to the Fs0 domain can bind to activin [Wang et al., 2000]. In support of this, hydrophobic residues critical for follistatin function have been identified in Fs0 [Sidis et al., 2001]. In addition to these reports, it has been shown that for optimal activin binding, full-length follistatin is required [Amthor et al., 2002]. Figure 4.2A shows the constructs used in this study, represented by bars, specifying residue number below the full length follistatin representation. The functional analysis focuses upon several single, double and triple domain constructs in an attempt to characterise a minimal activin-inhibiting fragment of follistatin. Full length follistatin is also used for a comparison of activity.

Figure 4.2B shows animal cap explants treated with various follistatin fragments in the presence or absence of activin A. 30U of human recombinant activin

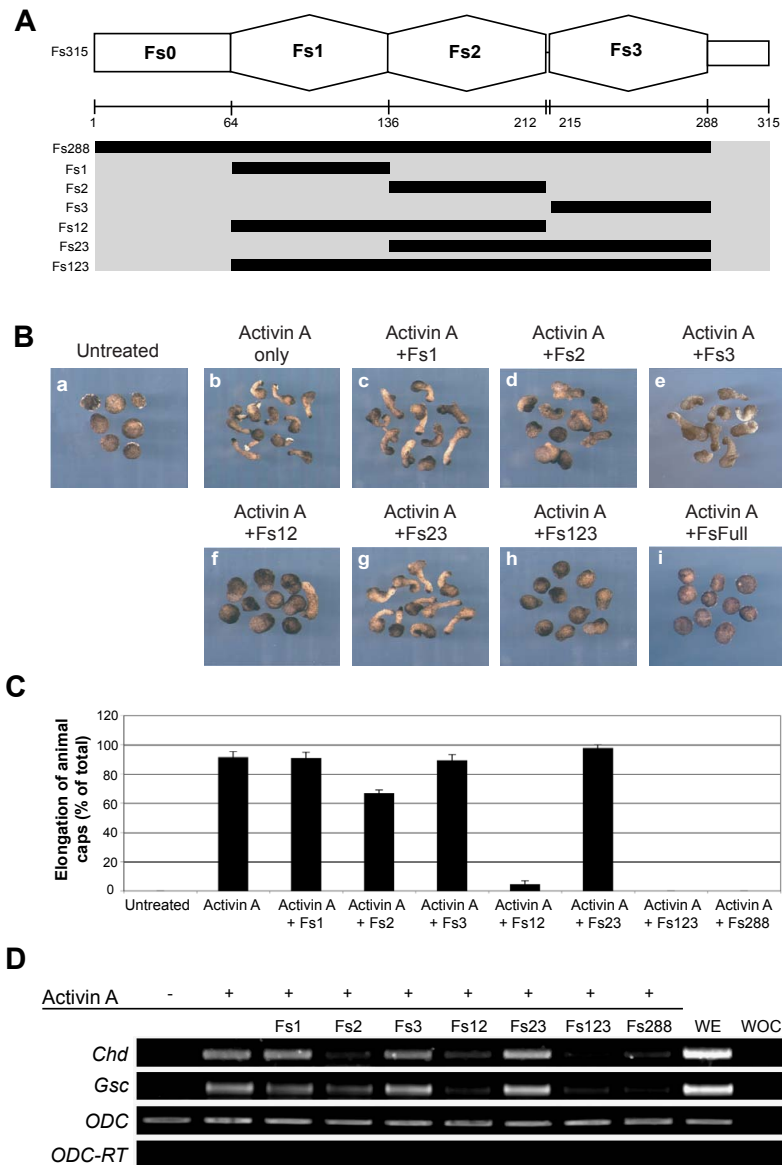


Figure 4.2: Inhibition of activin A by follistatin fragments in *Xenopus* animal cap explants

(A) The domain structure of follistatin. Bars below refer to the domains analysed, with numbers corresponding to the first and last residues of each fragment in the mature, full-length follistatin sequence. (B) Response of *Xenopus* animal caps to 30U activin A in the presence or absence of follistatin fragments as indicated above each panel. (C) Quantification of phenotypic data shown in (B) pooled from several experiments. (D) Semiquantitative animal cap analysis of the effects of follistatin fragments on activin A-induced expression of the mesoderm markers *Chordin* (*Chd*) and *Goosecoid* (*Gsc*) in *Xenopus* animal caps. n is in the range of 50-60 for each data set.

A produced elongation in almost all (Over 90%, figure 4.2C) of the caps treated, compared to the rounded untreated caps. This effect of activin is not abrogated by the addition of follistatin fragments Fs1, Fs3 or Fs23, whereas treatment of animal caps with fragments Fs2, Fs12, or Fs123 shows clear inhibitory effects upon activin-induced elongation. This inhibition is most pronounced with Fs12 and Fs123 (5% and 0% of the caps elongating, respectively, figure 4.2C) while the Fs2 domain alone elicits only partial inhibition (66% of caps elongating).

In addition to phenotypic analysis of animal cap explants, semiquantitative RT-PCR was also performed to analyse levels of mesodermal gene expression in response to activin and follistatin. Upon treatment of animal caps with 30U activin A, expression of the dorsal mesoderm markers *chordin* (*Chd*) and *goosecoid* (*Gsc*) is induced relative to control, untreated animal caps, figure 4.2D [Green et al., 1992, Sasai et al., 1994]. Induction of these dorsal mesoderm markers is not perturbed by the addition of follistatin fragments, Fs1, Fs3 or Fs23. Conversely, addition of Fs2, Fs12 or Fs123 results in the inhibition of activin-induced *Chd* and *Gsc* gene expression. Neither the phenotype of the animal caps nor the levels of marker gene expression differ from that of the control caps when the animal caps are treated with any of the follistatin fragments in the absence of follistatin (data not shown).

Together, these functional analyses in the *Xenopus* animal cap system suggest that the follistatin constructs Fs12 and Fs123, and to a lesser extent, Fs2, are sufficient for the inhibition of activin-mediated mesoderm induction, suggesting the Fs2 domain contains the main epitope for activin binding. The unique N-terminal Fs0 domain, as well as the Fs3 domain, appear dispensable for activin inhibition in this analysis.

4.2 Crystal structure of the activin-Fs12 complex

The functional analysis in the *Xenopus* animal cap system suggesting Fs2 as an important site for activin binding is in agreement with the crystal structure of the activin-Fs12 complex. This structural analysis was performed by our collaborators as stated at the beginning of this chapter, and is briefly summarised

here for the sake of completion.

4.2.1 Formation of activin-follistatin complexes

To confirm direct binding between particular follistatin domains and activin, and hence to determine if the inhibition is by direct association, complex formation between the proteins was determined by analytical gel filtration. The solubility of activin A is poor in aqueous buffers, but under these conditions after incubation with Fs12 or Fs123 before column loading, a complex corresponding to activin and the associated follistatin fragment is observed. This is not the case with any other follistatin fragments, including Fs2, suggesting Fs2 is important for binding to activin, but Fs1 is also required for formation of a stable complex, in agreement with the *Xenopus* functional analysis. This gel filtration analysis in combination with subsequent nondissociative mass spectrometry shows the stoichiometry of the activin-Fs12 complex is 1:2 (one activin dimer to two follistatin fragments).

4.2.2 Activin A-Fs12 structure

Figure 4.3A demonstrates the activin-Fs12 structure, which was solved to 2 Å resolution. The follistatin Fs12 fragments wrap around the convex outer surfaces of the activin protomers. Each Fs12 fragment only interacts with one activin protomer and there are no contacts between the two Fs12 fragments. The binding site on activin for Fs12 almost exactly overlaps the binding site for the activin type II receptor [Greenwald et al., 2004].

A potential key residue emerged from the activin-Fs12 structure, located at the edge of the binding area. The residue is arginine 192 (R192), located in the Fs2 domain. Figure 4.3B shows this area in closer detail. The R192 residue is inserted between the ‘fingertips’ of activin, and forms part of a hydrogen bonding network with surrounding residues. This R192 residue is conserved between all forms of follistatin and the follistatin related protein, FSRP/FSL-3 [Schneyer et al., 2001]. This particular region containing the R192 residue is also the most highly conserved region between the follistatins, further emphasising its critical role in activin binding.

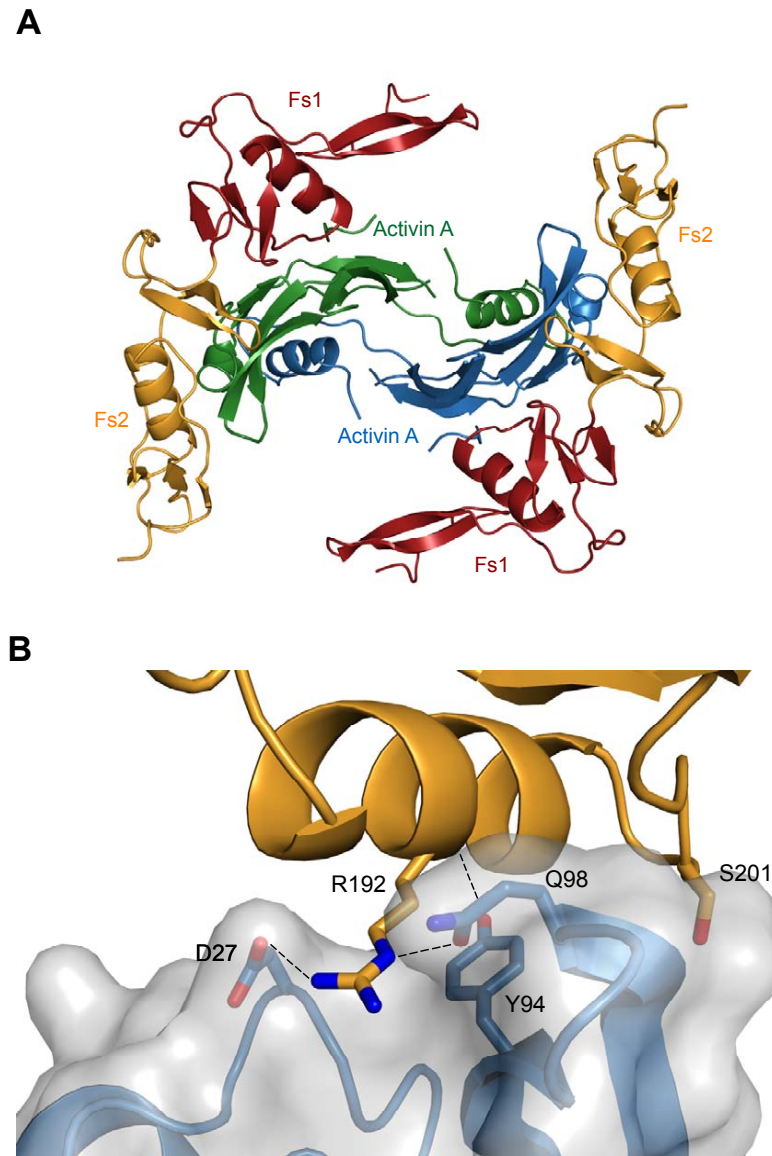


Figure 4.3: **Overall architecture of the activin-Fs12 complex**
(A) View down the two-fold axis of symmetry showing the two follistatin fragments binding to the back of the activin A fingers. Activin protomers are shown in green and blue. Follistatin domains Fs1 and Fs2 are shown in red and orange respectively **(B)** Detailed view of R192 'hook' of Fs2 (orange) interacting with activin A 'fingers' (blue).

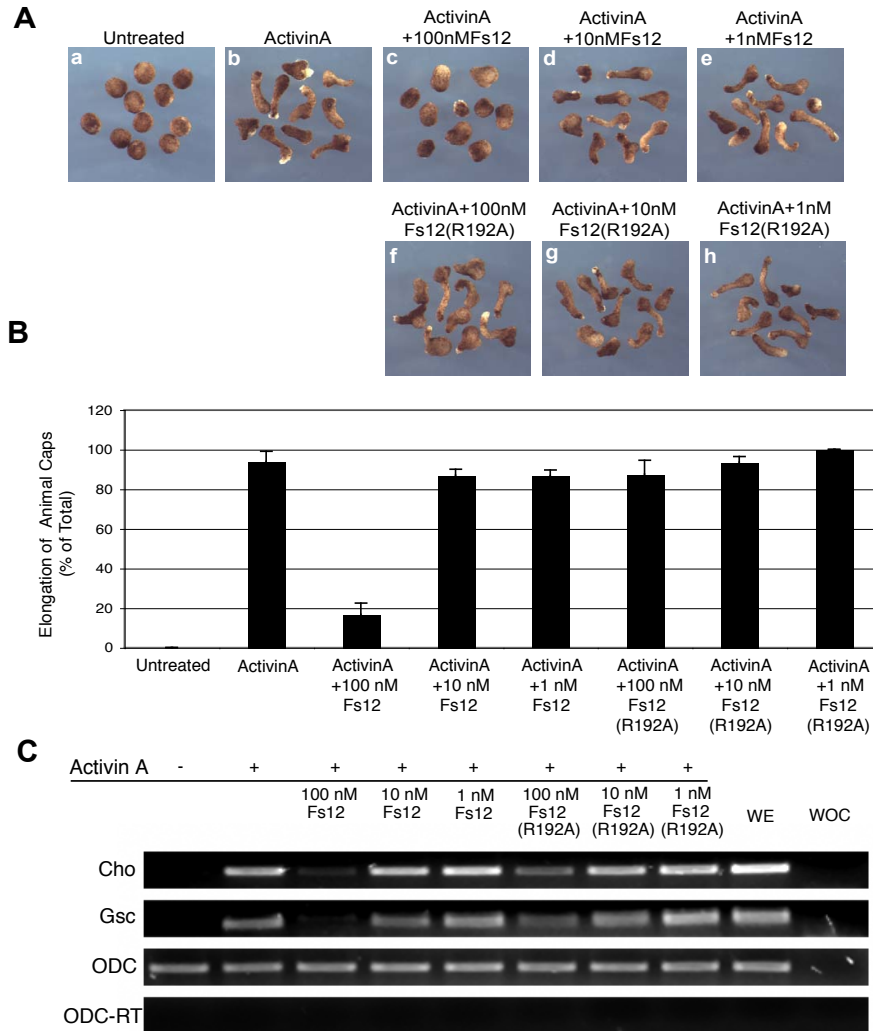


Figure 4.4: **Activity of R192A Fs12 mutant to inhibit activin A in *Xenopus* animal cap explants**

(A) Comparative phenotype response of *Xenopus* animal caps to activin A in the presence of wildtype versus mutant Fs12. (B) Quantification of phenotypic data shown in (A) pooled from several experiments. (C) Semiquantitative animal cap analysis of the effects of wildtype and mutant follistatin fragments on activin A-induced expression of the mesoderm markers *Chordin* (*Chd*) and *Goosecoid* (*Gsc*) in *Xenopus* animal caps. n is in the range of 40-50 for each data set.

4.3 Mutational analysis of the follistatin Fs12 domain, importance of R192

In order to test the hypothesis that the R192 residue is critical for activin binding by follistatin, mutational analysis was performed. The arginine residue at position 192 was mutated to alanine, and its ability to interact with and inhibit activin A studied. Analytical gel filtration demonstrated that the mutant Fs12 fails to form a stable complex with activin. This is supported by isothermal titration calorimetry data for affinity measurements, showing that no binding occurs between activin and Fs12(R192A).

In support of the biochemical analyses, the *Xenopus* embryo was again employed to test the functionality of the mutant Fs12. Figure 4.4A shows animal cap explants treated with wildtype versus mutant Fs12 in the presence or absence of activin. The concentration of follistatin fragments were titrated from 100nM to 1nM to identify differences in activity between the wildtype and mutant proteins. Almost all caps, (over 90%), Figure 4.4B), elongate in response to treatment with 30U activin. This response to activin is inhibited by the addition of 100nM wildtype Fs12. In contrast to this, addition of 100nM Fs12 mutant (R192A) does not result in a significant decrease in the number of caps elongating in response to activin treatment. No significant differences are observed at lower doses of Fs12 fragments applied.

In addition to the above phenotypic analysis, semiquantitative RT-PCR was performed to confirm the findings. Figure 4.4C shows induction of *Chd* and *Gsc* expression in response to treatment with 30U activin, compared to the untreated control. This induction of mesodermal marker expression is inhibited by the addition of 100nM wildtype Fs12. In contrast to this, addition of 100nM Fs12(R192A) mutant clearly demonstrates diminished inhibition of activin. This data in combination with the phenotypic, biochemical and structural analysis suggests that the R192 residue on the Fs2 domain of follistatin is indeed a critical residue for follistatin binding to activin, as shown by the loss of function when the Fs2 domain is absent from follistatin, and also when the R192 residue from Fs2 is absent.

Part IV

Results II: TSK, a novel regulator of the TGF- β superfamily

Chapter 5

TSK features and expression

5.1 Features of Tsukushi, a novel secreted protein

5.1.1 TSK sequence analysis and orthologues

Chick TSK (C-TSK) was identified by signal sequence trap screening [Klein et al., 1996] as coding for a 369 amino acid protein. At present, orthologues of TSK have been identified in 13 organisms. These are covered in table 5.1.1 along with variants and length in number of amino acid residues. The significance of the chick and *Xenopus* TSK variants will be discussed shortly.

Analysis of the aligned TSK sequences in figure 5.2 (upper 16 sequences) reveals 12 leucine rich repeats (LRRs) within every TSK sequence identified thus far. These sequences have been identified in Ensembl and NCBI database searches, the database references of which are shown in table 5.1.1 below. The LRRs are located between two cysteine clusters, at the N- and C-termini. Each individual LRR of TSK consists of 21-26 amino acid residues with the consensus ‘XXLXXXXFXLXXLXXLXLXXNXL’. The N-terminal cysteine cluster has the C-X₃-C-X-C-X₁₇-C pattern. In addition to this, there are potential sites of glycosaminoglycan (GAG) attachment (Ser-Gly consensus) and N-glycosylation (Asn-X-Ser/Thr consensus)(Figure 5.1).

These features of TSK, i.e. LRRs, cysteine clusters and sites for potential carbohydrate posttranslational modifications, identify TSK as a new member of the small leucine rich repeat proteoglycan (SLRP) family (reviewed by Hocking et al. [1998], Iozzo [1997]). Figure 5.2, shows an alignment of all currently identified SLRP family members from *H.sapiens*, including H-TSK (lower 13

Table 5.1: TSK orthologues

TSK orthologue	Residue length	Ensembl ID
<i>Gallus gallus</i> C-TSK-A	369	ENSGALG00000000761
<i>Gallus gallus</i> C-TSK-B	352	AB195969.1(NCBI)
<i>Xenopus laevis</i> X-TSK-B1	351	AB176536.1(NCBI)
<i>Xenopus laevis</i> X-TSK-B2	351	AB176537.1(NCBI)
<i>Xenopus tropicalis</i> TSK	350	ENSXETG00000019449
<i>Danio rerio</i> TSK	347	ENSDARG00000040815
<i>Fugu rubripes</i> TSK	348	NEWSINFRUG00000153817
<i>Tetraodon nigris</i> TSK	333	GSTENG00010533001
<i>Bos taurus</i> TSK	376	ENSBTAG00000001537
<i>Rattus norvegicus</i> TSK	353	ENSRNOG00000027784
<i>Mus musculus</i> TSK-A	354	ENSMUSP00000057071
<i>Mus musculus</i> TSK-B	354	ENSMUSP00000091713
<i>Canis familiaris</i> TSK	361	ENSCAFG00000005203
<i>Macaca mulatta</i> TSK	353	ENSMMUG00000008443
<i>Pan troglodytes</i> TSK	353	ENSPTRG00000004095
<i>Homo sapiens</i> TSK	353	ENSG00000182704

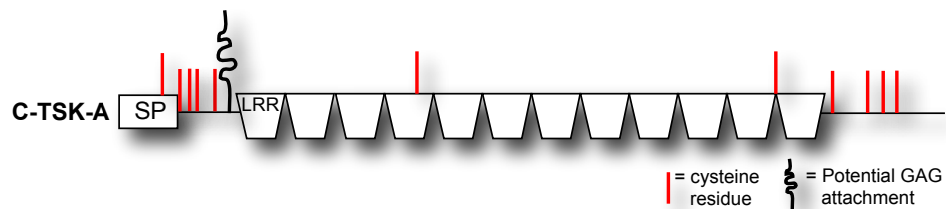


Figure 5.1: **Features of C-TSK-A identified from the amino acid sequence**

Features of C-TSK-A as identified from the amino acid sequence. SP: Signal peptide, LRR: Leucine rich repeat, GAG: Glycosaminoglycan.

sequences).

5.1.2 TSK is a new member of the Small Leucine Rich Repeat Proteoglycan family

The SLRP family currently comprises of 12 related members. Four classes have so far been identified, based upon protein conservation, N-terminal cysteine-rich cluster and number of LRRs. The initially identified member of the SLRP family, decorin, is 359 amino acids in length and has 10 LRR repeats flanked by N- and C-terminal cysteine rich clusters [Krusius and Ruoslahti, 1986]. In the phylogenetic tree of figure 5.3A, decorin is placed in class I of the SLRP family, along with biglycan [Fisher et al., 1989] and asporin [Lorenzo et al., 2001], by virtue of their unique N-terminal cysteine cluster consensus: 'CX₃CXCX₆C'. Class I SLRPs contain a pro-peptide and a N-terminal domain that is usually substituted with one or two chondroitin/dermatan sulphate side chains. SLRPs are all secreted proteins as has also been previously confirmed with TSK, whereupon after transient transfection into COS-7 cells, secreted TSK is detected in the cell supernatant [Ohta et al., 2004].

In each subfamily within the SLRP family, the N-terminal cysteine-rich cluster consensus is conserved. Class II, including fibromodulin [Oldberg et al., 1989], lumican [Blochberger et al., 1992], keratocan [Corpuz et al., 1996], PRELP [Bengtsson et al., 1995] and osteoadherin [Wendel et al., 1998] contain the consensus 'CX₃CXCX₉C'. These class II family members are primarily substituted with keratan sulphate chains and also contain 10 LRRs. Belonging to Class III are mimecan [Bentz et al., 1989] and opticin [Reardon et al., 2000], based upon the 'CX₂CXCX₆C' unique cysteine rich cluster and the presence of only 6 LRRs. The three remaining members, Tsukushi, Nyctalopin [Bech-Hansen et al., 2000] and Chondroadherin [Neame et al., 1994] do not fall into any of the existing classes due to unique N-terminal cysteine clusters; 'C-X₃-C-X-C-X₁₇-C', 'C-X₃-C-X₃-C-X₈CX₃-C' and 'C-X₃-C-X-C-X₈-C' respectively. Thus TSK falls into a new branch of the family, although based on sequence homology alone, appears to be most closely related to nyctalopin (Figure 5.3).

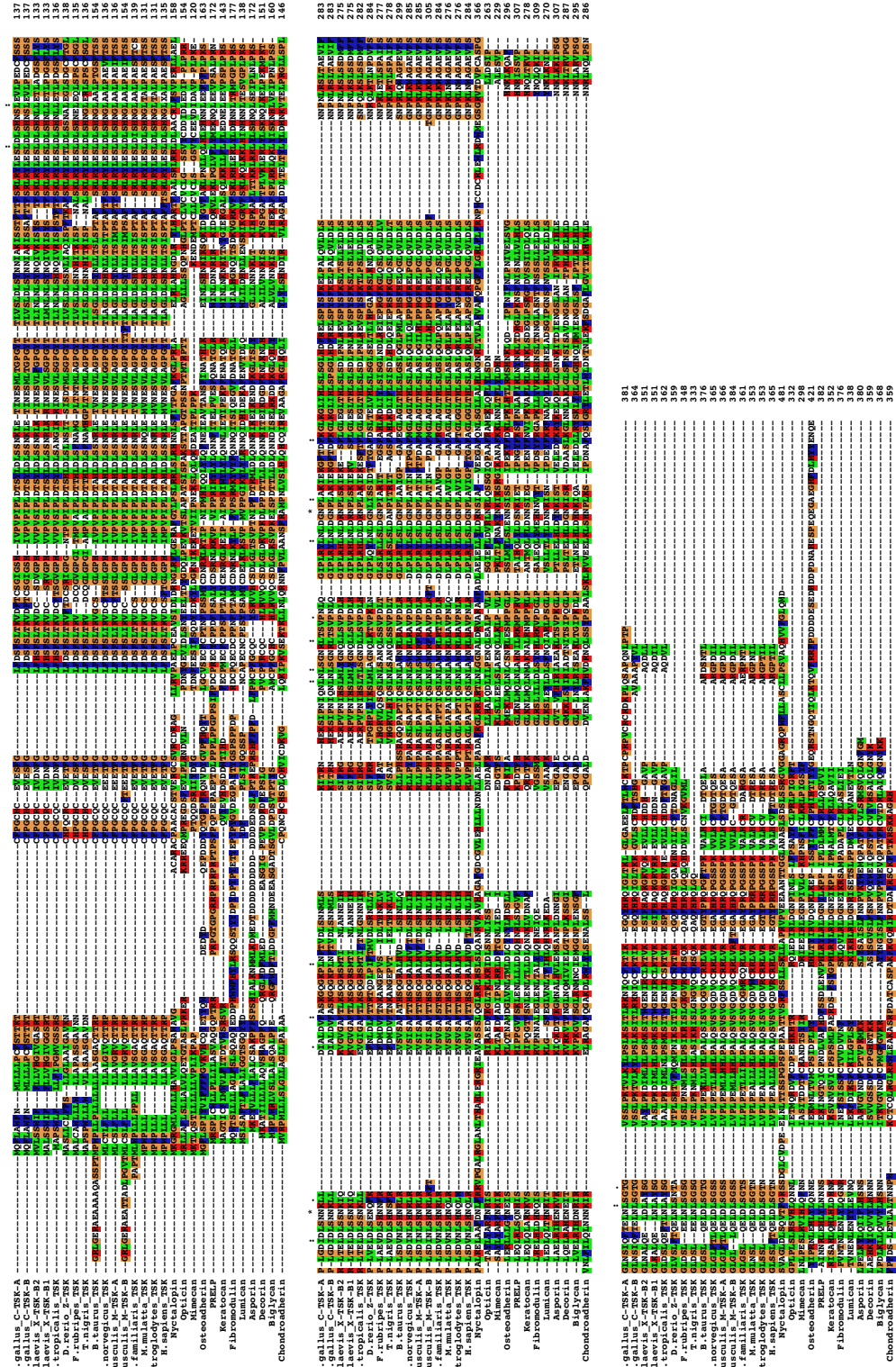


Figure 5.2: Multiple sequence alignment of TSKs and SLRPs
 Alignment of identified TSK sequences (upper 16 sequences) against other known SLRP sequences from H.sapiens (lower 12 sequences). Orange (GPST), Red (HKR), Blue (FWY), Green (ILMV).

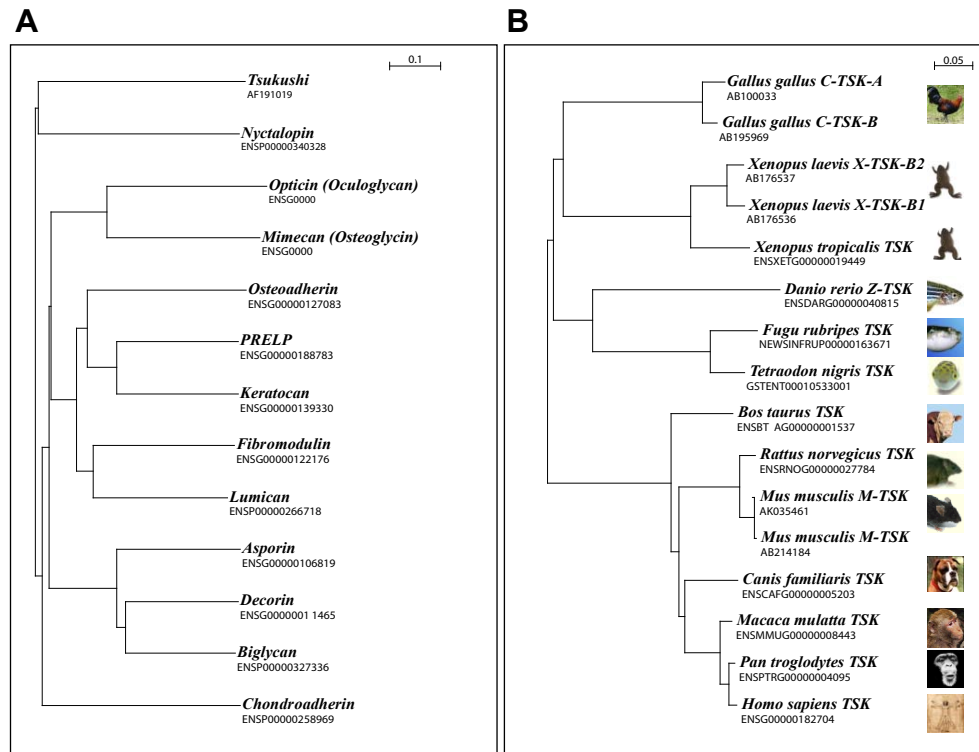


Figure 5.3: **Phylogenetic trees of SLRPs and TSKs**
(A) Phylogenetic tree of *H.sapiens* SLRPs, including TSK (left panel). **(B)** Phylogenetic tree of TSK from the indicated species. Underlying texts refer to Ensembl/NCBI database references.

5.1.3 TSK is post-translationally modified with addition of N-linked carbohydrates

Upon expression of mRNA for 6-myc tagged *C-TSK-A* or *X-TSK-B1* in *Xenopus* embryos, several specific bands are detected by Western blotting (see Figure 5.4).

Sizes of TSKs are predicted at 40.7kDa for C-TSK-A and 39kDa for X-TSK-B1 (Predicted using the Protparam programme, ExPASy, <http://www.expasy.ch/tools/protparam.html>) In the case of C-TSK-A, three distinct bands are detected, ranging from around 45 to 49 kDa in size. Similarly, for X-TSK, three bands are also evident, but running at a smaller size range, from around 40 to 45 kDa. The presence of several bands suggests both chick and *Xenopus* forms of TSK are being post-translationally modified

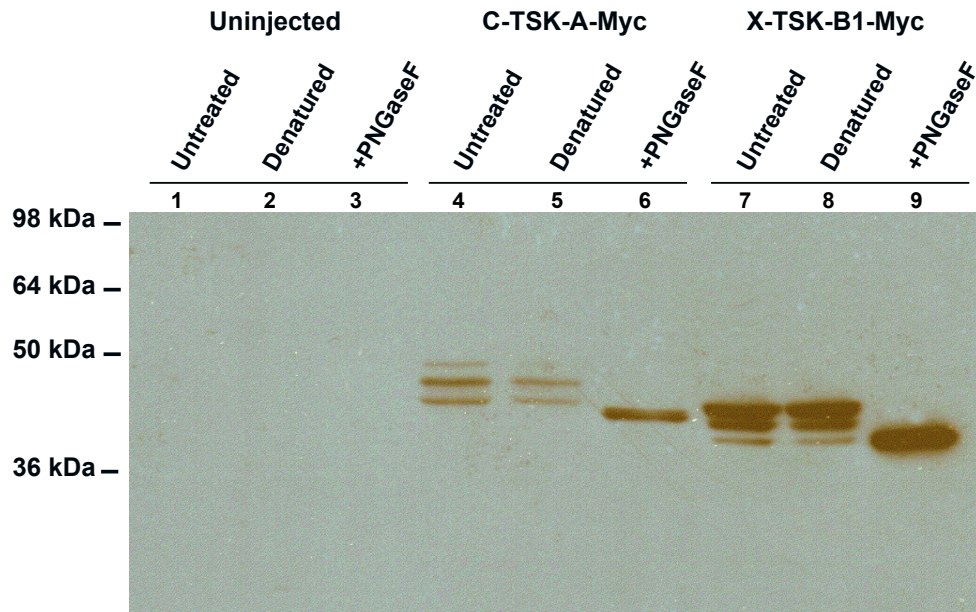


Figure 5.4: **Removal of N-linked carbohydrates from C-TSK-A and X-TSK-B1**

Treatment of 6-myc-tagged *C-TSK-A* and *X-TSK-B1* microinjected embryo lysate with PNGaseF in order to remove N-linked carbohydrates. Uninjected embryos (lanes 1, 2, 3). C-TSK-A-Myc (lanes 4, 5, 6). X-TSK-B1-Myc (lanes 7, 8, 9). Untreated lysates (lanes 1, 4, 7). Denatured lysates, no PNGaseF treatment (lanes 2, 5, 8). Denatured and PNGaseF treated lysates (lanes 3, 6, 9).

in *Xenopus*. This possibility was explored by treating lysates of injected embryos with PNGaseF, an enzyme which digests N-linked oligosaccharides from the main polypeptide chain. Upon treatment with PNGaseF the previously detected multiple bands collapse into a single band. This suggests that TSK is differentially modified in several specific manners, although after PNGaseF treatment the size of TSKs are comparable to the predicted sizes, indicating that there may be no GAG modifications in these conditions. Differential modification of SLRP family members is not unusual, with different forms of decorin previously reported [Blochberger et al., 1992].

5.1.4 Chick TSK and *Xenopus* TSK have some functional differences and differ in their C-termini compositions

In *Xenopus* ventral marginal zone explants and animal cap explants, expression of *C-TSK-A* is able to dorsalise mesoderm and directly induce neural tissue respectively [Ohta et al., 2004]. X-TSK has the same dorsalising and neuralising activity when overexpressed in *Xenopus* ventral or animal explants respectively [Kuriyama et al., 2006]. In the alignments of TSK orthologues (Figure 5.2) there are two different forms of C-TSK which have been identified, referred to as C-TSK-A and C-TSK-B. These two forms of C-TSK are produced by alternate splicing, and differ in that the A form of chick TSK has a longer C-terminal region with an additional 3 cysteine residues. The functional significance of this is not yet fully understood. These cysteine residues in the extended C-terminal region are absent from the chick B form of TSK (See figure 5.5A).

Xenopus also has two different forms of TSK. These forms, represented in figure 5.5A, show most homology to the chick TSK B form, and hence are referred to X-TSK-B1 and X-TSK-B2. So far, no A form of TSK has been identified in *Xenopus* or any other organisms. Chick appears to be unique in this respect. The two X-TSK forms are highly homologous, their differences localised to several amino acid substitutions throughout the sequence. The functional analysis performed in Kuriyama et al. [2006] was based upon the X-TSK-B1 form first identified. Subsequent functional analysis performed with the latter identified X-TSK-B2 has not shown any functional difference to that of X-TSK-B1 (Kunimasa Ohta, unpublished data). The sequence alignments and phylogenetic tree in figure 5.3B show that *Xenopus laevis* and *Xenopus tropicalis* TSK sequences are most closely related to chick TSK sequences.

5.1.5 Primary structure of TSK may be directly comparable to that of decorin

The LRRs of SLRP family members, including TSK, are a common structural feature of many proteins. At present, the LRR motif has been identified in more than 100 proteins, of widely varying function. Figure 5.5B shows the predicted structure of a TSK monomer, based upon the presence of 12 LRRs in the TSK

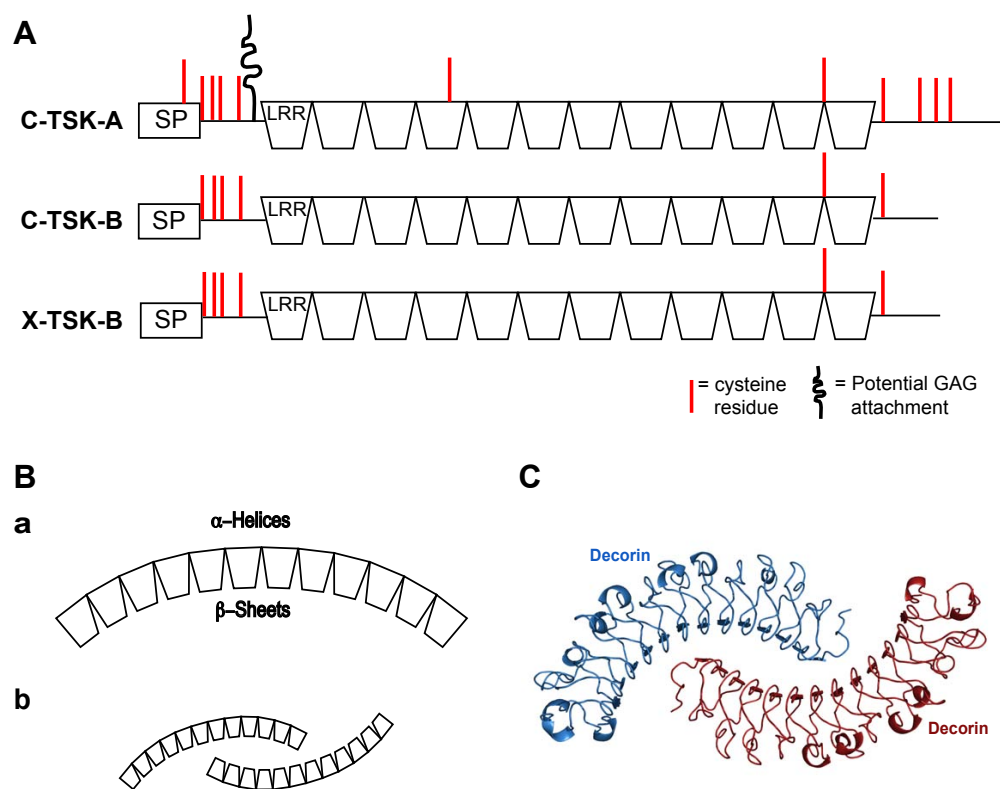


Figure 5.5: **Primary structure of TSK and SLRP family member, Decorin**

(A) Comparison of primary structure of C-TSK-A, C-TSK-B and X-TSK-B. SP: Signal Peptide. LRR: Leucine Rich Repeat. (Ba) Predicted structure of TSK monomer with packing of alpha helices. (Bb) Predicted structure of TSK dimers. (C) Solved structure of Decorin, the initially identified member of the SLRP family.

sequence. It is expected that on the concave surface of the protein lies the parallel β -sheets of each LRR repeat. On the convex surface of the monomer, the α helices (and other secondary structures) are expected to be situated. Due to the tighter packing of β sheets in comparison to the ‘splayed’ α helices, this will create a curvature of the monomer as the LRRs are situated adjacent to one another. This is termed a ‘curved solenoid fold’. In addition to this, TSK may form dimers in solution by binding via the concave surfaces, as has been reported for decorin [Scott et al., 2004] and biglycan [Scott et al., 2006].

This possible structure of TSK is supported by the crystal structures of

decorin and biglycan, which have been solved, [Scott et al., 2004, 2006] (Figure 5.5C). As expected for a protein with numerous LRRs, the parallel β sheet on the interior of the protein with the alpha helices on the outside create the curved solenoid fold. Decorin dimerises through these concave surfaces, with a great amount of surface buried between the two monomers. Previous structures of LRR-containing proteins such as RNaseA [Kobe and Deisenhofer, 1993] have revealed a ‘horseshoe’ shape to the curvature of the protein. The SLRPs are unique in this respect, forming more of a ‘banana’ shape and thus potentially leaving the C-termini of the monomers free to interact with other ligands.

5.2 *TSK* expression pattern

To look at the function of **X-TSK-B1**¹ in *Xenopus laevis* embryogenesis, the spatial and temporal expression pattern was examined by *in situ* hybridisation of whole embryos, sectioned embryos and semi-quantitative RT-PCR analysis of *TSK* mRNA levels.

5.2.1 *TSK* is expressed zygotically in the dorsal mesoderm and endoderm, in addition to maternal and zygotic expression in the ectoderm.

Figure 5.6 shows whole mount *in situ* hybridisation of *X-TSK* in *Xenopus* embryos from blastula stages through gastrula, neurula and tailbud stages to late embryogenesis. At stage 8, blastula (Panel a), *TSK* is expressed in the animal hemisphere and excluded from the vegetal hemisphere. At this stage, no differences in expression can be detected between the ventral and dorsal sides of the embryo. In early gastrula stages (stage 10, appearance of the dorsal blastopore lip), expression of *TSK* extends from the animal pole, to the dorsal blastopore lip (Panels b,c) but remains diminished in ventral and lateral marginal zone (d). Faint, punctate staining is observed in the vegetal region (b).

Expression of *TSK* in the dorsal blastopore lip is detected in the early gastrula, stage 10. By stage 10.5, when the blastopore has fully formed, *TSK*

¹For the functional analysis of TSK in this study, X-TSK-B1 was used. Therefore, any reference to X-TSK will refer to B1 form.

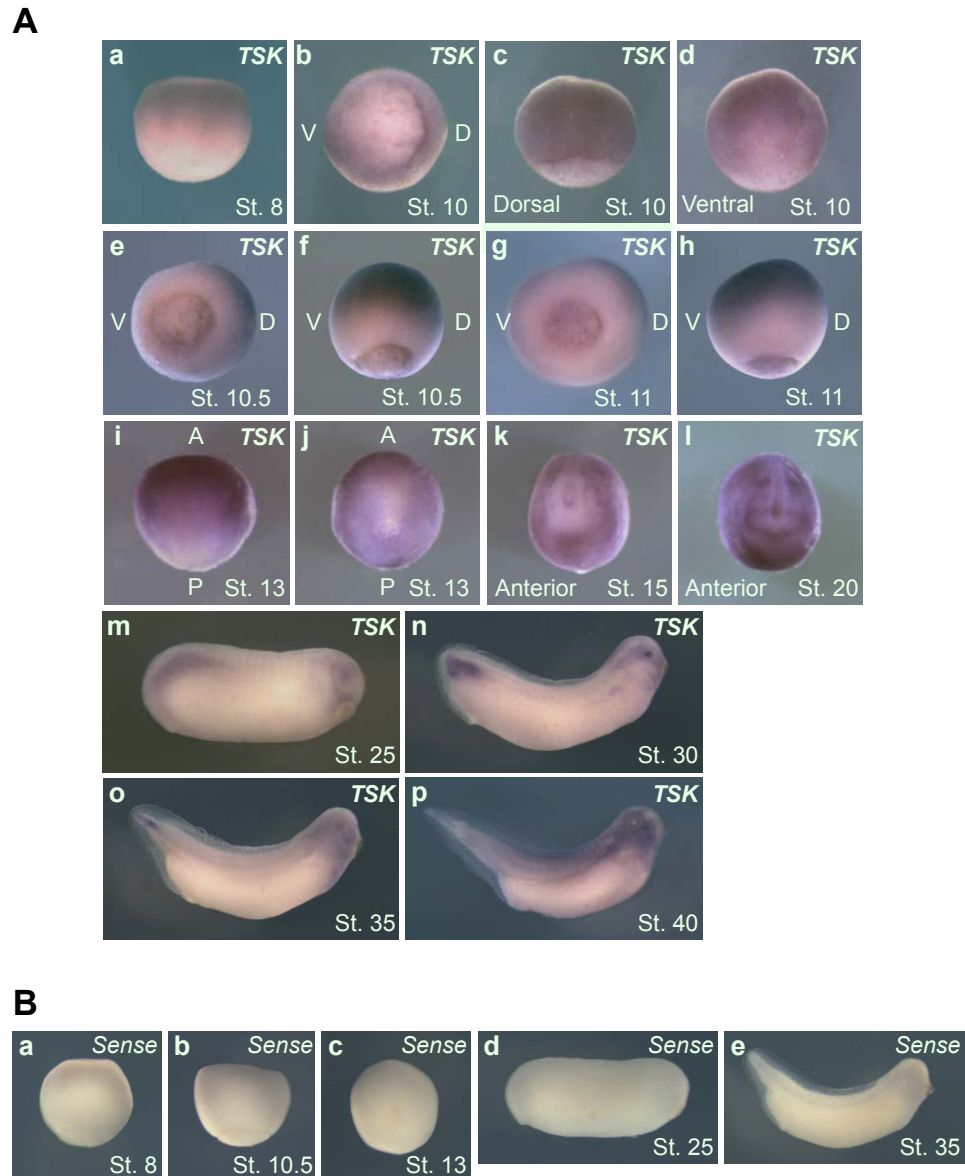


Figure 5.6: **Endogenous *TSK* mRNA expression in *Xenopus laevis* embryos**

(A) Whole mount *in situ* hybridisation of *Xenopus* embryos, stages as indicated with antisense *TSK* probe. Orientations as indicated (D: Dorsal, V: Ventral, A: Anterior, P: Posterior). Panels m, n, o, p: Anterior, right. Posterior, left. (B) Control whole mount *in situ* hybridisation with *TSK* sense probe.

expression levels are elevated within the blastopore itself (e, f). At this stage, expression is still strong in the animal hemisphere. This expression pattern is evident through to stage 11 (g, h). At stage 13, *TSK* expression is localised to the presumptive epidermal region. At stage 15, expression is localised to the anterior neural plate folds and outside the neural plate. At stage 25, *TSK* is expressed in the mandibular neural crest. Figure 5.6B shows *in situ* hybridisation of *Xenopus* embryos of selected stages with sense *TSK* probe. No significant staining is observed with the sense probe, demonstrating the *TSK* expression pattern in (A) is specific.

The whole mount *in situ* hybridisation of *TSK* in *Xenopus* embryos, in blastula and gastrula stages, shows expression in the endoderm, ectoderm and dorsal mesoderm with far lower levels detected in the lateral and ventral mesoderm. This data suggests that *TSK* may play a role in patterning the embryo with respect to germ layer formation at these early stages. Later expression in the neural region is consistent with published data, demonstrating a role for *TSK* in neural crest formation [Kuriyama et al., 2006] as discussed in the introduction.

5.2.2 *TSK* expression pattern in sectioned embryos, *TSK* is expressed in endoderm from early gastrula stages

In order to analyse the expression pattern of *TSK* in further detail, *in situ* hybridisation for *TSK* was carried out on sectioned embryos from stages 7 to 13, as these stages proved to be of most interest from the *TSK* expression pattern in whole embryos.

For comparison, Figure 5.7B shows expression of the pan-mesoderm marker *Xbrachury* (*Xbra*, panel a), the dorsal mesoderm marker *Goosecoid* (*Gsc*, panel b) and the endoderm marker, (*Sox17 α* panel c). *Xbra* is expressed around the blastopore in presumptive mesodermal cells. *Xbra* expression is an immediate-early response to mesoderm induction and in response to the mesoderm inducing factors, activin A and basic FGF [Smith et al., 1991]. Expression of *Xbra* is sufficient to induce development of mesodermal tissues in cells of the early embryo [Cunliffe and Smith, 1992]. Specifically, *Xbra* is a transcriptional acti-

vator required for posterior mesoderm formation and axial development. *Xbra* functions to activate mesoderm-specific gene transcription, and its loss results in defects of mesodermal patterning [Conlon et al., 1996].

Gsc was identified as a homeobox gene expressed in the organizer region with the ability to induce a complete secondary axis [Cho et al., 1991]. *Gsc* expression is detected before the dorsal blastopore lip forms and was thus proposed to be an important component of organizer formation [Robertis et al., 1992]. Loss of goosecoid function with antisense depletion ventralises mesodermal tissue, confirming the importance of goosecoid for dorsal patterning [Steinbeisser et al., 1995]. In contrast to *Xbra*, *Gsc* expression is not impaired by inhibition of FGF signalling [Amaya et al., 1993]. Interestingly, *Gsc* can repress expression of *Xbra* [Artinger et al., 1997, Latinkic and Smith, 1999].

GATA4, localised to endodermal derivatives, is one of six members belonging to the family of transcription factors, called the GATA factors [Patient and McGhee, 2002]. *GATA4* is first expressed in the endoderm, just prior to gastrulation [Afouda et al., 2005]. Antisense depletion of *GATA4* inhibits activin mediated induction of the endodermal markers, *Sox17 α* and *HNF1 β* [Afouda et al., 2005]. *Sox17 α* is a transcription factor also expressed in the gastrula presumptive endoderm whose ectopic expression induces endoderm gene expression in animal caps [Hudson et al., 1997]. Engleka et al. [2001] found that *Sox17 α* misexpression in the marginal zone prevents induction of *Xbra* and *MyoD* and thus is important for distinction between the endoderm and mesoderm.

Figure 5.7A, Panels a, b and c show *TSK* expression in sectioned blastula stage embryos (Stages 7, 8 and 9 respectively). *TSK* is strongly expressed in the ectoderm, in agreement with the whole mount expression pattern. This expression is clear from stage 7, pre-MBT, and is therefore maternal. During blastula stages, no *TSK* expression is detected in the vegetal region.

At early gastrula stages, 10 and 10.5 (Figure 5.7A, panels d and e respectively), the vegetal expression of *TSK* appears more uniform in intensity and reaches from beneath the blastocoel to the vegetal pole. At stage 10, the dor-

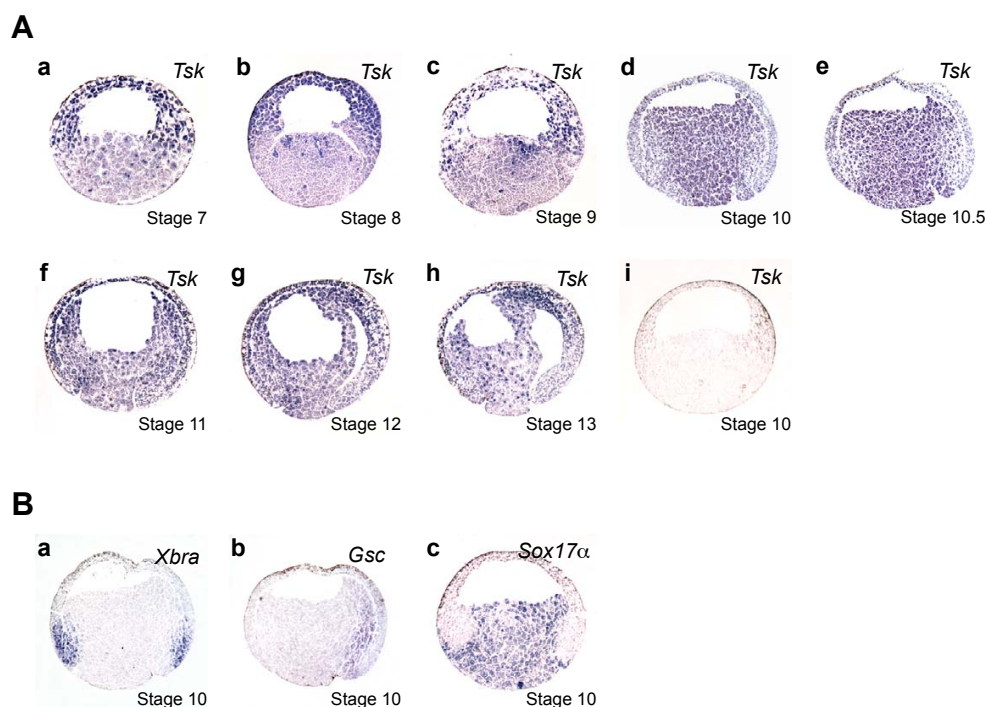


Figure 5.7: **Endogenous TSK mRNA expression in sectioned *Xenopus laevis* embryos**

(A) *in situ* hybridisation of sectioned *Xenopus* embryos, stages indicated with antisense *TSK* probe. (i) Control *in situ* hybridisation with *TSK* sense probe. (B) Endogenous expression of the pan-mesoderm marker, *Xbra*, dorsal mesoderm marker *Gsc*, and endoderm marker, *Sox17α*.

sal blastopore lip is evident, as marked on panel d. *TSK* expression is seen in the mesodermal region, slightly beyond the dorsal blastopore lip, in agreement with the whole mount expression pattern at the same stage. At later gastrula stages, 11, 12 and 13 (panels f, g and h), the blastopore is becoming progressively smaller and *TSK* expression does not appear as pronounced in this area. At stages 12 and 13, formation of the archenteron is evident as cells invaginate through the blastopore and move under the ectoderm. At these stages, *TSK* expression appears to be strongest in the region where the migrating anterior dorsal mesoderm cells meet the cells of the ectoderm. To show these stainings for *TSK* expression are specific, a control with sense *TSK* probe is included at stage 10 (panel i) and shows no specific staining.

The expression pattern of *TSK* in sectioned embryos is in agreement with the

whole mount *in situ* expression pattern for *TSK* in Figure 5.6. This confirms the presence of *TSK* expression throughout the vegetal hemisphere in early gastrula stages, after increasing from blastula stages. Expression is also confirmed in the ectoderm and diminished from the lateral and ventral mesoderm, further supporting a role for *TSK* in patterning of the germ layers at these early stages. In stage 10, early gastrula embryos. Comparison of these early gastrula embryos shows that expression of *Xbra* and *TSK* overlap in the dorsal mesoderm but not in the ventral mesoderm, whereas in the case of dorsal mesoderm at the blastopore lip periphery, *Gsc* and *TSK* expression do indeed overlap. Finally, staining of the endoderm with *Sox17a* overlaps with *TSK* expression at the same stage.

5.2.3 *TSK* mRNA expression levels peak during blastula and gastrula stages of development

To provide further confirmation of a role for *TSK* in patterning in the early embryo, expression levels of *TSK* in the whole embryo throughout development were comparatively analysed by semi-quantitative RT-PCR.

Expression levels of total *TSK* mRNA are shown in Figure 5.8A, from the egg to stage 40. *TSK* expression is detected in the egg (e), increasing in blastula stages (7, 8, 9). This expression is maintained in the early gastrula, stage 10, but then begins to decline as gastrulation proceeds (stages 10.5 to 13) and is present until stage 40 at lower levels. RT-PCR for the ODC ‘housekeeping’ gene product is included to control for relative levels of total RNA. An ODC control in the absence of reverse transcription (RT) is also included to demonstrate the absence of DNA contaminants in the original samples.

Expression levels of *TSK* throughout development as demonstrated in figure 5.8A show that *TSK* expression is present in the egg and highest throughout blastula and early gastrula stages. Expression before MBT at stage 8 is clear and indicates that *TSK* is maternally expressed. This further supports a possible role for *TSK* in early development, and in combination with spatial analysis of *TSK* expression, suggests this role may indeed lie in patterning of the germ layers. This window of elevated *TSK* expression temporally overlaps with *Vg1*

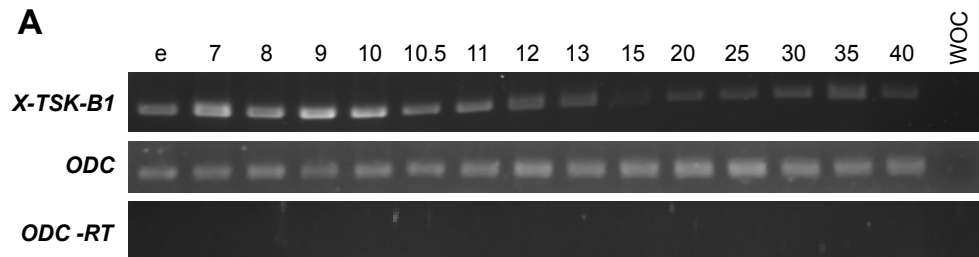


Figure 5.8: *TSK* mRNA expression in *Xenopus laevis* as measured by RT-PCR

(A) RT-PCR for *TSK* transcripts in *Xenopus laevis* at the indicated stages, including *ODC* (*Ornithine Decarboxylase*) control and -RT (no reverse transcriptase in the reaction) control.

expression in the early blastula [Weeks and Melton, 1987]. In addition to this, *TSK* expression also temporally overlaps with expression of *Xnrs* during development [Jones et al., 1995, Agius et al., 2000] in addition to the dorsal mesoderm marker *Gsc* [Robertis et al., 1992] and endoderm markers *GATAs* [Patient and McGhee, 2002] and *Sox17* [Hudson et al., 1997] and suggests *TSK* may play an important role in this regulatory network.

5.3 Gain-of-function analysis of *TSK* in early *Xenopus laevis* embryogenesis.

The spatial and temporal expression pattern of *TSK* suggested a potential role in patterning/formation of the early embryonic germ layers. *TSK* is expressed in the ectoderm, dorsal mesoderm and endoderm, but significantly diminished in the lateral and ventral mesoderm. To learn more about the function of *TSK* in these early stages, *TSK* was overexpressed in the mesoderm in a gain-of-function approach, covered in the following chapter.

Chapter 6

TSK gain-of-function analysis

6.1 Analysis of TSK function in *Xenopus laevis*

6.1.1 *TSK* overexpression in the ventral marginal zone does not result in secondary axis formation

As discussed in detail, above, chick has two forms of TSK, A and B, whilst *Xenopus* also has two forms, both similar to the chick B form, B1 and B2. Expression of C-TSK-A in the ventral marginal zone (VMZ) of *Xenopus* embryos results in secondary axis formation [Ohta et al., 2004] in around 30% of embryos injected (Figure 6.1Aa and B). In contrast to this, expression of C-TSK-B in the VMZ does not result in any secondary axis formation (Figure 6.1Ab). Similarly, overexpression of *X-TSK-B1* and *X-TSK-B2* does not produce secondary axes (Figure 6.1A c and d respectively).

Figure 6.1C summarises the primary structure differences between TSK orthologues. The main difference between the A and B TSK forms lies in the 3 extra cysteine residues in the C-terminal cysteine cluster in C-TSK-A. This may possibly account for the differences in secondary axis formation frequency in *Xenopus*, although this is only speculative at this stage. Even so, it is important to consider that X-TSK is unable to induce secondary axis formation, although still able to inhibit BMP and directly induce neural tissue [Kuriyama et al., 2006] when evaluating subsequent analyses of X-TSK behaviour in early embryogenesis.

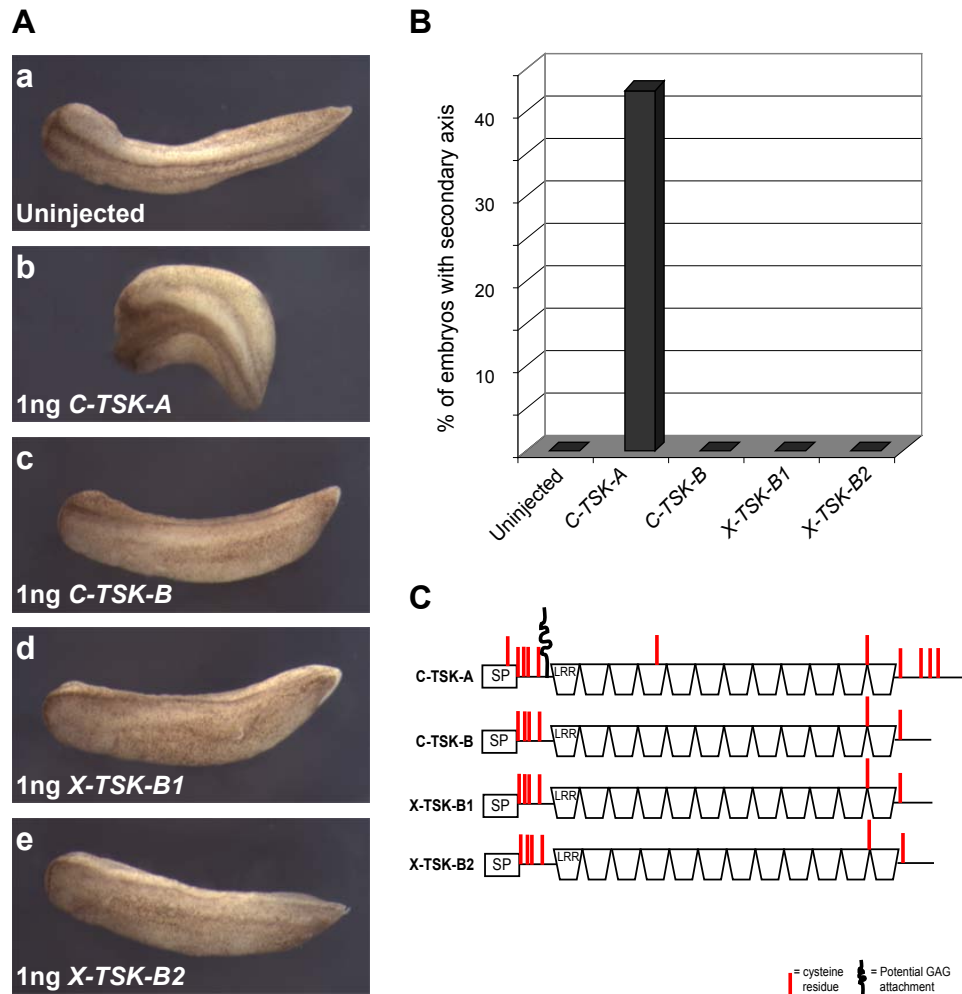


Figure 6.1: **Secondary axis formation by TSK orthologues in *Xenopus laevis***

(A) TSK orthologue microinjected embryos. *TSK* mRNA was targeted to the ventral marginal zone at the 8 cell stage. (B) Graphical representation of secondary axis formation frequency by TSK orthologues, n=45 to 50. (C) Summary of TSK orthologue primary structures.

6.1.2 Overexpression of *X-TSK* in *Xenopus* marginal zone inhibits pan-mesoderm marker expression whilst expanding expression of dorsal mesoderm and endoderm markers

To further explore a possible role for TSK in early embryonic patterning of the *Xenopus* embryo, the effect of *TSK* overexpression was analysed in the region of lowest *TSK* expression, the lateral and ventral marginal zone at stage 10.5. At this early stage of gastrulation when the blastopore has fully formed, strong expression of *Xbra*, *Gsc*, *Sox17 α* and *GATA4* is observed by *in situ* hybridisation. Thus any effect of *TSK* overexpression upon embryonic patterning may be reflected in distribution of these well-documented markers. 1ng of *X-TSK* was co-injected with 500pg β -Galactosidase¹ at the four-cell stage in the marginal zone. After incubation until stage 10.5, nuclear β -Gal staining was developed to identify correctly targeted marginal zone.

Figure 6.2 shows the effect of *TSK* overexpression within marginal zone, on expression of markers, *Xbra* (pan-mesoderm [Smith et al., 1991]), *Gsc* (dorsal mesoderm [Robertis et al., 1992]) and *Sox17 α* and *GATA4* (endoderm [Hudson et al., 1997, Afouda et al., 2005]). Normal expression of *Xbra* (Figure 6.2A panels a, b, c) is seen in a distinct band in the marginal zone around the blastopore, with expression of β -Gal having no effect upon this distribution. Upon overexpression of *TSK* though, *Xbra* expression is diminished in the targeted region (panels d, e and f). 65% of *TSK* injected embryos demonstrate this phenotype, as represented in Figure 6.2E. In contrast to this, expression of the organizer-specific marker, *Gsc* is expanded further around the dorsal blastopore lip (Figure 6.2C, panels d, e, f) upon *TSK* overexpression, in contrast to control β -Gal expressing embryos showing regular *Gsc* expression in a discrete area of the dorsal blastopore lip [Cho et al., 1991] (C, panels a,b,c). This expanded phenotype is observed in around 40% of *TSK* injected embryos, Figure 6.2E.

In addition to mesoderm markers, endoderm markers were also analysed by *in situ* hybridisation in *TSK*-injected embryos. Figure 6.2B (panels a,b,c) shows normal expression of *Sox17 α* in β -Gal injected embryos. *Sox17 α* expression is visible at low levels within the blastopore, displaying the highest levels

¹Any reference to β -Gal (Galactosidase) refers to the nucleus-targeted form of β -Gal

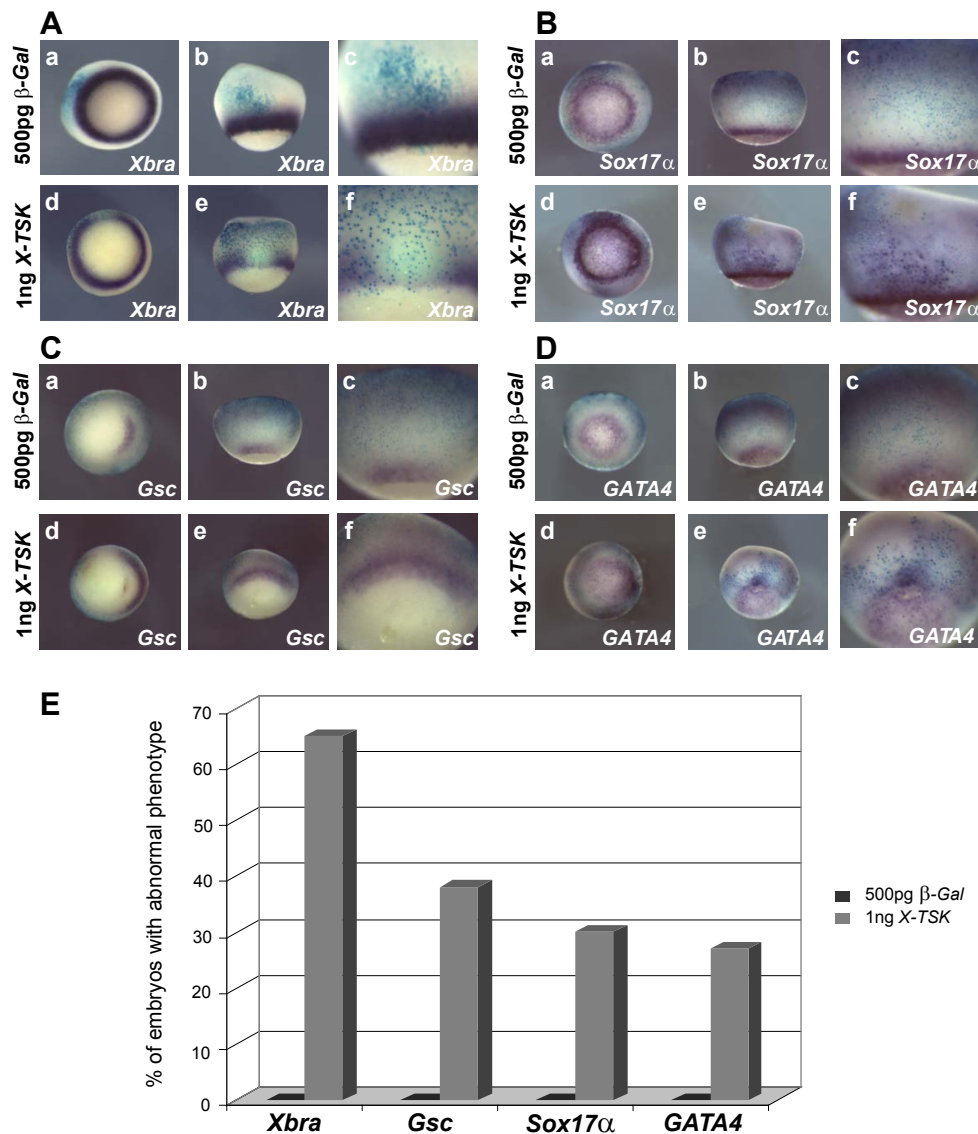


Figure 6.2: Overexpression of *TSK* in the marginal zone; analysis of mesoderm and endoderm marker expression

(A) *in situ* hybridisation with *Xbra* probe of *TSK* injected embryos. (B) As in A, with *Sox17 α* probe. (C) *Goosecoid* probe. (D) *GATA4* probe. All embryos were also coinjected and stained with β -Galactosidase to locate the targeted area (blue staining). Specific probe staining is purple. Orientation of embryos in each set of panels; (a,d) Vegetal view, dorsal right, ventral left. (b,c) Lateral view, animal top, vegetal bottom. (c, f) Zoom of lateral view. (E) Graphical representation of frequency of reported phenotypes. n = 100 to 120.

of expression at the blastopore periphery [Hudson et al., 1997]. This expression pattern appears to intensify in *TSK*-injected embryos, and in addition to this, slight expansion of *Sox17 α* expression is evident outside of the normal expression domain in the targeted area (Figure 6.2, panels d,e,f). This is also true in the case of an additional endoderm marker, *GATA4* which has a similar expression pattern as *Sox17 α* ([Afouda et al., 2005]) and expands similarly in *TSK*-injected embryos (Figure 6.2D, panels d,e,f). This endodermal marker expansion phenotype is present in around 30% and 25% of embryos for *Sox17 α* and *GATA4* respectively, Figure 6.2E.

6.1.3 TSK inhibition of the muscle marker, *MyoD*, is evident during gastrula and neurula stages

In addition to analysis of *Xbra* in early gastrulation, the effect of *TSK* overexpression upon a second marker, the myogenic regulatory factor, *MyoD*, was investigated. MyoD is a transcription factor, the earliest marker of muscle, expressed in gastrula stages in the presumptive muscle-forming region [Hopwood et al., 1989b, Steinbach et al., 1998]. Activin and FGF signalling can activate *MyoD* expression [Harvey, 1991], where eFGF is required for activation of *MyoD* expression in *Xenopus* [Fisher et al., 1989]. The most dorsal region of the marginal zone gives rise to notochord and the first muscle to develop arises from the lateral marginal zone [Dale and Slack, 1987], thus *MyoD* is expressed in both muscle and non-muscle precursors in the mesoderm [Frank and Harland, 1991].

Figure 6.4Aa shows normal expression of *MyoD* in stage 15 β -Gal expressing *Xenopus* embryos. *MyoD* is strongly expressed in two broad ‘stripes’ in the developing somites.² Embryos were injected at the 4-cell stage, into one animal-dorsal blastomere, with the intention to target only one side of the neural plate. Co-injection with β -Gal allowed for identification of correct targeting, and this approach also left one side of the neural plate uninjected, thus acting as an internal control. To look at differences in *MyoD* expression pattern, injected

²Somites: groups of cells that form just outside of and along the neural tube, and ultimately give rise to muscle and connective tissue.

sides were visually compared with the uninjected side. Overexpression of *TSK* results in a decrease in *MyoD* expression on the injected side in 25% of embryos (Figure 6.4A and B). This *TSK* inhibition of *MyoD* expression is also evident in the gastrula stage embryo (Figure 6.4). This is an interesting result as Zetser et al. [2001] have shown in *Xenopus* that inhibition of BMP signalling leads to activation of *MyoD* expression. In addition to BMP inhibition, MAPK activity is also required for muscle specific differentiation. This suggests that *TSK* may be functioning through a mechanism independent to its ability to antagonise BMP signalling.

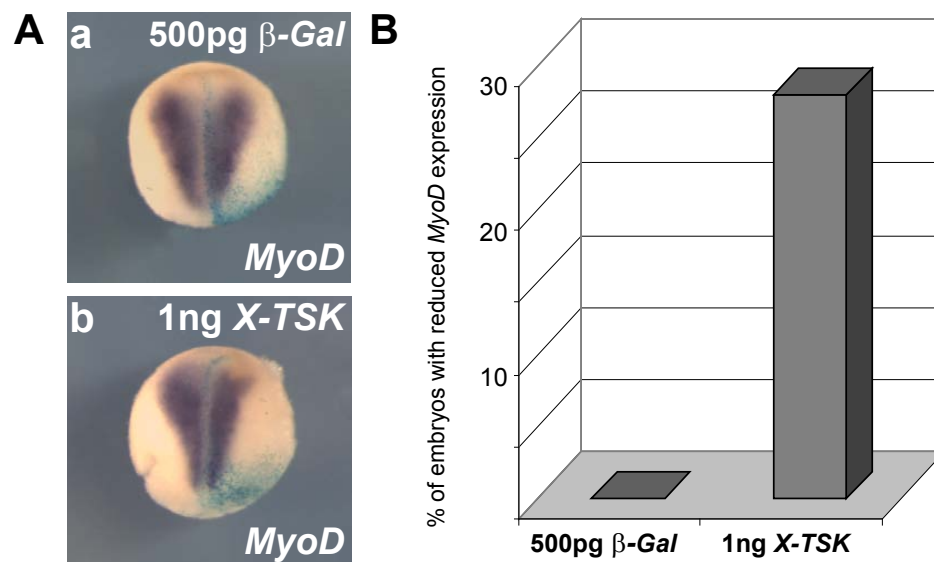


Figure 6.3: **Overexpression of *TSK* with analysis of the muscle marker, *MyoD* In neurula stages of development**

(A) *MyoD* expression in *TSK* injected embryos (b). Co-injection with β -Gal was also performed as a control (a) and to locate the targeted site. Orientation: anterior up, posterior down. (B) Graphical representation of *MyoD* areas of expression in injected embryos, n= 45 to 50.

This reduction of *MyoD* expression by *TSK* supports the inhibition of *Xbra* expression seen in Figure 6.2.

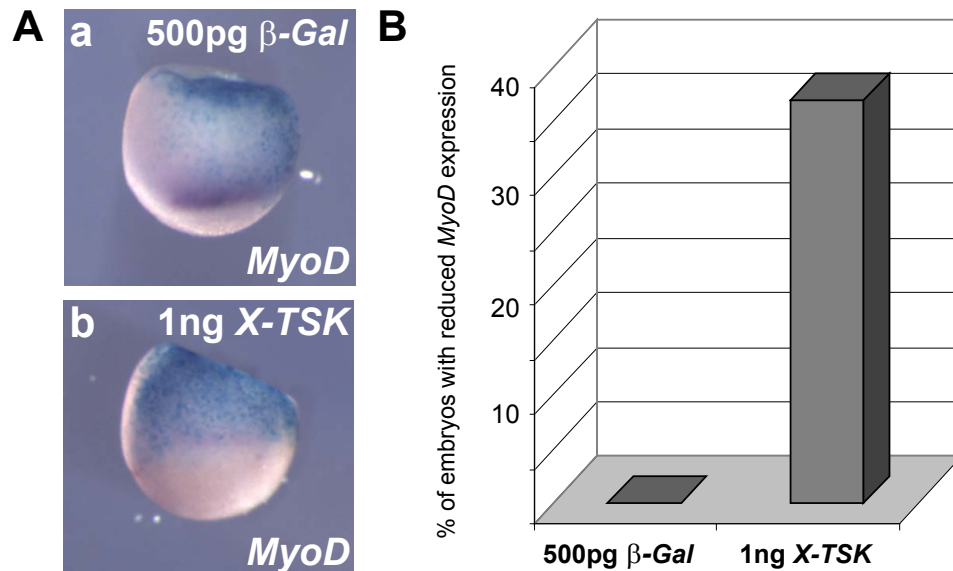


Figure 6.4: **Overexpression of *X-TSK* with analysis of the muscle marker, *MyoD* in gastrula stages of development** (A) *MyoD* expression in xTSK injected embryos (b). Co-injection with β -Gal was also performed as a control (a) and to locate the targeted site. Orientation: anterior up, posterior down. (B) Graphical representation of *MyoD* areas of expression in injected embryos, n=45 to 50.

6.2 Is the TSK gain-of-function phenotype explained by BMP inhibition?

TSK has been shown to be a BMP inhibitor, resulting in dorsalisation of mesoderm and direct neural induction [Ohta et al., 2004]. Can inhibition of mesoderm, activation of dorsal mesoderm and activation of endoderm gene expression be explained simply by the ability of TSK to inhibit BMP signalling in the *Xenopus* embryo?

6.2.1 BMP inhibition by chordin and truncated BMP receptor (tBR); effect on mesoderm and endoderm marker expression

Before analysis of gene expression in BMP activity-depleted embryos, titration of the dorsally expressed BMP inhibitor, Chordin, and a truncated BMP type I receptor, tBR [Graff et al., 1994, Suzuki et al., 1994] for induction of a sec-

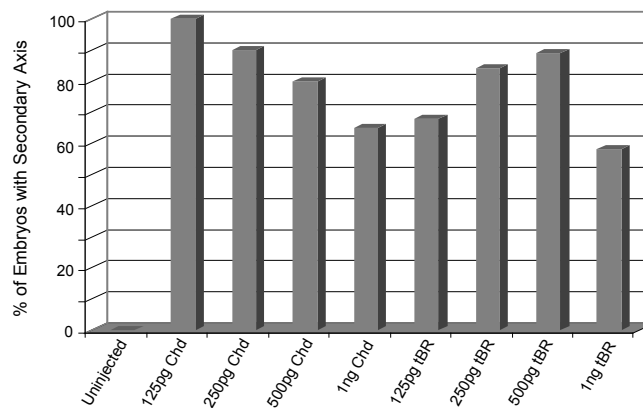
A**B**

Figure 6.5: **Titration of BMP inhibition by *chordin* or *tBR* mRNA levels required for secondary axis formation**

(A) Expression of *chordin* (125pg - 1ng, left column) and expression of *tBR* (125pg - 1ng, right column) in *Xenopus* ventral marginal zone with phenotypic analysis at tailbud stages. Orientation: anterior up, posterior down. (B) Graphical representation of secondary axis formation frequency by Chd and tBR, n = 80 to 90.

ondary axis was performed. Chordin has previously been shown by Sasai et al. [1994] to induce secondary axis formation. tBR is a type I BMP receptor, still able to specifically bind BMP ligands, although truncation of the intracellular domain results in no signal transduction, and hence acts as a dominant negative receptor.

To verify the mRNAs were functional and within an appropriate concentration range to induce secondary axis formation, microinjection of 125pg to 1ng *Chd* or *tBR* mRNA per embryo was performed. The ventral marginal zone was targeted by injecting the ventral vegetal blastomeres at the 8-cell stage. Figure 6.5 shows the resulting secondary axis formation after *Chd* and *tBR* expression. It is clear that both methods of BMP inhibition result in secondary axis formation over a range of concentrations (Figure 6.5A, B). In the case of *Chd*, the most efficient condition for secondary axis induction arises at 125pg, producing the reported phenotype in 100% of embryos injected. The optimum concentration is found at 250pg for *tBR*, with figures for both *Chd* and *tBR* in agreement with previous publications.

Figure 6.6 shows mesoderm and endoderm marker expression after injection of *Chd* and *tBR* RNAs at functional concentrations determined from titration as shown in Figure 6.5. Analysis was performed as above with TSK, with mRNAs for *Chd* and *tBR* targeted to the marginal zone, along with β -Gal to mark the targeted area. The upper three panels in 6.6 A, B and C show normal expression of *Xbra*, *Sox17 α* and *Gsc* respectively in β -Gal injected embryos. Expression of *tBR* (panels d, e and f in each case), results in perturbation of *Xbra* expression in 35% of injected embryos. This is a different phenotype to that seen upon *TSK* overexpression as *Xbra* expression appears to be expanded outside the normal boundaries after *tBR* expression. *Gsc* expression is slightly expanded in around 100% of cases, whilst expression of *Sox17 α* remains normal in the presence of *tBR*. *Chordin* overexpression (panels g, h and i in each case) does not result in changes of expression of *Xbra* and *Sox17 α* , relative to normal expression. As shown above, TSK overexpression results in inhibition of *Xbra*, expansion of *Gsc* and *Sox17 α* . These differential phenotypes between TSK and BMP inhibition

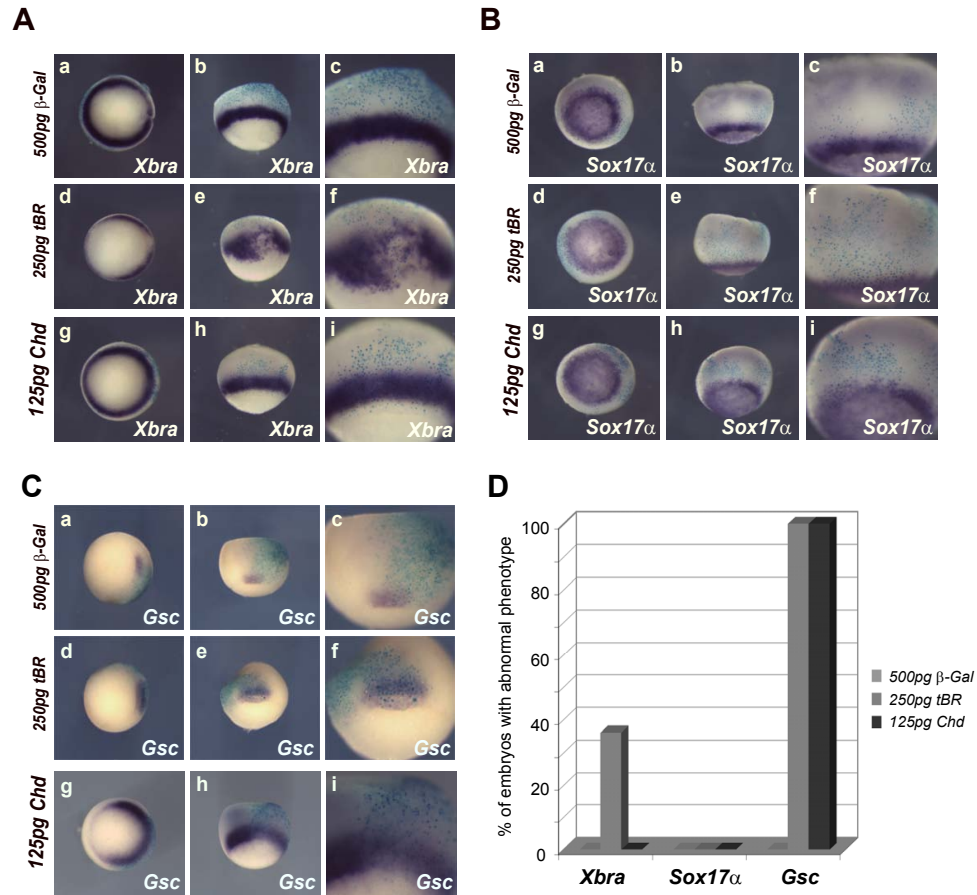


Figure 6.6: **Effect of BMP inhibition by chordin and tBR upon mesoderm and endoderm marker expression**

Embryos microinjected with *Chd* and *tBR* mRNA, β -Gal is used as a marker and injected in all cases. Expression of (A) *Xbra* (B) *Sox17 α* and (C) *Gsc* in injected embryos. (D) Graphical representation of phenotypes arising from *Chd* and *tBR* expression. Orientation of embryos in each set of panels; (a,d, g) Vegetal view, dorsal right, ventral left. (b,c, h) Lateral view, animal top, vegetal bottom. (c, f, i) Zoom of lateral view. (E) Graphical representation of frequency of reported phenotypes, n= 80 to 90.

suggest that TSK is not functioning through BMP inhibition alone. To confirm if this is true, rescue of mesoderm inhibition and endoderm activation was attempted by activation of BMP signalling in the *Xenopus* embryo.

6.2.2 Induction of endoderm markers are partially blocked and expansion of dorsal mesoderm markers is blocked by BMP signal activation

BMP signalling can be activated with a constitutively active form of the BMP type I receptor, caALK3 [Onichtchouk et al., 1999]. This construct was previously used by Ohta et al. [2004] to block induction of neural markers by TSK inhibition of BMP signalling in animal caps. If TSK is expanding dorsal mesoderm marker expression and activating endoderm marker expression through BMP inhibition alone, expression of *caALK3* would be expected to block these TSK phenotypes.

Figure 6.7 shows expression of *Xbra*, *Gsc*, *Sox17 α* and *GATA4* in *TSK* and *caALK3* injected embryos. As shown previously, overexpression of 1ng *TSK* inhibits *Xbra* expression (Figure 6.7Ab), and expands *Gsc*, *Sox17 α* , and *GATA4* expression (Af, Aj, and An respectively). Expression of 500pg *caALK3* similarly inhibits *Xbra* expression (Ac). In addition to inhibition of *Gsc* expression (Ag) *caALK3* also appears to inhibit *Sox17 α* , and *GATA4* (Ak and o) expression. In the presence of *caALK3*, *TSK* continues to inhibit *Xbra* expression (Ad) whereas expansion of *Gsc* expression by *TSK* is blocked by *caALK3* (Ah) This data is represented graphically in Figure 6.7B. Interestingly, expansion of the endoderm markers, *Sox17 α* and *GATA4* by *TSK* is only partially blocked by *caALK3* (Al, Ap and represented graphically in B. This data suggests that whilst the function of *TSK* in dorsal mesoderm may be explained by BMP antagonism by *TSK*, the function of *TSK* in endoderm may be independent, or in addition to BMP inhibition. This leads to the possibility of *TSK* acting through an additional pathway in the *Xenopus* embryo, and thus a more detailed mechanism of *TSK* function has to be constructed.

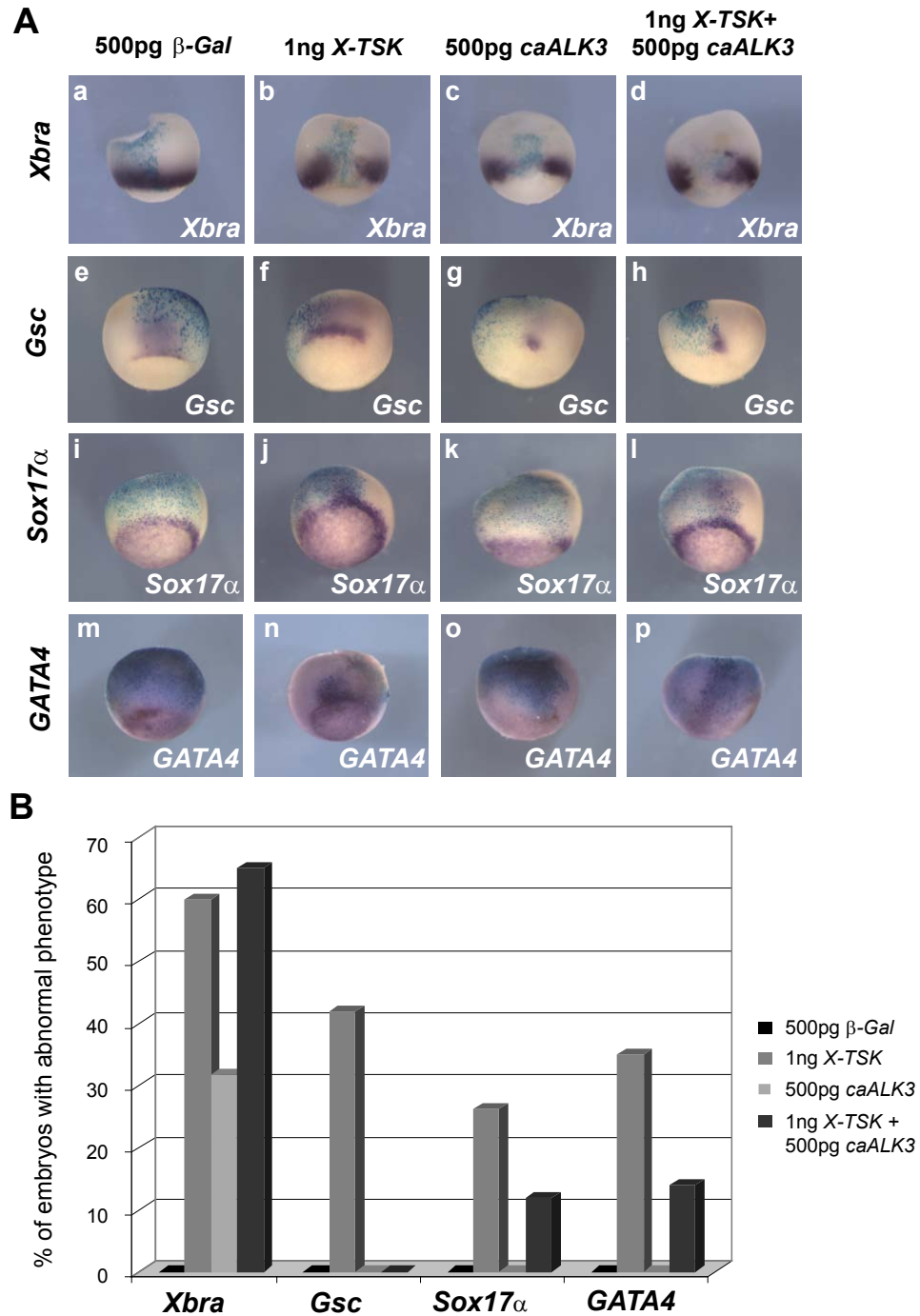


Figure 6.7: Mesoderm and endoderm marker expression in *TSK* and *caALK3* injected embryos

(A) Effect of *TSK* expression of *Xbra* (panels a, b, c, and d), *Gsc* (panels e, f, g, and h), *Sox17 α* (panels i, j, k and l) and *GATA4* (panels m, n, o and p) in *TSK* and *caALK3* injected embryos. Orientation of embryos: lateral, animal top, vegetal bottom. (B) Graphical representation of resultant phenotypes, n = 45 to 50.

Chapter 7

TSK loss of function analysis

In order to verify that TSK is indeed playing an important role in germ layer formation/patterning, loss of TSK function analysis was performed using TSK antisense morpholino. This morpholino has previously been shown to specifically deplete TSK protein levels in *Xenopus* embryos [Ohta et al., 2004, Kuriyama et al., 2006].

7.1 Loss of TSK function results in expansion of the mesoderm marker, *MyoD*

In the preceding chapter (Chapter 6), gain-of-TSK-function was shown to diminish the expression domain of the mesoderm markers, *Xbra* and *MyoD*. Figure 7.1 shows the effect of morpholino depletion of TSK upon *MyoD* expression in stage 15 (neurula) embryos. Panels a and b show normal *MyoD* expression in uninjected and control injected embryos, respectively. In contrast to gain-of-function, loss of TSK function by introduction of *TSK* morpholino results in expansion of *MyoD* expression (panel c) in around 20% of embryos injected (Figure 7.1B). Only one side of the embryo was targeted in order for the uninjected side to act as an internal control.

In contrast to the effect of TSK depletion upon *MyoD* expression, the effect observed in the case of *Xbra* expression in gastrula stage embryos is much weaker (Figure 7.2). Although in a small number of embryos, the regular distribution of *Xbra* around the blastopore (panels a and b) appears more unevenly distributed in the area of *TSK* morpholino introduction (panels c and d).

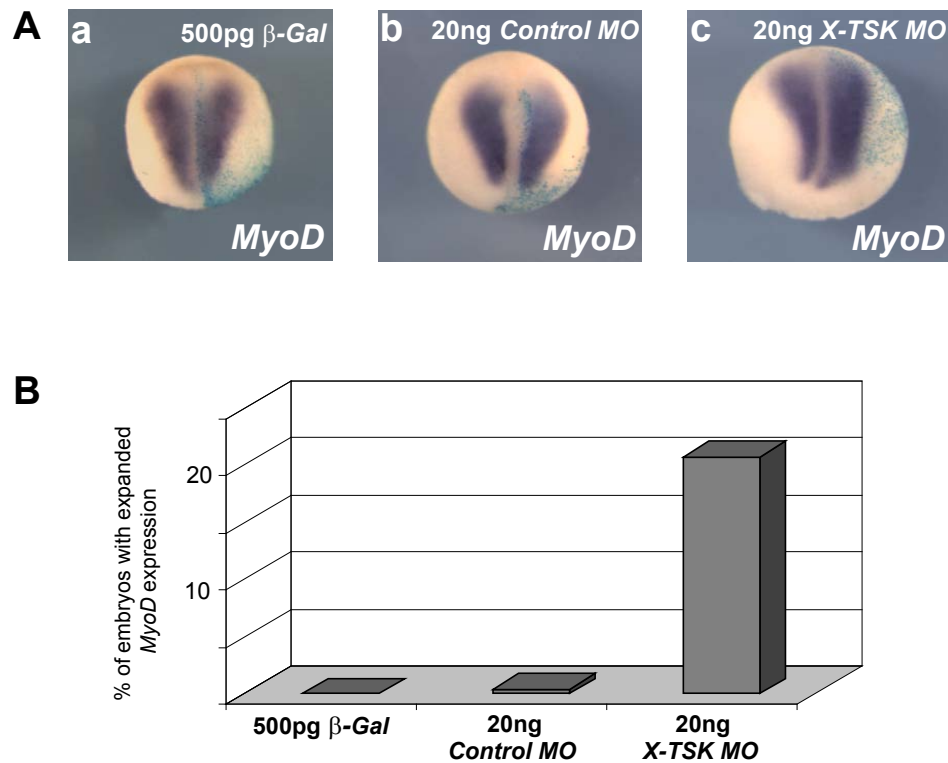


Figure 7.1: *MyoD* expression in *TSK* morpholino injected embryos (A) Expression of *MyoD*, in uninjected (panel A), control morpholino injected (b) and *TSK* morpholino injected embryos (c). Site of injection marked by β -Gal staining in each case (positioned to the right). Anterior top, Posterior towards bottom of page. (B) Graphical representation of phenotypic frequency in (A). n=21 to 27.

7.2 Loss of TSK function results in expansion of the organizer-specific marker, *gooseoid*

In the previous chapter, overexpression of *TSK* in the dorsal region produced an expansion in expression of the organizer specific gene, *Gsc* (Figure 6.2, page 75). Antisense morpholino depletion of *TSK* results in relatively diminished *Gsc* expression in over 40% of targeted embryos (Figure 7.3A and B). Interestingly, expression of *MyoD* is not induced in the dorsal-most region in *TSK*-depleted embryos (Figure 7.3C).

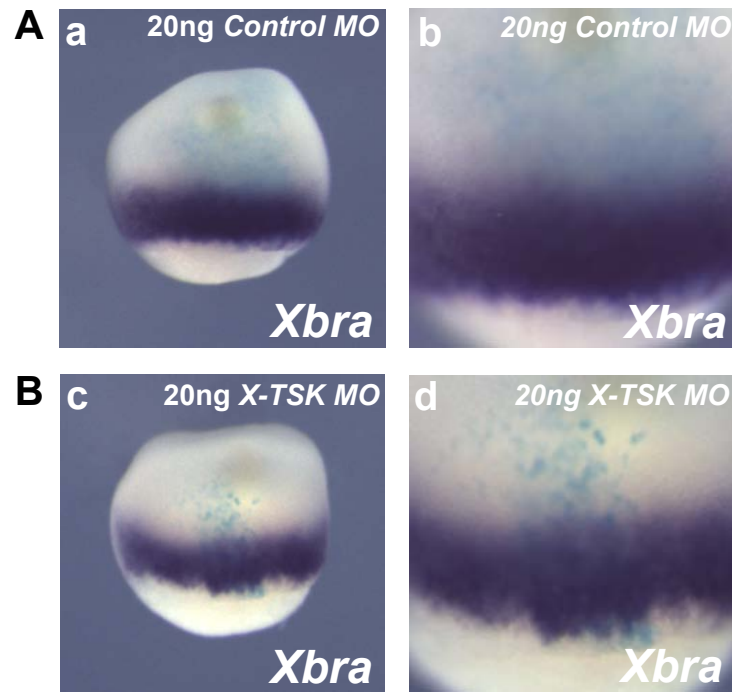


Figure 7.2: *Xbra* expression in *TSK* morpholino injected embryos (A) Expression of *Xbra*, control morpholino injected embryos and (B) *TSK* morpholino injected embryos. Site of injection marked by β -Gal staining in each case. Lateral view, animal top, vegetal towards bottom of page (Panels a and c). Zoom of lateral view (Panels b and d). n= 45 to 50.

7.3 Loss of TSK function results in diminished expression of the endoderm markers, *Sox17 α* and *GATA4*

In contrast to the inhibition of mesoderm markers, *Xbra* and *MyoD* expression resulting from TSK gain-of function, expression of endoderm markers is induced by *TSK* overexpression. In order to look at the effect of TSK loss of function in terms of endoderm formation, morpholino against *TSK* was coinjected with β -Gal to identify the site of injection, into one vegetal cell of a 16-cell stage embryo, thus targeting endoderm at later stages, i.e. during gastrulation. At stage 10, embryos were sectioned and analysed for expression of *Sox17 α* , *GATA4* and *Xbra* by *in situ* hybridisation.

Figure 7.4 shows TSK loss of function in the endoderm, an area in

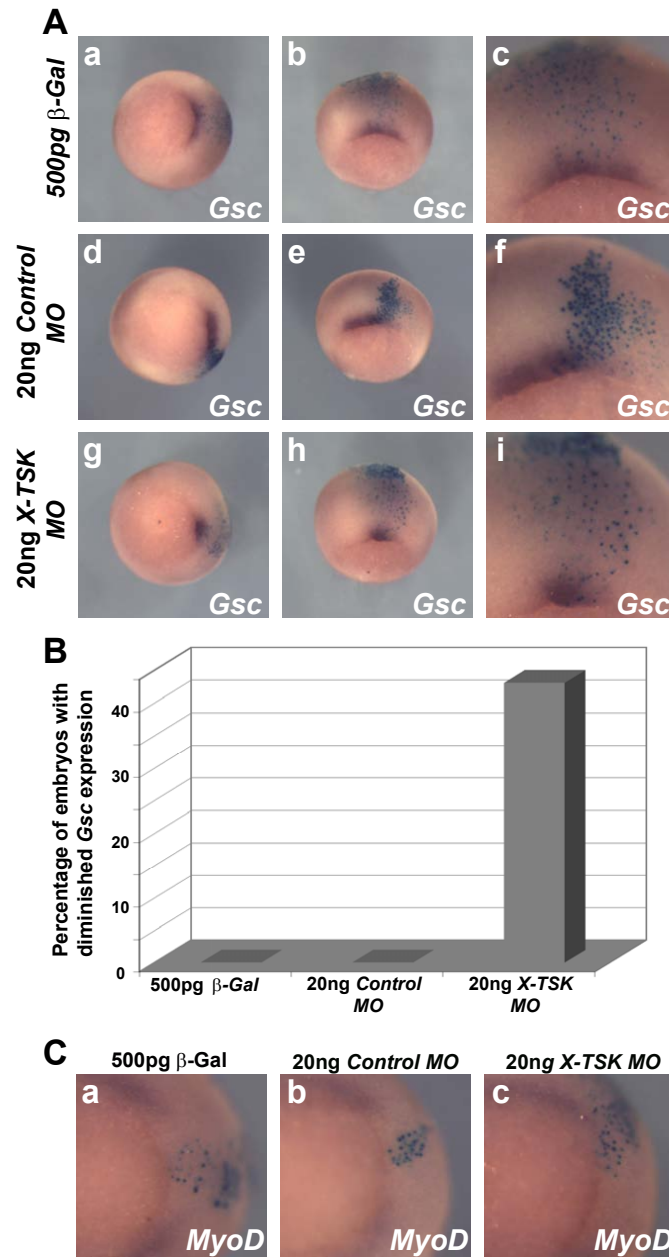


Figure 7.3: *Gsc* and *MyoD* expression in *TSK* MO injected embryos (A) Normal expression of *Gsc*, in β -Gal injected embryos (panels a, b, c). *Gsc* expression in control morpholino injected embryos (panels d, e f) and in *TSK* morpholino injected embryos (panels g, h, i). Orientation; first column: vegetal view, dorsal right. Second column: dorsal view, animal top, vegetal bottom. Third column: dorsal zoom. (B) Graphical representation of phenotypes from (A), n= 40 to 45. (C) *MyoD* expression in β -Gal (Panel a), control morpholino (panel b) and *TSK* morpholino injected embryos. Orientation; vegetal view, zoom on dorsal region.

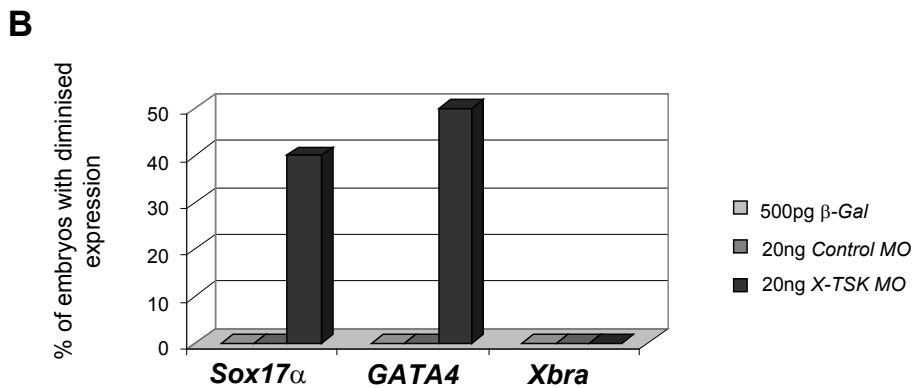
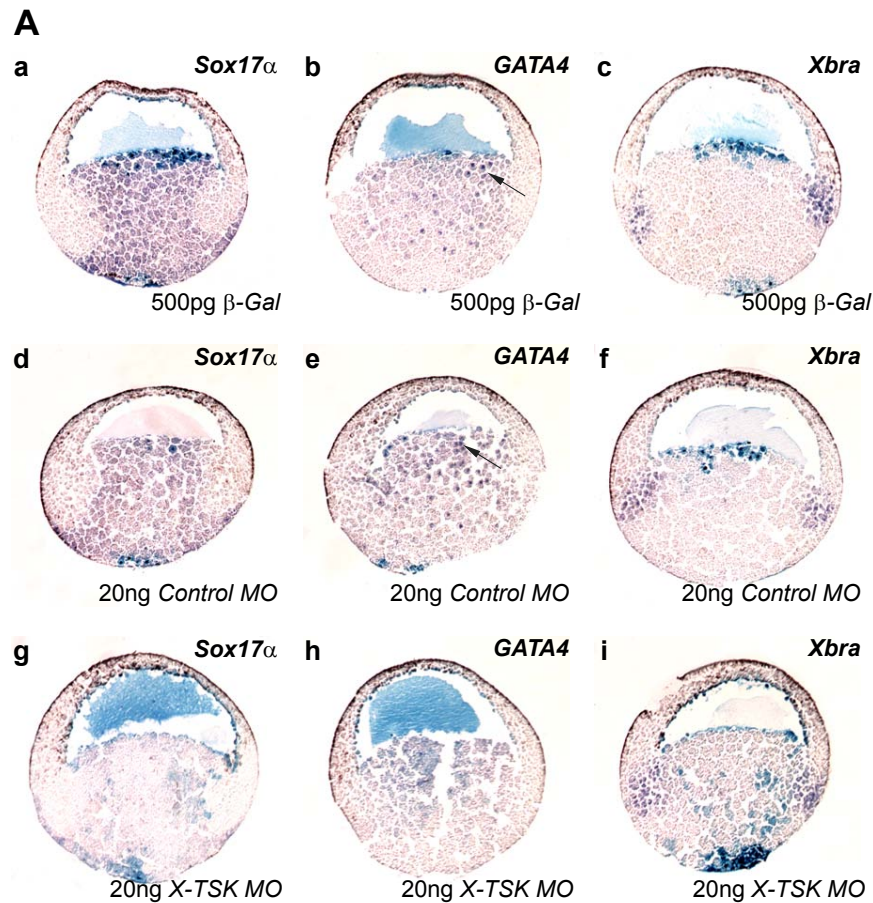


Figure 7.4: *Sox17 α* , *GATA4* and *Xbra* expression in *TSK* MO injected embryos

(A) Expression of *Sox17 α* (first column), *GATA4* (Second column) and *Xbra* (Third column) in uninjected (First row, panels a, b and c), control morpholino injected (Second row, panels d, e and f) and *TSK* morpholino injected embryos (Third row, panels g, h and i). Site of injection marked by β -Gal staining in each case. Animal pole positioned to the top of the page, vegetal to the bottom. (B) Graphical representation of phenotypes arising in (A) n=10 to 12.

which *TSK* is expressed during gastrulation, as shown in chapter 5. Control morpholino-injected embryos (panels d, e and f) do not differ from uninjected embryos (panels a, b and c) in normal expression of *Sox17 α* , *GATA4* and *Xbra* respectively, also discussed previously in Chapter 5 (Figures 5.6, 5.7, pages 66 and 69 respectively). Injection of 20ng *TSK* morpholino results in a clear reduction of *Sox17 α* staining in the endoderm (panel g). In addition to this, the punctate expression pattern of *GATA4* seen in normal embryos is lost in *TSK* morpholino-injected embryos (panel h). In contrast to this, significant changes are not detected in *Xbra* expression levels in sectioned embryos.

The reduction of endoderm marker expression upon loss of TSK function, and expansion of endoderm marker expression domains upon *TSK* overexpression in combination with the temporal expression of *TSK* during germ layer formation and gastrulation, coupled with the spatial expression of *TSK* with the endoderm during gastrulation suggests that *TSK* plays a specific role in formation of endodermal tissues in the embryo. To test this hypothesis further, TSK-depleted embryos were grown to late stages to confirm the role of TSK.

7.4 Loss of TSK function in late-stage embryos

Figure 7.5 A shows late-stage embryos which have been targeted with 40ng morpholino into one vegetal cell at the 16-cell stage, as above. Development of control morpholino-injected embryos proceeds normally to these later stages. In contrast to this, TSK-depleted embryos show clear defects in pigmentation and gut development. The diminished pigmentation observed can most likely be explained as a defect in melanocyte development, associated with the function of TSK during neural crest formation. Of interest here, and in agreement with the phenotype seen in early-stage TSK depleted embryos, gut dimensions in these late-stage TSK depleted embryos is clearly abnormal. To analyse this in further detail, dimension of gut area, length and width were measured using the NIH Image program. These measurements are represented graphically in figure 7.5 B. Dimensions between uninjected and control morpholino-injected embryos do not significantly differ. In TSK depleted embryos, gut length is

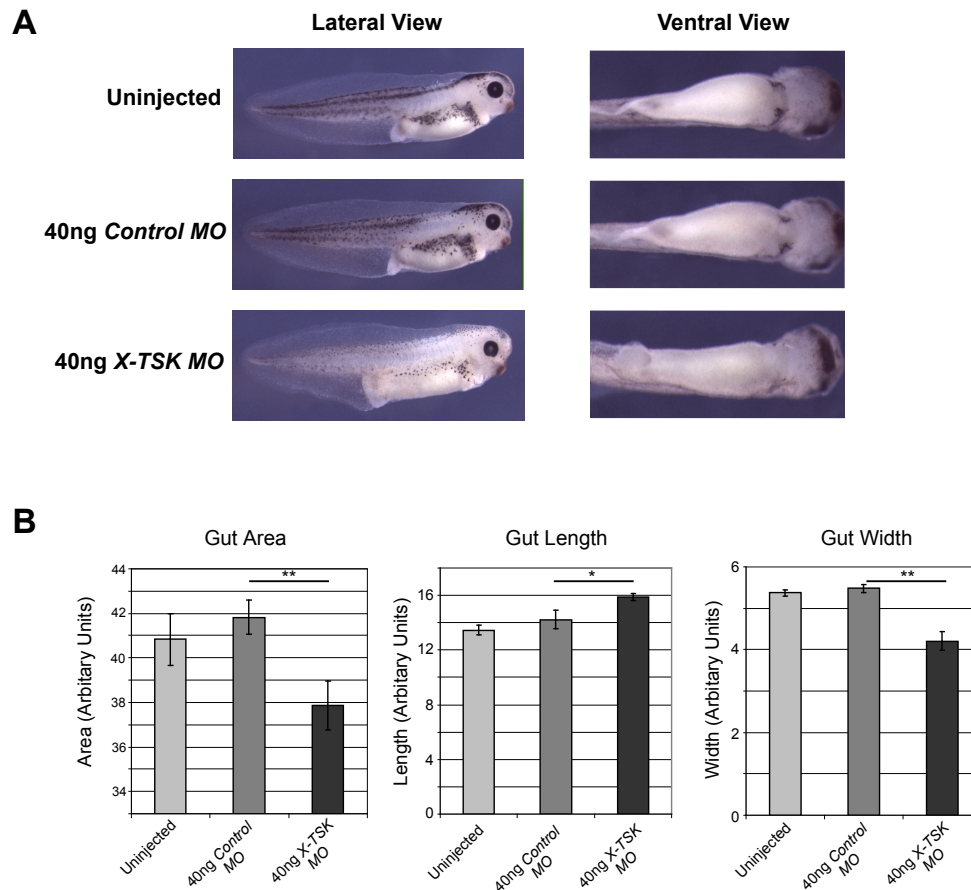


Figure 7.5: Measurement of gut dimensions in late stage *TSK* morpholino injected embryos

(A) Late-stage uninjected (top row), control morpholino-injected (middle-row) and *TSK* morpholino-injected (bottom row) embryos. Left column, lateral view. Right column, ventral view. (B) Graphical representation of changes in gut area, gut length and gut width as measured from the above ventral views. $n=37$ to 45. Significance measured by t-test. * = p is less than 0.05, ** = p is less than 0.01.

slightly increased although gut width is more significantly decreased (p is less than 0.01). This is reflected in the measurement of gut area, showing that the size is overall and consistently reduced (p is less than 0.01). These perturbations in gut dimensions suggest the early effects of TSK depletion in germ layer formation/patterning are significant and carry through to later stages of *Xenopus* development.

7.5 Rescue of gastrula stage TSK-depletion phenotype with expression human TSK in endoderm

In order to confirm that the effect of TSK-depletion upon formation of endoderm is specific, rescue of the phenotype was performed by coinjection of *TSK* morpholino with *human TSK* (*H-TSK*) mRNA. Injected embryos were analysed by *in situ* hybridisation of *Sox17 α* and *GATA4* in sectioned gastrula-stage embryos. The antisense *TSK* morpholino is not expected to be effective against H-TSK as the target sites against the 5'UTR are sufficiently different. *H-TSK* is also used for the rescue as overexpression in *Xenopus* embryos has shown similar phenotypes as *Xenopus TSK* overexpression (data not shown).

Figure 7.6 shows reduction of *Sox17 α* and *GATA4* expression in TSK depleted embryos (panels c and d) relative to normal expression in uninjected embryos (panels a and b) as shown above. introduction of 1ng *H-TSK* mRNA in addition to *Xenopus TSK* morpholino effectively rescues the TSK depletion phenotype and partially restores *Sox17 α* expression whilst punctate expression of *GATA4* appears to be fully restored. The rescue of the TSK depletion phenotype with *H-TSK* confirms the effect of TSK loss of function upon endoderm formation is specific. This loss of function analysis in combination with the previous gain of function analysis confirms that TSK plays an important role in germ layer formation in early *Xenopus* development.

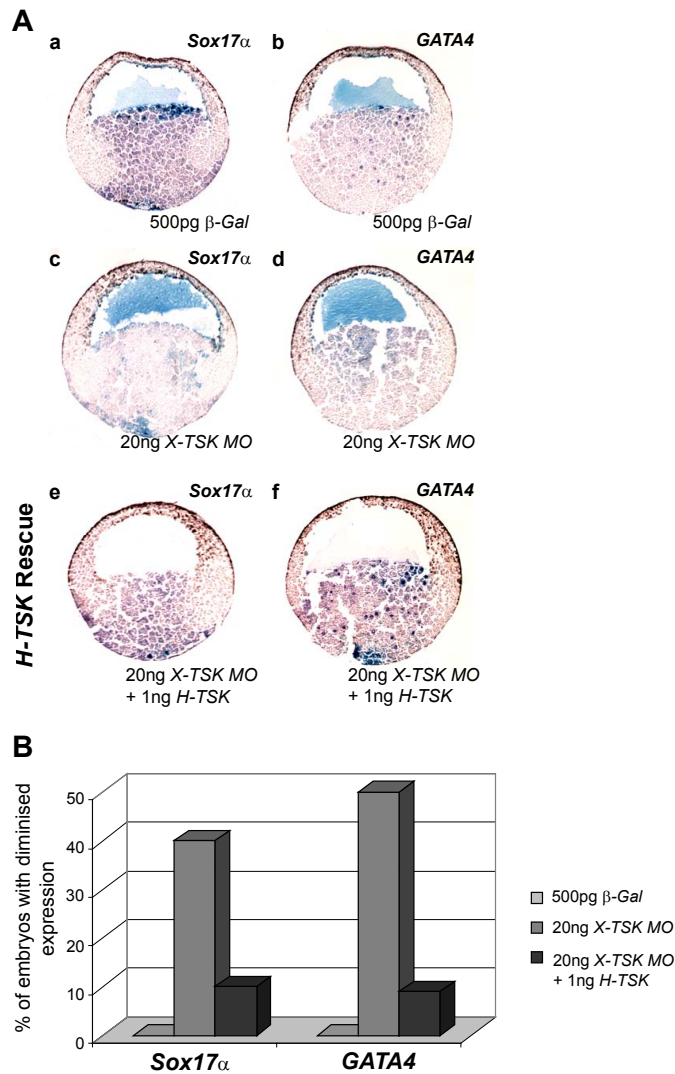


Figure 7.6: **Rescue of gastrula stage TSK-depletion phenotype with expression human TSK in endoderm**

(A) Expression of *Sox17 α* (first column) and *GATA4* (Second column) in uninjected (panels a, b), *Xenopus TSK* depleted (c, d) and *Xenopus TSK* depleted-*H-TSK* rescued embryos (g, h). Animal pole towards top of page. (B) Graphical representation of phenotype frequencies from (A), n = 11 to 12.

7.6 Effect of TSK depletion in neurula stage embryos

To further confirm that TSK depletion is behaving to consistently oppose the effects of TSK overexpression, the effects of TSK gain and loss of function were analysed in neurula stage (specifically, stage 18) embryos. Microinjection of mRNA or morpholino in conjunction with β -Gal, to identify the site of injection, was targeted to one side of the neural plate by injection into one animal dorsal cell of a four-cell stage embryo. Following incubation to stage 18, whole mount *in situ* hybridisation for the neural markers, *Krox20*, *Engrailed2* (*En2*) and *Otx2* was performed.

Krox20 is a zinc finger protein and was found by Sham et al. [1993] to be expressed in a segment-restricted domain in the hindbrain, and regulates *HoxB2* during hindbrain segmentation. In *Xenopus*, *Krox20* has been used as a hindbrain marker to study the mechanism anterior and posterior neural development [Itoh and Sokol, 1997]. In addition to this *Krox20* expression has been shown to be regulated by BMP and FGF signalling [Ishimura et al., 2000] and thus is interesting within the scope of this study as TSK may have functions in addition to BMP inhibition. In contrast to this, *En2* is a homeobox-containing protein expressed at the midbrain-hindbrain boundary [Hemmati-Brivanlou et al., 1990, 1991]. Finally *Otx2* is a homeobox gene expressed in a broad anterior domain covering presumptive anterior neural and cement gland ectoderm in addition to mesoderm and endoderm responsible for inducing them [Blitz and Cho, 1995, Pannese et al., 1995]. *Otx2* activates anterior neural development in *Xenopus* [Gammill and Sive, 2001]. Shifts of these three neural markers towards the anterior or posterior part of the neural plate as observed by *in situ* hybridisation can give an indication of possible TSK function in the neural plate.

Figure 7.7 A shows the effect of TSK overexpression and depletion in the neural plate. Expression of *Krox20* (Hindbrain), *En2* (Midbrain), and *Otx2* (Anterior) is not shifted by expression of β -Gal or introduction of control morpholino. In contrast to this, overexpression of 1ng *TSK* produces a shift of all

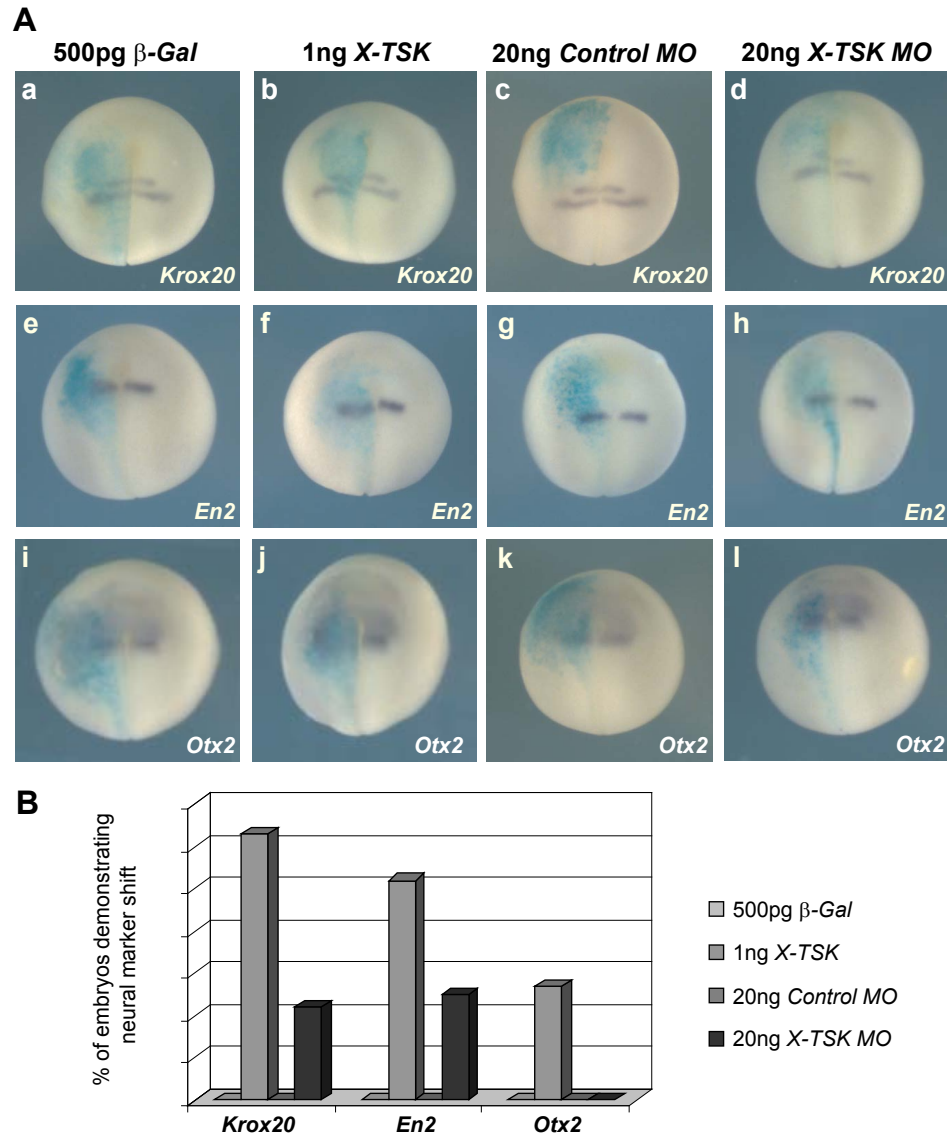


Figure 7.7: Shift of neural markers in response to *TSK* overexpression or morpholino injection

(A) Expression of *Krox20* (First row), *En2* (Second row), and *Otx2* (Third row) in β -Gal (Panels a, e, i), *TSK* (Panels b, f, j), Control morpholino (Panels c, g, k) and *TSK* morpholino (Panels d, h, l). Injected sides marked by β -Gal staining positioned to the left. Anterior neural plate positioned to the top of the page. (B) Graphical representation of neural marker shifts. n=40 to 50.

three neural markers towards the posterior of the embryo (Panels b, f, j), whilst depletion of 20ng *TSK* morpholino produces an opposite shift of *Krox20* and *En2* towards the anterior of the embryo. No significant shift is observed with *Otx2*. The posterior shift of neural markers resultant from TSK overexpression suggests an expansion of the anterior neural plate, whereas loss of function suggests the opposite, reduced anterior, or perhaps expansion of the posterior neural plate. As FGF can induce/posteriorise the neuroderm [Cox and Hemmati-Brivanlou, 1995, Lamb and Harland, 1995, Isaacs et al., 1998] this raised the possibility that TSK may function with FGF signalling in *Xenopus*.

Chapter 8

Mechanism of TSK action

8.1 Major signalling pathways in the *Xenopus* embryos

To identify potential candidate pathways downstream of TSK, we may consider pathways downstream of TGF- β superfamily members and also consider pathways known to be involved in germ layer formation and patterning. This covers Smad1, downstream of BMP signals and Smad2 downstream of activin-like signalling [Massagué, 1998, Whitman, 1998, Hill, 2001]. Smad1 is important for patterning of the mesoderm, and endoderm. In addition to this, MAPK kinase signals play an important role in patterning of germ layers [LaBonne et al., 1995, Faure et al., 2000, Schohl and Fagotto, 2002]. BMP-Smad1 signalling functions to impose ventral fate during gastrulation [Sasai and Robertis, 1997, Lemaire and Yasuo, 1998, Dale and Wardle, 1999]. Whilst mesoderm and endoderm formation require activin-like-Smad2 signals from the vegetal pole [Hemmati-Brivanlou and Melton, 1992, Schulte-Merker et al., 1994, Harland and Gerhart, 1997]. In addition to this, FGF-MAPK signalling is essential for mesoderm induction [Amaya et al., 1991, Harland and Gerhart, 1997]. Hence these signalling pathways have important roles during germ layer formation and patterning. Considering the importance of Smad2, Smad1 and MAPK kinase in these aspects of early embryogenesis, these were the most interesting aspects in terms of TSK function.

8.2 Intracellular signalling downstream of TSK

To analyse intracellular signalling downstream of TSK, overexpression of *TSK* RNA at a concentration range of 125pg to 1ng per embryo was injected into the animal hemisphere at the 2-cell stage. At stage 9, animal caps were dissected and harvested at stage 10. Figure 8.1 shows Western blotting of TSK injected animal caps, probed for (a) Phosphorylated MAPK, (b) Phosphorylated Smad2 and (c) Phosphorylated Smad1. In each case, total levels of each unphosphorylated signalling component are probed as a control for equal protein loading.

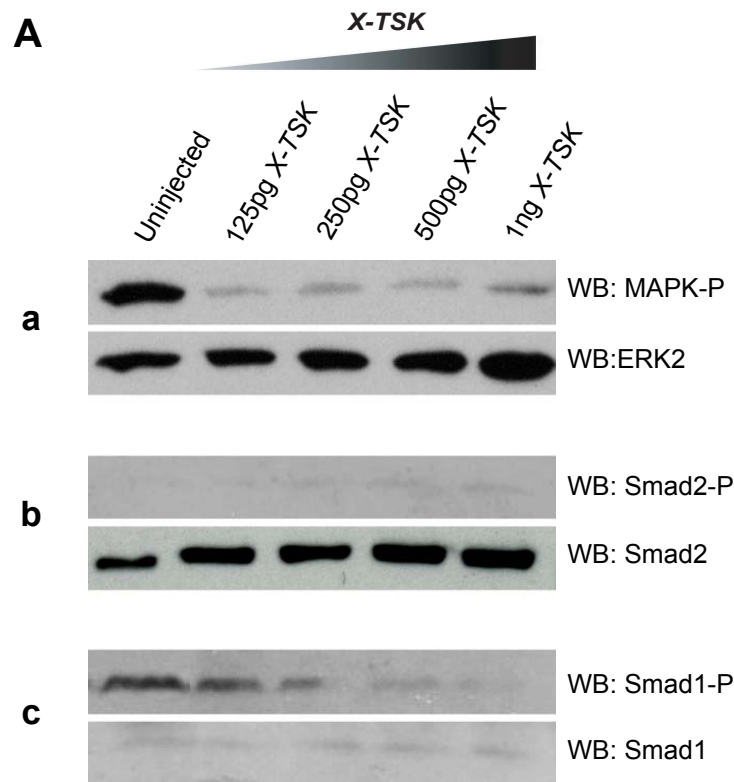


Figure 8.1: **Intracellular signalling downstream of TSK; MAPK, Smad 2 and Smad1**

(A) Overexpression of *TSK* in *Xenopus* animal caps followed by Western blotting of lysates for (a upper) Phosphorylated MAPK (a lower) Total MAPK, (b upper) Phosphorylated Smad2 (b lower) Total Smad2, (c upper) Phosphorylated Smad1 (c lower) Total Smad1.

Overexpression of 125pg - 1ng *TSK* mRNA produces a clear inhibition of MAPK phosphorylation, relative to uninjected animal caps (Figure 8.1 a lane

1). This inhibition is evident at the lowest concentration of 125pg *TSK*, with increasing concentration not significantly inhibiting MAPK phosphorylation further. This suggests that lower doses of *TSK* are effectively inhibiting MAPK activity in the animal cap. In contrast to this, overexpression of *TSK* within the same range weakly activates phosphorylation of Smad2 over levels seen in uninjected animal caps (Figure 8.1 b). In the case of Smad1, *TSK* inhibits phosphorylation in a dose dependent manner with the greatest inhibition of phosphorylation seen at 1ng *TSK* (Figure 8.1 c). This data indicates that whilst TSK has a weak effect on Smad2 signalling, MAPK and Smad1 signals are inhibited by *TSK* overexpression. Inhibition of Smad1 signalling is also in agreement with previous findings of TSK as a BMP inhibitor [Ohta et al., 2004, Kuriyama et al., 2006]. Conversely, MAPK phosphorylation is activated in *TSK* morpholino injected embryos, and Smad1 phosphorylation is also slightly activated (Figure 8.2).

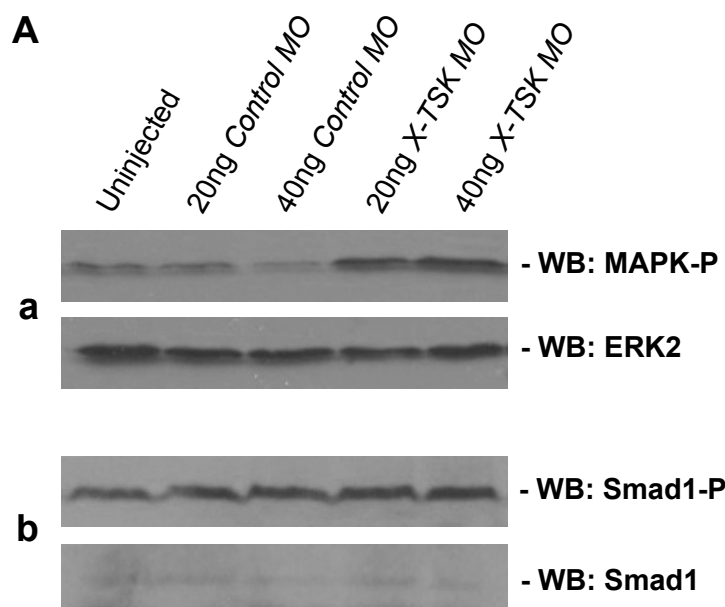


Figure 8.2: **Cell signalling downstream of *TSK* morpholino**
(A) Injection of *TSK* morpholino in *Xenopus* animal caps followed by Western blotting of lysates for (a upper) Phosphorylated MAPK (a lower) Total MAPK, (b upper) Phosphorylated Smad1 (b lower) Total Smad1.

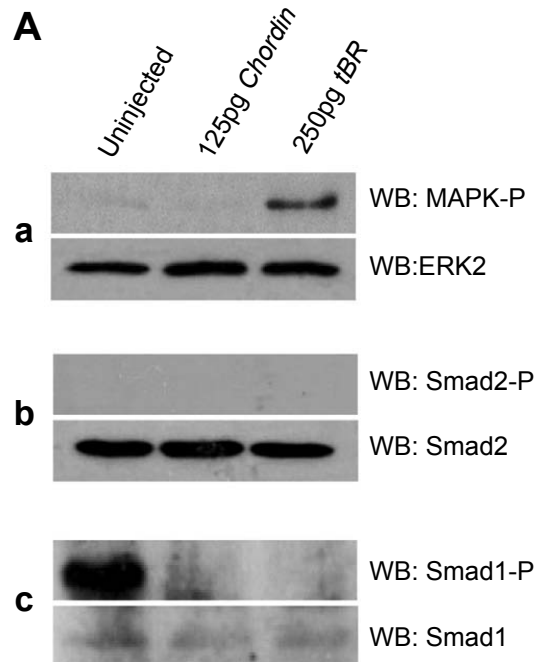


Figure 8.3: **Intracellular signalling downstream of Chd, tBR; MAPK, Smad2 and Smad1**

(A) Overexpression of 125pg *Chd* and 250pg *tBR* in *Xenopus* animal cap followed by Western blotting of lysates for (a upper) Phosphorylated MAPK (a lower) Total MAPK, (b upper) Phosphorylated Smad2 (b lower) Total Smad2, (c upper) Phosphorylated Smad1 (c lower) Total Smad1.

To make an additional comparison between TSK activity and BMP inhibition, 125pg *Chd* and 250pg *tBR* were overexpressed in animal caps and signalling analysed by Western blotting as above. Figure 8.3 shows MAPK, Smad2 and Smad1 signalling in *Chd* and *tBR* injected animal caps. Overexpression of 125pg *Chd* may slightly inhibit MAPK phosphorylation, whereas no effect is observed for Smad2 phosphorylation levels ((Figure 8.3 a and b respectively). Smad1 phosphorylation is inhibited by *Chd* expression, as expected for a known BMP inhibitor (Figure 8.3 c). Expression of *tBR* also shows no changes in Smad2 phosphorylation and inhibition of Smad1 phosphorylation (Figure 8.3 b and c respectively). In contrast to this, 250pg *tBR* RNA expression results in activation of MAPK phosphorylation in animal caps (Figure 8.3 a), thus highlighting differences between TSK function and BMP inhibition. The main difference

in the signal output created by TSK overexpression in comparison to BMP inhibition appears to lie with MAPK. *tBR* activates MAPK signals, which is in contrast to TSK inhibition of MAPK signalling. Firstly the consequence of MAPK inhibition by TSK in the mesoderm will be addressed, as FGF-MAPK has been shown to be essential for mesoderm formation [Amaya et al., 1991, 1993].

8.3 Consequence of MAPK inhibition by TSK in the *Xenopus* marginal zone

Amaya et al. [1991] showed that a mutant FGF receptor produced specific defects in gastrulation and posterior development, and that embryos expressing the mutant receptor failed to induce mesoderm in response to FGF. The mutant receptor, termed XFD, was constructed by deletion of the entire tyrosine kinase domain of the wildtype *Xenopus* FGF receptor (XFR). The authors proposed that this truncated receptor forms non-functional heterodimers with endogenous FGF receptors, leading to a block in phosphorylation of the intracellular catalytic domains and thus blocking signal transduction from the receptor.

The authors went on to confirm the importance of FGF signalling in mesoderm formation by showing that the XFD protein inhibits expression of *Xbra* throughout the marginal zone, but does not inhibit *Gsc* expression [Amaya et al., 1993]. Figure 8.4A shows normal expression of *Xbra* around the blastopore in β -Gal injected embryos. In XFD expressing embryos (Figure 8.4B), *Xbra* expression is completely inhibited in the targeted area, as identified by β -Gal staining. Since FGF signalling is blocked in these embryos, levels of MAPK phosphorylation will be dramatically decreased. This leads to the possibility that the inhibition of MAPK activation by TSK may be the possible mechanism by which TSK also *Xbra* expression in the marginal zone.

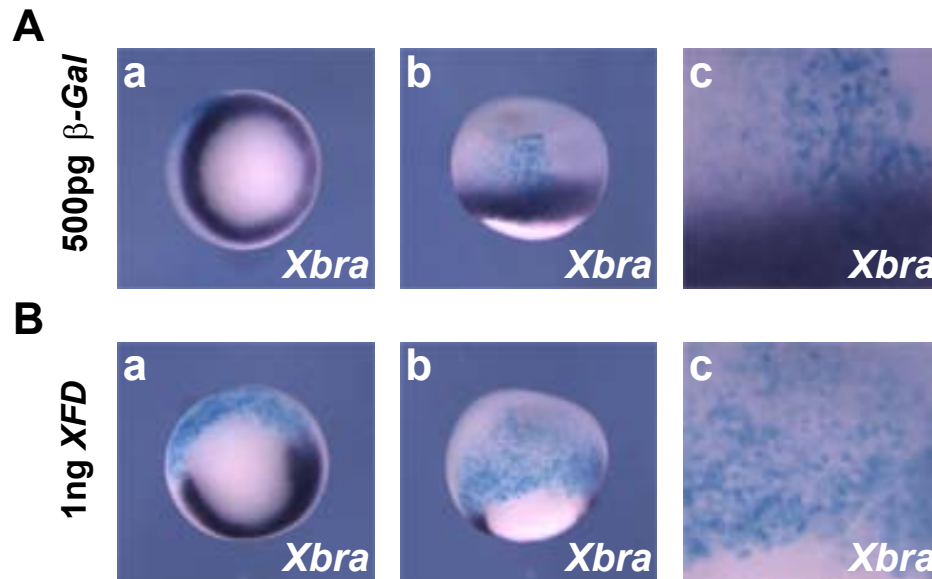


Figure 8.4: **Expression of *Xbra* is inhibited by the dominant negative FGF receptor, XFD**

(A) Expression pattern of *Xbra* by whole mount *in situ* hybridisation in β -Gal injected embryos (B) Expression pattern of *Xbra* in embryos injected with 1ng of the dominant negative FGF receptor, XFD.

8.4 TSK inhibits the activity of FGF8 in the *Xenopus* embryo

Two FGF8 spliceforms exist in the *Xenopus* embryo; FGF8a and FGF8b [Fletcher et al., 2006]. FGF8a has little effect on mesoderm whereas FGF8b is a potent mesoderm inducer. Thus, FGF8b was coinjected with *TSK* to observe the effect upon the activity of FGF8b in terms of MAPK phosphorylation and ectopic *Xbra* induction.

Figure 8.5 shows Western blotting for MAPK in animal caps and whole mount *in situ* hybridisation for *Xbra* in *TSK* and *FGF8b* injected embryos. Animal caps were injected at the two cell stage with *TSK* and *FGF8b* RNAs, dissection of caps proceeded at stage 9, followed by Western blotting for phosphorylated MAPK at stage 10. *TSK* clearly inhibits FGF8b mediated activation of MAPK phosphorylation.

In addition to analysing rescue of the *TSK* phenotype with Western blot-

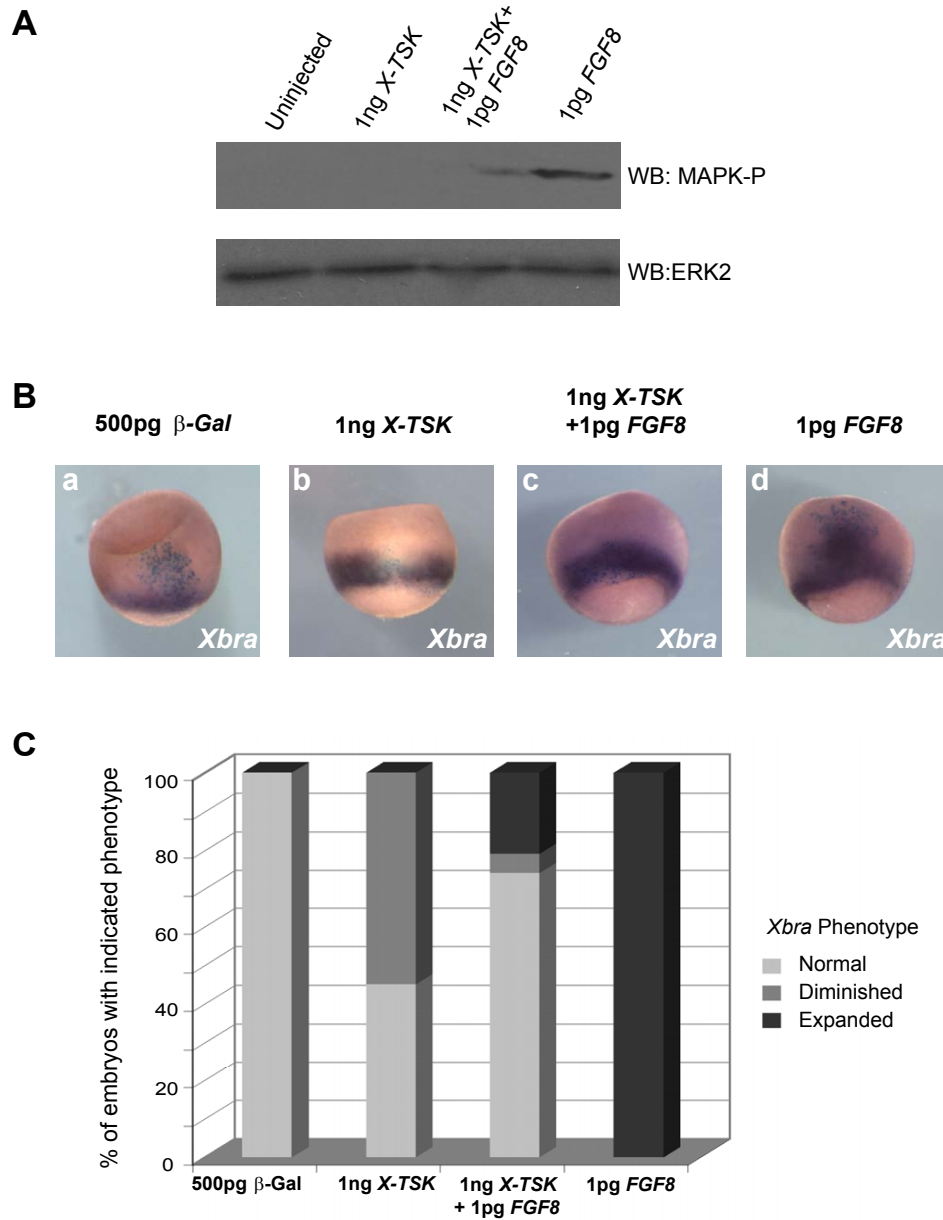


Figure 8.5: **TSK partially blocks FGF8b expansion of *Xbra* expression**
(A) Western blotting for MAPK in *TSK* and *FGF8b* injected animal caps.
(B) Whole mount *in situ* hybridisation for *Xbra* in *TSK* and *FGF8* injected embryos.
(C) Graphical representation of *Xbra* phenotype frequency arising from *TSK* and *FGF8* injected embryos, n = 45 to 50.

ting, whole mount *in situ* hybridisation for *Xbra* was also performed in *TSK* and *FGF8b* injected embryos (Figure 8.5B). As in previous experiments, injection of 1ng *TSK* results in inhibition of *Xbra* expression (panel b). Activation of MAPK phosphorylation by expression of 1pg *FGF8* in the marginal zone induces expression of *Xbra* ectopically into the animal hemisphere (panel d). Overexpression of TSK partially rescues this FGF8b phenotype with lower levels of *Xbra* expression evident.

This data, showing inhibition of the FGF8b expansion of *Xbra* expression with overexpression of *TSK* suggests that TSK is indeed inhibiting expression of the early mesoderm marker, *Xbra* through inhibition of the FGF-MAPK signalling pathway. To confirm this and characterise it in further detail, other components of the FGF-MAPK were analysed in combination with TSK.

8.5 Rescue of TSK mediated *Xbra* expression inhibition by *vras*

Activation of the FGF signalling cascade activates the GTPase, Ras, which in turn activates a cascade of kinases resulting in activation of MAPK and activation of gene expression [Fambrough et al., 1999]. Thus, a constitutively active form of ras was employed in an attempt to rescue TSK mediated inhibition of *Xbra* expression.

Figure 8.6 shows Western blotting for MAPK in animal caps and whole mount *in situ* hybridisation for *Xbra* in *TSK* and *vras* injected embryos. Animal caps were injected at the two cell stage with *TSK* and *vras* RNAs, dissection of caps proceeded at stage 9, followed by Western blotting for phosphorylated MAPK at stage 10. 1ng *TSK* inhibits MAPK phosphorylation as above (Figure 8.6A) relative to the uninjected control. 50pg *vras* strongly activates phosphorylation of MAPK, with this activation rescuing inhibition of MAPK phosphorylation by TSK.

In addition to analysing rescue of the TSK phenotype with Western blotting, whole mount *in situ* hybridisation for *Xbra* was also performed in *TSK* and *vras* injected embryos (Figure 8.6B). As in previous experiments, injection

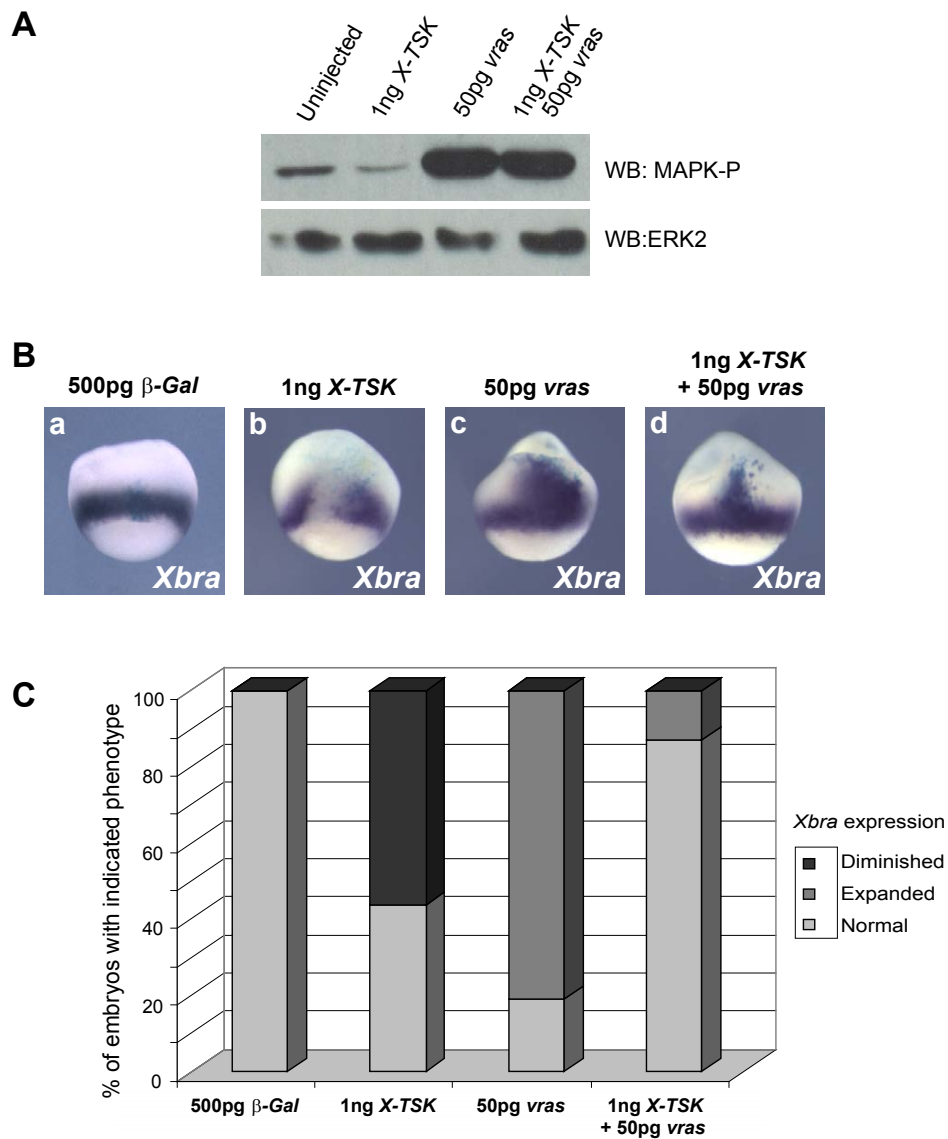


Figure 8.6: **TSK Inhibition of *Xbra* expression is rescued by vras**
(A) Western blotting for MAPK in *TSK* and *vras* injected animal caps. **(B)** Whole mount *in situ* hybridisation for *Xbra* in *TSK* and *vras* injected embryos. **(C)** Graphical representation of *Xbra* phenotype frequency arising from *TSK* and *vras* injected embryos, n = 45 to 50.

of 1ng *TSK* results in inhibition of *Xbra* expression (panel b). Activation of MAPK phosphorylation by expression of 50pg *vras* in the marginal zone induces expression of *Xbra* ectopically into the animal hemisphere, overlapping with the targeted area as identified by β -Gal staining (panel c). In agreement with the analysis of MAPK phosphorylation, *vras* rescues TSK inhibition of *Xbra* expression (panel d). Inhibition of *Xbra* expression is seen in 55% of *TSK* injected embryos, whereas in the presence of *vras*, this figure drops to less than 10% (Figure 8.6C).

This data, showing rescue of the TSK phenotype with a constitutively active component of the FGF signal cascade further suggests that TSK is inhibiting expression of *Xbra* through inhibition of the FGF-MAPK signalling pathway.

8.6 Dimerisation of a caFGF Receptor may be inhibited by TSK

In order to look at the association between TSK and FGF-MAPK signalling in closer detail, rescue of the TSK mesoderm phenotype was performed at the level of the FGF receptor. A constitutively active form of the FGF receptor is available (C249Y) and has been shown by [Neilson and Friesel, 1996] to activate FGF signalling in the *Xenopus* embryo by dimerising independently of ligand binding.

Figure 8.7A shows Western blotting for MAPK in animal caps. 1ng *TSK* inhibits MAPK phosphorylation relative to the uninjected control. Expression of 25pg *caFGFR* strongly activates phosphorylation of MAPK. In contrast to the rescue of TSK MAPK inhibition by *vras* above, *caFGFR* is able to partially rescue the TSK phenotype, although TSK is clearly inhibiting the ability of *caFGFR* to activate MAPK.

Figure 8.7B again shows *in situ* hybridisation for *Xbra*. As in previous experiments, injection of 1ng *TSK* results in inhibition of *Xbra* expression (panel b). Activation of MAPK phosphorylation by expression of 25pg *caFGFR* in the marginal zone induces expression of *Xbra* beyond the boundaries of normal expression. In agreement with the analysis of MAPK phosphorylation where

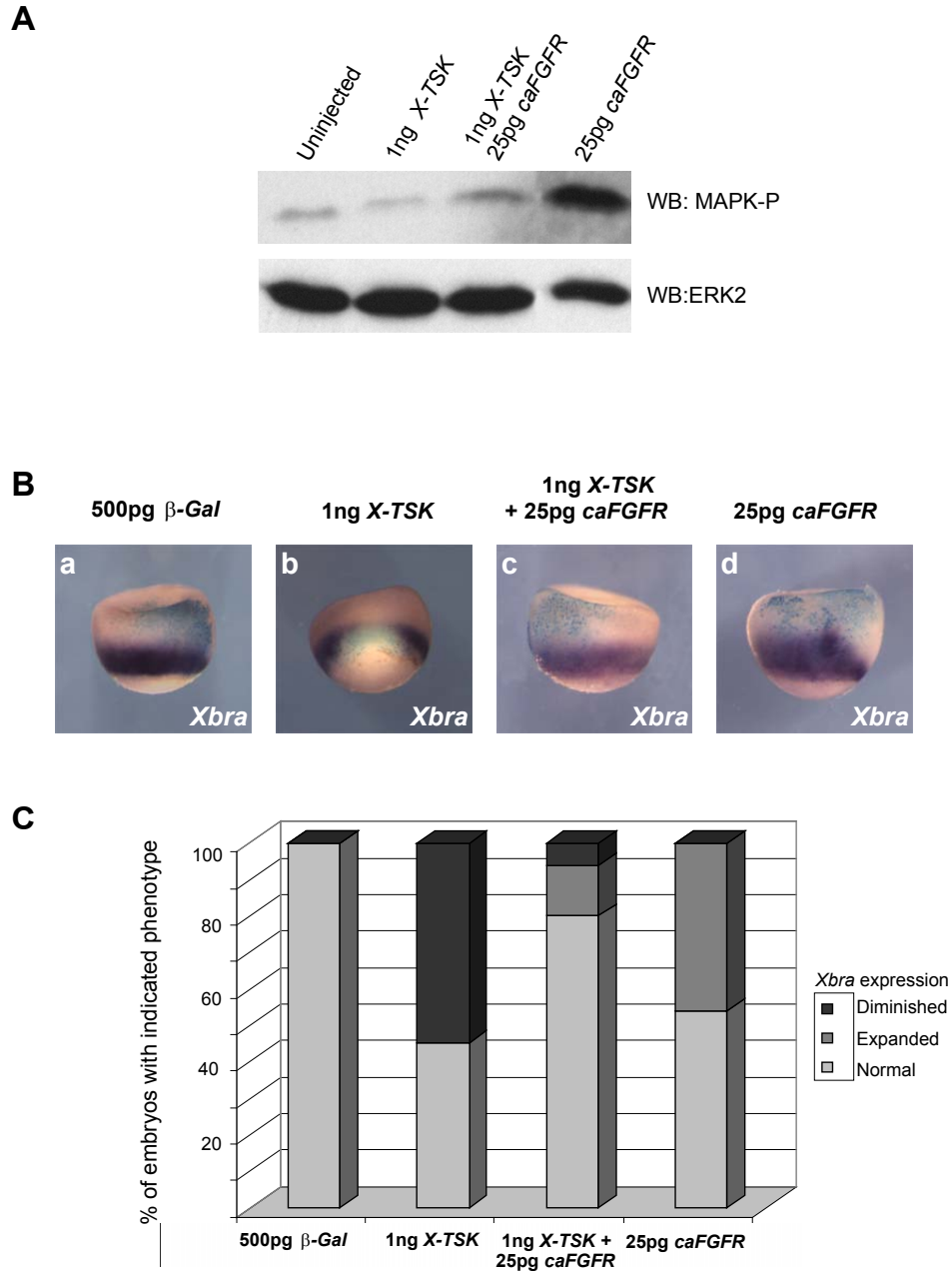


Figure 8.7: *TSK* blocks *caFGFR* activation of MAPK phosphorylation and expansion of *Xbra* expression

(A) Western blotting for MAPK in *TSK* and *caFGFR* injected animal caps. (B) Whole mount *in situ* hybridisation for *Xbra* in *TSK* and *caFGFR* injected embryos. (C) Graphical representation of *Xbra* phenotype frequency arising from *TSK* and *caFGFR* injected embryos.

a combination of TSK and caFGFR produces MAPK phosphorylation levels similar to those seen in uninjected caps, caFGFR rescues TSK inhibition of *Xbra* expression (panel c), although TSK clearly blocks the ability of caFGFR to expand *Xbra* expression. Inhibition of *Xbra* expression is seen in 55% of TSK injected embryos, whereas in the presence of caFGFR, no inhibition of *Xbra* expression is observed (Figure 8.6C).

This data, showing the inhibition of a constitutively active FGF receptor by TSK suggests that TSK may be working at the level of the FGF receptor, possibly inhibiting receptor dimerisation to produce the output of MAPK phosphorylation inhibition. This is supported by evidence above shown that an intracellular component of the FGF-MAPK pathway, downstream of receptor level, can rescue TSK mediated MAPK phosphorylation inhibition and inhibition of *Xbra* expression.

8.7 TSK function in mesoderm is blocked by chemically activated homodimerisation of a synthetic FGF receptor

In order to demonstrate that TSK is inhibiting MAPK phosphorylation and thus inhibiting *Xbra* expression at FGF receptor level, a synthetic FGF receptor which can be subject to chemical dimerisation was used. Pownall et al. [2003] showed the lipophilic, synthetic dimerising agent, AP20187 is able to rapidly activate signalling through a mutant of the FGF receptor, iFGFR in *Xenopus* embryos and thus activate FGF-MAPK signalling in a controlled manner.

Figure 8.8 shows Western blotting for MAPK in animal caps and whole mount *in situ* hybridisation for *Xbra* in *TSK* and *iFGFR* injected embryos, in the presence and absence of AP0187. Animal caps were injected at the two cell stage with *TSK* and *iFGFR* RNAs, dissection of caps proceeded at stage 9 with incubation in AP20187 or carrier, followed by Western blotting for phosphorylated MAPK at stage 10. 1ng *TSK* inhibits MAPK phosphorylation as above (Figure 8.8 A) relative to the uninjected control. Expression of 0.5 to 50pg *iFGFR* does not activate phosphorylation of MAPK in the absence of

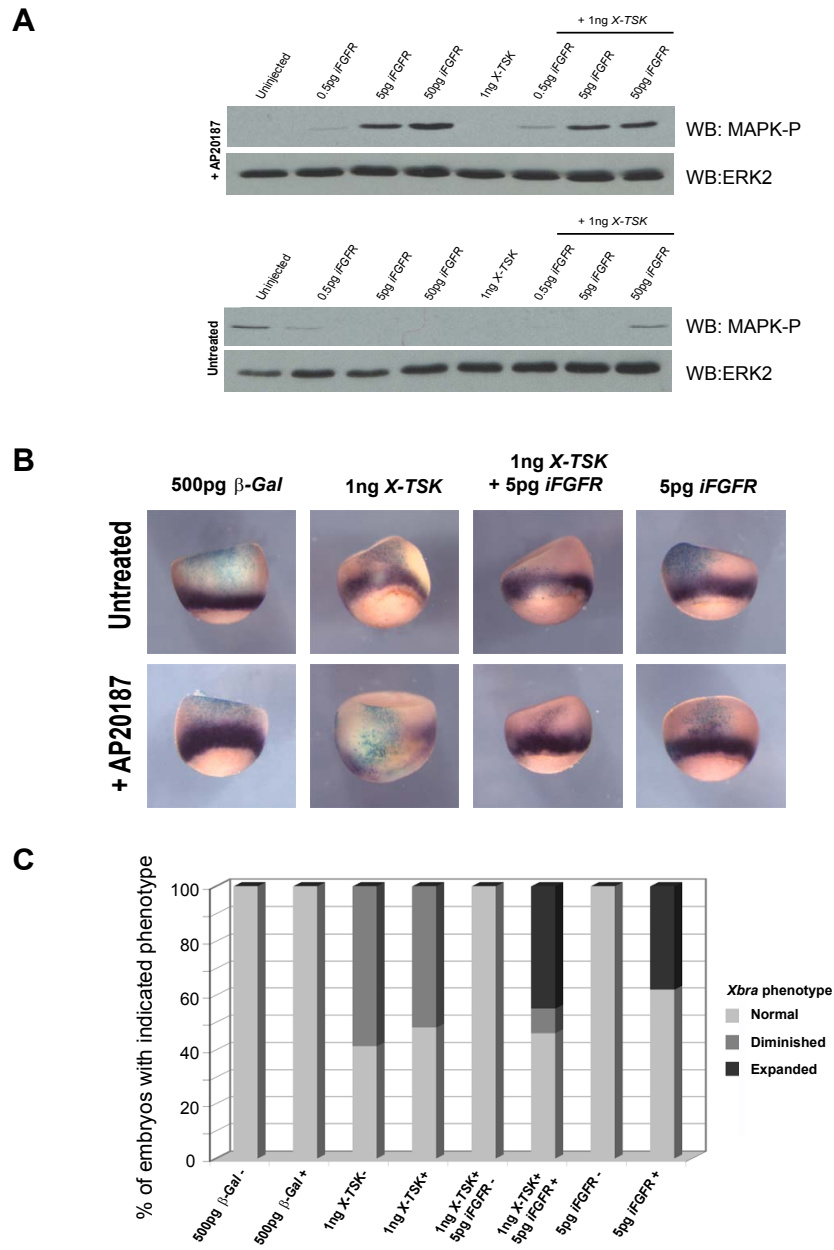


Figure 8.8: **TSK inhibition of *Xbra* expression is rescued by chemical activation of FGF Receptor dimerisation**

(A) Western blotting for MAPK in *TSK* and *iFGFR* injected animal caps, treated with dimerisation activator, AP20187 (upper) or in the absence of activator (lower). (B) Whole mount *in situ* hybridisation for *Xbra* in *TSK* and *iFGFR* injected embryos, untreated (upper) and AP20187 treated (lower) (C) Graphical representation of *Xbra* phenotype frequency arising from *TSK* and *iFGFR* injected embryos in the presence and absence of AP20187, n= 45 to 50.

AP20187. Upon addition of this homodimerization reagent, MAPK phosphorylation is activated, most strongly with 50pg *iFGFR*. In the presence of TSK and AP20187, *iFGFR* continues to activate MAPK, suggesting that TSK is unable to inhibit dimerisation of the synthetic receptor, and is not functioning downstream of the receptor.

To confirm rescue of the TSK phenotype as seen by Western blotting, whole mount *in situ* hybridisation for *Xbra* was also performed in *TSK* and *iFGFR* injected embryos in the presence or absence of AP20187 (Figure 8.8B). Again, injection of 1ng *TSK* results in inhibition of *Xbra* expression in the presence and absence of AP20187 (panels b and e, respectively). Activation of MAPK phosphorylation by expression of 5pg *iFGFR* and AP20187 addition in the marginal zone induces expression of *Xbra* beyond the boundaries of normal expression (panel h). In agreement with the analysis of MAPK phosphorylation where a combination of TSK and *iFGFR* in the presence of AP20187 produces continued elevation of MAPK phosphorylation, *iFGFR* dimerisation rescues TSK inhibition of *Xbra* expression (panel h).

This data, showing the inhibition of MAPK phosphorylation and inhibition of *Xbra* expression is blocked by chemically activated dimerisation of a synthetic FGF receptor strongly suggests that TSK is acting externally to the cell. This is supported by evidence above showing that the activity of a constitutively active form of the FGF receptor is inhibited by *TSK* overexpression.

8.8 Is TSK functioning to induce endoderm through inhibition of FGF signalling?

Overexpression of *TSK* in *Xenopus* marginal zone induces expression of endoderm markers (Figure 6.2, page 75). It has been shown that inhibition of FGF signalling expands endoderm in *Xenopus* [Cha et al., 2004]. Thus it is likely that FGF-MAPK inhibition by TSK may form part of the endoderm induction mechanism by TSK. Figure 8.9 shows *in situ* hybridisation of the endoderm marker, *Sox17 α* in *TSK* and *vras* injected embryos. *TSK* alone induces *Sox17 α* expression, although interestingly, in the presence of *vras* this induction is par-

tially blocked. It is important to note that the inhibition upon TSK by *vras* is only partial in this context, suggesting that other mechanisms may be employed by TSK in the context of endoderm formation, which will be considered in the following chapter.

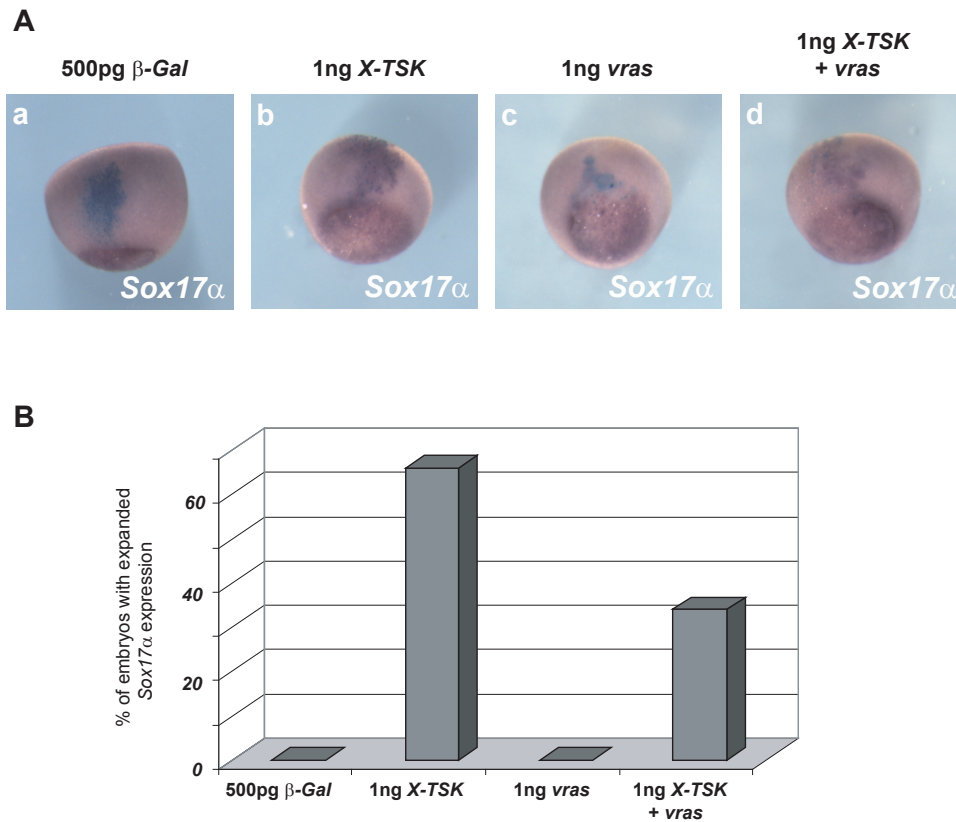


Figure 8.9: *Sox17α* expression in *TSK* and *vras* injected embryos (A) *In situ* hybridisation of *Sox17α* in *TSK* and *vras* injected embryos. Orientation lateral, animal top, vegetal bottom. (B) Graphical representation of phenotypes arising in (A), n = 45 to 50.

Chapter 9

TSK mechanism II; TGF- β signals

9.1 TGF- β signal candidates for TSK function in germ layer formation

In addition to FGF signalling, TGF- β signals are also important for patterning of the germ layers in early *Xenopus* embryogenesis, as described in the introduction. TSK has previously been shown to function as a BMP inhibitor, although in this study, it has been shown that inhibition of BMP by TSK cannot simply account for patterning of the germ layers by TSK. This raises the possibility that there is a separate or additional function of TSK in addition to BMP inhibition. In terms of mesoderm inhibition and endoderm induction, this may be due to FGF-MAPK signal inhibition by TSK, as shown in the previous chapter. This does appear to be the case, although other mechanisms cannot be ruled out at this point, for example interaction of TSK with other members of the TGF- β superfamily.

9.2 TGF- β candidate for TSK mechanism: Nodal

Nodal was identified as a gene in mouse essential for embryonic patterning. Disruption of the nodal gene in mice results in absence or reduction of mesoderm formation, failed primitive streak formation and arrest of development at gastrulation [Conlon et al., 1991, 1994, Iannaccone et al., 1992]. In addition to this, it was found in mouse that intact nodal signalling is required for formation

of mesoderm cell lineages [Conlon et al., 1994, Zhou et al., 1993]. In *Xenopus* Jones et al. [1995] identified two nodal related genes, *Xnr1* and *Xnr2*. These two related genes are 87% identical to each other [Kingsley, 1994] although their expression patterns and functions differ slightly in the *Xenopus* embryo. By RT-PCR, no transcription of either *Xnr1* or *Xnr2* is detected before the onset of zygotic transcription, indicating these genes are not maternally transcribed. Expression of both genes is detected in the late blastula (stage 9) until the end of gastrulation (stage 13). No further expression of *Xnr2* is detected, this is in contrast to *Xnr1* where transcripts can be detected at neurula stages (stage 17) [Jones et al., 1995]. *In situ* hybridisation showed that expression of *Xnr1* and *Xnr2* is detected in a punctate staining pattern all over the vegetal hemisphere at stage 9. At stage 10.25, *Xnr1* is restricted to the dorsal marginal zone, whereas *Xnr2* is detected in the dorsal marginal zone in addition to nearby dorsovegetal cells at pregastrula stage 10. By stage 10.5, *Xnr2* is expressed most strongly in the dorsal blastopore lip at superficial levels and deeper staining. At this stage, some vegetal cells also still express *Xnr2* [Jones et al., 1995]. In the *Xenopus* embryo, *Xnr2* expression is induced in response to dorsal mesoderm inducing signals and *Xnr2* itself dorsalises ventral mesoderm during gastrula stages. This is in contrast to activin which is unable to dorsalise the ventral marginal zone [Smith et al., 1993].

In addition to a role in mesoderm induction, *Xnr2* has also been shown to be important for endoderm formation in the *Xenopus* embryo. A two step model for fate determination of presumptive endoderm was proposed by Yasuo and Lemaire [1999] in which the initial activation of early endodermal genes by maternal factors, including VegT is relayed by the action of zygotic TGF- β superfamily members, including *Xnr1* and *Xnr2*. In addition to this Xanthos et al. [2001] showed that VegT is the maternal regulator of endoderm formation and *Xnr* members are located downstream.

Xnr2: the foremost candidate for interaction with TSK

This spatial and temporal expression pattern of *Xnr2* in particular, combined with its role in germ layer patterning makes it a possible candidate for interaction with TSK. Expression levels of TSK begin to peak at stage 7 and remain relatively high until the end of gastrulation, although it is only at the start of gastrulation where TSK is observed in the endoderm and dorsal blastopore lip. This spatial and temporal expression pattern overlaps with that of *Xnr2* in addition to functions within germ layer patterning. It may also be a possibility that TGF- β superfamily members such as activin and Vg1 are good candidates for the mechanism of TSK action. This remains a possibility, although TSK has not been shown to physically interact with activin [Ohta et al., 2004] and the importance of activin remains debated in the *Xenopus* embryo. Previously, a dominant negative activin receptor has been shown to block mesoderm induction in *Xenopus* [Hemmati-Brivanlou and Melton, 1992] although the use of this artificial receptor may block other TGF- β signals. An approach using follistatin, an inhibitor of activin (as discussed in chapter 4) demonstrates that activin is not required for mesoderm induction in *Xenopus* [Schulte-Merker et al., 1994]. This combined with the role of Xnr2 in endoderm formation thus makes Xnr2 a more likely candidate for TSK function. In the case of Vg1, spatial and temporal expression is not synchronised to TSK in such a way that would suggest interaction in *Xenopus* with Vg1 expression arising too early to complement TSK function. In addition to this, it has been recently shown that Vg1 may not be properly processed in the *Xenopus* embryo [Birsoy et al., 2005]. Finally, Xnr2 can dorsalise ventral mesoderm during *Xenopus* gastrula stages, an activity shared with TSK [Ohta et al., 2004, Kuriyama et al., 2006] further supporting a possible relationship between TSK and Xnr2.

9.3 Endoderm marker expression induction by TSK is blocked by inhibition of nodal signalling

To determine if TSK induction of endoderm markers can be explained through its functional interaction with Xnr signalling, induction of ectopic *GATA4* ex-

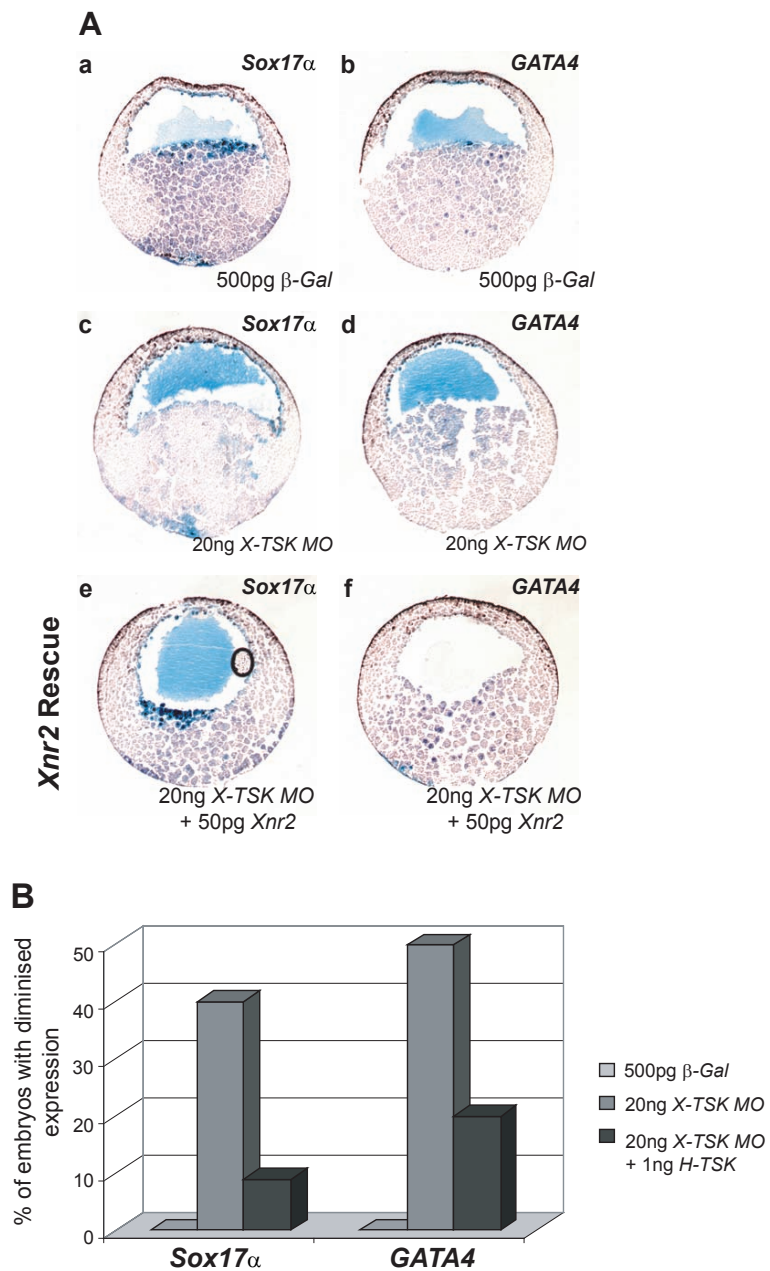


Figure 9.1: **Partial rescue of *TSK* morpholino mediated endoderm depletion by *Xnr2***

(A) Expression of *Sox17 α* (first column) and *GATA4* (Second column) in uninjected (panels a, b), *Xenopus TSK* depleted (c, d) and *Xenopus TSK* depleted-*Xnr2* rescued embryos (g, h). Animal pole towards top of page. (B) Graphical representation of phenotype frequencies from (A), n = 11 to 12.

pression by TSK was analysed by whole mount *in situ* hybridisation in embryos in which nodal signalling has been inhibited. Cerberus Short (CerS) is a form of Cerberus which has been shown to specifically inhibit nodal signalling in the *Xenopus* embryo [Takahashi et al., 2000]. Similarly, dnALK4 (dominant negative ALK4 receptor) can block nodal function [Chen et al., 2004]. Figure 9.1 demonstrates that TSK induction of endoderm marker expression is blocked by co-expression with CerS, and almost fully blocked by dnALK4. This data strongly suggests that nodal signalling is important for TSK function, thus interaction between TSK and *Xnr2* was analysed.

9.4 Rescue of TSK depletion phenotype with *Xnr2*

In addition to blocking the function of TSK in endoderm induction by inhibition of nodal signalling, rescue of the *TSK* morpholino phenotype was performed with *Xnr2*. Figure 9.2 shows that *TSK* morpholino depletes expression of endoderm markers, whilst co-expression of *Xnr2* can partially rescue this phenotype.

9.5 Complex formation between TSK and *Xnr2*: Nickel bead pulldown assay

In order to determine if TSK interacts with other TGF- β superfamily members other than BMPs, pulldown assays were performed between TSK and the main candidate, *Xnr2*. A Myc-Histidine tagged form of TSK was used in conjunction with a Myc-tagged *Xnr2*. Tagged *TSK* and tagged *Xnr2* mRNAs were coinjected into 1-cell stage embryos, followed by incubation until stage 10 and lysis of the embryos. Incubation with Nickel beads followed to pull down tagged TSK, followed by Western blot detection of possible tagged *Xnr2* pulled down in complex with TSK.

Figure 9.3 shows the pulldown of *Xnr2* in complex with TSK. *Xnr2* is only detected in association with the nickel beads in the presence of TSK (top panel, lane 3). No *Xnr2* is detected in association with the beads in the absence of TSK (top panel, lane 2), indicating that the complex with TSK is specific.

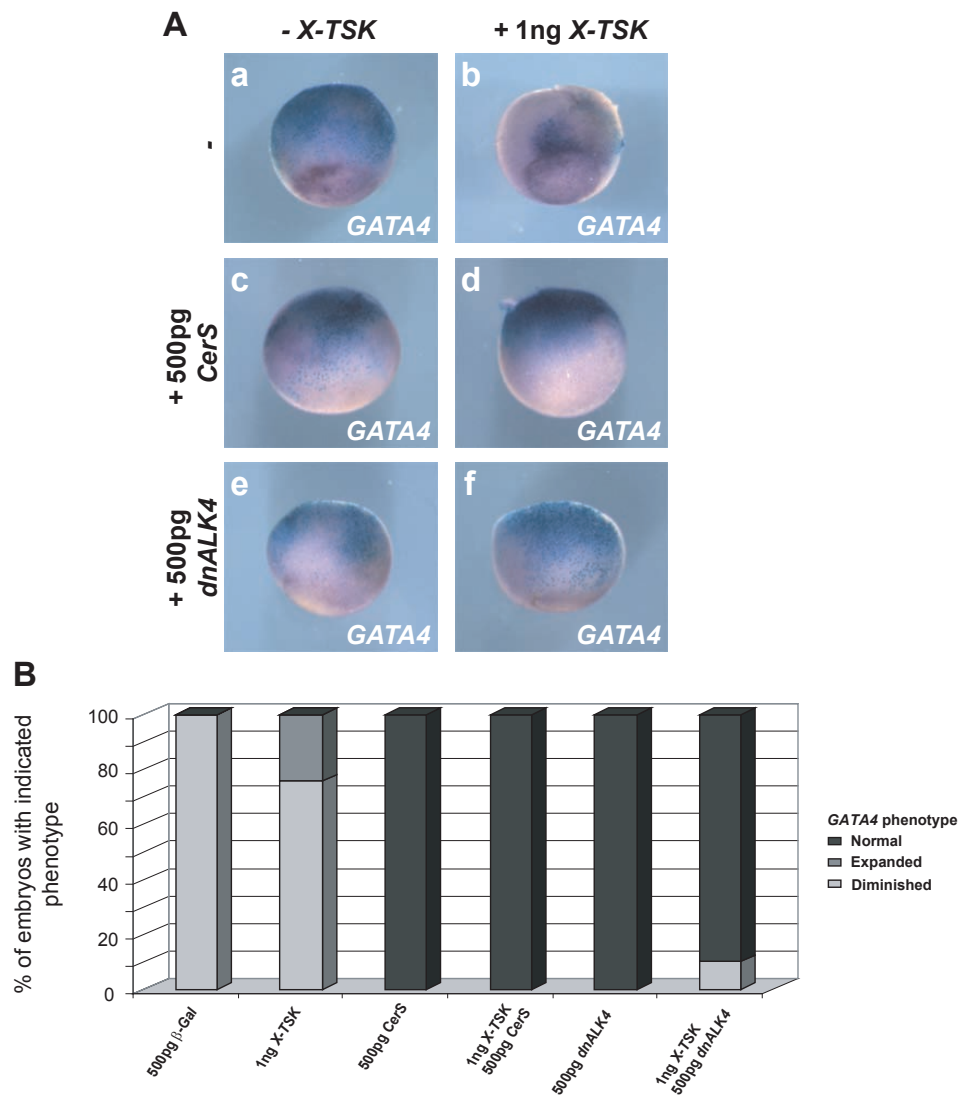


Figure 9.2: **Rescue of *TSK* mediated endoderm expansion by nodal signal inhibition**

(A) Whole mount *in situ* hybridisation for *GATA4* in *TSK* and *CerS* or *dnALK4* injected embryos. β -Gal (a), 1ng *TSK* (b), 500pg *CerS* (c) 500pg *CerS* with 1ng *TSK* (d), 500pg *dnALK4*(e), and 500pg *dnALK4* with 1ng *TSK* (f). All RNAs were coinjected with β -Gal to identify the targeted area. (B) Graphical representation of *GATA4* phenotype frequency arising from *TSK* and *CerS* or *dnALK4* injected embryos, n = 45 to 50.

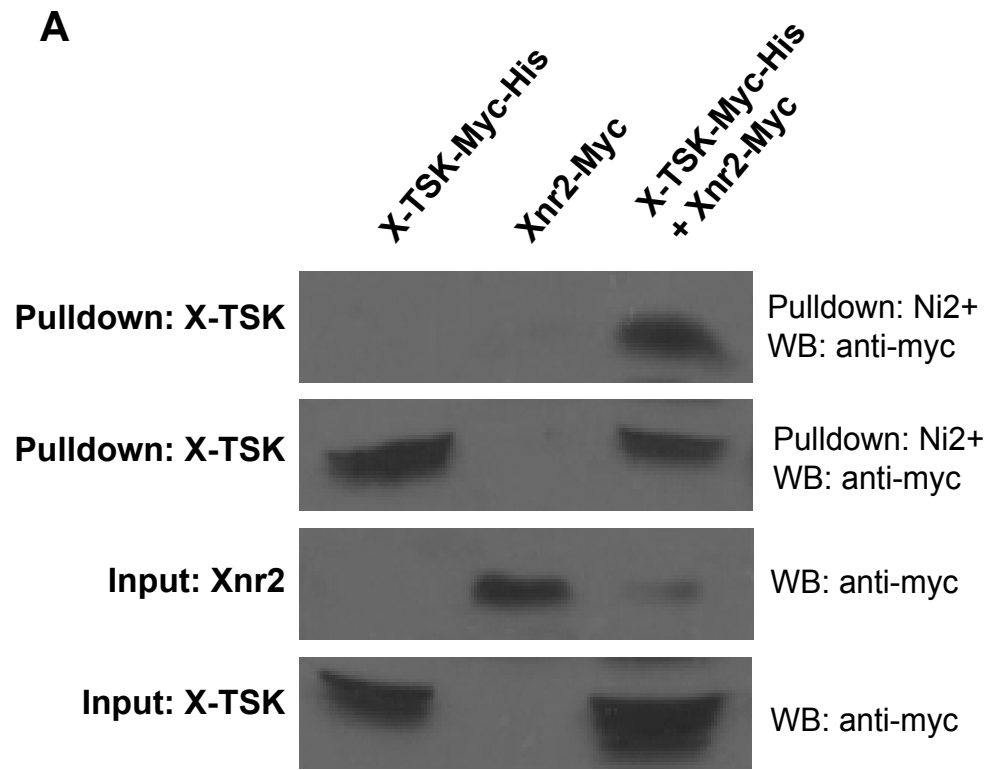


Figure 9.3: **Xnr2 is pulled down in complex with TSK**
(A) Western blotting for pull-down of Xnr2-Myc in complex with X-TSK-Myc-His (top, panel 1). Pull-down of X-TSK-Myc-His (Panel 2). Input of Xnr2-Myc into the pull-down reaction (Panel 3). Input of X-TSK-Myc-His into the pull-down reaction (Panel 4).

Pull-down of TSK is shown in the second panel (lanes 1 and 3). Inputs of Xnr2 and TSK into the pull-downs are shown in panels 3 and 4. This data indicates that TSK does indeed form a complex with Xnr2, in addition to other TGF- β family members such as BMP-2, BMP-4 and BMP-7 [Ohta et al., 2004], [Kuriyama et al., 2006]. In addition to this, complex formation with the EGF-CFC cofactor FRL1/CR1 was analysed as shown in Figure 9.4. This shows that FRL1/CR1 is also pulled down in complex with TSK, thus raising the possibility of ternary complex formation between TSK, Xnr2 and FRL1/CR1, which will require further investigation.

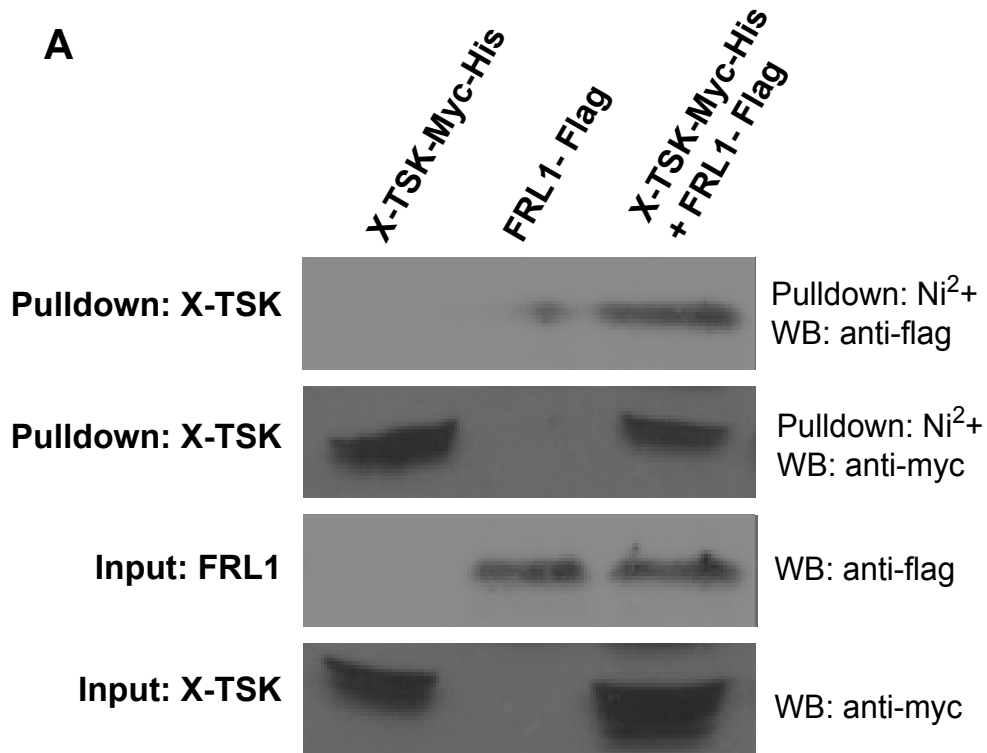


Figure 9.4: **FRL1/CR1 is pulled down in complex with X-TSK**
(A) Western blotting for pull-down of FRL1/CR1-Flag in complex with X-TSK-Myc-His (top, panel 1). Pull-down of X-TSK-Myc-His (Panel 2). Input of FRL1/CR1-Flag into the pull-down reaction (Panel 3). Input of X-TSK-Myc-His into the pull-down reaction (Panel 4).

9.6 Signalling downstream of the TSK-Xnr2 interaction

In order to analyse the possible functional interaction between TSK and Xnr2 in *Xenopus*, signalling pathways were analysed in *TSK* and *Xnr2* injected embryos, as in previous chapters. Namely, phosphorylation of Smad2, downstream of the ALK4 receptor for Xnr2 [Yeo and Whitman, 2001] and phosphorylation of MAPK. Activation of Xnr2 signalling activates Smad2 in addition to MAPK phosphorylation, where Ohkawara et al. [2004] have shown that activin signalling activates MAPK phosphorylation.

Figure 9.5 shows phosphorylated MAPK and phosphorylated Smad2 levels in *TSK* and *Xnr2* injected animal caps by Western blot analysis. Injection

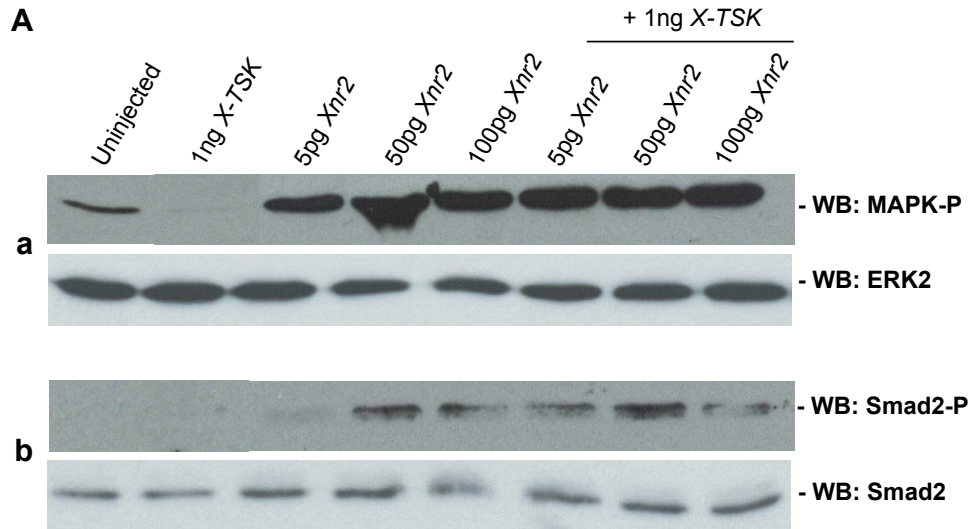


Figure 9.5: **MAPK and Smad2 signals downstream of TSK and Xnr2** (A) Western blotting of *TSK* (1ng) and *Xnr2* (5pg - 100pg) injected embryos probed for (a) phosphorylated MAPK (Upper panel) and ERK2 (Lower panel), (b) phosphorylated Smad2 (Upper panel) and total Smad2 (Lower panel).

of 1ng *TSK* inhibits MAPK phosphorylation (Panel a) as shown previously in chapter 8. Injection of 5, 50 and 100pg *Xnr2* activates MAPK phosphorylation, increasing slightly from 5pg to 100pg. Coinjection of *TSK* and *Xnr2* strikingly results in no inhibition of MAPK phosphorylation as seen with single overexpression of *TSK*. In terms of Smad2 phosphorylation, injection of 1ng *TSK* has relatively little effect in comparison to *Xnr2*. Injection of 5pg to 100pg *Xnr2*, as expected, activates Smad2 phosphorylation, peaking at 50pg *Xnr2*. With coinjection of *TSK* and *Xnr2*, phosphorylation of Smad2 is enhanced at 5pg and 50pg *Xnr2*, with no difference in levels detected at 100pg *Xnr2* with *TSK*. The ability of *Xnr2* to block MAPK phosphorylation inhibition by *TSK*, and the enhanced *Xnr2* activated Smad2 phosphorylation by *TSK* suggests that *TSK* potentiates *Xnr2* signalling in the *Xenopus* animal cap. To analyse this in further detail, a gain of function approach was carried out in the marginal zone of the whole embryo.

9.7 *Xbra* expression in *TSK* and *Xnr2* injected embryos

The approach of analysing the functional interaction between *TSK* and *Xnr2* in the marginal zone involves whole mount *in situ* hybridisation of *Xnr2* targets in *TSK* and *Xnr2* injected embryos, *Xbra*, *Gsc*, *Sox17 α* and *GATA4*.

Figure 9.6 A shows expression of *Xbra* in *TSK* and *Xnr2* injected embryos. Panels a, b and c show normal *Xbra* expression in β -Gal injected embryos around the blastopore of a stage 10.5 embryo. Injection of 1pg *Xnr2* dramatically expands *Xbra* expression through the animal hemisphere of the embryo. Similarly, injection of 10pg *Xnr2* expands *Xbra* expression although this is partially non-overlapping with the area of β -Gal expression. At levels of 100pg *Xnr2* injection, *Xbra* expression remains expanded into the animal hemisphere but clearly at lower levels than observed with the lower doses of *Xnr2* injected. Injection of 1ng *TSK* inhibits expression of *Xbra* as shown previously in chapter 6. Panels p, q and r show coinjection of 1ng *TSK* and 1pg *Xnr2*. Expression of *Xbra* is expanded although in comparison to expression of 1pg *Xnr2* alone, this expansion is restricted in the animal hemisphere, especially in the targeted area as shown by β -Gal staining. This is also seen with coinjection of *TSK* and 10pg *Xnr2* where overall expression of *Xbra* expression appears weaker, this phenotype becomes more pronounced with coinjection of *TSK* and 100pg *Xnr2*.

9.8 *Gsc* expression in *TSK* and *Xnr2* injected embryos

Figure 9.7 A shows expression of the dorsal mesoderm marker, *Gsc* in *TSK* and *Xnr2* injected embryos. Panels a, b and c show normal *Gsc* expression in β -Gal injected embryos in the dorsal blastopore lip of a stage 10.5 embryo. Injection of 1pg *Xnr2* slightly expands *Gsc* expression beyond the normal domain of expression. Similarly, injection of 10pg *Xnr2* expands *Gsc* expression further into the animal hemisphere. At levels of 100pg *Xnr2* injection, *Gsc* expression remains expanded into the animal hemisphere at levels similar to 10pg *Xnr2*. Injection of 1ng *TSK* expands expression of *Gsc* in a small proportion of embryos

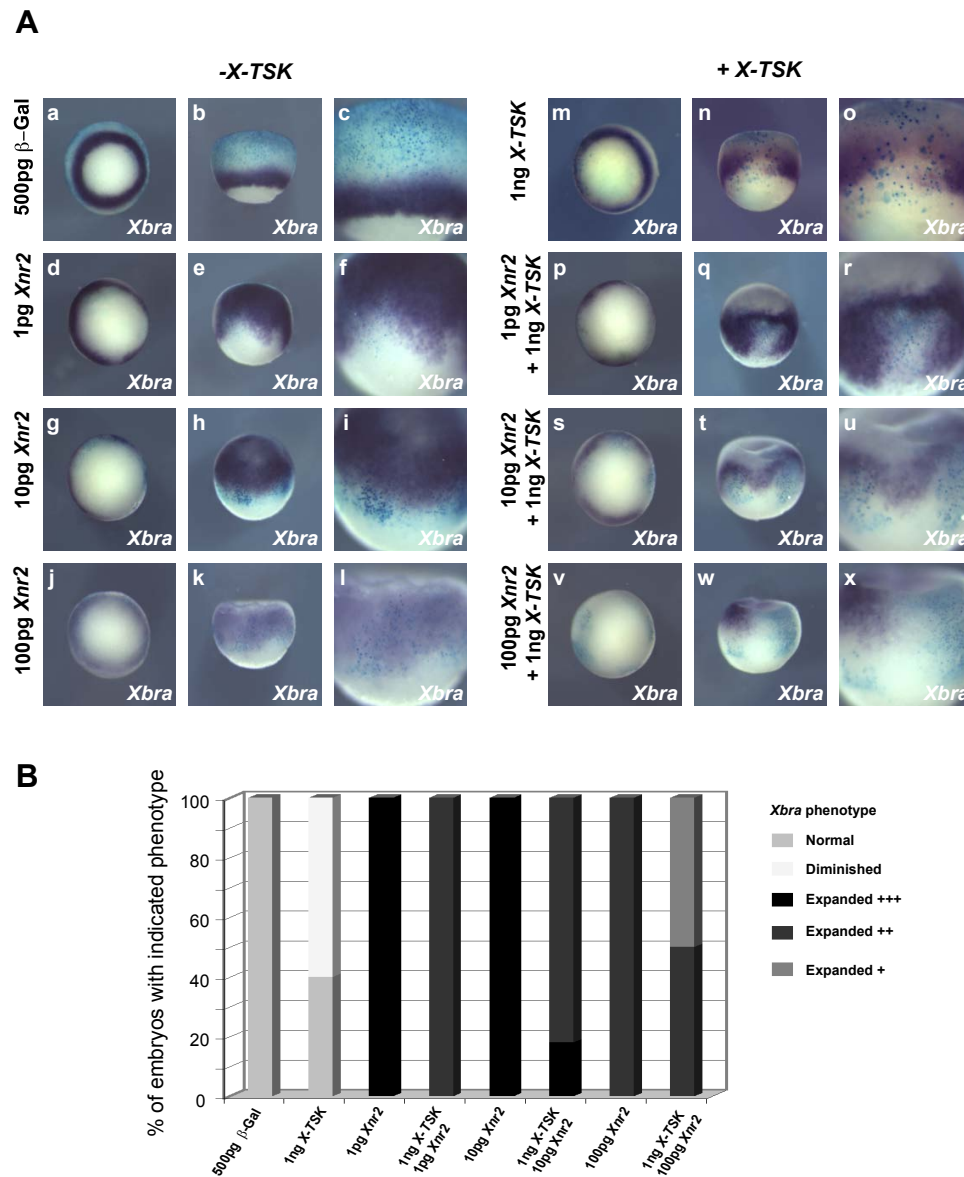


Figure 9.6: *Xbra* expression in *TSK* and *Xnr2* injected embryos
(A) Whole mount *in situ* hybridisation for *Xbra* in *TSK* and *Xnr2* injected embryos. Left panels, β -Gal (a, b, c), 1pg *Xnr2* (d, e, f), 10pg *Xnr2* (g, h, i) and 100pg *Xnr2* injected embryos (j, k, l). Right panels, coinjection of 1ng *TSK* with β -Gal (m, n, o), 1pg *Xnr2* (p, q, r), 10pg *Xnr2* (s, t, u) and 100pg *Xnr2* (v, w, x). In each set of panels, vegetal view (First column), lateral view (Second column), lateral zoom (Third column). **(B)** Graphical representation of *Xbra* phenotype frequency arising from *TSK* and *Xnr2* injected embryos, n = 50 to 60.

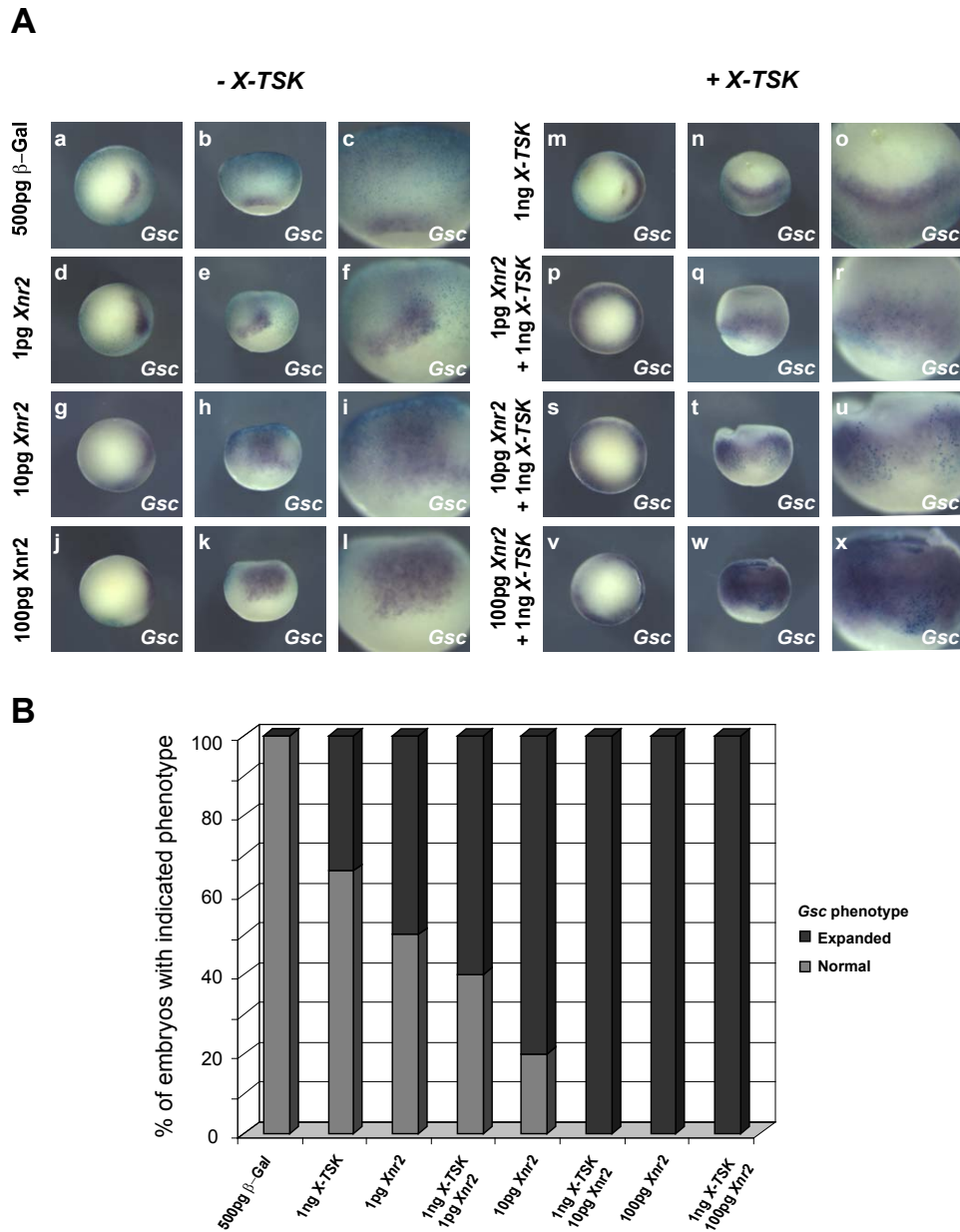


Figure 9.7: *Gsc* expression in *TSK* and *Xnr2* injected embryos
(A) Whole mount *in situ* hybridisation for *Gsc* in *TSK* and *Xnr2* injected embryos. Left panels, β -Gal (a, b, c), 1pg *Xnr2* (d, e, f), 10pg *Xnr2* (g, h, i) and 100pg *Xnr2* injected embryos (j, k, l). Right panels, coinjection of 1ng *TSK* with β -Gal (m, n, o), 1pg *Xnr2* (p, q, r), 10pg *Xnr2* (s, t, u) and 100pg *Xnr2* (v, w, x). In each set of panels, vegetal view (First column), lateral view (Second column), lateral zoom (Third column). **(B)** Graphical representation of *Gsc* phenotype frequency arising from *TSK* and *Xnr2* injected embryos, n = 50 to 60.

as shown previously in chapter 6. Panels p, q and r show coinjection of 1ng *TSK* and 1pg *Xnr2*. Expression of *Gsc* is expanded much further in comparison to injection of 1pg *Xnr2* alone. This is also seen with coinjection of *TSK* and 10pg *Xnr2* where overall expression of *Gsc* expression is elevated, this phenotype becomes more pronounced with coinjection of *TSK* and 100pg *Xnr2*, where strong expansion and expression of *Gsc* is clear.

9.9 *Sox17 α* expression in *TSK* and *Xnr2* injected embryos

Figure 9.8 A shows expression of the endoderm marker, *Sox17 α* in *TSK* and *Xnr2* injected embryos. Panels a, b and c show normal *Sox17 α* expression in β -Gal injected embryos in and around the blastopore of a stage 10.5 embryo. Injection of 1pg *Xnr2* slightly expands *Sox17 α* expression beyond the normal domain of expression. Similarly, injection of 10pg *Xnr2* expands *Sox17 α* expression further into the animal hemisphere. At levels of 100pg *Xnr2* injection, *Sox17 α* expression remains expanded into the animal hemisphere at levels similar to 10pg *Xnr2*. Injection of 1ng *TSK* expands expression of *Sox17 α* as shown previously in chapter 6. Panels p, q and r show coinjection of 1ng *TSK* and 1pg *Xnr*. Expression of *Sox17 α* is expanded, although in a much more restricted domain in comparison to injection of 1pg *Xnr2* alone. This is also seen with coinjection of *TSK* and 10pg *Xnr2* where overall expression of *Sox17 α* expression is less diffuse than with 10pg *Xnr2* alone.

9.10 *GATA4* expression in *TSK* and *Xnr2* injected embryos

Figure 9.9 A shows expression of the endoderm marker, *GATA4* in *TSK* and *Xnr2* injected embryos. Panels a, b and c show normal *GATA4* expression in β -Gal injected embryos in and around the blastopore of a stage 10.5 embryo. Injection of 1pg *Xnr2* only very slightly expands *GATA4* expression beyond the normal domain of expression. Injection of 10pg *Xnr2* expands *GATA4* expression further into the animal hemisphere. At levels of 100pg *Xnr2* injection,

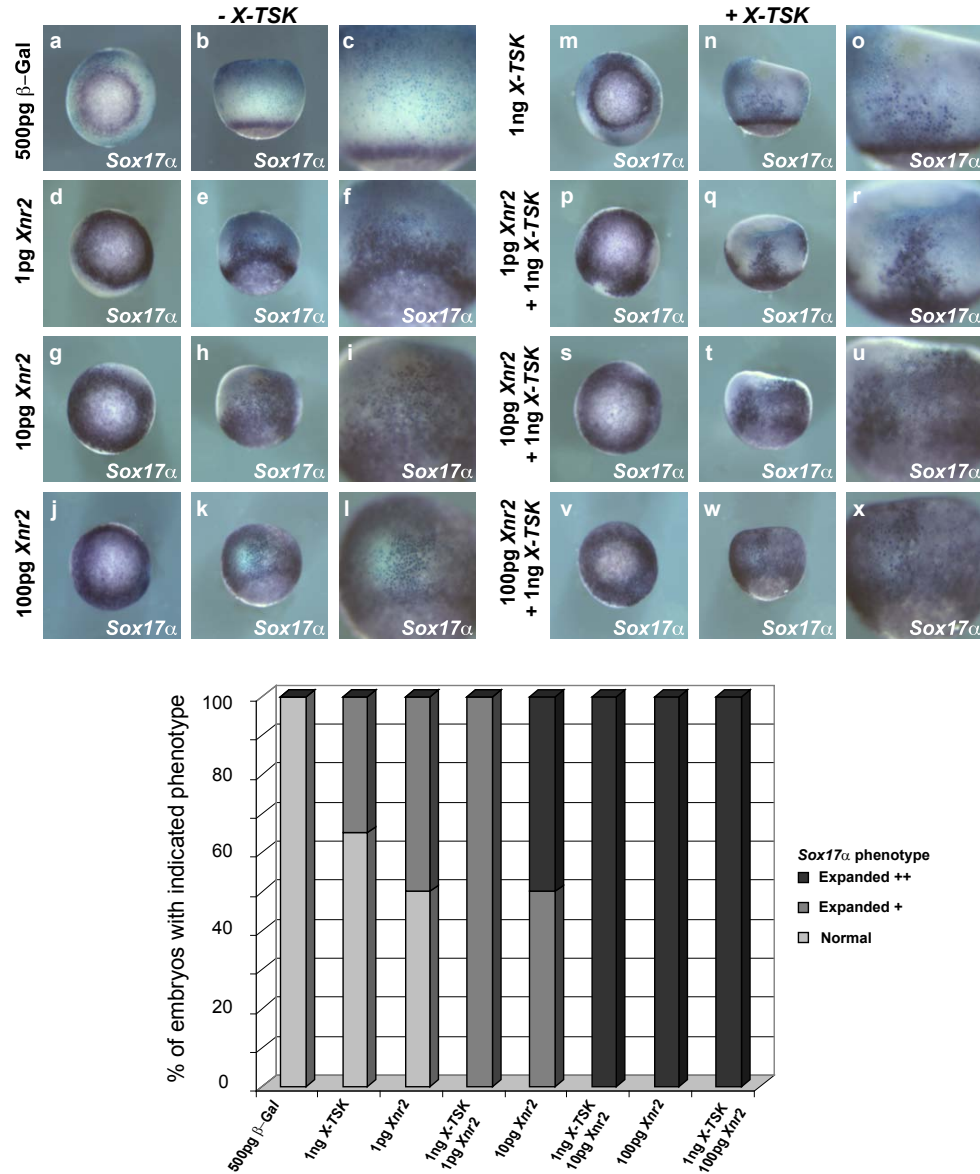


Figure 9.8: *Sox17 α* expression in *TSK* and *Xnr2* injected embryos
(A) Whole mount *in situ* hybridisation for *Sox17 α* in *TSK* and *Xnr2* injected embryos. Left panels, β -Gal (a, b, c), 1pg *Xnr2* (d, e, f), 10pg *Xnr2* (g, h, i) and 100pg *Xnr2* injected embryos (j, k, l). Right panels, coinjection of 1ng *TSK* with β -Gal (m, n, o), 1pg *Xnr2* (p, q, r), 10pg *Xnr2* (s, t, u) and 100pg *Xnr2* (v, w, x). In each set of panels, vegetal view (First column), lateral view (Second column), lateral zoom (Third column). **(B)** Graphical representation of *Sox17 α* phenotype frequency arising from *TSK* and *Xnr2* injected embryos, n = 50 to 60.

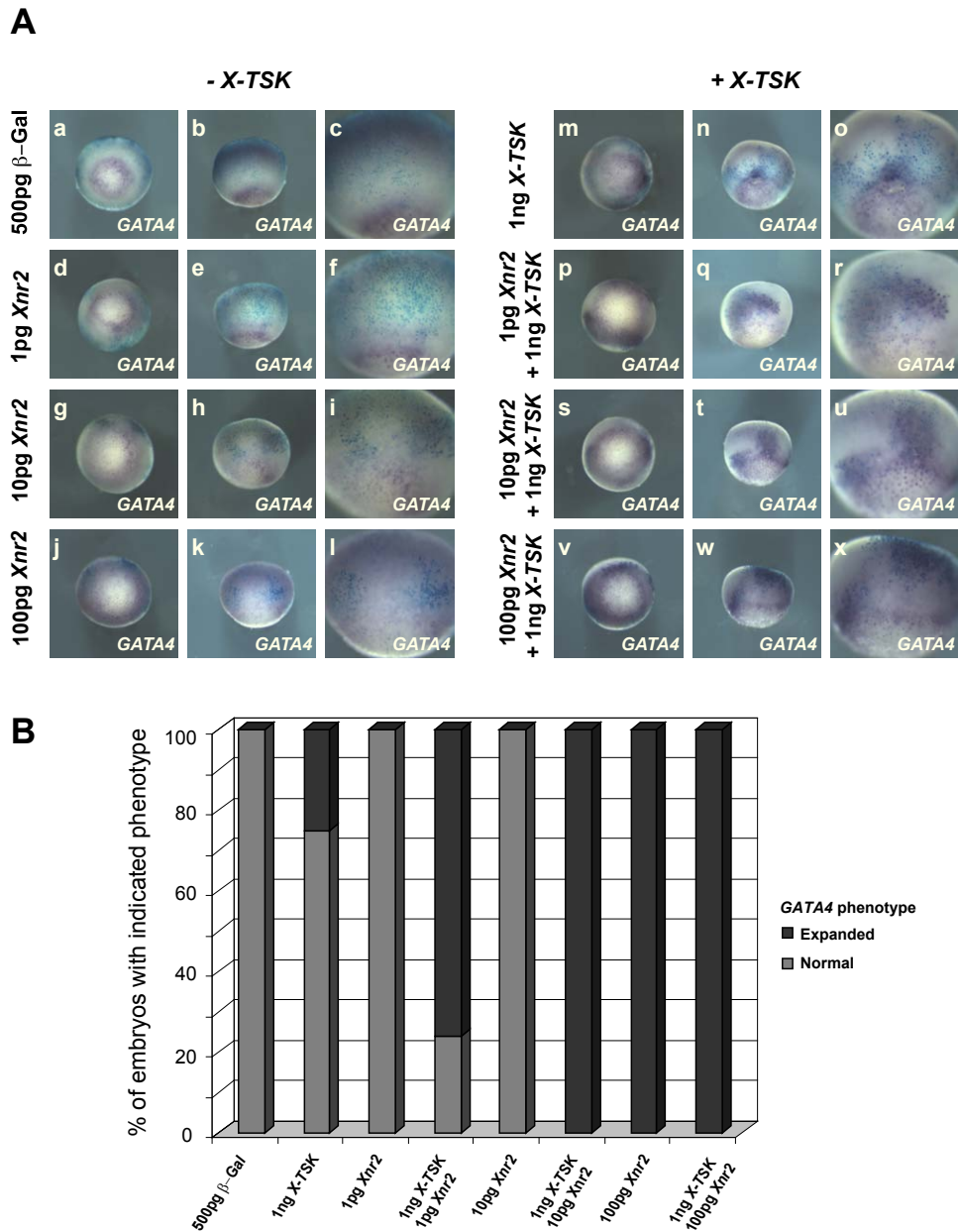


Figure 9.9: *GATA4* expression in *TSK* and *Xnr2* injected embryos
(A) Whole mount *in situ* hybridisation for *GATA4* in *TSK* and *Xnr2* injected embryos. Left panels, β -Gal (a, b, c), 1pg *Xnr2* (d, e, f), 10pg *Xnr2* (g, h, i) and 100pg *Xnr2* injected embryos (j, k, l). Right panels, coinjection of 1ng *TSK* with β -Gal (m, n, o), 1pg *Xnr2* (p, q, r), 10pg *Xnr2* (s, t, u) and 100pg *Xnr2* (v, w, x). In each set of panels, vegetal view (First column), lateral view (Second column), lateral zoom (Third column). **(B)** Graphical representation of *GATA4* phenotype frequency arising from *TSK* and *Xnr2* injected embryos.

GATA4 expression is expanded into the animal hemisphere even further than 10pg *Xnr2*. Injection of 1ng *TSK* expands expression of *GATA* as shown previously in chapter 6. Panels p, q and r show coinjection of 1ng *TSK* and 1pg *Xnr2*. Expression of *GATA4* is strongly induced in comparison to 1pg *Xnr2* alone. This is also seen with coinjection of *TSK* and 10pg and 100pg *Xnr2* where expression of *GATA4* expression is enhanced in comparison to expression of *Xnr2* alone.

Interaction with EGF-CFCs

These data, showing 1) inhibition of nodal signalling blocks *TSK* function, 2) *Xnr2* partially rescues *TSK* morpholino depletion of endoderm markers 3) *TSK* is pulled down in complex with *Xnr2* and *FRL1/CR1*, 4) *TSK* potentiates nodal signalling and 5) results in enhanced induction of mesoderm and endoderm markers strongly indicates that *TSK* functions with nodal signalling in the *Xenopus* embryo. Functional interaction with EGF-CFC family members, *FRL1/CR1* and *CR3s* was also analysed (Figure 9.10) although the phenotypes were not very clear, hence this area requires further investigation.

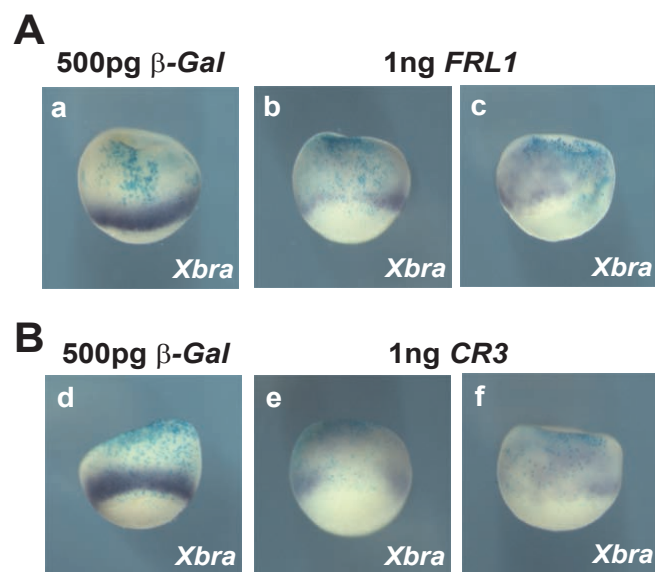


Figure 9.10: *Xbra* expression in *FRL1/CR1* and *CR3s* injected embryos
A Expression of *FRL1* (panels a, b). **B** Expression of *CR3s* (panels c, d)
 Orientation: Lateral, animal top, vegetal bottom.

9.11 Interaction between nodal, BMP and FGF signalling in endoderm formation

TSK can clearly enhance nodal signalling to induce expression of endoderm markers, as demonstrated in this chapter. Inhibition of nodal signalling blocks the ability of TSK to induce endoderm (Figure 9.1, page 114) whilst activation of BMP signalling and FGF signalling (Figures 6.7 , page 83 and 8.9 , page 110 respectively) partially blocks TSK function in the endoderm. This suggests that TSK multiply coordinates nodal, BMP and FGF signalling in endoderm induction. This is supported by findings in Zebrafish showing that endoderm formation is regulated by the combined activation of nodal signalling with inhibition of FGF and BMP signalling [Poulain et al., 2006]. Although this has yet to be confirmed in *Xenopus*, figure 9.11 shows the effect of combined nodal, BMP and FGF signal regulation on endoderm marker induction. Individual expression of *Xnr2*, *tBR* or *XFD* has very little effect. The strongest induction of *Sox17 α* expression is produced by overexpression of all three components, thus supporting the findings in Zebrafish. The activity of TSK to activate nodal signalling whilst inhibiting BMP and FGF signalling fits well with this model of endoderm induction.

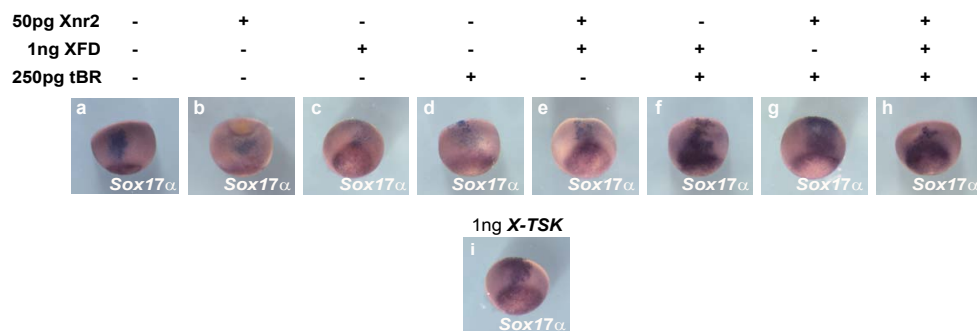


Figure 9.11: *Sox17 α* expression in *Xnr2*, *tBR* and *XFD* injected embryos
A Expression of *Sox17 α* (panels a, b). Orientation: Lateral, animal top, vegetal bottom.

Chapter 10

Regulation of TSK expression

10.1 TSK expression is regulated by FGF-MAPK, Vg1 and Notch signalling activities in the embryo

As shown in chapter 8, overexpression of TSK in *Xenopus* marginal zone inhibits expression of *Xbra* expression through inhibition of FGF-MAPK signalling. In the *Xenopus* embryo, *TSK* is expressed in ectoderm, dorsal mesoderm and endoderm with far lower levels of expression in the lateral and ventral marginal zone. In contrast to this, MAPK is activated in the marginal zone [Schohl and Fagotto, 2002], thus raising the possibility that TSK may be largely excluded from the marginal zone to maintain activity of FGF signalling. Therefore it must be asked if TSK expression is regulated by FGF-MAPK activity in the embryo.

Figure 8.8 shows whole mount *in situ* hybridisation of *TSK* in *Xenopus* embryos injected with XFD, vras and caFGFR. Inhibition of FGF-MAPK signalling by the dominant negative FGF receptor, XFD, produces a more intense TSK expression in the animal hemisphere of the embryo. In contrast to this, activation of FGF-MAPK signalling with caFGFR or vras produces a lighter staining of *TSK*. This suggests that FGF-MAPK activity downregulates *TSK* expression in the *Xenopus* embryo. In addition to this, preliminary data shown below indicates that Vg1 activates expression of TSK, whereas activated notch signalling via the notch intracellular domain construct inhibits expression of *TSK*. This preliminary observation with notch signalling is very interesting as

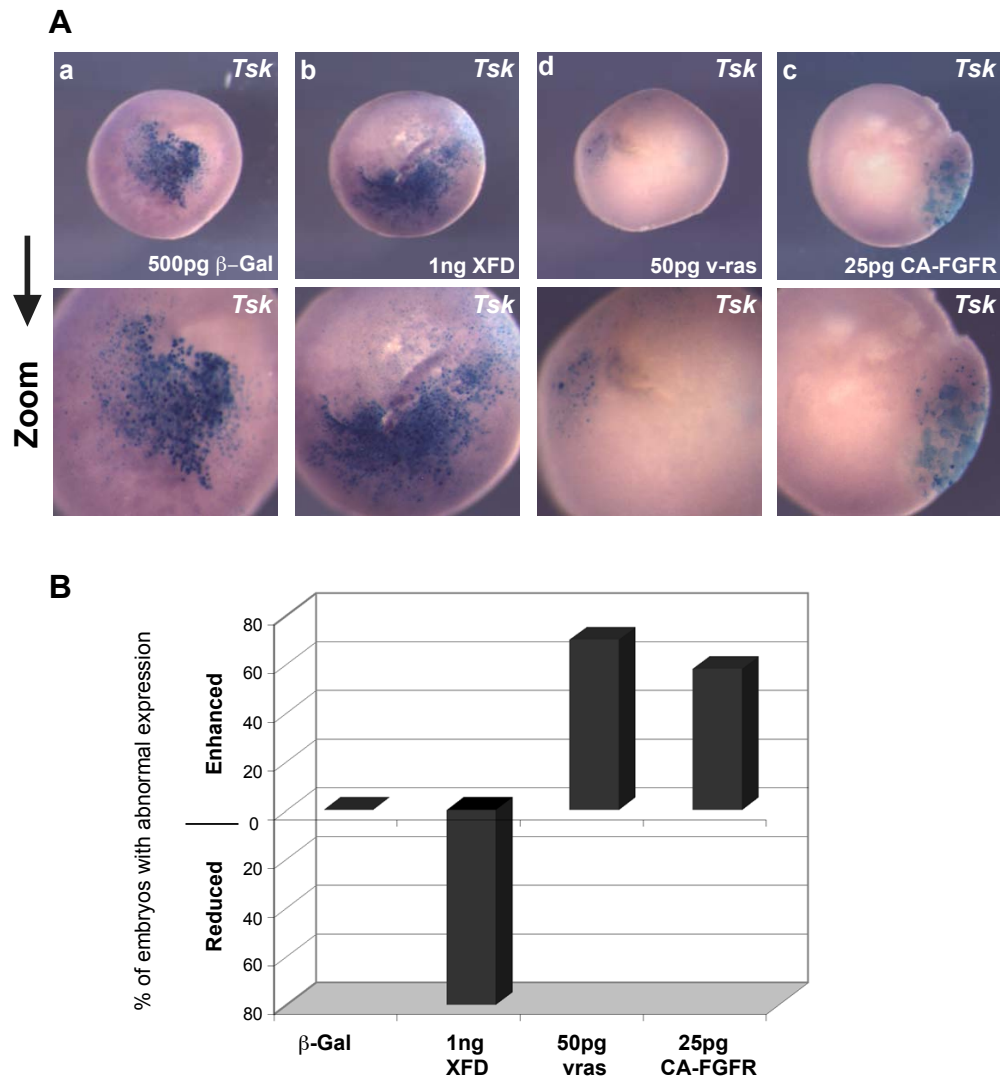


Figure 10.1: *TSK* expression is regulated by MAPK activity
 (A) Whole mount *in situ* hybridisation of *TSK* in XFD, vras and caFGFR injected embryos. (B) Graphical representation of phenotypes arising in (A).
 Orientation: animal view.

it has been shown in sea urchin that notch signalling regulates position of the ectoderm-endoderm boundary [Sherwood and McClay, 2001]. Thus it will be interesting to study the potential function of TSK with notch in this context.

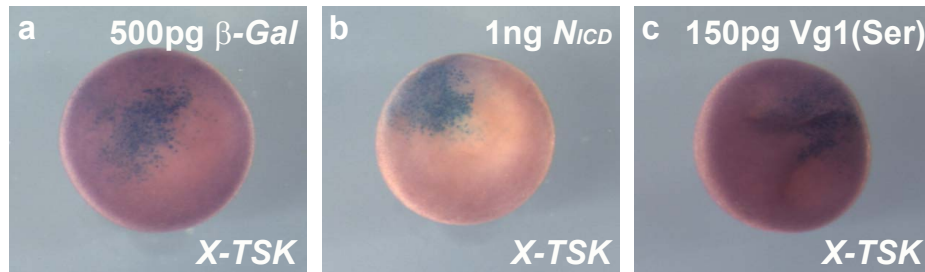


Figure 10.2: ***TSK* expression is regulated by Vg1 and Notch activity**
(A) Whole mount *in situ* hybridisation of *TSK* in β -Gal, Notch Intracellular Domain and Vg1 injected embryos. (B) Graphical representation of phenotypes arising in (A). Orientation: animal view.

Part V

Discussion

Chapter 11

Discussion

11.1 TSK features and expression pattern

11.1.1 TSK is a secreted proteoglycan belonging to the SLRP family

SLRPs are post-translationally modified by the addition of oligosaccharides and dermatan/keratan sulphates in some cases [Hocking et al., 1998, Iozzo, 1997]. Expression of both *C-TSK* and *X-TSK-B1* in the *Xenopus* embryo yields three clear bands corresponding to TSK, as seen by Western blotting which indicate as many different types of modification. Removal of N-linked carbohydrates with PNGaseF results in collapse of the bands into one faster-migrating band, suggesting that all the identified bands are due to N-linked glycosylation (See Figure 5.4, page 62). Further analysis of other potential sugar modifications will be required. Decorin has been shown to be differentially post-translationally modified in a context-specific manner [Blochberger et al., 1992] and it will be interesting to see if the same applies to TSK, and indeed, the importance of these post-translational modifications for TSK function.

The originally identified chick *TSK* gene encodes for a 369 amino acid secreted protein. *TSK* orthologues have been identified in 13 organisms at present, ranging from 333 to 369 amino acids in length. Sequence analysis of *TSK* orthologues identifies 12 LRRs within the sequence between N- and C- terminal cysteine rich clusters (See Figure 5.2, page 60). This in combination with the potential sugar modification sites identifies TSK as belonging to the SLRP family of secreted proteoglycans. Members of this family, biglycan, decorin and fibro-

modulin have previously been found to bind to TGF- β [Hildebrand et al., 1994] and decorin in particular inhibits TGF- β signalling in Chinese hamster ovary cells [Yamaguchi et al., 1990]. Recently, biglycan has been shown to interact with BMP and chordin in a similar manner to TSK in *Xenopus* [Moreno et al., 2005]. Members of the SLRP family, including TSK are emerging as important regulators of TGF- β superfamily signalling. The N-terminal cysteine-rich cluster of TSK has a unique consensus (C-X₃-C-X-C-X₁₇-C) to those of other SLRPs for TSK to form a new branch of the family (See Figure 5.3, page 61). Even so, TSK shares a similarity of function with members such as biglycan in development, although there are differences in expression pattern. It will remain to be seen if further members of the SLRP family play significant roles during early development, and there may be redundancy between family members to consider. All members of the SLRP family are secreted, although the extent to which TSK is secreted and diffuses, or remains close to the source cell remains to be determined.

Differences between TSK A and B forms

Two forms of TSK, generated by alternate splicing have been identified in chick (C-TSK-A and C-TSK-B, Figure 5.5, page 64). In addition to differential expression of *TSK* isoforms in the chick embryo, functional analysis in *Xenopus* has shown crucial differences in TSK isoform activity. Microinjection of *C-TSK-A* mRNA results in axis duplication in *Xenopus* [Ohta et al., 2004]. In contrast to this, microinjection of *C-TSK-B* does not result in axis duplication, as is also the case upon microinjection of both *X-TSK-B1* and *X-TSK-B2* (Kunimasa Ohta, unpublished data and also shown in Figure 6.1, page 73). In addition to this, other TSK orthologues (Z-TSK and H-TSK) have been shown to lack the axis duplication properties of C-TSK-A (Kunimasa Ohta, unpublished). The functional differences between TSK A and B isoforms may be due to their differential abilities to antagonise BMP signalling. It is postulated that the weaker BMP antagonism by TSK B isoforms leads to the inability to suppress BMP signals to a level to permit axis duplication. While this may be the case,

at present, other unidentified functional differences between the isoforms leading to these phenotypic differences cannot be ruled out, because excess TSK-B cannot induce secondary axes even though Smad1 phosphorylation is strongly inhibited.

11.2 Expression and function of TSK in early *Xenopus* development

11.2.1 *TSK* is expressed maternally and zygotically in the ectoderm

TSK is clearly expressed in the animal hemisphere prior to the mid-blastula transition and *TSK* expression is also detected in the egg, suggesting that *TSK* is maternally expressed in this location. In addition to this, *TSK* expression is maintained in the ectoderm post-MBT, this zygotic expression persisting throughout gastrulation. Figures 5.6, 5.7 and 5.8, pages 66, 69 and 71 respectively.

Maternal TSK expression

Maternal mRNAs play important roles in determination of cell fate. *VegT* is such a maternal determinant coding for a transcription factor which is localised to the vegetal region [Zhang and King, 1996, Stennard et al., 1999]. At MBT, VegT activates expression of many zygotic genes excluded from the ectoderm [Xanthos et al., 2002]. The expression patterns of *VegT* and *TSK* are largely non-overlapping, and thus the function of *TSK* pre-MBT may lie with other maternal determinants and pathways. Good candidates for maternal TSK function are localised to the animal hemisphere, i.e. BMPs which are also maternally encoded. It has been hypothesised that maternal BMP proteins activate the first signal transduction events in the Smad1 pathway [Heasman, 2006]. As BMPs are capable of inducing mesoderm, their activity must be inhibited to maintain the fate of the ectoderm, where they are expressed at high levels [Fainsod et al., 1994].

Ectodermin is one example of a maternally encoded ectoderm localised in-

hibitor of BMP signalling. Ectodermin inhibits the cellular response to mesoderm-inducers of the TGF- β superfamily by promoting the degradation of Smad4 [Dupont et al., 2005]. Coco is a second example of a maternal ectodermally localised BMP inhibitor which functions to maintain the competence of the ectoderm [Bell et al., 2003]. As TSK is known to inhibit BMP signalling, maternal TSK may also function to inhibit BMP in the ectoderm and thus contribute to the maintenance of ectodermal competence. In addition to this, TSK also inhibits FGF-MAPK signalling (Chapter 8) which is required for mesoderm formation [Amaya et al., 1991, 1993]. Hence is is a possibility that TSK may also play a role in ectodermal competence in this manner also. In order to test these possibilities, TSK will have to be depleted with antisense morpholino in oocytes followed by analysis of relative mesoderm/ectoderm formation in the corresponding maternal *TSK* depleted embryos.

Zygotic TSK expression in the ectoderm

Zygotic *TSK* expression in the ectoderm clearly persists post-MBT, through gastrula stages of development. This expression pattern supports previous evidence for TSK acting as a BMP inhibitor, and thus it can be proposed that a major role for zygotic TSK in patterning the ectoderm is related to its BMP inhibitory activity. This has been demonstrated in previous work by Kuriyama et al. [2006] in which depletion of TSK with morpholino influences the balance between epidermis and neural ectoderm by modulation of BMP signalling. In addition to this, BMP signalling has been shown to induce *TSK* expression, which may explain the presence of *TSK* throughout the ectoderm. Other examples of BMP inhibitors expressed in the ectoderm include Coco and FRL1/CR1 which act to lower overall levels of BMP signals and facilitate neural induction [Bell et al., 2003], [Yabe et al., 2003]. TSK may also be acting in the same way, as it has also been shown to directly induce neural tissue [Ohta et al., 2004].

11.2.2 *TSK* is expressed in dorsal mesoderm and may play a role in dorsal patterning

In addition to expression in endoderm tissue, *TSK* expression in the dorsal mesoderm (Figure 5.6, page 66) suggests that *TSK* may also play a role in organiser activities and patterning of the mesoderm. Again, this hypothesis is supported by the fact that *TSK* inhibits BMP in cooperation with Chordin [Ohta et al., 2004]. BMP signalling and chordin are well-known to play important roles in patterning the mesoderm in terms of dorsal-ventral polarity (reviewed in Robertis et al. [2000] and Robertis and Kuroda [2004]).

TSK expression in the dorsal mesoderm overlaps with expression of the dorsal mesoderm markers *Gooseoid* [Cho et al., 1991] and *Chordin* [Sasai et al., 1994], and non-overlapping with *MyoD* [Hopwood et al., 1989b, Steinbach et al., 1998] expression. *TSK* may function with dorsal mesoderm inducers, such as members of the TGF- β superfamily. One such candidate, also detected in the endoderm is *Xnr2*, expressed in the dorsal mesoderm in addition to the endoderm [Jones et al., 1995]. Several BMP inhibitors function in the dorsal region, including chordin, noggin and follistatin, to oppose BMP signalling. Thus, *TSK* may also play a role in dorsal-ventral patterning of the mesoderm through its capacity to inhibit BMP in cooperation with chordin, and possibly other members of the TGF- β superfamily such as *Xnr2*.

TSK expands expression of the organizer-specific gene, *gooseoid*

Antisense morpholino depletion of *TSK* from the dorsal region diminishes *Gsc* expression (Figure 7.3, page 87). Conversely, overexpression of *TSK* in the dorsal region expands expression of the organizer-specific marker, *Gsc* (Figure 6.2, page 75). This suggests that *TSK* is indeed involved in the formation and function of the organizer and mesoderm patterning.

The organizer is responsible for induction of dorsal ectoderm into neural tissue, formation of the anteroposterior body axis from the surrounding mesoderm, initiation of gastrulation movements, whilst itself differentiates into dorsal mesoderm derivatives [Harland and Gerhart, 1997]. As *TSK* can function

as a direct neural inducer [Ohta et al., 2004], this complements the activity of the organizer. Overexpression of *Xenopus TSK* in the ventral marginal zone cannot induce secondary axis formation and in addition to this, cannot directly induce dorsal mesoderm in animal cap explants [Ohta et al., 2004]. Also, we have only observed an expansion of *Gsc* expression (Figure 6.2, page 75) but no ectopic induction of *Gsc* expression outside the dorsal region (data not shown). Goosecoid is an important component of organizer formation [Robertis et al., 1992] and has the ability to induce a complete secondary axis [Cho et al., 1991]. Thus the absence of secondary axis formation and ectopic *Gsc* expression is suggesting that TSK alone is not sufficient for organizer induction.

In consideration of the mechanism by which TSK may participate with the function of the organizer, inhibition of BMP by TSK is again a possible factor. BMP signalling in the embryo suppresses dorsal fate specification. Dorsal-ventral patterning of the mesoderm is executed in part by BMP inhibitors expressed in the organizer region to define the dorsal territory [Robertis and Kuroda, 2004, Harland and Gerhart, 1997]. Thus TSK may function to provide further BMP inhibition in the dorsal region to pattern the mesoderm, this seems reasonable as several redundant mechanisms are employed in the dorsal region to inhibit BMP signalling [Robertis and Kuroda, 2004, Harland and Gerhart, 1997].

From the evidence we have thus far on the role of TSK in organizer formation and function, it is difficult to determine exactly where TSK may be acting. It is possible that TSK is a component in the initial induction of the organizer. Although it may be just as likely that TSK lies downstream of organizer induction and is more involved in the functions of the organizer. This does not rule out the initial steps of induction, thus positive factors in this process should be considered, such as nodals which are expressed in the Nieuwkoop center and induce the Spemann organizer in overlying cells [Agius et al., 2000, Takahashi et al., 2000]. Data presented in Chapter 9 demonstrates that TSK can potentiate nodal signalling, and thus this may be an important part of the mechanism of TSK function in the dorsal region. In addition to this, prelimi-

nary data shows that *Vg1* induces expression of *TSK* (Figure 10.2, page 130), which places *TSK* in the *Vg1*-Nodal pathway of mesoderm formation. Further work is required with additional markers of both dorsal and ventral mesoderm markers to determine more precisely the mechanism and timing of *TSK* action in this context.

11.2.3 Expression levels of *TSK* are diminished in ventro-lateral mesoderm where *TSK* functions to inhibit mesoderm formation

TSK expression levels are markedly decreased in the lateral and ventral mesoderm in comparison to dorsal mesoderm during gastrulation (Figure 5.6, page 66). This raises the possibility that *TSK* must be downregulated in this region of marginal zone for mesoderm formation to proceed. Overexpression of *TSK* in the marginal zone inhibits expression of the early immediate mesoderm gene, *Xbra* (Figure 6.2, page 75) and inhibits expression of *MyoD* (Figure 6.4, page 78) in the area of lateral/ventral mesoderm. Conversely, depletion of *TSK* with antisense morpholino expands the area of later *MyoD* expression (Figure 7.1, page 85) and in a small number of cases expands *Xbra* (Figure 7.2, page 86) expression, suggesting indeed that *TSK* may function to constrain lateral/ventral mesoderm formation.

Interestingly depletion of *TSK* with antisense morpholino in and around the marginal zone, and in endoderm has only a minor effect on *Xbra* expression in the early gastrula. This indicates that depletion of *TSK* is not sufficient to induce ectopic *Xbra* expression¹. It may be the case that another positive factor is required in order for mesoderm to be induced, thus depletion of *TSK* alone is not sufficient to induce ectopic mesoderm. Depletion of *TSK* would be expected to expand mesoderm as higher levels of BMP signalling are expected in this situation, although activation of BMP may not expand mesoderm itself. It is also a possibility that *TSK* interacts with other pathways involved in mesoderm formation/patterning and hence depletion of *TSK* is unpredictable in this respect. In addition to this, *TSK* depletion may not show an expansion

¹The morpholino has been shown to be sufficient to inhibit *TSK* function in studies on the epidermis and neuroectoderm [Kuriyama et al., 2006]

of mesoderm as another negative factor upon mesoderm formation may have to be removed for an effect. Examples of such factors include the B2 form of X-TSK or other members of the SLRP family such as biglycan². Thus depletion of TSK in combination with depletion of these additional candidates will have to be performed to learn more about the mechanism and possible redundancy of TSK in inhibition of mesoderm formation.

TSK may be inhibiting mesoderm formation via several mechanisms. Primarily, the inhibition of BMP signalling by TSK must be considered as BMPs are mesoderm inducers [Köster et al., 1991] thus inhibition of BMP by TSK may lead to inhibition of mesoderm formation, although this is not the case as will be discussed shortly. Other candidates include other mesoderm inducing factors of the TGF- β superfamily such as activin [Green and Smith, 1990, Arizumi et al., 1991], Vg1 [Kessler and Melton, 1995, Melton, 1987, Thomsen and Melton, 1993, Weeks and Melton, 1987] and Nodals [Jones et al., 1995, Joseph and Melton, 1997, Takahashi et al., 2000]. FGF signalling is also required for mesoderm formation [Amaya et al., 1991, 1993] and thus this pathway is also a candidate in the mechanism of TSK-mediated mesoderm inhibition as TSK inhibits FGF-MAPK signalling (Figure 8.2, page 98) and its expression is regulated by FGF-MAPK activity (Figure 10.1, page 129). The link between *Xbra* expression and *Gsc* should also be considered as *Gsc* can inhibit expression of *Xbra* [Artinger et al., 1997, Latinkic and Smith, 1999]. This could be a possible mechanism by which TSK inhibits *Xbra* expression, but this does not seem likely as *Gsc* expression is only expanded, ectopic expression is not induced outside the dorsal region where *Xbra* downregulation is observed.

11.2.4 *TSK* is expressed in the endoderm and has a role in induction of endoderm tissue

The presence of *TSK* in the vegetal region during endoderm formation (Figures 5.6, 5.7, pages 66 and 5.7 respectively) suggests that TSK may play a role in this aspect of germ layer patterning. This suggestion that TSK may be involved

²Depletion of biglycan shows no phenotype, redundancy with TSK has been suggested by the authors, Moreno et al. [2005]

in establishment/ patterning of the endoderm is supported by overexpression of TSK in the marginal zone, resulting in ectopic expression of the endoderm markers *Sox17 α* and *GATA4* (Figure 6.2, page 75). In addition to this, loss of TSK function in the endoderm with antisense morpholino against TSK results in loss of endoderm markers (Figure 7.4, page 88) and a reduction in gut size in later stages of development (Figure 7.5, page 90). This is supported by the fact that TSK has previously been established to inhibit BMP in cooperation with Chordin [Ohta et al., 2004]. Both BMP signalling and chordin have been implicated in endoderm formation [Poulain et al., 2006, Sasai et al., 1996]. In addition to this, data in Chapter 9 demonstrates that TSK can potentiate nodal signalling, a key player in endoderm formation [Yasuo and Lemaire, 1999, Clements et al., 1999, Takahashi et al., 2000]. In order to understand this in further detail, this must be considered in the context of the endoderm induction mechanism.

TSK expression in the vegetal region/endoderm overlaps with expression of the endoderm markers *Sox17 α* and *GATA4* [Hudson et al., 1997], [Afouda et al., 2005] (Figure 5.7, page 69), and TGF- β superfamily members/endoderm inducers Vg1 [Melton, 1987, Weeks and Melton, 1987] and Xnrs [Yasuo and Lemaire, 1999]. The vegetally localised T-box transcription factor, *VegT* is essential for initiation of endoderm formation by activating expression of *Xnr* family members, *Derrière* and *Sox17* [Zhang et al., 2005, Clements et al., 1999, Kofron et al., 1999, Engleka et al., 2001, Xanthos et al., 2001, 2002]. At the early blastula stage, this achieves a high level of TGF- β signalling [Agius et al., 2000, Clements et al., 1999]. *Sox17* expression is activated early by VegT, with later nodal signals required for maintenance of its expression [Clements and Woodland, 2003]. At the late blastula stage, expression of the transcription factors of the Mix and GATA families is induced (reviewed in [Loose and Patient, 2004]). Continuing into the gastrula stages, the mesoderm and endoderm cell populations become distinct [Lemaire et al., 1998].

Vegetal *TSK* expression is detected in the late blastula embryo (Figure 5.7, page 69), but increases in early gastrula stages. This suggests that expression of

TSK lies downstream of endoderm inducers, such as *Vg1* and *VegT*, and indeed *TSK* expression may be induced by *Vg1* (Figure 10.2, page 130). Vegetal *Xnr* expression from stage 8 is induced by *Vg1*, forming a relay mechanism for endoderm induction [Yasuo and Lemaire, 1999]. The majority of *TSK* expression in the endoderm is detected after *Vg1* and *Xnr* expression, raising that possibility that *TSK* expression is regulated by *Vg1* and *Xnr* expression and thus forms part of this relay mechanism.

Endoderm specification begins in gastrula stages and by early gastrulation, vegetal cells have become committed to form endoderm [Heasman et al., 1984, Wylie et al., 1987]. TGF- β superfamily signalling is important in endoderm formation. Expression of endoderm specific genes such as members of the Sox and GATA families, can be induced by activin or *Vg1* in animal cap explants [Henry et al., 1996, Rosa, 1989, Hudson et al., 1997, Ecochard et al., 1995]. *Xnr1*, 2 and 4 are also expressed in vegetal cells from late blastula stages onwards and can induce endoderm markers in animal cap assays [Yasuo and Lemaire, 1999, Clements et al., 1999]. In addition to this, *Derrière* can also induce endoderm [Sun et al., 1999]. Thus it is a possibility that *TSK* may positively interact with these candidates to promote endoderm formation.

In contrast to the above TGF- β factors exerting a positive role in endoderm formation, it may be the case that BMP signalling has to be inhibited for endoderm induction to proceed in *Xenopus*. There are several lines of evidence for this, the first of which the BMP inhibitors chordin and noggin can induce endoderm marker expression in *Xenopus* [Sasai et al., 1996]. Also, in sea urchin, BMP inhibition by noggin is enhances endoderm differentiation [Angerer et al., 2000]. Furthermore in Zebrafish, Poulain et al. [2006] have shown that a combination of Nodal, FGF and BMP signalling regulates endoderm formation. In this context, inhibition of both FGF and BMP signalling is required for endoderm formation. This is supported by data in *Xenopus* showing that inhibition of FGF signalling expands the endoderm [Cha et al., 2004]. Interestingly, activation of BMP signalling with caALK3 inhibits expression of endoderm markers, suggesting that BMP inhibition is indeed important for endoderm induction

(Figure 6.7, page 83).

TGF- β signalling is important for endoderm formation. Although little work has been carried out on the role of BMP inhibition in endoderm formation, this is a candidate mechanism for TSK endoderm function as TSK inhibits BMP signalling in cooperation with chordin. It is also a possibility that chordin has additional roles in endoderm formation, and thus this may also be a possible facet of TSK function in the endoderm. Inhibition of FGF signalling also appears to be important for endoderm formation, this is in contrast to the requirement of FGF signalling for mesoderm formation. It also provides a common link between the mechanics of mesoderm and endoderm and is therefore an additional candidate for TSK function. In addition to this, nodals also provide a common link between dorsal mesoderm and endoderm, and hence remain an interesting candidate for TSK function in both germ layers. These possibilities are supported by the findings that TSK induction of endoderm is partially blocked by activation of BMP signalling (Figure 6.7, page 83), blocked by inhibition of nodal signalling (Figure 9.1, page 114) and blocked by activation of FGF signalling (Figure 8.6, page 104).

11.2.5 *TSK* functions in germ layer formation and patterning in *Xenopus*

In this study, it has been shown that *TSK* is expressed maternally in the ectoderm in addition to zygotic maternal expression. At the onset of gastrulation, zygotic *TSK* expression is also seen in the endoderm and dorsal mesoderm with the lowest/absent expression in the lateral and ventral mesoderm. *TSK* expression is positively regulated by BMP [Kuriyama et al., 2006] and Vg1 (Figure 10.2, page 130) and negatively regulated by FGF-MAPK (Figure 10.1, page 129) and Notch (Figure 10.2, page 130) signalling (Summarised in figure 11.1). Gain and loss of function studies show that *TSK* functions in mesoderm patterning, organizer formation/function and endoderm induction. This evidence suggests that *TSK* plays a role in germ layer formation/patterning of the whole embryo. This is supported by the elevated expression of levels of *TSK* detected during these stages of development (Figure 5.8, page 71).

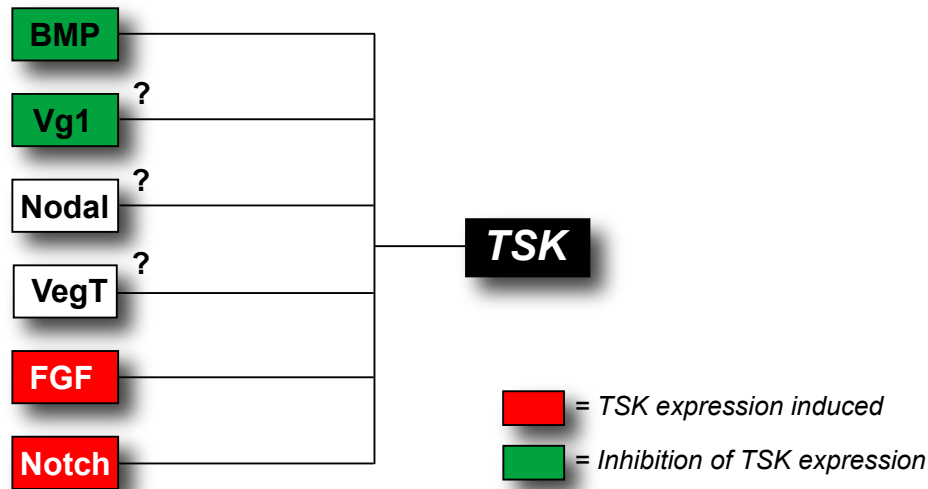


Figure 11.1: **Regulation of *TSK* expression in *Xenopus***
 Schematic representation of regulation of *TSK* expression by BMP, Nodal, Vg1, VegT, FGF-MAPK and Notch signalling in the *Xenopus* embryo. Positive regulation denoted by green colour. Negative regulation denoted by red colour.

11.3 TSK function in germ layer patterning cannot be explained by BMP inhibition alone

The multiple functions of TSK during *Xenopus* embryogenesis must be considered within the context of BMP inhibition by TSK. TSK consistently inhibits Smad1 signalling as demonstrated in this study in figure 6.6, page 81. This supports previous reports showing TSK is a dorsalisng factor of ventral explants, a direct neural inducer in animal explants and regulator of neural crest development, all roles associated with the capacity of TSK to antagonise BMP signalling in cooperation with chordin [Ohta et al., 2004], [Kuriyama et al., 2006]. The expansion of *gooseoid* expression can be explained well by the ability of TSK to inhibit BMP signalling, as it has been shown previously that inhibition of BMP in ventral mesoderm results in dorsalisation [Suzuki et al., 1994, Maéno et al., 1994, Steinbeisser et al., 1995]. However, it is difficult to explain mesoderm inhibition in ventrolateral mesoderm by TSK and induction of endoderm by TSK in terms of BMP inhibition alone. This is supported by the following evidence from both previous work and this study.

Mesoderm inhibition by TSK cannot be attributed to inhibition of BMP signalling

- In this study, introduction of tBR into the marginal zone does not inhibit expression of *Xbra*. Similarly, overexpression of the BMP inhibitor, chordin does not result in inhibition of *Xbra* expression (Figure 6.6, page 81). It must be noted here that the mechanisms of BMP inhibition employed here, i.e. chordin overexpression and expression of tBR are functioning normally as shown by induction of secondary axis formation.
- Expression of tBR in *Xenopus* results in activation of MAPK phosphorylation as demonstrated in Figure 8.3, page 99. This is not compatible with mesoderm inhibition which can result from inhibition of FGF signalling [Amaya et al., 1991, 1993]. In contrast to BMP inhibition, TSK inhibits MAPK phosphorylation, (Figure 8.1, page 97) and thus this is a fundamental difference between BMP inhibition and TSK function.
- BMP4 has the ability to induce mesoderm in animal caps [Köster et al., 1991], although inhibition of BMP function with a truncated BMP receptor does not result in loss of mesoderm, but rather, results in dorsalisation of ventral tissue [Suzuki et al., 1994], [Maéno et al., 1994]. In addition to this loss of BMP4 function using antisense morpholino also results in dorsalisation of mesoderm [Steinbeisser et al., 1995].

Endoderm induction by TSK cannot be attributed to inhibition of BMP signalling alone

- Induction of endoderm by TSK is only partially rescued by introduction of a constitutively active BMP receptor, Figure 6.7, page 83. This strongly suggests that TSK is not functioning through BMP inhibition alone to induce endoderm.
- Inhibition of BMP signalling by expression of tBR alone in the *Xenopus* marginal zone does not result in induction of mesoderm markers as is the case with TSK overexpression. It may be the case that additional

signalling is required in addition to BMP inhibition as is the case in Zebrafish where a combination of Nodal, FGF and BMP signalling regulates endoderm formation [Poulain et al., 2006]. Chordin and noggin have been reported to induce expression of endoderm markers in animal cap explants [Sasai et al., 1996].

Thus, BMP inhibition alone by TSK cannot explain the phenotypes observed in the ventrolateral mesoderm and endoderm with TSK gain and loss of function. Although there is clearly a possibility that BMP inhibition contributes to TSK function, there is a strong possibility that TSK is functioning with other factors in these contexts. This is demonstrated by the shift in neural markers upon TSK gain- and loss-of-function (Figure 7.7, page 94) as inhibition of FGF signalling in particular inhibits posterior neural development [Cox and Hemmati-Brivanlou, 1995], identifying FGF signalling as a potential candidate. In addition to this, two interesting candidate pathways to repeatedly feature in the mesoderm and endoderm are nodal signalling and FGF signalling, thus analysis of these in the context of TSK function was performed.

11.4 Signalling in early *Xenopus* development

11.4.1 FGF signalling and mesoderm formation

The BMP inhibitory activity of TSK is not likely to inhibit mesoderm formation, thus other pathways were considered. The clear inhibition of *Xbra* expression by TSK is particularly reminiscent of *Xbra* expression inhibition by the dominant negative FGF receptor, XFD (Figure 8.4, page 101). FGF signalling is required for mesoderm formation and upon expression of XFD, *Xbra* expression is completely blocked, even in the presence of mesoderm inducers such as activin [Amaya et al., 1991, 1993]. FGF signalling is also likely to be required for maintenance of mesodermal tissue as loss of mesoderm markers results from XFD expression subsequent to initial mesoderm induction [Kroll and Amaya, 1996]. Expression of *Xbra* is maintained by FGF signalling. *Xbra* then forms an autocrine loop by inducing *eFGF* expression [Isaacs et al., 1994, Schulte-Merker and Smith, 1995]. Activation of FGF signalling with *vras* rescues TSK

inhibition of *Xbra* expression (Figure 8.6, page 104) and partially blocks expansion of endoderm markers by TSK, strongly implicating FGF signalling in the mechanism of TSK function.

FGFs bind to their cognate receptors, FGFR to induce dimerisation and autophosphorylation of more than 6 intracellular tyrosine residues [Mohammadi et al., 1996]. Src homology 2 (SH2) domain-containing proteins dock with the phosphorylated tyrosines. An example of an SH2 domain containing protein is phospholipase C- γ which stimulates phosphatidylinositol hydrolysis and mobilisation of Ca^{2+} in the cell [Mohammadi et al., 1992, Peters et al., 1992]. In addition to mobilisation of Ca^{2+} , receptor autophosphorylation also activates the GTPase, Ras, which activates a cascade of kinases resulting in activation of MAPK and activation of gene expression [Fambrough et al., 1999]. PI3K (downstream of which is Akt) is also able to connect to Ras in FGFR signalling [Browaeys-Poly et al., 2000]

Binding of PLC- γ to the FGFR is not essential for *Xbra* expression and mesoderm formation [Muslin et al., 1994]. In contrast to this, Ras/MAPK signalling is required for FGF-mediated mesoderm induction, as dominant negative components of the pathway including Ras [Whitman and Melton, 1992] and Raf [MacNicol et al., 1993] block *Xbra* expression and mesoderm formation.

The most striking finding here in terms of signalling pathways activated downstream of TSK is the inhibition of FGF-MAPK signalling (Figure 8.1, page 97). There is the possibility that FGF-MAPK inhibition by TSK is a result of BMP-Smad1 inhibition by TSK. This is not the case as inhibition of BMP signalling activates MAPK phosphorylation as shown in this study (Figure 8.3, page 99) Thus FGF-MAPK signal inhibition is independent of the BMP inhibitory activity of BMP, further supporting that TSK functions through additional pathways in the *Xenopus* embryo.

11.4.2 Regulation of FGF-MAPK signalling by TSK functions to inhibit mesoderm formation

TSK overexpression in the mesoderm produces the same phenotype as inhibition of FGF signalling in the mesoderm, i.e. inhibition of *Xbra* expression (Figure

6.2, page 75) and it has been demonstrated that TSK can inhibit FGF-MAPK signalling (Figure 8.1, page 97). Thus it is highly likely that TSK inhibits mesoderm formation through inhibition of FGF signalling. This hypothesis was confirmed by rescue to TSK inhibition of *Xbra* expression with a constitutively active form of ras, vras (Figure 8.6, page 104). As this inhibition of FGF-MAPK is not mediated by TSK inhibition of BMP signalling, the mechanism of FGF-MAPK inhibition by TSK was studied by activation of FGF signalling in different approaches.

TSK can inhibit MAPK phosphorylation activated by the FGFR ligand, FGF8b [Fletcher et al., 2006] (Figure 8.5, page 102) and this places TSK either extracellularly, or raised the possibility of cross-talk from other intracellular pathways. TSK could also inhibit MAPK phosphorylation activated by a constitutively active FGFR (Figure 8.7, page 106). This particular receptor (caFGFR-C249Y) can be partially inhibited if dimerisation is inhibited by an extracellular factor, thus TSK was potentially working at the extracellular receptor level or again downstream. This was confirmed with an inducible FGFR dimerisation system, which does not possess extracellular domains of the FGF receptor [Isaacs et al., 1994]. TSK was unable to negate activation of FGF-MAPK signalling promoted by chemical dimerisation (Figure 8.8, page 108). Combined, these data strongly suggest that TSK inhibits FGF-MAPK signalling in the extracellular space at the level of the FGF receptor.

At this point there are several possibilities for the exact mechanism of TSK action in this respect. Primarily, we need to determine if FGF is pulled down in complex with TSK. FRL1/CR1 is a ligand of the FGF receptor and activates FGF-MAPK signalling [Kinoshita et al., 1995]. This study has shown that FRL1/CR1 is pulled down in complex with TSK (Figure 9.4, page 118). TSK mediated MAPK inhibition may be mediated by interaction with CR proteins, including FRL1/CR1. It is a possibility that TSK may sequester FRL1/CR1 from that FGF receptor, thus inhibiting FGF-MAPK signalling. This hypothesis could possibly be tested on the basis of competition of TSK, FRL-1 and FGFR binding to determine if TSK can out-compete FGFR in FRL1/CR1

binding. The finding that FRL1/CR1 activates FGF-MAPK signalling by Kinoshita et al. [1995] conflicts with Dorey and Hill [2006], thus this area remains confusing at present.

11.4.3 Akt signalling

A second example of an intracellular signalling pathway important for mesoderm formation is the Phosphatidylinositol-3 kinase pathway (PI3K). In addition to connecting to Ras in FGFR signalling [Browaeys-Poly et al., 2000], PI3K can act in parallel to FGF-MAPK signalling to convert ectoderm into mesoderm [Carballada et al., 2001]. Akt is downstream of PI3K although a direct role for Akt in mesoderm has not yet been tested. Interestingly though, PI3K signalling is involved in promotion of neurogenesis, in which Akt is an essential target of PI3K [Peng et al., 2004]. We currently have preliminary data showing that TSK can activate Akt signalling (data not shown here), hence this is an interesting possibility for TSK function.

Thus, it appears that FGF-MAPK, Activin-like-Smad2 and PI3K, in addition to BMP-Smad1 signalling is important in mesoderm formation in the *Xenopus* embryo, thus the effect of TSK upon these pathways was analysed to learn more about the role of TSK in the mesoderm. Indeed, TSK overexpression in animal cap explants inhibits MAPK phosphorylation, thus accounting for the inhibition in *Xbra* expression observed. TSK also inhibits phosphorylation of Smad1 (Figure 8.1, page 97) which is in full agreement with the BMP inhibitory activity of TSK. In addition to this TSK overexpression also weakly activates Smad2 signalling in addition to activation of Akt signalling. These activations may be related to the function of TSK in expansion of dorsal mesoderm. Elsewhere in the mesoderm, the MAPK inhibition may dominate in *Xbra* inhibition. Interestingly, there is an element of cross-talk between the PI3K/Akt and TGF- β /Smad pathway. In some instances, PI3K/Akt enhances Smad3 signalling [Runyan et al., 2004], whereas in others, PI3K/Akt is responsible for suppressing Smad3 [Song et al., 2003]. Smad3 inhibits activin signalling by competing with Smad4 for FAST-2 (transcription factor) binding [Nagarajan

et al., 1999]. Thus activation of PI3K/Akt by TSK may have a positive effect on Smad2 signal transduction. This area is currently complicated though by further data showing that PI3K/Akt can inhibit Smad2 in neuroblastoma cells [Qiao et al., 2006]. Thus the cross-talk between PI3K/Akt and TGF- β /Smad signalling appears to be context specific hence remains elusive in the *Xenopus* embryo.

11.4.4 The role of nodal signalling in mesoderm and endoderm formation

In addition to FGF-MAPK signalling, other signalling pathways are important for mesoderm formation. One such example is Smad2 signalling³ which activates the activin-inducible dorsal gene, forkhead1 in *Xenopus*, and thus reveals Smad2 as a transducer of activin signals [Howell and Hill, 1997]. In addition to this, dominant negative Smad2 mutants disrupt axis formation by inhibiting activin/Vg1 signalling in *Xenopus* [Hoodless et al., 1999]. Also, Smad2 has been shown to mediate nodal signalling [Kumar et al., 2001]. Thus Smad2 is an important intracellular signalling component in mesoderm formation, interestingly the loss of mesodermal competence has been shown to be related to the phosphorylation-dependent inability of Smad2 to localise to the nucleus [Grimm and Gurdon, 2002]. Loss of mesodermal competence is also related to the ability of Notch signal activation to modulate Smad2-Smad4 complex formation [Abe et al., 2005].

11.5 TSK functionally interacts with nodal signalling to pattern the germ layers

It has been suggested by Schier and Shen [2000] that many of the roles attributed to TGF- β signalling during development may be accounted for by nodal signalling. Interest has shifted to the role of nodal family members as it has thus far been difficult to demonstrate essential roles in mesoderm formation for activin and Vg1. Derrière, another member of the TGF- β superfamily related to Vg1 has been shown to be a potent mesoderm and endoderm in-

³Used by activin-like (Activin, nodals, Vg1, derriere) signals in the embryo.

ducer, important for posterior mesoderm formation, but not general mesoderm formation [Sun et al., 1999].

In contrast to this, nodal signalling has been shown to be essential for mesoderm formation. In mouse, disruption of the *Nodal* gene disrupts mesoderm formation [Zhou et al., 1993], also in these mice, a primitive streak fails to form [Conlon et al., 1994]. Zebrafish, mutant for the *nodal*-related genes, *squint* and *cyclops* do not form head and trunk mesoderm in addition to lacking the germ-ring [Feldman et al., 2000]. Nodals are expressed zygotically, but this does not necessarily rule out their involvement in mesoderm induction. VegT can induce *nodal* expression [Yasuo and Lemaire, 1999], [Clements et al., 1999]. Nodal signalling also defines pattern in the mesoderm where Xnr2 can dorsalise ventral mesoderm during gastrulation [Smith et al., 1993].

Nodal signalling is also important in endoderm formation in *Xenopus*⁴. In zebrafish mutants for the *nodal-related* genes, *squint* and *cyclops*, endoderm differentiation, in addition to mesoderm, is defective [Sampath et al., 1998], [Feldman et al., 1998]. In *Xenopus*, Xnr1 and 2, 4, 5 and 6 are potent inducers of endoderm [Yasuo and Lemaire, 1999], [Clements et al., 1999], [Takahashi et al., 2000].

A two step model for fate determination of presumptive endoderm was proposed by Yasuo and Lemaire [1999] in which the initial activation of early endodermal genes by maternal factors, including VegT is relayed by the action of zygotic TGF- β superfamily members, including Xnr1 and Xnr2. In addition to this Xanthos et al. [2001] showed that VegT is the maternal regulator of endoderm formation and Xnr members are located downstream. GATA4, 5 and 6, belonging to the GATA family of transcription factors function to mediate this TGF- β maintenance of endodermal gene expression [Afouda et al., 2005], [Weber et al., 2000]. GATA family members are potent inducers of early endoderm markers, Sox17 α HNF1 β [Afouda et al., 2005], [Weber et al., 2000]. GATA5 is induced by activin levels above those required for dorsal mesoderm formation, thus indicating that endoderm induction is resultant from high levels of TGF β

⁴In addition to Vg1 [Gamer and Wright, 1995], [Henry et al., 1996], [Joseph and Melton, 1998] and *derrière* [Sun et al., 1999]

signalling, and in addition to this, FGF signalling must be absent [Weber et al., 2000].

11.5.1 Regulation and gradients of nodal signalling

The type I receptor, ALK4 and the type II receptors, ActRIIA and ActIIRB are very likely to be nodal receptors as indicated by loss and gain-of-function analyses [Gu et al., 1998, Oh and Li, 1997, Song et al., 1999]. In addition to this, ALK4 can co-immunoprecipitate Vg1, Xnr1 and Derrière [Chen et al., 2004] suggesting complex formation between Xnr1 and ALK4, although direct binding has not yet been demonstrated. As discussed earlier, EGF-CFC cofactors are required for Nodal signalling [Schier and Shen, 2000, Shen and Schier, 2000]. Interestingly, mouse and zebrafish nodal and EGF-CFC mutants display similar phenotypes, although *EGF-CFC* mutants form anterior neural structures whilst *nodal* mutants do not [Varlet et al., 1997, Ding et al., 1998] suggesting nodal may have EGF-CFC independent functions. This was confirmed by Yeo and Whitman [2001], showing that Cripto interaction with ALK4 is required for nodal binding and signaling through the receptor. In addition to this, nodal can antagonise BMP signalling in a cripto-independent manner.

Gradients of nodal signalling are important during *Xenopus* development. For instance *Xnr1*, *Xnr2* and *Xnr4* are expressed in a ventral to dorsal gradient in endodermal cells with highest levels in the dorsal region [Agius et al., 2000]. Thus it can be considered that lower levels of nodal signalling are required for ventral mesoderm formation whilst higher levels induce dorsal mesoderm formation. In addition to this, even higher levels of TGF- β signalling, very likely through nodal signalling, are required for endoderm. Thus differential expression is important in combination with regulation of signalling to achieve the appropriate levels of nodal signalling for the required biological outputs.

11.5.2 TSK and nodal interaction

Expression of *Xnr1* and *Xnr2* is detected in a punctate staining pattern all over the vegetal hemisphere at stage 9. At stage 10.25, *Xnr1* is restricted to the dorsal marginal zone, whereas *Xnr2* is detected in the dorsal marginal zone in

addition to nearby dorsovegetal cells at pregastrula stage 10. By stage 10.5, *Xnr2* is expressed most strongly in the dorsal blastopore lip at superficial levels and deeper staining. At this stage, some vegetal cells also still express *Xnr2* [Jones et al., 1995].

There are some common elements between TSK and Xnrs, *Xnr2* in particular. Namely the overlapping spatial and temporal expression patterns in the endoderm and dorsal mesoderm, and induction of dorsal mesoderm and endoderm. Also, *Xnr* expression is induced by *Vg1* [Agius et al., 2000], as is TSK, further suggesting that TSK may function with nodal signalling.

Also in chick, TSK is expressed in Koller's sickle and the posterior marginal zone. Koller's sickle is a ridge of small cells situated between the area pellucida and posterior marginal zone. *Vg1* is expressed in the posterior marginal zone and induces *nodal* expression in Koller's sickle [Stern, 2004]. Hence TSK and nodal expression is overlapping in the chick embryo in addition to *Xenopus*, further suggesting a possible conserved functional interaction between TSK and nodal signalling in development.

There are some common elements between TSK and Xnrs. Namely the overlapping spatial and temporal expression patterns in the endoderm and dorsal mesoderm, and induction of dorsal mesoderm and endoderm. *Xnr1*, 2, 5 and 6 show almost identical phenotypes on overexpression, indicating that their biochemical and cell biological activities are highly similar although regulation of their expressions are different. In the case of *Xnr2*, expression overlaps with that of TSK in the vegetal region and dorsal region during blastula and gastrula stages of development. *Xnr2* is also a strong dorsal mesoderm and endoderm inducer, thus the biochemical and functional interaction between TSK and *Xnr2* was analysed. TGF- β superfamily members, BMP2 and BMP4 have previously been shown to be pulled down in complex with TSK [Ohta et al., 2004, Kuriyama et al., 2006]. This study shows that *Xnr2* is also pulled down in complex with TSK in addition to the EGF-CFC cofactor, FRL1/CR1 required for nodal signalling through ALK4. TSK can form a ternary complex with BMP and chordin [Ohta et al., 2004], thus raising the possibility that TSK also forms

a ternary complex with Xnr2 and FRL1/CR1. Work is now in progress to test this hypothesis using the chemical cross-linker, DTSSP. In addition to Xnr2, preliminary data also suggests that Xnr1, Xnr5 and Xnr6 are also pulled down in complex with TSK (Data not shown).

There are several findings suggesting that TSK functionally interacts with Xnr2. First of all, Xnr2 is pulled down in complex with TSK (Figure 9.3, page 117). In addition to this, expression patterns of TSK and Xnr2 are spatially and temporally overlapping in the endoderm and dorsal mesoderm. Also, expression regulation of TSK and Xnr2 are similar in that expression of both is induced by Vg1. Finally, Xnr2 activates Smad2 phosphorylation, and although Smad2 activation by TSK is weak in the animal cap, it may be stronger in the endoderm where nodal-related proteins are also expressed.

Upon co-overexpression of TSK and Xnr2, several observations were made, strongly suggesting that TSK and Xnr2 functionally interact. This included the finding that TSK potentiates Xnr2 mediated Smad2 phosphorylation in the animal cap (Figure 9.5, page 119). This potentiation of Smad2 phosphorylation by TSK is reflected in the fact that TSK also activates ectopic endoderm formation by Xnr2 in the marginal zone of whole embryos, as shown by the markers, *Sox17 α* and *GATA4* (Figures 9.8, 9.9, pages 124, 125). In addition to this, TSK mediated activation of endoderm formation is blocked by the specific nodal inhibitor, Ces-S and a dominant negative ALK4 receptor (Figure 9.2, 116). Also, loss of endoderm markers in TSK depleted embryos is partially rescued by Xnr2 overexpression (Figure 9.1, page 114). This indicates that endoderm induction by TSK is mediated in part by nodal signalling. These observations demonstrate that TSK mediated regulation of Smad2 phosphorylation is mediated by nodal signalling, where this regulation acts to induce endoderm formation. Xnr2 activates MAPK signalling. However, this is not ideal for endoderm formation [Weber et al., 2000]. Thus TSK also functions to reduce MAPK activation to permit endoderm formation. This remains unclear at present because MAPK phosphorylation is clearly not inhibited in the animal cap. This may be an artifact of MAPK activation upon cap cutting.

Alternatively, there be another factor in the animal cap which changes the response to TSK in the presence of Xnr2. Ideally, coinjection of TSK and Xnr2 will be performed in the endoderm followed by MAPK signal activation.

Within the context of dorsal mesoderm formation, TSK expands *Gsc* expression. Smad2 signalling is essential for expression of *Gsc* in the dorsal region of the embryo, and thus it is reasonable to suggest that the expansion of *Gsc* is resultant from the ability of TSK to potentiate Smad2 signalling. In contrast to this, *Gsc* expression is not dependent on MAPK signalling [Amaya et al., 1993] and thus TSK mediated FGF-MAPK signalling inhibition has no effect, unlike the situation with inhibition of *Xbra* expression. TSK in concert with Xnr2 produces a much stronger expansion of *Gsc* expression, supporting that TSK potentiates nodal signalling in the embryo.

11.6 Model of TSK function in early *Xenopus* embryogenesis

In early *Xenopus laevis* embryogenesis TGF- β signalling is important for regulation of mesoderm and endoderm formation and thus crucial for establishment of the germ layers. In addition to this, FGF signalling has also been shown to play an important role in mesoderm and endoderm specification. This study has described a novel secreted regulator of pathways involved in germ layer establishment, Tsukushi (TSK). *TSK* is expressed during germ layer formation and gastrulation, with highest expression levels detected in the ectoderm and endoderm. Overexpression of *TSK* in the lateral/ventral marginal zone, where expression levels are lowest, results in inhibition of mesoderm marker (*Xbra*) expression. In contrast to this ectopic expression of endoderm markers (*Sox17 α* , *GATA4*) is induced at the site of this TSK misexpression. In addition to this, loss of function analysis with morpholino against TSK produces an expansion of mesoderm whilst inhibiting endoderm formation. This demonstrates that TSK has an important function during germ layer formation and patterning during early *Xenopus* embryogenesis.

To look at the mechanism by which loss and gain of TSK function affects

germ layer formation, interactions with pathways important for mesoderm and endoderm formation have been studied here. Activity of Xnr2, a member of the TGF- β superfamily is required for mesoderm and endoderm induction whilst FGF signal activation is required for mesoderm, whereas inhibition is required for endoderm, in addition to inhibition of BMP signalling. TSK has previously been shown to interact with and inhibit BMP signalling. Here we show TSK also interacts with Xnr2, potentiating its activity. This combined regulation of Xnr2, BMP and FGF by TSK results in segregation between mesoderm and endoderm in the *Xenopus* embryo.

11.7 Multiple pathway regulation

Coordination of multiple signalling pathways is essential for the precise regulation of developmental processes. In early embryogenesis, extracellular molecules such as morphogens and their inhibitors have fundamental roles in regulation of signalling pathways that are important for embryogenesis. However, studies about coordination of these pathways are largely restricted to intracellular cross talk. Several extracellular regulators such as follistatin and cerberus are known to interact with extracellular proteins of more than one signalling pathway [Tashiro et al., 1991, Fainsod et al., 1997, Piccolo et al., 1999]. For example, follistatin binds with activin and BMP and inhibits both signalling pathways. Our analyses have demonstrated that, in the extracellular space, TSK has three activities and co-ordinately regulates nodal, BMP and FGF activities in the extracellular space to maximize their functions in endoderm induction and mesoderm inhibition. This is summarised in figures 11.2 11.3, 11.4. Also, in ectoderm, TSK regulates BMP activity, which contributes to the process of segregation between epithelial and neural tissues. In addition to this, the MAPK inhibitory activity of TSK regulates anterior-posterior polarity in neural tissues. Combined, the data presented in this study clearly shows the importance of extracellular cross talk of these pathways and suggests that extracellular coordination of multiple signalling pathways has important roles in cell signalling.

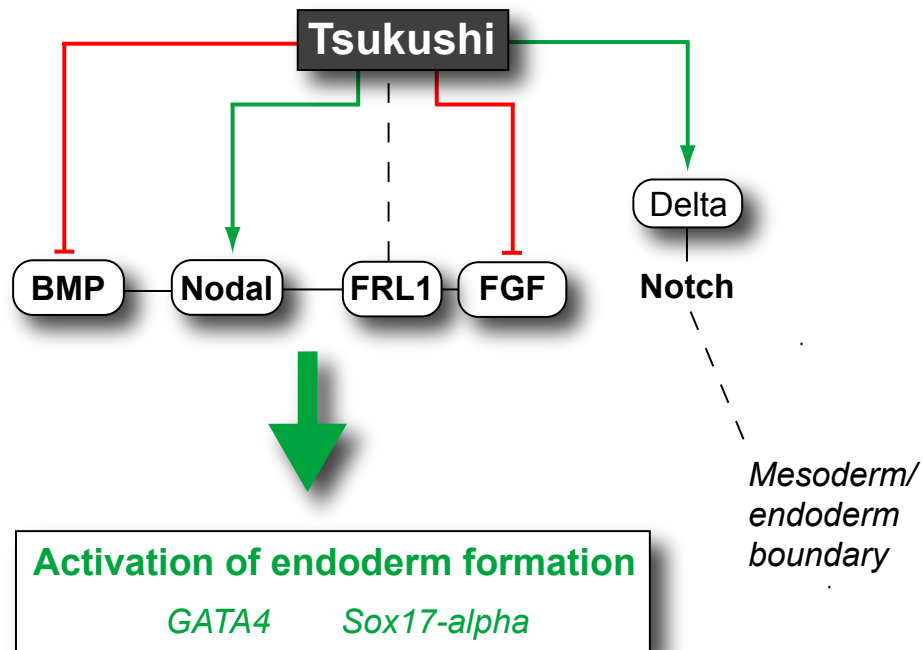


Figure 11.2: **Model of TSK function mechanism in *Xenopus* endoderm formation**

Schematic representation of *TSK* functional model in endoderm formation in the *Xenopus* embryo. Positive regulation denoted by green colour. Negative regulation denoted by red colour. See text for detailed explanation.

11.7.1 Morphogen gradients and border formation

Morphogens such as activin-like proteins and FGF are known to create distinct fates depending on their concentrations [Slack, 1987; Green, 1990]. It has been reported that responses of cells to activin depend on the absolute number of receptors occupied by activin [Dyson and Gurdon, 1998], suggesting the importance of regulation of morphogen diffusion to create a concentration gradient. This importance of diffusion control has been demonstrated recently. *Drosophila* mutants *toutvelu* and *dally*, which have defects in the synthesis of extracellular heparan sulfate proteoglycans, prevents Wingless morphogen diffusion [Lin and Perrimon, 2000]. However, the role of such matrix factors in morphogen diffusion is still poorly understood. Members of the SLRP family, which also have sugar modifications, might be good candidates in this context.

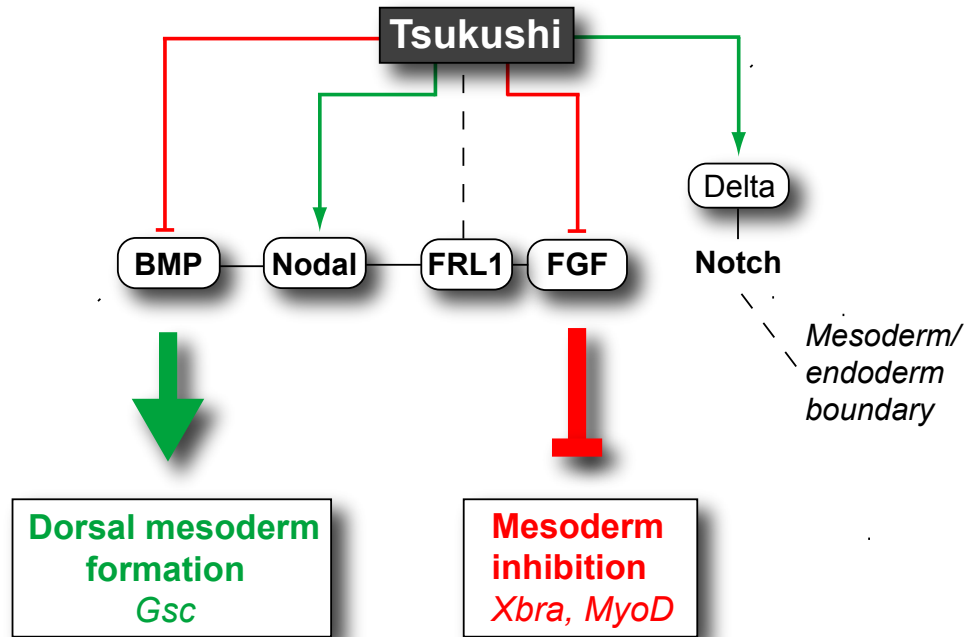


Figure 11.3: **Model of TSK function in *Xenopus* mesoderm formation**
 Schematic representation of *TSK* functional model in mesoderm formation (including dorsal mesoderm formation) in the *Xenopus* embryo. Positive regulation denoted by green colour. Negative regulation denoted by red colour. See text for detailed explanation.

Xnr proteins produce mesoderm and endoderm depending on their concentration. However, the concentration dependence is very vague. Thus, there is no sharp change between mesoderm and endoderm. However, we have demonstrated that the combination of two morphogens, Xnr2 and TSK, makes a clear border between mesoderm and endoderm (Figures 9.6, 9.7, 9.8, 9.9, chapter 9). Our analyses indicate that this is caused by a combination of three main factors. Firstly, these two molecules have a distinct functional range. For example, Xnr2 works as a long-range morphogen [Williams et al., 2004], whilst TSK works at short-range. Secondly, these two proteins regulate distinct sets of signalling pathways. Thirdly, the proteins make a complex that synergistically potentiates or inhibits activities of these proteins. This interaction changes effective concentration or diffusion of proteins. Thus, in the co-overexpression experiment (Figure 9.8), TSK stays near cells expressing the two proteins to

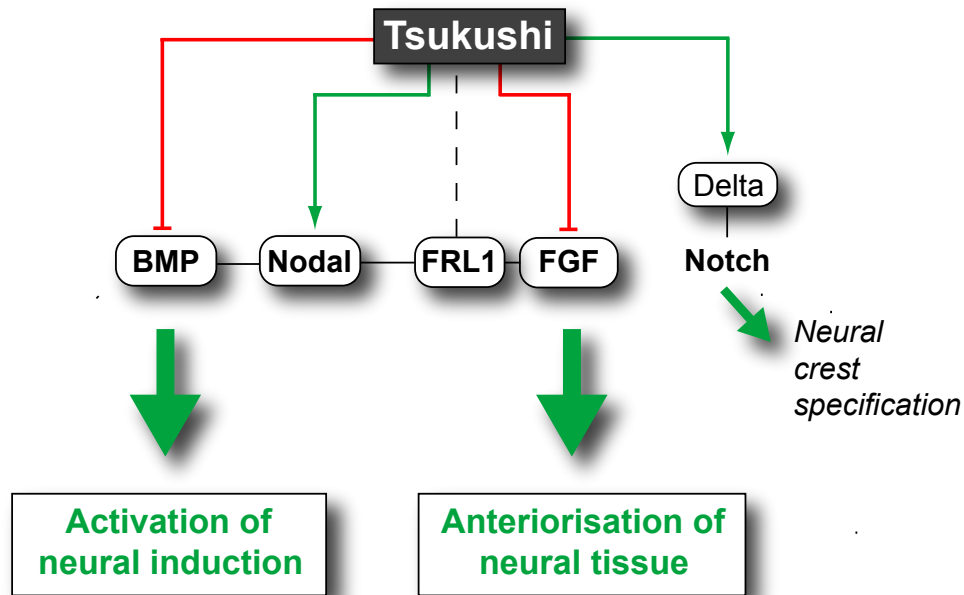


Figure 11.4: **Model of TSK function in *Xenopus* ectoderm formation**
Schematic representation of *TSK* functional model in ectoderm formation (including neural induction and anterior-posterior patterning) in the *Xenopus* embryo. Positive regulation denoted by green colour. Negative regulation denoted by red colour.

create a competent area in which TSK makes a complex with Xnr2 and synergistically potentiates signalling pathways of both proteins; i.e. activation of the nodal-Smad2 pathway and inhibition of the FGF-MAPK pathway. This simultaneous regulation, in which endoderm formation is activated and mesoderm formation is inhibited, contributes to create a clear border between mesoderm and endoderm.

In the case of natural embryogenesis, we need to consider a fourth important factor: spatially and temporally regulated transcription of morphogens. Zygotic TSK is expressed in endoderm, dorsal mesoderm, and ectoderm with exclusion from lateral/ventral mesoderm. This expression pattern may be initially produced by Smad2 activation through Vg1 and then matured by a combination of Smad2 mediated positive regulation and negative regulation by MAPK. Thus, this regulation creates some distinct competent areas for germ layer specification. The Notch signalling pathway may also have a role here, as it has funda-

mental roles in border formation [Sherwood and McClay, 2001]. Although the role of Notch signalling in *Xenopus* embryogenesis is not clearly elucidated yet, TSK may have contribution in Notch mediated border formation.

Based on our observations, the following model is proposed for endoderm and mesoderm specification. In the absence of TSK, Xnr proteins create a pattern of Smad2 activation with a vegetal-animal linear gradient. Activated *TSK* expression in the endoderm creates a competent area, in which the potential short-range morphogen, TSK, traps Xnr proteins to increase their effective concentration. This results in the ideal coordination for endoderm formation: nodal-Smad2 activation, FGF-MAPK inhibition, and BMP-Smad1 inhibition. In terms of mesoderm formation, MAPK activation inhibits expression of *TSK* in lateral/ventral mesoderm where a combination of MAPK activation and Smad2 activation contributes to mesoderm induction. In addition to this *TSK* expression in the dorsal mesoderm effectively contributes to organizer formation and function, mainly through BMP-Smad1 inhibition by synergistic ternary complex formation between TSK, BMP, and chordin [Ohta et al., 2006] and nodal-Smad2 activation. In conclusion, through regulation of these multiple factors, TSK coordinates all germ layer specification.

11.7.2 Future directions: formation of an extracellular network hypothesis

The findings presented in this study exemplify the nature of the extracellular network in biological systems. There are a growing number of factors, inclusive of TSK, that are localised to the extracellular matrix and are responsible for coordinated regulation of multiple pathways. We plan to use TSK as a ‘model factor’ in this context and to determine in further detail the precise mechanisms by which TSK functions. This approach will combine biochemical and embryological techniques to determine ratios of specific complex formation, and how this relates to biological output. The challenge is to begin detailed construction of the ‘extracellular network’ (Figure 11.5) and to document in further detail events outside the cell.

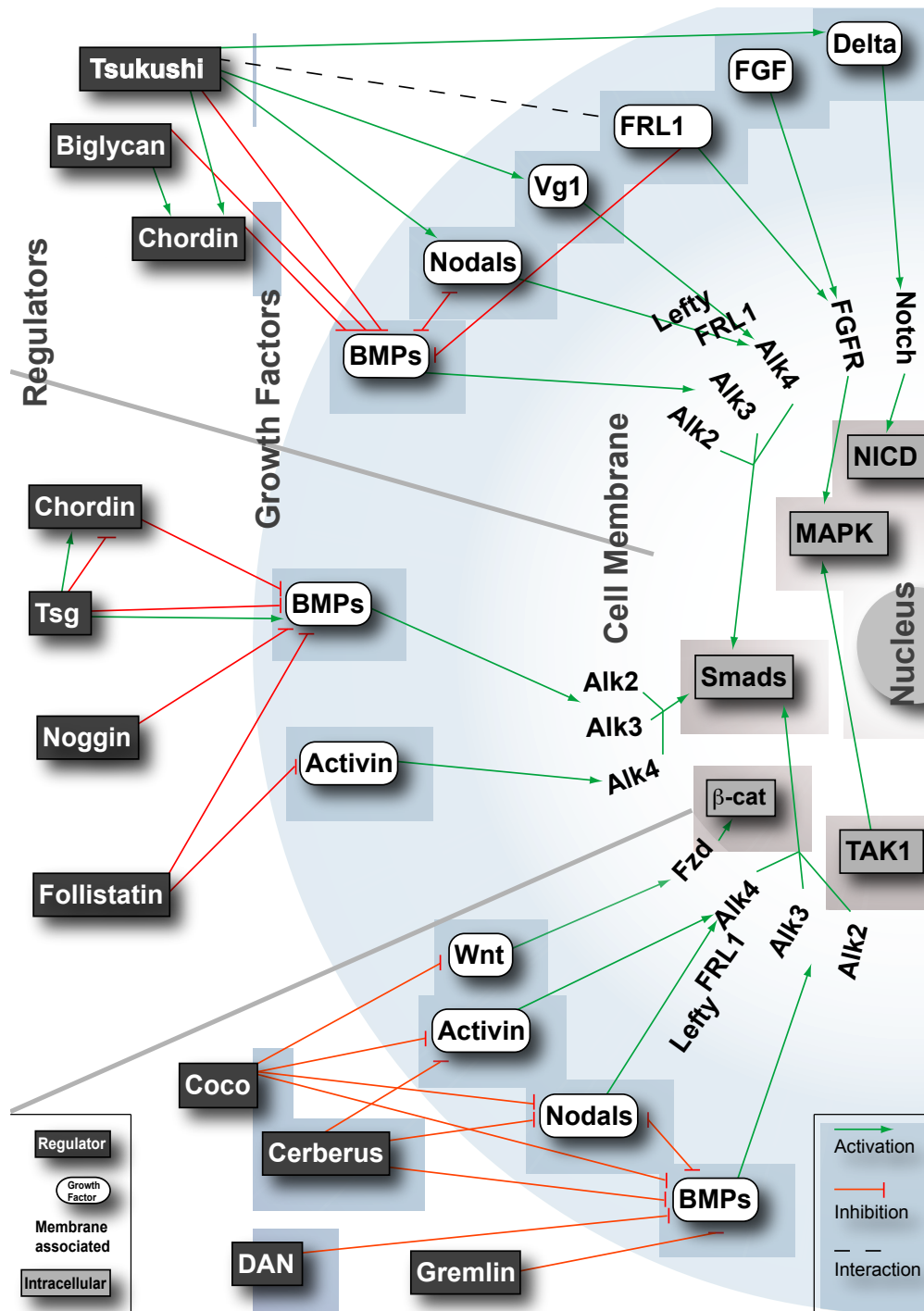


Figure 11.5: **Model of the extracellular network in *Xenopus laevis***
 Schematic representation of the extracellular network in the *Xenopus* embryo. Interactions between components are denoted by red, green or blue lines. This is by no means an exhaustive representation of factors in the extracellular matrix. Dark grey boxes: Extracellular regulators. White boxes: Secreted growth factors. No boxes: membrane associated proteins and regulators. Light grey boxes: Intracellular signalling.

Acknowledgments

Principally I would like to express gratitude to my supervisor, Dr. Shin-ichi Ohnuma. I am indebted to him for the opportunity he has provided me to study *Xenopus* development in his laboratory and the continuous source of inspiration he has provided.

I would also like to thank members of the Ohnuma group, past and present; Iris Chan, Maki Daniels, Kamran Hussein, Maiko Kurosawa, Toshiaki Mochizuki, Caroline Waters and Julie Watson. In particular, much appreciation goes to Xana Almeida and Katerina Bilitou for help, support, friendship and much laughter. Acknowledgments also go to the Philpott lab; Anna Philpott for guidance and ‘constructive criticism’, Helen Wise for her friendship for many years, Jon Vosper for his alternative teachings, Hector Boix-Perales for missions to the LMB tea room, Ruth Cosgrove for her patience in teaching me *Xenopus* techniques and Mehregan Movassagh for entertainment during lengthy animal capping sessions. Thanks also go to Ian Horan, Cristelle Fiore-Heriche, Kasumi Murai, Kate Wilson and Ryan Roark of the Philpott group and countless other members of ‘The Hutch’ who have made my time there so enjoyable.

In terms of collaborations, appreciation is shown to Kunimasa Ohta, Sei Kuriyama, Giuseppe Lupo and Marko Hyvönen for technical advice and reagents. Special thanks go to Kunimasa for his crash-course to Japan and Marko for all his support.

Deep gratitude goes to my parents, whose continuous love, support and encouragement has carried me to this point. These sentiments are also extended to my Grandmother, with much respect for her input over the years.

Thank you to Miraz, for his undivided support and the strength he has

given me.

I would also like to Acknowledge the Medical Research Council and Clare College for financial support. I am also very appreciative to the Department of Oncology and Hutchison/MRC, Professor Bruce Ponder and Professor Ron Laskey respectively for creating such a stimulating scientific environment to belong to.

Cambridge 5th September 2006

Bibliography

Bibliography

- T. Abe, M. Furue, A. Kondow, K. Matsuzaki, and M. Asashima. Notch signaling modulates the nuclear localization of carboxy-terminal-phosphorylated Smad2 and controls the competence of ectodermal cells for activin A. *Mech Dev*, 122(5):671–680, May 2005.
- B. A. Afouda, A. Ciau-Uitz, and R. Patient. GATA4, 5 and 6 mediate TGF β maintenance of endodermal gene expression in *Xenopus* embryos. *Development*, 132(4):763–774, Feb 2005.
- E. Agius, M. Oelgeschläger, O. Wessely, C. Kemp, and E. M. D. Robertis. Endodermal Nodal-related signals and mesoderm induction in *Xenopus*. *Development*, 127(6):1173–1183, Mar 2000.
- E. Amaya, T. J. Musci, and M. W. Kirschner. Expression of a dominant negative mutant of the FGF receptor disrupts mesoderm formation in *Xenopus* embryos. *Cell*, 66(2):257–270, Jul 1991.
- E. Amaya, P. A. Stein, T. J. Musci, and M. W. Kirschner. FGF signalling in the early specification of mesoderm in *Xenopus*. *Development*, 118(2):477–487, Jun 1993.
- H. Amthor, B. Christ, F. Rashid-Doubell, C. F. Kemp, E. Lang, and K. Patel. Follistatin regulates bone morphogenetic protein-7 (BMP-7) activity to stimulate embryonic muscle growth. *Dev Biol*, 243(1):115–127, Mar 2002.
- H. Amthor, G. Nicholas, I. McKinnell, C. F. Kemp, M. Sharma, R. Kambadur, and K. Patel. Follistatin complexes Myostatin and antagonises Myostatin-mediated inhibition of myogenesis. *Dev Biol*, 270(1):19–30, Jun 2004.

- L. M. Angerer, D. W. Oleksyn, C. Y. Logan, D. R. McClay, L. Dale, and R. C. Angerer. A BMP pathway regulates cell fate allocation along the sea urchin animal-vegetal embryonic axis. *Development*, 127(5):1105–1114, Mar 2000.
- T. Ariizumi, K. Sawamura, H. Uchiyama, and M. Asashima. Dose and time-dependent mesoderm induction and outgrowth formation by activin A in *Xenopus laevis*. *Int J Dev Biol*, 35(4):407–414, Dec 1991.
- M. Artinger, I. Blitz, K. Inoue, U. Tran, and K. W. Cho. Interaction of goosecoid and brachyury in *Xenopus* mesoderm patterning. *Mech Dev*, 65(1-2):187–196, Jul 1997.
- N. T. Bech-Hansen, M. J. Naylor, T. A. Maybaum, R. L. Sparkes, B. Koop, D. G. Birch, A. A. Bergen, C. F. Prinsen, R. C. Polomeno, A. Gal, A. V. Drack, M. A. Musarella, S. G. Jacobson, R. S. Young, and R. G. Weleber. Mutations in NYX, encoding the leucine-rich proteoglycan nyctalopin, cause X-linked complete congenital stationary night blindness. *Nat Genet*, 26(3):319–323, Nov 2000.
- R. Beddington. Left, right, left... turn. *Nature*, 381(6578):116–117, May 1996.
- E. Bell, I. Muñoz-Sanjuán, C. R. Altmann, A. Vonica, and A. H. Brivanlou. Cell fate specification and competence by Coco, a maternal BMP, TGF β and Wnt inhibitor. *Development*, 130(7):1381–1389, Apr 2003.
- E. Bengtsson, P. J. Neame, D. Heinegård, and Y. Sommarin. The primary structure of a basic leucine-rich repeat protein, PRELP, found in connective tissues. *J Biol Chem*, 270(43):25639–25644, Oct 1995.
- H. Bentz, R. M. Nathan, D. M. Rosen, R. M. Armstrong, A. Y. Thompson, P. R. Segarini, M. C. Mathews, J. R. Dasch, K. A. Piez, and S. M. Seyedin. Purification and characterization of a unique osteoinductive factor from bovine bone. *J Biol Chem*, 264(34):20805–20810, Dec 1989.
- B. Birsoy, L. Berg, P. H. Williams, J. C. Smith, C. C. Wylie, J. L. Christian, and J. Heasman. XPACE4 is a localized pro-protein convertase required for

- mesoderm induction and the cleavage of specific TGF β proteins in xenopus development. *Development*, 132(3):591–602, Feb 2005.
- I. L. Blitz and K. W. Cho. Anterior neurectoderm is progressively induced during gastrulation: the role of the *Xenopus* homeobox gene orthodenticle. *Development*, 121(4):993–1004, Apr 1995.
- I. L. Blitz, O. Shimmi, K. Wünnenberg-Stapleton, M. B. O'Connor, and K. W. Cho. Is chordin a long-range- or short-range-acting factor? roles for BMP1-related metalloproteases in chordin and BMP4 autofeedback loop regulation. *Dev Biol*, 223(1):120–138, Jul 2000.
- I. L. Blitz, K. W. Y. Cho, and C. Chang. Twisted gastrulation loss-of-function analyses support its role as a BMP inhibitor during early *Xenopus* embryogenesis. *Development*, 130(20):4975–4988, Oct 2003.
- T. C. Blochberger, P. K. Cornuet, and J. R. Hassell. Isolation and partial characterization of lumican and decorin from adult chicken corneas. A keratan sulfate-containing isoform of decorin is developmentally regulated. *J Biol Chem*, 267(29):20613–20619, Oct 1992.
- T. Bouwmeester, S. Kim, Y. Sasai, B. Lu, and E. M. D. Robertis. Cerberus is a head-inducing secreted factor expressed in the anterior endoderm of Spemann's organizer. *Nature*, 382(6592):595–601, Aug 1996.
- W. W. Branford and H. J. Yost. Lefty-dependent inhibition of Nodal- and Wnt-responsive organizer gene expression is essential for normal gastrulation. *Curr Biol*, 12(24):2136–2141, Dec 2002.
- E. Browaeys-Poly, K. Cailliau, and J. P. Vilain. Signal transduction pathways triggered by fibroblast growth factor receptor 1 expressed in *Xenopus laevis* oocytes after fibroblast growth factor 1 addition. role of Grb2, phosphatidylinositol 3-kinase, Src tyrosine kinase, and phospholipase C γ . *Eur J Biochem*, 267(20):6256–6263, Oct 2000.

- K. Butler, A. M. Zorn, and J. B. Gurdon. Nonradioactive in situ hybridization to *Xenopus* tissue sections. *Methods*, 23(4):303–312, Apr 2001.
- R. Carballada, H. Yasuo, and P. Lemaire. Phosphatidylinositol-3 kinase acts in parallel to the ERK MAP kinase in the FGF pathway during *Xenopus* mesoderm induction. *Development*, 128(1):35–44, Jan 2001.
- S.-W. Cha, Y.-S. Hwang, J.-P. Chae, S.-Y. Lee, H.-S. Lee, I. Daar, M. J. Park, and J. Kim. Inhibition of FGF signaling causes expansion of the endoderm in *Xenopus*. *Biochem Biophys Res Commun*, 315(1):100–106, Feb 2004.
- Y. R. Cha, S. Takahashi, and C. V. E. Wright. Cooperative non-cell and cell autonomous regulation of Nodal gene expression and signaling by Lefty/Antivin and Brachyury in *Xenopus*. *Dev Biol*, 290(2):246–264, Feb 2006.
- C. Chang and A. Hemmati-Brivanlou. *Xenopus* GDF6, a new antagonist of noggin and a partner of BMPs. *Development*, 126(15):3347–3357, Aug 1999.
- C. Chang, D. A. Holtzman, S. Chau, T. Chickering, E. A. Woolf, L. M. Holmgren, J. Bodorova, D. P. Gearing, W. E. Holmes, and A. H. Brivanlou. Twisted gastrulation can function as a BMP antagonist. *Nature*, 410(6827):483–487, Mar 2001.
- C. Chang, B. J. L. Eggen, D. C. Weinstein, and A. H. Brivanlou. Regulation of nodal and BMP signaling by tomoregulin-1 (X7365) through novel mechanisms. *Dev Biol*, 255(1):1–11, Mar 2003.
- S. C. Chapman, F. R. Schubert, G. C. Schoenwolf, and A. Lumsden. Analysis of spatial and temporal gene expression patterns in blastula and gastrula stage chick embryos. *Dev Biol*, 245(1):187–199, May 2002.
- Y. Chen, E. Mironova, L. L. Whitaker, L. Edwards, H. J. Yost, and A. F. Ramsdell. ALK4 functions as a receptor for multiple TGF β -related ligands to regulate left-right axis determination and mesoderm induction in *Xenopus*. *Dev Biol*, 268(2):280–294, Apr 2004.

- A. M. Cheng, B. Thisse, C. Thisse, and C. V. Wright. The lefty-related factor *Xatv* acts as a feedback inhibitor of nodal signaling in mesoderm induction and L-R axis development in *Xenopus*. *Development*, 127(5):1049–1061, Mar 2000.
- S. K. Cheng, F. Olale, J. T. Bennett, A. H. Brivanlou, and A. F. Schier. EGF-CFC proteins are essential coreceptors for the TGF- β signals *Vg1* and *GDF1*. *Genes Dev*, 17(1):31–36, Jan 2003.
- S. K. Cheng, F. Olale, A. H. Brivanlou, and A. F. Schier. Lefty blocks a subset of TGF β signals by antagonizing EGF-CFC coreceptors. *PLoS Biol*, 2(2):E30, Feb 2004.
- K. W. Cho, B. Blumberg, H. Steinbeisser, and E. M. D. Robertis. Molecular nature of Spemann’s organizer: the role of the *Xenopus* homeobox gene *gooseoid*. *Cell*, 67(6):1111–1120, Dec 1991.
- A. Ciccociola, R. Dono, S. Obici, A. Simeone, M. Zollo, and M. G. Persico. Molecular characterization of a gene of the ‘EGF family’ expressed in undifferentiated human NTERA2 teratocarcinoma cells. *EMBO J*, 8(7):1987–1991, Jul 1989.
- D. Clements and H. R. Woodland. VegT induces endoderm by a self-limiting mechanism and by changing the competence of cells to respond to TGF- β signals. *Dev Biol*, 258(2):454–463, Jun 2003.
- D. Clements, R. V. Friday, and H. R. Woodland. Mode of action of VegT in mesoderm and endoderm formation. *Development*, 126(21):4903–4911, Nov 1999.
- F. L. Conlon, K. S. Barth, and E. J. Robertson. A novel retrovirally induced embryonic lethal mutation in the mouse: assessment of the developmental fate of embryonic stem cells homozygous for the 413.d proviral integration. *Development*, 111(4):969–981, Apr 1991.

- F. L. Conlon, K. M. Lyons, N. Takaesu, K. S. Barth, A. Kispert, B. Herrmann, and E. J. Robertson. A primary requirement for nodal in the formation and maintenance of the primitive streak in the mouse. *Development*, 120(7):1919–1928, Jul 1994.
- F. L. Conlon, S. G. Sedgwick, K. M. Weston, and J. C. Smith. Inhibition of *xbra* transcription activation causes defects in mesodermal patterning and reveals autoregulation of Xbra in dorsal mesoderm. *Development*, 122(8):2427–2435, Aug 1996.
- L. M. Corpuz, J. L. Funderburgh, M. L. Funderburgh, G. S. Bottomley, S. Prakash, and G. W. Conrad. Molecular cloning and tissue distribution of keratocan. bovine corneal keratan sulfate proteoglycan 37a. *J Biol Chem*, 271(16):9759–9763, Apr 1996.
- W. G. Cox and A. Hemmati-Brivanlou. Caudalization of neural fate by tissue recombination and bFGF. *Development*, 121(12):4349–4358, Dec 1995.
- V. Cunliffe and J. C. Smith. Ectopic mesoderm formation in *Xenopus* embryos caused by widespread expression of a Brachyury homologue. *Nature*, 358(6385):427–430, Jul 1992.
- V. Cunliffe and J. C. Smith. Specification of mesodermal pattern in *Xenopus laevis* by interactions between Brachyury, noggin and Xwnt-8. *EMBO J*, 13(2):349–359, Jan 1994.
- N. S. Cunningham, V. Paralkar, and A. H. Reddi. Osteogenin and recombinant bone morphogenetic protein 2b are chemotactic for human monocytes and stimulate Transforming Growth Factor Beta 1 mRNA expression. *Proc Natl Acad Sci U S A*, 89(24):11740–11744, Dec 1992.
- L. Dale and J. M. Slack. Regional specification within the mesoderm of early embryos of *Xenopus laevis*. *Development*, 100(2):279–295, Jun 1987.
- L. Dale and F. C. Wardle. A gradient of BMP activity specifies dorsal-ventral

- fates in early *Xenopus* embryos. *Semin Cell Dev Biol*, 10(3):319–326, Jun 1999.
- L. Dale, G. Howes, B. M. Price, and J. C. Smith. Bone morphogenetic protein 4: a ventralizing factor in early *Xenopus* development. *Development*, 115(2): 573–585, Jun 1992.
- S. Darras, Y. Marikawa, R. P. Elinson, and P. Lemaire. Animal and vegetal pole cells of early *Xenopus* embryos respond differently to maternal dorsal determinants: implications for the patterning of the organiser. *Development*, 124(21):4275–4286, Nov 1997.
- J. Ding, L. Yang, Y. T. Yan, A. Chen, N. Desai, A. Wynshaw-Boris, and M. M. Shen. Cripto is required for correct orientation of the anterior-posterior axis in the mouse embryo. *Nature*, 395(6703):702–707, Oct 1998.
- K. Dorey and C. S. Hill. A novel Cripto-related protein reveals an essential role for EGF-CFCs in Nodal signalling in *Xenopus* embryos. *Dev Biol*, 292(2): 303–316, Apr 2006.
- S. Dupont, L. Zacchigna, M. Cordenonsi, S. Soligo, M. Adorno, M. Rugge, and S. Piccolo. Germ-layer specification and control of cell growth by ectodermin, a Smad4 ubiquitin ligase. *Cell*, 121(1):87–99, Apr 2005.
- S. Dyson and J. B. Gurdon. Activin signalling has a necessary function in *Xenopus* early development. *Curr Biol*, 7(1):81–84, Jan 1997.
- S. Dyson and J. B. Gurdon. The interpretation of position in a morphogen gradient as revealed by occupancy of activin receptors. *Cell*, 93(4):557–568, May 1998.
- V. Ecochard, C. Cayrol, F. Foulquier, A. Zaraisky, and A. M. Duprat. A novel TGF- β -like gene, fugacin, specifically expressed in the Spemann organizer of *Xenopus*. *Dev Biol*, 172(2):699–703, Dec 1995.
- P. M. Eimon and R. M. Harland. In *Xenopus* embryos, BMP heterodimers

are not required for mesoderm induction, but BMP activity is necessary for dorsal/ventral patterning. *Dev Biol*, 216(1):29–40, Dec 1999.

P. M. Eimon and R. M. Harland. *Xenopus* Dan, a member of the Dan gene family of BMP antagonists, is expressed in derivatives of the cranial and trunk neural crest. *Mech Dev*, 107(1-2):187–189, Sep 2001.

P. M. Eimon and R. M. Harland. Effects of heterodimerization and proteolytic processing on derrière and Nodal activity: implications for mesoderm induction in *Xenopus*. *Development*, 129(13):3089–3103, Jul 2002.

M. J. Engleka, E. J. Craig, and D. S. Kessler. VegT activation of Sox17 at the midblastula transition alters the response to nodal signals in the vegetal endoderm domain. *Dev Biol*, 237(1):159–172, Sep 2001.

F. S. Esch, S. Shimasaki, M. Mercado, K. Cooksey, N. Ling, S. Ying, N. Ueno, and R. Guillemin. Structural characterization of follistatin: a novel follicle-stimulating hormone release-inhibiting polypeptide from the gonad. *Mol Endocrinol*, 1(11):849–855, Nov 1987.

C. H. Ezal, C. D. Marion, and W. C. Smith. Primary structure requirements for *Xenopus* nodal-related 3 and a comparison with regions required by *Xenopus* nodal-related 2. *J Biol Chem*, 275(19):14124–14131, May 2000.

A. Fainsod, H. Steinbeisser, and E. M. D. Robertis. On the function of BMP-4 in patterning the marginal zone of the *Xenopus* embryo. *EMBO J*, 13(21):5015–5025, Nov 1994.

A. Fainsod, K. Deissler, R. Yelin, K. Marom, M. Epstein, G. Pillemer, H. Steinbeisser, and M. Blum. The dorsalizing and neural inducing gene follistatin is an antagonist of BMP-4. *Mech Dev*, 63(1):39–50, Apr 1997.

D. Fambrough, K. McClure, A. Kazlauskas, and E. S. Lander. Diverse signaling pathways activated by growth factor receptors induce broadly overlapping, rather than independent, sets of genes. *Cell*, 97(6):727–741, Jun 1999.

- S. Faure, M. A. Lee, T. Keller, P. ten Dijke, and M. Whitman. Endogenous patterns of TGF β superfamily signaling during early *Xenopus* development. *Development*, 127(13):2917–2931, Jul 2000.
- B. Feldman, M. A. Gates, E. S. Egan, S. T. Dougan, G. Rennebeck, H. I. Sirotkin, A. F. Schier, and W. S. Talbot. Zebrafish organizer development and germ-layer formation require nodal-related signals. *Nature*, 395(6698):181–185, Sep 1998.
- B. Feldman, S. T. Dougan, A. F. Schier, and W. S. Talbot. Nodal-related signals establish mesendodermal fate and trunk neural identity in zebrafish. *Curr Biol*, 10(9):531–534, May 2000.
- L. W. Fisher, J. D. Termine, and M. F. Young. Deduced protein sequence of bone small proteoglycan I (biglycan) shows homology with proteoglycan II (decorin) and several nonconnective tissue proteins in a variety of species. *J Biol Chem*, 264(8):4571–4576, Mar 1989.
- R. B. Fletcher, J. C. Baker, and R. M. Harland. FGF8 spliceforms mediate early mesoderm and posterior neural tissue formation in *Xenopus*. *Development*, 133(9):1703–1714, May 2006.
- V. Francois and E. Bier. *Xenopus* chordin and *Drosophila* short gastrulation genes encode homologous proteins functioning in dorsal-ventral axis formation. *Cell*, 80(1):19–20, Jan 1995.
- V. Francois, M. Solloway, J. W. O’Neill, J. Emery, and E. Bier. Dorsal-ventral patterning of the *Drosophila* embryo depends on a putative negative growth factor encoded by the short gastrulation gene. *Genes Dev*, 8(21):2602–2616, Nov 1994.
- D. Frank and R. M. Harland. Transient expression of XMyoD in non-somitic mesoderm of *Xenopus* gastrulae. *Development*, 113(4):1387–1393, Dec 1991.
- A. Fukui, T. Nakamura, K. Sugino, K. Takio, H. Uchiyama, M. Asashima, and

- H. Sugino. Isolation and characterization of *Xenopus* follistatin and activins. *Dev Biol*, 159(1):131–139, Sep 1993.
- A. Fukui, T. Nakamura, H. Uchiyama, K. Sugino, H. Sugino, and M. Asashima. Identification of activins A, AB, and B and follistatin proteins in *Xenopus* embryos. *Dev Biol*, 163(1):279–281, May 1994.
- D. Gaddy-Kurten, K. Tsuchida, and W. Vale. Activins and the receptor serine kinase superfamily. *Recent Prog Horm Res*, 50:109–129, 1995.
- L. W. Gamer and C. V. Wright. Autonomous endodermal determination in *Xenopus*: regulation of expression of the pancreatic gene *XlHbox 8*. *Dev Biol*, 171(1):240–251, Sep 1995.
- L. S. Gammill and H. Sive. *Otx2* expression in the ectoderm activates anterior neural determination and is required for *Xenopus* cement gland formation. *Dev Biol*, 240(1):223–236, Dec 2001.
- S. F. Gilbert. *Developmental Biology; Seventh Edition*. Sinauer, 2003.
- A. Glavic, F. Silva, M. J. Aybar, F. Bastidas, and R. Mayor. Interplay between Notch signaling and the homeoprotein *Xiro1* is required for neural crest induction in *Xenopus* embryos. *Development*, 131(2):347–359, Jan 2004.
- A. Glinka, H. Delius, C. Blumenstock, and C. Niehrs. Combinatorial signalling by *Xwnt-11* and *Xnr3* in the organizer epithelium. *Mech Dev*, 60(2):221–231, Dec 1996.
- A. Glinka, W. Wu, D. Onichtchouk, C. Blumenstock, and C. Niehrs. Head induction by simultaneous repression of *Bmp* and *Wnt* signalling in *Xenopus*. *Nature*, 389(6650):517–519, Oct 1997.
- C. Glister, C. F. Kemp, and P. G. Knight. Bone morphogenetic protein (BMP) ligands and receptors in bovine ovarian follicle cells: actions of BMP-4, -6 and -7 on granulosa cells and differential modulation of Smad-1 phosphorylation by follistatin. *Reproduction*, 127(2):239–254, Feb 2004.

- J. M. Graff, R. S. Thies, J. J. Song, A. J. Celeste, and D. A. Melton. Studies with a *Xenopus* BMP receptor suggest that ventral mesoderm-inducing signals override dorsal signals in vivo. *Cell*, 79(1):169–179, Oct 1994.
- P. Grant and J. F. Wacaster. The amphibian gray crescent region—a site of developmental information? *Dev Biol*, 28(3):454–471, Jul 1972.
- J. B. Green and J. C. Smith. Graded changes in dose of a *Xenopus* activin a homologue elicit stepwise transitions in embryonic cell fate. *Nature*, 347(6291):391–394, Sep 1990.
- J. B. Green, H. V. New, and J. C. Smith. Responses of embryonic *Xenopus* cells to activin and FGF are separated by multiple dose thresholds and correspond to distinct axes of the mesoderm. *Cell*, 71(5):731–739, Nov 1992.
- J. Greenwald, M. E. Vega, G. P. Allendorph, W. H. Fischer, W. Vale, and S. Choe. A flexible activin explains the membrane-dependent cooperative assembly of TGF- β family receptors. *Mol Cell*, 15(3):485–489, Aug 2004.
- O. H. Grimm and J. B. Gurdon. Nuclear exclusion of Smad2 is a mechanism leading to loss of competence. *Nat Cell Biol*, 4(7):519–522, Jul 2002.
- K. Gritsman, J. Zhang, S. Cheng, E. Heckscher, W. S. Talbot, and A. F. Schier. The EGF-CFC protein one-eyed pinhead is essential for nodal signaling. *Cell*, 97(1):121–132, Apr 1999.
- J. Groppe, J. Greenwald, E. Wiater, J. Rodriguez-Leon, A. N. Economides, W. Kwiatkowski, M. Affolter, W. W. Vale, J. C. I. Belmonte, and S. Choe. Structural basis of BMP signalling inhibition by the cystine knot protein Noggin. *Nature*, 420(6916):636–642, Dec 2002.
- L. Grotewold, M. Plum, R. Dildrop, T. Peters, and U. R  ther. Bambi is coexpressed with Bmp-4 during mouse embryogenesis. *Mech Dev*, 100(2):327–330, Feb 2001.
- Z. Gu, M. Nomura, B. B. Simpson, H. Lei, A. Feijen, J. van den Eijnden-van Raaij, P. K. Donahoe, and E. Li. The type I activin receptor ActRIB is

- required for egg cylinder organization and gastrulation in the mouse. *Genes Dev*, 12(6):844–857, Mar 1998.
- J. B. Gurdon, S. Fairman, T. J. Mohun, and S. Brennan. Activation of muscle-specific actin genes in *Xenopus* development by an induction between animal and vegetal cells of a blastula. *Cell*, 41(3):913–922, Jul 1985.
- J. B. Gurdon, P. Harger, A. Mitchell, and P. Lemaire. Activin signalling and response to a morphogen gradient. *Nature*, 371(6497):487–492, Oct 1994.
- J. B. Gurdon, A. Mitchell, and D. Mahony. Direct and continuous assessment by cells of their position in a morphogen gradient. *Nature*, 376(6540):520–521, Aug 1995.
- B. Hall. *The Neural Crest in Development and Evolution*. New York: Springer Verlag., 1999.
- J. Hama and D. C. Weinstein. Is Chordin a morphogen? *Bioessays*, 23(2):121–124, Feb 2001.
- C. S. Hansen, C. D. Marion, K. Steele, S. George, and W. C. Smith. Direct neural induction and selective inhibition of mesoderm and epidermis inducers by Xnr3. *Development*, 124(2):483–492, Jan 1997.
- R. Harland and J. Gerhart. Formation and function of Spemann’s organizer. *Annu Rev Cell Dev Biol*, 13:611–667, 1997.
- R. M. Harland. In situ hybridization: an improved whole-mount method for *Xenopus* embryos. *Methods Cell Biol*, 36:685–695, 1991.
- R. M. Harland. The transforming growth factor beta family and induction of the vertebrate mesoderm: bone morphogenetic proteins are ventral inducers. *Proc Natl Acad Sci U S A*, 91(22):10243–10246, Oct 1994.
- A. E. Harrington, S. A. Morris-Triggs, B. T. Ruotolo, C. V. Robinson, S.-I. Ohnuma, and M. Hyvönen. Structural basis for the inhibition of activin signalling by follistatin. *EMBO J*, 25(5):1035–1045, Mar 2006.

- R. P. Harvey. Widespread expression of MyoD genes in *Xenopus* embryos is amplified in presumptive muscle as a delayed response to mesoderm induction. *Proc Natl Acad Sci U S A*, 88(20):9198–9202, Oct 1991.
- J. Heasman. Patterning the *Xenopus* blastula. *Development*, 124(21):4179–4191, Nov 1997.
- J. Heasman. Maternal determinants of embryonic cell fate. *Semin Cell Dev Biol*, 17(1):93–98, Feb 2006.
- J. Heasman, C. C. Wylie, P. Hausen, and J. C. Smith. Fates and states of determination of single vegetal pole blastomeres of *X. laevis*. *Cell*, 37(1):185–194, May 1984.
- A. Hemmati-Brivanlou and D. A. Melton. A truncated activin receptor inhibits mesoderm induction and formation of axial structures in *Xenopus* embryos. *Nature*, 359(6396):609–614, Oct 1992.
- A. Hemmati-Brivanlou and G. H. Thomsen. Ventral mesodermal patterning in *Xenopus* embryos: expression patterns and activities of BMP-2 and BMP-4. *Dev Genet*, 17(1):78–89, 1995.
- A. Hemmati-Brivanlou, R. M. Stewart, and R. M. Harland. Region-specific neural induction of an engrailed protein by anterior notochord in *Xenopus*. *Science*, 250(4982):800–802, Nov 1990.
- A. Hemmati-Brivanlou, J. R. de la Torre, C. Holt, and R. M. Harland. Cephalic expression and molecular characterization of *Xenopus* En-2. *Development*, 111(3):715–724, Mar 1991.
- A. Hemmati-Brivanlou, O. G. Kelly, and D. A. Melton. Follistatin, an antagonist of activin, is expressed in the Spemann organizer and displays direct neuralizing activity. *Cell*, 77(2):283–295, Apr 1994.
- G. L. Henry, I. H. Brivanlou, D. S. Kessler, A. Hemmati-Brivanlou, and D. A. Melton. TGF- β signals and a pattern in *Xenopus laevis* endodermal development. *Development*, 122(3):1007–1015, Mar 1996.

- C. Hensey, V. Dolan, and H. R. Brady. The *Xenopus* pronephros as a model system for the study of kidney development and pathophysiology. *Nephrol Dial Transplant*, 17 Suppl 9:73–74, 2002.
- A. Hildebrand, M. Romaris, L. M. Rasmussen, D. Heinegård, D. R. Twardzik, W. A. Border, and E. Ruoslahti. Interaction of the small interstitial proteoglycans biglycan, decorin and fibromodulin with transforming growth factor beta. *Biochem J*, 302 (Pt 2):527–534, Sep 1994.
- C. S. Hill. TGF- β signalling pathways in early *Xenopus* development. *Curr Opin Genet Dev*, 11(5):533–540, Oct 2001.
- A. M. Hocking, T. Shinomura, and D. J. McQuillan. Leucine-rich repeat glycoproteins of the extracellular matrix. *Matrix Biol*, 17(1):1–19, Apr 1998.
- B. L. Hogan. Bone morphogenetic proteins in development. *Curr Opin Genet Dev*, 6(4):432–438, Aug 1996.
- P. A. Hoodless, T. Tsukazaki, S. Nishimatsu, L. Attisano, J. L. Wrana, and G. H. Thomsen. Dominant-negative Smad2 mutants inhibit activin/Vg1 signaling and disrupt axis formation in *Xenopus*. *Dev Biol*, 207(2):364–379, Mar 1999.
- N. D. Hopwood, A. Pluck, and J. B. Gurdon. A *Xenopus* mRNA related to *Drosophila* twist is expressed in response to induction in the mesoderm and the neural crest. *Cell*, 59(5):893–903, Dec 1989a.
- N. D. Hopwood, A. Pluck, and J. B. Gurdon. MyoD expression in the forming somites is an early response to mesoderm induction in *Xenopus* embryos. *EMBO J*, 8(11):3409–3417, Nov 1989b.
- M. Howell and C. S. Hill. XSmad2 directly activates the activin-inducible, dorsal mesoderm gene XFKH1 in *Xenopus* embryos. *EMBO J*, 16(24):7411–7421, Dec 1997.
- D. R. Hsu, A. N. Economides, X. Wang, P. M. Eimon, and R. M. Harland.

- The *Xenopus* dorsalizing factor Gremlin identifies a novel family of secreted proteins that antagonize BMP activities. *Mol Cell*, 1(5):673–683, Apr 1998.
- C. Hudson, D. Clements, R. V. Friday, D. Stott, and H. R. Woodland. Xsox17 α and - β mediate endoderm formation in *Xenopus*. *Cell*, 91(3):397–405, Oct 1997.
- P. M. Iannaccone, X. Zhou, M. Khokha, D. Boucher, and M. R. Kuehn. Insertional mutation of a gene involved in growth regulation of the early mouse embryo. *Dev Dyn*, 194(3):198–208, Jul 1992.
- S. Iemura, T. S. Yamamoto, C. Takagi, H. Uchiyama, T. Natsume, S. Shimasaki, H. Sugino, and N. Ueno. Direct binding of follistatin to a complex of bone-morphogenetic protein and its receptor inhibits ventral and epidermal cell fates in early *Xenopus* embryo. *Proc Natl Acad Sci U S A*, 95(16):9337–9342, Aug 1998.
- R. V. Iozzo. The family of the small leucine-rich proteoglycans: key regulators of matrix assembly and cellular growth. *Crit Rev Biochem Mol Biol*, 32(2):141–174, 1997.
- H. V. Isaacs, M. E. Pownall, and J. M. Slack. eFGF regulates Xbra expression during *Xenopus* gastrulation. *EMBO J*, 13(19):4469–4481, Oct 1994.
- H. V. Isaacs, M. E. Pownall, and J. M. Slack. Regulation of Hox gene expression and posterior development by the *Xenopus* caudal homologue Xcad3. *EMBO J*, 17(12):3413–3427, Jun 1998.
- A. Ishimura, R. Maeda, M. Takeda, M. Kikkawa, I. O. Daar, and M. Maéno. Involvement of BMP-4/msx-1 and FGF pathways in neural induction in the *Xenopus* embryo. *Dev Growth Differ*, 42(4):307–316, Aug 2000.
- F. Itoh, H. Asao, K. Sugamura, C. H. Heldin, P. ten Dijke, and S. Itoh. Promoting bone morphogenetic protein signaling through negative regulation of inhibitory Smads. *EMBO J*, 20(15):4132–4142, Aug 2001.

- K. Itoh and S. Y. Sokol. Graded amounts of *Xenopus* dishevelled specify discrete anteroposterior cell fates in prospective ectoderm. *Mech Dev*, 61(1-2):113–125, Jan 1997.
- C. M. Jones and J. C. Smith. Establishment of a BMP-4 morphogen gradient by long-range inhibition. *Dev Biol*, 194(1):12–17, Feb 1998.
- C. M. Jones, K. M. Lyons, P. M. Lapan, C. V. Wright, and B. L. Hogan. DVR-4 (bone morphogenetic protein-4) as a posterior-ventralizing factor in *Xenopus* mesoderm induction. *Development*, 115(2):639–647, Jun 1992.
- C. M. Jones, M. R. Kuehn, B. L. Hogan, J. C. Smith, and C. V. Wright. Nodal-related signals induce axial mesoderm and dorsalize mesoderm during gastrulation. *Development*, 121(11):3651–3662, Nov 1995.
- C. M. Jones, N. Armes, and J. C. Smith. Signalling by TGF- β family members: short-range effects of Xnr-2 and BMP-4 contrast with the long-range effects of activin. *Curr Biol*, 6(11):1468–1475, Nov 1996.
- E. M. Joseph and D. A. Melton. Xnr4: a *Xenopus* nodal-related gene expressed in the Spemann organizer. *Dev Biol*, 184(2):367–372, Apr 1997.
- E. M. Joseph and D. A. Melton. Mutant Vg1 ligands disrupt endoderm and mesoderm formation in *Xenopus* embryos. *Development*, 125(14):2677–2685, Jul 1998.
- K. Joubin and C. D. Stern. Molecular interactions continuously define the organizer during the cell movements of gastrulation. *Cell*, 98(5):559–571, Sep 1999.
- M. R. Kalt. The relationship between cleavage and blastocoel formation in *Xenopus laevis*. I. light microscopic observations. *J Embryol Exp Morphol*, 26(1):37–49, Aug 1971.
- D. S. Kessler and D. A. Melton. Induction of dorsal mesoderm by soluble, mature Vg1 protein. *Development*, 121(7):2155–2164, Jul 1995.

- H. T. Keutmann, A. L. Schneyer, and Y. Sidis. The role of follistatin domains in follistatin biological action. *Mol Endocrinol*, 18(1):228–240, Jan 2004.
- M. K. Khokha, J. Yeh, T. C. Grammer, and R. M. Harland. Depletion of three BMP antagonists from Spemann’s organizer leads to a catastrophic loss of dorsal structures. *Dev Cell*, 8(3):401–411, Mar 2005.
- D. M. Kingsley. The TGF- β superfamily: new members, new receptors, and new genetic tests of function in different organisms. *Genes Dev*, 8(2):133–146, Jan 1994.
- N. Kinoshita, J. Minshull, and M. W. Kirschner. The identification of two novel ligands of the FGF receptor by a yeast screening method and their activity in *Xenopus* development. *Cell*, 83(4):621–630, Nov 1995.
- T. Kirsch, W. Sebald, and M. K. Dreyer. Crystal structure of the BMP-2-BRIA ectodomain complex. *Nat Struct Biol*, 7(6):492–496, Jun 2000.
- R. D. Klein, Q. Gu, A. Goddard, and A. Rosenthal. Selection for genes encoding secreted proteins and receptors. *Proc Natl Acad Sci U S A*, 93(14):7108–7113, Jul 1996.
- B. Kobe and J. Deisenhofer. Crystal structure of porcine ribonuclease inhibitor, a protein with leucine-rich repeats. *Nature*, 366(6457):751–756, 1993.
- M. Kofron, T. Demel, J. Xanthos, J. Lohr, B. Sun, H. Sive, S. Osada, C. Wright, C. Wylie, and J. Heasman. Mesoderm induction in *Xenopus* is a zygotic event regulated by maternal VegT via TGF β growth factors. *Development*, 126(24):5759–5770, Dec 1999.
- M. Kolb, P. J. Margetts, P. J. Sime, and J. Gauldie. Proteoglycans decorin and biglycan differentially modulate TGF- β -mediated fibrotic responses in the lung. *Am J Physiol Lung Cell Mol Physiol*, 280(6):L1327–L1334, Jun 2001.
- M. Köster, S. Plessow, J. H. Clement, A. Lorenz, H. Tiedemann, and W. Knöchel. Bone morphogenetic protein 4 (BMP-4), a member of the TGF-

- β family, in early embryos of *Xenopus laevis*: analysis of mesoderm inducing activity. *Mech Dev*, 33(3):191–199, Mar 1991.
- K. L. Kroll and E. Amaya. Transgenic *Xenopus* embryos from sperm nuclear transplantations reveal FGF signaling requirements during gastrulation. *Development*, 122(10):3173–3183, Oct 1996.
- T. Krusius and E. Ruoslahti. Primary structure of an extracellular matrix proteoglycan core protein deduced from cloned cDNA. *Proc Natl Acad Sci U S A*, 83(20):7683–7687, Oct 1986.
- A. Kumar, V. Novoselov, A. J. Celeste, N. M. Wolfman, P. ten Dijke, and M. R. Kuehn. Nodal signaling uses activin and transforming growth factor- β receptor-regulated Smads. *J Biol Chem*, 276(1):656–661, Jan 2001.
- S. Kuriyama, G. Lupo, K. Ohta, S.-I. Ohnuma, W. A. Harris, and H. Tanaka. Tsukushi controls ectodermal patterning and neural crest specification in *Xenopus* by direct regulation of BMP4 and X-delta-1 activity. *Development*, 133(1):75–88, Jan 2006.
- H. Kuroda, O. Wessely, and E. M. D. Robertis. Neural induction in *Xenopus*: requirement for ectodermal and endomesodermal signals via Chordin, Noggin, β -Catenin, and Cerberus. *PLoS Biol*, 2(5):E92, May 2004.
- T. Kurth, S. Meissner, S. Schäckel, and H. Steinbeisser. Establishment of mesodermal gene expression patterns in early *Xenopus* embryos: the role of repression. *Dev Dyn*, 233(2):418–429, Jun 2005.
- C. LaBonne and M. Bronner-Fraser. Neural crest induction in *Xenopus*: evidence for a two-signal model. *Development*, 125(13):2403–2414, Jul 1998.
- C. LaBonne, B. Burke, and M. Whitman. Role of MAP kinase in mesoderm induction and axial patterning during *Xenopus* development. *Development*, 121(5):1475–1486, May 1995.

- T. M. Lamb and R. M. Harland. Fibroblast growth factor is a direct neural inducer, which combined with noggin generates anterior-posterior neural pattern. *Development*, 121(11):3627–3636, Nov 1995.
- T. M. Lamb, A. K. Knecht, W. C. Smith, S. E. Stachel, A. N. Economides, N. Stahl, G. D. Yancopoulos, and R. M. Harland. Neural induction by the secreted polypeptide noggin. *Science*, 262(5134):713–718, Oct 1993.
- J. Larrain, D. Bachiller, B. Lu, E. Agius, S. Piccolo, and E. M. D. Robertis. BMP-binding modules in chordin: a model for signalling regulation in the extracellular space. *Development*, 127(4):821–830, Feb 2000.
- J. Larrain, M. Oelgeschläger, N. I. Ketpura, B. Reversade, L. Zakin, and E. M. D. Robertis. Proteolytic cleavage of Chordin as a switch for the dual activities of Twisted gastrulation in BMP signaling. *Development*, 128(22):4439–4447, Nov 2001.
- B. V. Latinkic and J. C. Smith. Goosecoid and mix.1 repress Brachyury expression and are required for head formation in *Xenopus*. *Development*, 126(8):1769–1779, Apr 1999.
- N. Le Douarin and C. Kalcheim. *The Neural Crest, 2nd edn.*. Cambridge University Press: Cambridge., 1999.
- H. X. Lee, A. L. Ambrosio, B. Reversade, and E. M. D. Robertis. Embryonic dorsal-ventral signaling: secreted frizzled-related proteins as inhibitors of tolloid proteinases. *Cell*, 124(1):147–159, Jan 2006.
- M. A. Lee, J. Heasman, and M. Whitman. Timing of endogenous activin-like signals and regional specification of the *Xenopus* embryo. *Development*, 128(15):2939–2952, Aug 2001.
- P. Lemaire and H. Yasuo. Developmental signalling: a careful balancing act. *Curr Biol*, 8(7):R228–R231, Mar 1998.
- P. Lemaire, S. Darras, D. Caillol, and L. Kodjabachian. A role for the vegetally expressed *Xenopus* gene Mix.1 in endoderm formation and in the restriction

- of mesoderm to the marginal zone. *Development*, 125(13):2371–2380, Jul 1998.
- X. Lin and N. Perrimon. Role of heparan sulfate proteoglycans in cell-cell signaling in drosophila. *Matrix Biol*, 19(4):303–307, Aug 2000.
- J. L. Lohr, M. C. Danos, and H. J. Yost. Left-right asymmetry of a nodal-related gene is regulated by dorsoanterior midline structures during *Xenopus* development. *Development*, 124(8):1465–1472, Apr 1997.
- M. Loose and R. Patient. A genetic regulatory network for *Xenopus* mesoderm formation. *Dev Biol*, 271(2):467–478, Jul 2004.
- P. Lorenzo, A. Aspberg, P. Onnerfjord, M. T. Bayliss, P. J. Neame, and D. Heinegard. Identification and characterization of asporin. A novel member of the leucine-rich repeat protein family closely related to decorin and biglycan. *J Biol Chem*, 276(15):12201–12211, Apr 2001.
- K. D. Lustig, K. Kroll, E. Sun, R. Ramos, H. Elmendorf, and M. W. Kirschner. A *Xenopus* nodal-related gene that acts in synergy with noggin to induce complete secondary axis and notochord formation. *Development*, 122(10):3275–3282, Oct 1996.
- A. M. MacNicol, A. J. Muslin, and L. T. Williams. Raf-1 kinase is essential for early *Xenopus* development and mediates the induction of mesoderm by FGF. *Cell*, 73(3):571–583, May 1993.
- M. Maéno, R. C. Ong, A. Suzuki, N. Ueno, and H. F. Kung. A truncated bone morphogenetic protein 4 receptor alters the fate of ventral mesoderm to dorsal mesoderm: roles of animal pole tissue in the development of ventral mesoderm. *Proc Natl Acad Sci U S A*, 91(22):10260–10264, Oct 1994.
- G. M. Malacinski. Biological properties of a presumptive morphogenetic determinant from the amphibian oocyte germinal vesicle nucleus. *Cell Differ*, 3(1):31–44, Jun 1974.

- L. Marchant, C. Linker, and R. Mayor. Inhibition of mesoderm formation by follistatin. *Dev Genes Evol*, 208(3):157–160, May 1998a.
- L. Marchant, C. Linker, P. Ruiz, N. Guerrero, and R. Mayor. The inductive properties of mesoderm suggest that the neural crest cells are specified by a BMP gradient. *Dev Biol*, 198(2):319–329, Jun 1998b.
- J. Massagué. The transforming growth factor-beta family. *Annu Rev Cell Biol*, 6:597–641, 1990.
- J. Massagué. TGF- β signal transduction. *Annu Rev Biochem*, 67:753–791, 1998.
- J. Massagué and Y. G. Chen. Controlling TGF- β signaling. *Genes Dev*, 14(6):627–644, Mar 2000.
- R. Mayor, R. Morgan, and M. G. Sargent. Induction of the prospective neural crest of *Xenopus*. *Development*, 121(3):767–777, Mar 1995.
- N. McDowell, A. M. Zorn, D. J. Crease, and J. B. Gurdon. Activin has direct long-range signalling activity and can form a concentration gradient by diffusion. *Curr Biol*, 7(9):671–681, Sep 1997.
- L. L. McGrew, C. J. Lai, and R. T. Moon. Specification of the anteroposterior neural axis through synergistic interaction of the Wnt signaling cascade with noggin and follistatin. *Dev Biol*, 172(1):337–342, Nov 1995.
- R. McKendry, S. C. Hsu, R. M. Harland, and R. Grosschedl. LEF-1/TCF proteins mediate wnt-inducible transcription from the *Xenopus* nodal-related 3 promoter. *Dev Biol*, 192(2):420–431, Dec 1997.
- A. C. McPherron, A. M. Lawler, and S. J. Lee. Regulation of skeletal muscle mass in mice by a new tgf-beta superfamily member. *Nature*, 387(6628):83–90, May 1997.
- M. F. Mehler, P. C. Mabie, D. Zhang, and J. A. Kessler. Bone morphogenetic proteins in the nervous system. *Trends Neurosci*, 20(7):309–317, Jul 1997.

- D. A. Melton. Translocation of a localized maternal mRNA to the vegetal pole of *Xenopus* oocytes. *Nature*, 328(6125):80–82, 1987.
- C. Meno, Y. Ito, Y. Saijoh, Y. Matsuda, K. Tashiro, S. Kuhara, and H. Hamada. Two closely-related left-right asymmetrically expressed genes, *lefty-1* and *lefty-2*: their distinct expression domains, chromosomal linkage and direct neuralizing activity in *Xenopus* embryos. *Genes Cells*, 2(8):513–524, Aug 1997.
- G. Minchiotti, S. Parisi, G. Liguori, M. Signore, G. Lania, E. D. Adamson, C. T. Lago, and M. G. Persico. Membrane-anchorage of Cripto protein by glycosylphosphatidylinositol and its distribution during early mouse development. *Mech Dev*, 90(2):133–142, Feb 2000.
- G. Minchiotti, G. Manco, S. Parisi, C. T. Lago, F. Rosa, and M. G. Persico. Structure-function analysis of the EGF-CFC family member Cripto identifies residues essential for nodal signalling. *Development*, 128(22):4501–4510, Nov 2001.
- K. Miyazawa, M. Shinozaki, T. Hara, T. Furuya, and K. Miyazono. Two major Smad pathways in TGF- β superfamily signalling. *Genes Cells*, 7(12):1191–1204, Dec 2002.
- M. Mohammadi, C. A. Dionne, W. Li, N. Li, T. Spivak, A. M. Honegger, M. Jaye, and J. Schlessinger. Point mutation in FGF receptor eliminates phosphatidylinositol hydrolysis without affecting mitogenesis. *Nature*, 358(6388):681–684, Aug 1992.
- M. Mohammadi, I. Dikic, A. Sorokin, W. H. Burgess, M. Jaye, and J. Schlessinger. Identification of six novel autophosphorylation sites on fibroblast growth factor receptor 1 and elucidation of their importance in receptor activation and signal transduction. *Mol Cell Biol*, 16(3):977–989, Mar 1996.
- M. Moreno, R. Muñoz, F. Aroca, M. Labarca, E. Brandan, and J. Larrain. Biglycan is a new extracellular component of the Chordin-BMP4 signaling pathway. *EMBO J*, 24(7):1397–1405, Apr 2005.

- A. Moustakas, S. Souchelnytskyi, and C. H. Heldin. Smad regulation in TGF- β signal transduction. *J Cell Sci*, 114(Pt 24):4359–4369, Dec 2001.
- A. J. Muslin, K. G. Peters, and L. T. Williams. Direct activation of phospholipase C- γ by fibroblast growth factor receptor is not required for mesoderm induction in *Xenopus* animal caps. *Mol Cell Biol*, 14(5):3006–3012, May 1994.
- R. P. Nagarajan, J. Liu, and Y. Chen. Smad3 inhibits transforming growth factor- β and activin signaling by competing with Smad4 for FAST-2 binding. *J Biol Chem*, 274(44):31229–31235, Oct 1999.
- P. J. Neame, Y. Sommarin, R. E. Boynton, and D. Heinegård. The structure of a 38-kDa leucine-rich protein (chondroadherin) isolated from bovine cartilage. *J Biol Chem*, 269(34):21547–21554, Aug 1994.
- K. M. Neilson and R. Friesel. Ligand-independent activation of fibroblast growth factor receptors by point mutations in the extracellular, transmembrane, and kinase domains. *J Biol Chem*, 271(40):25049–25057, Oct 1996.
- H. V. New, A. I. Kavka, J. C. Smith, and J. B. Green. Differential effects on *Xenopus* development of interference with type IIA and type IIB activin receptors. *Mech Dev*, 61(1-2):175–186, Jan 1997.
- J. Newport and M. Kirschner. A major developmental transition in early *Xenopus* embryos: II. control of the onset of transcription. *Cell*, 30(3):687–696, Oct 1982a.
- J. Newport and M. Kirschner. A major developmental transition in early *Xenopus* embryos: I. characterization and timing of cellular changes at the midblastula stage. *Cell*, 30(3):675–686, Oct 1982b.
- V. H. Nguyen, B. Schmid, J. Trout, S. A. Connors, M. Ekker, and M. C. Mullins. Ventral and lateral regions of the zebrafish gastrula, including the neural crest progenitors, are established by a bmp2b/swirl pathway of genes. *Dev Biol*, 199(1):93–110, Jul 1998.

- P. D. Nieuwkoop. The "organization centre". 3. segregation and pattern formation in morphogenetic fields. *Acta Biotheor*, 17(4):178–194, 1967a.
- P. D. Nieuwkoop. The "organization centre". II. field phenomena, their origin and significance. *Acta Biotheor*, 17(4):151–177, 1967b.
- P. D. Nieuwkoop. The organization center of the amphibian embryo: its origin, spatial organization, and morphogenetic action. *Adv Morphog*, 10:1–39, 1973.
- P. D. Nieuwkoop. Origin and establishment of embryonic polar axes in amphibian development. *Curr Top Dev Biol*, 11:115–132, 1977.
- M. Oelgeschläger, J. Larrain, D. Geissert, and E. M. D. Robertis. The evolutionarily conserved BMP-binding protein Twisted gastrulation promotes BMP signalling. *Nature*, 405(6788):757–763, Jun 2000.
- M. Oelgeschläger, H. Kuroda, B. Reversade, and E. M. D. Robertis. Chordin is required for the Spemann organizer transplantation phenomenon in *Xenopus* embryos. *Dev Cell*, 4(2):219–230, Feb 2003a.
- M. Oelgeschläger, B. Reversade, J. Larrain, S. Little, M. C. Mullins, and E. M. D. Robertis. The pro-BMP activity of Twisted gastrulation is independent of BMP binding. *Development*, 130(17):4047–4056, Sep 2003b.
- M. Oelgeschläger, U. Tran, K. Grubisic, and E. M. D. Robertis. Identification of a second *Xenopus* twisted gastrulation gene. *Int J Dev Biol*, 48(1):57–61, Feb 2004.
- S. P. Oh and E. Li. The signaling pathway mediated by the type IIB activin receptor controls axial patterning and lateral asymmetry in the mouse. *Genes Dev*, 11(14):1812–1826, Jul 1997.
- B. Ohkawara, K. Shirakabe, J. Hyodo-Miura, R. Matsuo, N. Ueno, K. Matsumoto, and H. Shibuya. Role of the TAK1-NLK-STAT3 pathway in TGF- β -mediated mesoderm induction. *Genes Dev*, 18(4):381–386, Feb 2004.

- K. Ohta, G. Lupo, S. Kuriyama, R. Keynes, C. E. Holt, W. A. Harris, H. Tanaka, and S. ichi Ohnuma. Tsukushi functions as an organizer inducer by inhibition of BMP activity in cooperation with chordin. *Dev Cell*, 7(3):347–358, Sep 2004.
- K. Ohta, S. Kuriyama, T. Okafuji, R. Gejima, S. ichi Ohnuma, and H. Tanaka. Tsukushi cooperates with VG1 to induce primitive streak and Hensen’s node formation in the chick embryo. *Development*, Aug 2006.
- A. Oldberg, P. Antonsson, K. Lindblom, and D. Heinegård. A collagen-binding 59-kd protein (fibromodulin) is structurally related to the small interstitial proteoglycans PG-S1 and PG-S2 (decorin). *EMBO J*, 8(9):2601–2604, Sep 1989.
- D. Onichtchouk, Y. G. Chen, R. Dosch, V. Gawantka, H. Delius, J. Massagué, and C. Niehrs. Silencing of TGF- β signalling by the pseudoreceptor BAMBI. *Nature*, 401(6752):480–485, Sep 1999.
- Y. Onuma, C.-Y. Yeo, and M. Whitman. XCR2, one of three *Xenopus* EGF-CFC genes, has a distinct role in the regulation of left-right patterning. *Development*, 133(2):237–250, Jan 2006.
- S. I. Osada and C. V. Wright. *Xenopus* nodal-related signaling is essential for mesendodermal patterning during early embryogenesis. *Development*, 126(14):3229–3240, Jun 1999.
- K. Osafune, R. Nishinakamura, S. Komazaki, and M. Asashima. In vitro induction of the pronephric duct in *Xenopus* explants. *Dev Growth Differ*, 44(2):161–167, Apr 2002.
- M. Pannese, C. Polo, M. Andreazzoli, R. Vignali, B. Kablar, G. Barsacchi, and E. Boncinelli. The *Xenopus* homologue of Otx2 is a maternal homeobox gene that demarcates and specifies anterior body regions. *Development*, 121(3):707–720, Mar 1995.

- R. K. Patient and J. D. McGhee. The GATA family (vertebrates and invertebrates). *Curr Opin Genet Dev*, 12(4):416–422, Aug 2002.
- Y. Peng, B.-H. Jiang, P.-H. Yang, Z. Cao, X. Shi, M. C. M. Lin, M.-L. He, and H.-F. Kung. Phosphatidylinositol 3-kinase signaling is involved in neurogenesis during *Xenopus* embryonic development. *J Biol Chem*, 279(27):28509–28514, Jul 2004.
- K. G. Peters, J. Marie, E. Wilson, H. E. Ives, J. Escobedo, M. D. Rosario, D. Mirda, and L. T. Williams. Point mutation of an FGF receptor abolishes phosphatidylinositol turnover and Ca^{2+} flux but not mitogenesis. *Nature*, 358(6388):678–681, Aug 1992.
- S. Piccolo, Y. Sasai, B. Lu, and E. M. D. Robertis. Dorsoventral patterning in *Xenopus*: inhibition of ventral signals by direct binding of chordin to BMP-4. *Cell*, 86(4):589–598, Aug 1996.
- S. Piccolo, E. Agius, B. Lu, S. Goodman, L. Dale, and E. M. D. Robertis. Cleavage of Chordin by Xolloid metalloprotease suggests a role for proteolytic processing in the regulation of Spemann organizer activity. *Cell*, 91(3):407–416, Oct 1997.
- S. Piccolo, E. Agius, L. Leyns, S. Bhattacharyya, H. Grunz, T. Bouwmeester, and E. M. D. Robertis. The head inducer Cerberus is a multifunctional antagonist of Nodal, BMP and Wnt signals. *Nature*, 397(6721):707–710, Feb 1999.
- O. Piepenburg, D. Grimmer, P. H. Williams, and J. C. Smith. Activin redux: specification of mesodermal pattern in *Xenopus* by graded concentrations of endogenous activin B. *Development*, 131(20):4977–4986, Oct 2004.
- M. Poulain, M. Fürthauer, B. Thisse, C. Thisse, and T. Lepage. Zebrafish endoderm formation is regulated by combinatorial Nodal, FGF and BMP signalling. *Development*, 133(11):2189–2200, Jun 2006.

- M. E. Pownall, B. E. Welm, K. W. Freeman, D. M. Spencer, J. M. Rosen, and H. V. Isaacs. An inducible system for the study of FGF signalling in early amphibian development. *Dev Biol*, 256(1):89–99, Apr 2003.
- J. Qiao, J. Kang, T. C. Ko, B. M. Evers, and D. H. Chung. Inhibition of transforming growth factor- β /Smad signaling by phosphatidylinositol 3-kinase pathway. *Cancer Lett*, Jan 2006.
- A. J. Reardon, M. L. Goff, M. D. Briggs, D. McLeod, J. K. Sheehan, D. J. Thornton, and P. N. Bishop. Identification in vitreous and molecular cloning of opticin, a novel member of the family of leucine-rich repeat proteins of the extracellular matrix. *J Biol Chem*, 275(3):2123–2129, Jan 2000.
- Y. Re'em-Kalma, T. Lamb, and D. Frank. Competition between noggin and bone morphogenetic protein 4 activities may regulate dorsalization during *Xenopus* development. *Proc Natl Acad Sci U S A*, 92(26):12141–12145, Dec 1995.
- E. M. D. Robertis and H. Kuroda. Dorsal-ventral patterning and neural induction in *Xenopus* embryos. *Annu Rev Cell Dev Biol*, 20:285–308, 2004.
- E. M. D. Robertis, M. Blum, C. Niehrs, and H. Steinbeisser. Goosecoid and the organizer. *Dev Suppl*, pages 167–171, 1992.
- E. M. D. Robertis, J. Larrain, M. Oelgeschläger, and O. Wessely. The establishment of Spemann's organizer and patterning of the vertebrate embryo. *Nat Rev Genet*, 1(3):171–181, Dec 2000.
- F. M. Rosa. Mix.1, a homeobox mRNA inducible by mesoderm inducers, is expressed mostly in the presumptive endodermal cells of *Xenopus* embryos. *Cell*, 57(6):965–974, Jun 1989.
- J. J. Ross, O. Shimmi, P. Vilmos, A. Petryk, H. Kim, K. Gaudenz, S. Hermanson, S. C. Ekker, M. B. O'Connor, and J. L. Marsh. Twisted gastrulation is a conserved extracellular BMP antagonist. *Nature*, 410(6827):479–483, Mar 2001.

- C. E. Runyan, H. W. Schnaper, and A.-C. Poncelet. The phosphatidylinositol 3-kinase/akt pathway enhances smad3-stimulated mesangial cell collagen i expression in response to transforming growth factor- β 1. *J Biol Chem*, 279(4):2632–2639, Jan 2004.
- D. S. Saloman, C. Bianco, A. D. Ebert, N. I. Khan, M. D. Santis, N. Normanno, C. Wechselberger, M. Seno, K. Williams, M. Sanicola, S. Foley, W. J. Gullick, and G. Persico. The EGF-CFC family: novel epidermal growth factor-related proteins in development and cancer. *Endocr Relat Cancer*, 7(4):199–226, Dec 2000.
- K. Sampath, A. M. Cheng, A. Frisch, and C. V. Wright. Functional differences among *Xenopus* nodal-related genes in left-right axis determination. *Development*, 124(17):3293–3302, Sep 1997.
- K. Sampath, A. L. Rubinstein, A. M. Cheng, J. O. Liang, K. Fekany, L. Solnica-Krezel, V. Korzh, M. E. Halpern, and C. V. Wright. Induction of the zebrafish ventral brain and floorplate requires cyclops/nodal signalling. *Nature*, 395(6698):185–189, Sep 1998.
- Y. Sasai and E. M. D. Robertis. Ectodermal patterning in vertebrate embryos. *Dev Biol*, 182(1):5–20, Feb 1997.
- Y. Sasai, B. Lu, H. Steinbeisser, D. Geissert, L. K. Gont, and E. M. D. Robertis. *Xenopus* chordin: a novel dorsalizing factor activated by organizer-specific homeobox genes. *Cell*, 79(5):779–790, Dec 1994.
- Y. Sasai, B. Lu, H. Steinbeisser, and E. M. D. Robertis. Regulation of neural induction by the Chd and Bmp-4 antagonistic patterning signals in *Xenopus*. *Nature*, 376(6538):333–336, Jul 1995.
- Y. Sasai, B. Lu, S. Piccolo, and E. M. D. Robertis. Endoderm induction by the organizer-secreted factors chordin and noggin in *Xenopus* animal caps. *EMBO J*, 15(17):4547–4555, Sep 1996.

- A. F. Schier. Nodal signaling in vertebrate development. *Annu Rev Cell Dev Biol*, 19:589–621, 2003.
- A. F. Schier and M. M. Shen. Nodal signalling in vertebrate development. *Nature*, 403(6768):385–389, Jan 2000.
- S. G. Schiffer, S. Foley, A. Kaffashan, X. Hronowski, A. E. Zichittella, C. Y. Yeo, K. Miatkowski, H. B. Adkins, B. Damon, M. Whitman, D. Salomon, M. Sanicola, and K. P. Williams. Fucosylation of Cripto is required for its ability to facilitate nodal signaling. *J Biol Chem*, 276(41):37769–37778, Oct 2001.
- J. Schmidt, V. Francois, E. Bier, and D. Kimelman. *Drosophila* short gastrulation induces an ectopic axis in *Xenopus*: evidence for conserved mechanisms of dorsal-ventral patterning. *Development*, 121(12):4319–4328, Dec 1995.
- V. A. Schneider and M. Mercola. Spatially distinct head and heart inducers within the *Xenopus* organizer region. *Curr Biol*, 9(15):800–809, 1999.
- A. Schneyer, D. Tortoriello, Y. Sidis, H. Keutmann, T. Matsuzaki, and W. Holmes. Follistatin-related protein (FSRP): a new member of the follistatin gene family. *Mol Cell Endocrinol*, 180(1-2):33–38, Jun 2001.
- A. Schohl and F. Fagotto. β -catenin, MAPK and Smad signaling during early *Xenopus* development. *Development*, 129(1):37–52, Jan 2002.
- S. Schulte-Merker and J. C. Smith. Mesoderm formation in response to brachyury requires FGF signalling. *Curr Biol*, 5(1):62–67, Jan 1995.
- S. Schulte-Merker, J. C. Smith, and L. Dale. Effects of truncated activin and FGF receptors and of follistatin on the inducing activities of BVg1 and activin: does activin play a role in mesoderm induction? *EMBO J*, 13(15):3533–3541, Aug 1994.
- I. C. Scott, I. L. Blitz, W. N. Pappano, S. A. Maas, K. W. Cho, and D. S. Greenspan. Homologues of Twisted gastrulation are extracellular cofactors in antagonism of BMP signalling. *Nature*, 410(6827):475–478, Mar 2001.

- P. G. Scott, P. A. McEwan, C. M. Dodd, E. M. Bergmann, P. N. Bishop, and J. Bella. Crystal structure of the dimeric protein core of decorin, the archetypal small leucine-rich repeat proteoglycan. *Proc Natl Acad Sci U S A*, 101(44):15633–15638, Nov 2004.
- P. G. Scott, C. M. Dodd, E. M. Bergmann, J. K. Sheehan, and P. N. Bishop. Crystal structure of the biglycan dimer and evidence that dimerization is essential for folding and stability of class I small leucine-rich repeat proteoglycans. *J Biol Chem*, 281(19):13324–13332, May 2006.
- M. H. Sham, C. Vesque, S. Nonchev, H. Marshall, M. Frain, R. D. Gupta, J. Whiting, D. Wilkinson, P. Charnay, and R. Krumlauf. The zinc finger gene *Krox20* regulates *HoxB2* (*Hox2.8*) during hindbrain segmentation. *Cell*, 72(2):183–196, Jan 1993.
- M. M. Shen and A. F. Schier. The EGF-CFC gene family in vertebrate development. *Trends Genet*, 16(7):303–309, Jul 2000.
- M. M. Shen, H. Wang, and P. Leder. A differential display strategy identifies *Cryptic*, a novel EGF-related gene expressed in the axial and lateral mesoderm during mouse gastrulation. *Development*, 124(2):429–442, Jan 1997.
- D. R. Sherwood and D. R. McClay. *LvNotch* signaling plays a dual role in regulating the position of the ectoderm-endoderm boundary in the sea urchin embryo. *Development*, 128(12):2221–2232, Jun 2001.
- S. Shimasaki, M. Koga, M. L. Buscaglia, D. M. Simmons, T. A. Bicsak, and N. Ling. Follistatin gene expression in the ovary and extragonadal tissues. *Mol Endocrinol*, 3(4):651–659, Apr 1989.
- H. Shimizu, M. A. Julius, M. Giarre, Z. Zheng, A. M. Brown, and J. Kitajewski. Transformation by Wnt family proteins correlates with regulation of β -catenin. *Cell Growth Differ*, 8(12):1349–1358, Dec 1997.
- Y. Sidis, A. L. Schneyer, P. M. Sluss, L. N. Johnson, and H. T. Keutmann.

- Follistatin: essential role for the N-terminal domain in activin binding and neutralization. *J Biol Chem*, 276(21):17718–17726, May 2001.
- A. C. Silva, M. Filipe, K.-M. Kuerner, H. Steinbeisser, and J. A. Belo. Endogenous Cerberus activity is required for anterior head specification in *Xenopus*. *Development*, 130(20):4943–4953, Oct 2003.
- I. Skromne and C. D. Stern. A hierarchy of gene expression accompanying induction of the primitive streak by Vg1 in the chick embryo. *Mech Dev*, 114(1-2):115–118, Jun 2002.
- J. C. Smith. Mesoderm induction and mesoderm-inducing factors in early amphibian development. *Development*, 105(4):665–677, Apr 1989.
- J. C. Smith and J. M. Slack. Dorsalization and neural induction: properties of the organizer in *Xenopus laevis*. *J Embryol Exp Morphol*, 78:299–317, Dec 1983.
- J. C. Smith, B. M. Price, K. V. Nimmen, and D. Huylebroeck. Identification of a potent *Xenopus* mesoderm-inducing factor as a homologue of activin A. *Nature*, 345(6277):729–731, Jun 1990.
- J. C. Smith, B. M. Price, J. B. Green, D. Weigel, and B. G. Herrmann. Expression of a *Xenopus* homolog of Brachyury (T) is an immediate-early response to mesoderm induction. *Cell*, 67(1):79–87, Oct 1991.
- W. C. Smith and R. M. Harland. Expression cloning of noggin, a new dorsalizing factor localized to the Spemann organizer in *Xenopus* embryos. *Cell*, 70(5):829–840, Sep 1992.
- W. C. Smith, A. K. Knecht, M. Wu, and R. M. Harland. Secreted noggin protein mimics the Spemann organizer in dorsalizing *Xenopus* mesoderm. *Nature*, 361(6412):547–549, Feb 1993.
- W. C. Smith, R. McKendry, S. Ribisi, and R. M. Harland. A nodal-related gene defines a physical and functional domain within the Spemann organizer. *Cell*, 82(1):37–46, Jul 1995.

- J. Song, S. P. Oh, H. Schrewe, M. Nomura, H. Lei, M. Okano, T. Gridley, and E. Li. The type II activin receptors are essential for egg cylinder growth, gastrulation, and rostral head development in mice. *Dev Biol*, 213(1):157–169, Sep 1999.
- K. Song, S. C. Cornelius, M. Reiss, and D. Danielpour. Insulin-like growth factor-I inhibits transcriptional responses of transforming growth factor-beta by phosphatidylinositol 3-kinase/Akt-dependent suppression of the activation of Smad3 but not Smad2x. *J Biol Chem*, 278(40):38342–38351, Oct 2003.
- E. Stanley, C. Biben, S. Kotecha, L. Fabri, S. Tajbakhsh, C. C. Wang, T. Hatzistavrou, B. Roberts, C. Drinkwater, M. Lah, M. Buckingham, D. Hilton, A. Nash, T. Mohun, and R. P. Harvey. DAN is a secreted glycoprotein related to *Xenopus* cerberus. *Mech Dev*, 77(2):173–184, Oct 1998.
- O. C. Steinbach, A. Ulshöfer, A. Authaler, and R. A. Rupp. Temporal restriction of MyoD induction and autocatalysis during *Xenopus* mesoderm formation. *Dev Biol*, 202(2):280–292, Oct 1998.
- H. Steinbeisser, A. Fainsod, C. Niehrs, Y. Sasai, and E. M. D. Robertis. The role of gsc and BMP-4 in dorsal-ventral patterning of the marginal zone in *Xenopus*: a loss-of-function study using antisense RNA. *EMBO J*, 14(21):5230–5243, Nov 1995.
- F. Stenard, A. M. Zorn, K. Ryan, N. Garrett, and J. B. Gurdon. Differential expression of VegT and Antipodean protein isoforms in *Xenopus*. *Mech Dev*, 86(1-2):87–98, Aug 1999.
- C. Stern. *Gastrulation: from cells to embryo*. Cold Spring Harbor Press. pp. 219-232, 2004.
- A. Streit, K. J. Lee, I. Woo, C. Roberts, T. M. Jessell, and C. D. Stern. Chordin regulates primitive streak development and the stability of induced neural cells, but is not sufficient for neural induction in the chick embryo. *Development*, 125(3):507–519, Feb 1998.

- S. Sumitomo, S. Inouye, X. J. Liu, N. Ling, and S. Shimasaki. The heparin binding site of follistatin is involved in its interaction with activin. *Biochem Biophys Res Commun*, 208(1):1–9, Mar 1995.
- B. I. Sun, S. M. Bush, L. A. Collins-Racie, E. R. LaVallie, E. A. DiBlasio-Smith, N. M. Wolfman, J. M. McCoy, and H. L. Sive. *derrière*: a TGF- β family member required for posterior development in *Xenopus*. *Development*, 126(7):1467–1482, Apr 1999.
- P. D. Sun and D. R. Davies. The cystine-knot growth-factor superfamily. *Annu Rev Biophys Biomol Struct*, 24:269–291, 1995.
- A. Suzuki, R. S. Thies, N. Yamaji, J. J. Song, J. M. Wozney, K. Murakami, and N. Ueno. A truncated bone morphogenetic protein receptor affects dorsal-ventral patterning in the early *Xenopus* embryo. *Proc Natl Acad Sci U S A*, 91(22):10255–10259, Oct 1994.
- S. J. Symes KR. Gastrulation movements provide an early marker of mesoderm induction in *Xenopus laevis*. *Development*, 101:339–349, 1987.
- S. Takahashi, C. Yokota, K. Takano, K. Tanegashima, Y. Onuma, J. Goto, and M. Asashima. Two novel nodal-related genes initiate early inductive events in *Xenopus* Nieuwkoop center. *Development*, 127(24):5319–5329, Dec 2000.
- K. Tanegashima, C. Yokota, S. Takahashi, and M. Asashima. Expression cloning of Xantivin, a *Xenopus* lefty/antivin-related gene, involved in the regulation of activin signaling during mesoderm induction. *Mech Dev*, 99(1-2):3–14, Dec 2000.
- K. Tanegashima, Y. Haramoto, C. Yokota, S. Takahashi, and M. Asashima. Xantivin suppresses the activity of EGF-CFC genes to regulate nodal signaling. *Int J Dev Biol*, 48(4):275–283, Jun 2004.
- K. Tashiro, R. Yamada, M. Asano, M. Hashimoto, M. Muramatsu, and K. Shiohawa. Expression of mRNA for activin-binding protein (follistatin) during

- early embryonic development of *Xenopus laevis*. *Biochem Biophys Res Commun*, 174(2):1022–1027, Jan 1991.
- T. B. Thompson, T. K. Woodruff, and T. S. Jardetzky. Structures of an ActRIIB:activin A complex reveal a novel binding mode for TGF- β ligand:receptor interactions. *EMBO J*, 22(7):1555–1566, Apr 2003.
- T. B. Thompson, T. F. Lerch, R. W. Cook, T. K. Woodruff, and T. S. Jardetzky. The structure of the follistatin:activin complex reveals antagonism of both type I and type II receptor binding. *Dev Cell*, 9(4):535–543, Oct 2005.
- G. Thomsen, T. Woolf, M. Whitman, S. Sokol, J. Vaughan, W. Vale, and D. A. Melton. Activins are expressed early in *Xenopus* embryogenesis and can induce axial mesoderm and anterior structures. *Cell*, 63(3):485–493, Nov 1990.
- G. H. Thomsen and D. A. Melton. Processed Vg1 protein is an axial mesoderm inducer in *Xenopus*. *Cell*, 74(3):433–441, Aug 1993.
- H. Uchiyama, T. Nakamura, S. Komazaki, K. Takio, M. Asashima, and H. Sugino. Localization of activin and follistatin proteins in the *Xenopus* oocyte. *Biochem Biophys Res Commun*, 202(1):484–489, Jul 1994.
- C. G. Ullman and S. J. Perkins. The Factor I and follistatin domain families: the return of a prodigal son. *Biochem J*, 326 (Pt 3):939–941, Sep 1997.
- I. Varlet, J. Collignon, and E. J. Robertson. nodal expression in the primitive endoderm is required for specification of the anterior axis during mouse gastrulation. *Development*, 124(5):1033–1044, Mar 1997.
- S. Villanueva, A. Glavic, P. Ruiz, and R. Mayor. Posteriorization by FGF, Wnt, and retinoic acid is required for neural crest induction. *Dev Biol*, 241(2):289–301, Jan 2002.
- Q. Wang, H. T. Keutmann, A. L. Schneyer, and P. M. Sluss. Analysis of human follistatin structure: identification of two discontinuous N-terminal sequences

- coding for activin A binding and structural consequences of activin binding to native proteins. *Endocrinology*, 141(9):3183–3193, Sep 2000.
- F. C. Wardle, J. V. Welch, and L. Dale. Bone morphogenetic protein 1 regulates dorsal-ventral patterning in early *Xenopus* embryos by degrading chordin, a BMP4 antagonist. *Mech Dev*, 86(1-2):75–85, Aug 1999.
- H. Weber, C. E. Symes, M. E. Walmsley, A. R. Rodaway, and R. K. Patient. A role for GATA5 in *Xenopus* endoderm specification. *Development*, 127(20):4345–4360, Oct 2000.
- D. L. Weeks and D. A. Melton. A maternal mRNA localized to the vegetal hemisphere in *Xenopus* eggs codes for a growth factor related to TGF- β . *Cell*, 51(5):861–867, Dec 1987.
- M. Wendel, Y. Sommarin, and D. Heinegård. Bone matrix proteins: isolation and characterization of a novel cell-binding keratan sulfate proteoglycan (osteoaderin) from bovine bone. *J Cell Biol*, 141(3):839–847, May 1998.
- O. Wessely, E. Agius, M. Oelgeschläger, E. M. Pera, and E. M. D. Robertis. Neural induction in the absence of mesoderm: β -catenin-dependent expression of secreted BMP antagonists at the blastula stage in *Xenopus*. *Dev Biol*, 234(1):161–173, Jun 2001.
- M. Whitman. Smads and early developmental signaling by the TGF β superfamily. *Genes Dev*, 12(16):2445–2462, Aug 1998.
- M. Whitman and D. A. Melton. Involvement of p21ras in *Xenopus* mesoderm induction. *Nature*, 357(6375):252–254, May 1992.
- P. H. Williams, A. Hagemann, M. Gonzalez-Gaitn, and J. C. Smith. Visualizing long-range movement of the morphogen Xnr2 in the *Xenopus* embryo. *Curr Biol*, 14(21):1916–1923, Nov 2004.
- A. Wills, R. M. Harland, and M. K. Khokha. Twisted gastrulation is required for forebrain specification and cooperates with Chordin to inhibit BMP signaling during *X. tropicalis* gastrulation. *Dev Biol*, 289(1):166–178, Jan 2006.

- S. E. Witta, V. R. Agarwal, and S. M. Sato. XIPOU 2, a noggin-inducible gene, has direct neuralizing activity. *Development*, 121(3):721–730, Mar 1995.
- C. C. Wylie, A. Snape, J. Heasman, and J. C. Smith. Vegetal pole cells and commitment to form endoderm in *Xenopus laevis*. *Dev Biol*, 119(2):496–502, Feb 1987.
- J. B. Xanthos, M. Kofron, C. Wylie, and J. Heasman. Maternal VegT is the initiator of a molecular network specifying endoderm in *Xenopus laevis*. *Development*, 128(2):167–180, Jan 2001.
- J. B. Xanthos, M. Kofron, Q. Tao, K. Schaible, C. Wylie, and J. Heasman. The roles of three signaling pathways in the formation and function of the Spemann Organizer. *Development*, 129(17):4027–4043, Sep 2002.
- S.-I. Yabe, K. Tanegashima, Y. Haramoto, S. Takahashi, T. Fujii, S. Kozuma, Y. Taketani, and M. Asashima. FRL-1, a member of the EGF-CFC family, is essential for neural differentiation in *Xenopus* early development. *Development*, 130(10):2071–2081, May 2003.
- Y. Yamaguchi, D. M. Mann, and E. Ruoslahti. Negative regulation of transforming growth factor-beta by the proteoglycan decorin. *Nature*, 346(6281):281–284, Jul 1990.
- Y.-T. Yan, J.-J. Liu, Y. Luo, C. E. R. S. Haltiwanger, C. Abate-Shen, and M. M. Shen. Dual roles of Cripto as a ligand and coreceptor in the nodal signaling pathway. *Mol Cell Biol*, 22(13):4439–4449, Jul 2002.
- J. Yang, C. Tan, R. S. Darken, P. A. Wilson, and P. S. Klein. β -catenin/Tcf-regulated transcription prior to the midblastula transition. *Development*, 129(24):5743–5752, Dec 2002.
- H. Yasuo and P. Lemaire. A two-step model for the fate determination of presumptive endodermal blastomeres in *Xenopus* embryos. *Curr Biol*, 9(16):869–879, Aug 1999.

- C. Yeo and M. Whitman. Nodal signals to Smads through Cripto-dependent and Cripto-independent mechanisms. *Mol Cell*, 7(5):949–957, May 2001.
- C. Yokota, M. Kofron, M. Zuck, D. W. Houston, H. Isaacs, M. Asashima, C. C. Wylie, and J. Heasman. A novel role for a nodal-related protein; Xnr3 regulates convergent extension movements via the FGF receptor. *Development*, 130(10):2199–2212, May 2003.
- L. Zakin and E. M. D. Robertis. Inactivation of mouse Twisted gastrulation reveals its role in promoting Bmp4 activity during forebrain development. *Development*, 131(2):413–424, Jan 2004.
- A. Zetser, D. Frank, and E. Bengal. MAP kinase converts MyoD into an instructive muscle differentiation factor in *Xenopus*. *Dev Biol*, 240(1):168–181, Dec 2001.
- C. Zhang, T. Basta, S. R. Fawcett, and M. W. Klymkowsky. SOX7 is an immediate-early target of VegT and regulates Nodal-related gene expression in *Xenopus*. *Dev Biol*, 278(2):526–541, Feb 2005.
- J. Zhang and M. L. King. *Xenopus* VegT RNA is localized to the vegetal cortex during oogenesis and encodes a novel T-box transcription factor involved in mesodermal patterning. *Development*, 122(12):4119–4129, Dec 1996.
- J. Zhang, W. S. Talbot, and A. F. Schier. Positional cloning identifies zebrafish one-eyed pinhead as a permissive EGF-related ligand required during gastrulation. *Cell*, 92(2):241–251, Jan 1998.
- X. Zhou, H. Sasaki, L. Lowe, B. L. Hogan, and M. R. Kuehn. Nodal is a novel TGF- β -like gene expressed in the mouse node during gastrulation. *Nature*, 361(6412):543–547, Feb 1993.
- L. Zhu, M. J. Marvin, A. Gardiner, A. B. Lassar, M. Mercola, C. D. Stern, and M. Levin. Cerberus regulates left-right asymmetry of the embryonic head and heart. *Curr Biol*, 9(17):931–938, Sep 1999.

- L. B. Zimmerman, J. M. D. Jesús-Escobar, and R. M. Harland. The Spemann organizer signal noggin binds and inactivates bone morphogenetic protein 4. *Cell*, 86(4):599–606, Aug 1996.
- A. M. Zorn, K. Butler, and J. B. Gurdon. Anterior endomesoderm specification in *Xenopus* by Wnt/ β -catenin and TGF- β signalling pathways. *Dev Biol*, 209(2):282–297, May 1999.

Appendix: Original publication

A. E. Harrington, S. A. Morris-Triggs, B. T. Ruotolo, C. V. Robinson, S.-I. Ohnuma, and M. Hyvönen. Structural basis for the inhibition of activin signalling by follistatin. *EMBO J*, 25(5): 1035 - 1045, Mar 2006.

Structural basis for the inhibition of activin signalling by follistatin

Adrian E Harrington^{1,4}, Samantha A Morris-Triggs², Brandon T Ruotolo³, Carol V Robinson³, Shin-ichi Ohnuma² and Marko Hyvönen^{1,*}

¹Department of Biochemistry, University of Cambridge, Cambridge, UK, ²Hutchison/MRC Research Centre, Department of Oncology, University of Cambridge, Cambridge, UK and ³Department of Chemistry, University of Cambridge, Cambridge, UK

The secreted, multidomain protein follistatin binds activins with high affinity, inhibiting their receptor interaction. We have dissected follistatin's domain structure and shown that the minimal activin-inhibiting fragment of follistatin is comprised of the first and second Fs domains (Fs12). This protein can bind to activin dimer and form a stable complex containing two Fs12 molecules and one activin dimer. We have solved crystal structures of activin A alone and its complex with Fs12 fragment to 2 Å resolution. The complex structure shows how Fs12 molecules wrap around the back of the 'wings' of activin, blocking the type II receptor-binding site on activin A. Arginine 192 in Fs2 is a key residue in this interaction, inserting itself in between activin's fingers. Complex formation imposes a novel orientation for the EGF- and Kazal-like subdomains in the Fs2 domain and activin A shows further variation from the canonical TGF-β family fold. The structure provides a detailed description of the inhibitory mechanism and gives insights into interactions of follistatin with other TGF-β family proteins.

The EMBO Journal (2006) 25, 1035–1045. doi:10.1038/sj.emboj.7601000; Published online 16 February 2006

Subject Categories: signal transduction; structural biology

Keywords: activin; crystal structure; follistatin; growth factor signalling; regulation

Introduction

Activins and other members of the TGF-β superfamily are involved in regulating a wide range of cellular events, such as differentiation, repair, cell adhesion and apoptosis (Massagué, 1998). Their signalling originates from an oligomeric complex comprising the growth factor and its two receptors in which the type II receptor phosphorylates the type I receptor in the glycine/serine-rich sequence of the juxtamembrane region. The type I receptor in turn phosphory-

lates the receptor-regulated Smad (R-Smad) proteins, which form a complex with common-mediator Smads (Co-Smads), translocate to the nucleus and activate transcription of target genes (Massagué and Wotton, 2000).

There are four activin genes in humans, but most research has been focused on activins A and B. Different activins appear to have nonoverlapping functions as implicated by the distinct and additive phenotypes of activin knockout mice (Vassalli *et al*, 1994; Matzuk *et al*, 1995). Activins have been studied extensively as stimulators of follicle-stimulating hormone production in humans and as mesoderm inducers in *Xenopus laevis* embryos (Piepenburg *et al*, 2004). They are also able to support pluripotency, proliferation and differentiation of embryonic stem cells (Beattie *et al*, 2005; James *et al*, 2005; Shi *et al*, 2005).

The activities of activins are regulated by the high-affinity inhibitor follistatin, one of a growing group of proteins including also noggin, gremlin and chordin that antagonise signalling by activins and bone morphogenetic proteins (BMPs) (Esch *et al*, 1987; Hemmati-Brivanlou *et al*, 1994; Piccolo *et al*, 1996; Zimmerman *et al*, 1996; Fainsod *et al*, 1997; Hsu *et al*, 1998). It is common for these inhibitors to be expressed in close temporal and spatial proximity, and there is a degree of redundancy in their action and specificity for growth factors (Bachiller *et al*, 2000). However, it appears that multiple strategies for binding to proteins of the TGF-β superfamily have evolved as the sequences of these proteins reveal distinctly varied domain compositions. The crystal structure of a complex between BMP-7 and noggin, a disulphide-linked dimer, was solved recently and it showed occupation of both type I and type II receptor-binding epitopes by the antagonist (Groppe *et al*, 2002).

Mature follistatin consists of an N-terminal unique domain (Fs0) and three follistatin domains (Fs1, 2, 3; Shimasaki *et al*, 1989; Ullman and Perkins, 1997; see Figure 1A). There are three major isoforms of follistatin, which differ in their C-terminal sequences and are generated by a combination of alternative splicing and proteolytic processing. The main functional difference between the isoforms is in their ability to bind heparan sulphates (HS), with the shortest form (Fs288) having highest affinity for HS and the longest form (Fs315) with its acidic tail unable to bind HS at all (Sugino *et al*, 1993). The main binding site for heparan sulphate is located in the Fs1 domain, which bears a highly basic region in its EGF-like subdomain (Inouye *et al*, 1992; Innis and Hyvönen, 2003).

While activin appears to be the highest affinity ligand for follistatin, follistatin binds and inhibits many other TGF-β family members, such as myostatin and BMPs 2, 4, 6 and 7 (Iemura *et al*, 1998; Amthor *et al*, 2002, 2004; Glister *et al*, 2004).

Several groups have investigated the molecular basis of activin and BMP antagonism by follistatin in attempts to identify critical residues for growth factor binding. Synthetic polypeptides representing sequences from Fs0 can bind to

*Corresponding author. Department of Biochemistry, University of Cambridge, 80 Tennis Court Road, Cambridge CB2 1GA, UK. Tel.: +44 1223 766044; Fax: +44 1223 766002; E-mail: marko@cryst.bioc.cam.ac.uk

⁴Present address: Department of Biochemistry and Molecular Biology, AJ Drexel Institute of Basic and Applied Protein Science, Drexel University College of Medicine, Philadelphia, PA, USA

Received: 27 September 2005; accepted: 20 January 2006; published online: 16 February 2006

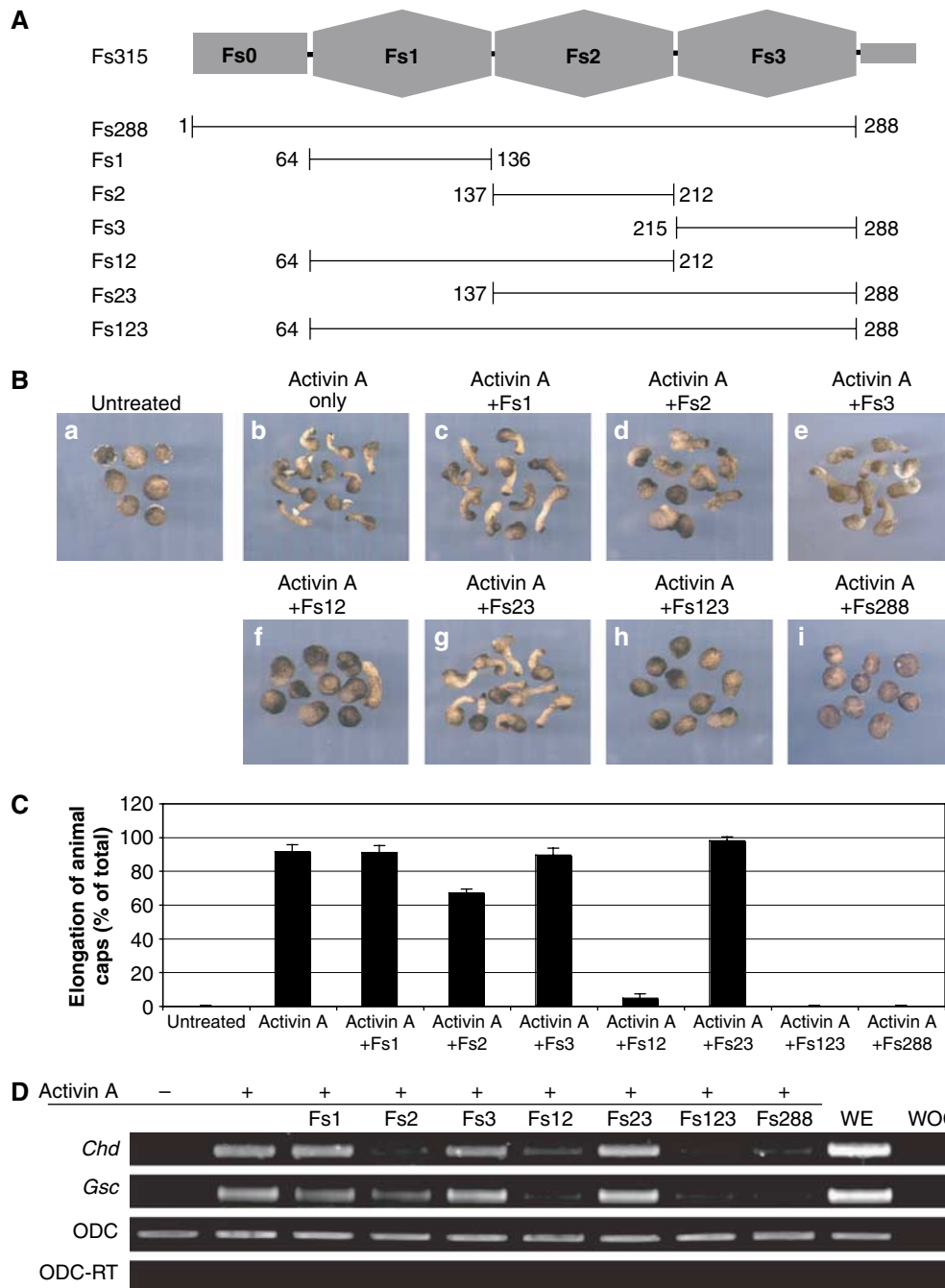


Figure 1 Inhibition of activin by follistatin fragments in the *Xenopus* animal cap system. **(A)** The domain structure of follistatin with constructs used in this study indicated by bars underneath it. Numbers refer to the first and last residues of each construct in mature, full-length follistatin sequence. **(B)** Response of *Xenopus* animal caps to 30 U of activin A in the presence or absence of follistatin fragments as indicated above each panel. **(C)** Quantitation of the phenotypic data shown in **(A)** using a larger number of animal caps. **(D)** Semiquantitative RT-PCR analysis of the effects of follistatin fragments on activin A-induced expression of mesodermal markers *Chordin* (*Chd*) and *Goosecoid* (*Gsc*) in *Xenopus* animal caps. WOC, water only control; WE, whole embryo; ODC, ornithine decarboxylase used for normalisation of RNA level; ODC-RT, ornithine decarboxylase PCR without reverse-transcriptase reaction.

activin (Wang *et al*, 2000), and hydrophobic residues in Fs0 that are critical for follistatin function have been identified (Sidis *et al*, 2001). Other studies suggest that the Kazal-type subdomains of Fs1 and Fs2 contain activin-binding sequences (Keutmann *et al*, 2004), and that a full-length follistatin chain is required for optimal growth factor binding (Amthor *et al*, 2004). Follistatin-related protein (FSRP/FSL3) is homologous to follistatin, and it can also antagonise activin

and BMP signalling (Schneyer *et al*, 2001). It has 20-fold lower affinity for activin and similar affinity for BMP-2 when compared to follistatin, and its second Fs domain has been implicated in activin binding (Tsuchida *et al*, 2000; Sidis *et al*, 2004).

We describe here functional and biochemical characterisation of a minimal activin-inhibiting fragment of follistatin, and describe its crystal structure in complex with activin A.

The structure provides insights into the mechanism of follistatin-mediated inhibition and specificity towards other substrates.

Results

Inhibition of activin-mediated elongation in *Xenopus* animal caps

In order to identify the minimal activin-binding fragment of follistatin, we have created a number of single, double and triple domain constructs of the inhibitor, and produced these proteins for functional and biochemical analysis of activin inhibition (Figure 1A). In the *Xenopus laevis* animal cap explant model, activin can act as a potent mesoderm-inducing factor, inducing the animal cap to undergo extensive morphogenetic movement and tissue elongation (Symes and Smith, 1987; Green *et al*, 1992). Follistatin can inhibit this process, and we have exploited this phenomenon to examine the biological effect the follistatin fragments might have on activin function (Schulte-Merker *et al*, 1994).

Animal cap explants were treated with various follistatin fragments in the presence or absence of activin. Almost all caps (>90%) elongate in response to treatment with activin, compared to the rounded control caps (Figure 1B). This effect of activin is not abrogated by the addition of follistatin fragments Fs1, Fs3 or Fs23, whereas treatment of animal caps with fragments Fs2, Fs12 or Fs123 shows clear inhibitory effects upon activin-induced elongation. This inhibition is most pronounced with Fs12 and Fs123 (5 and 0% of the caps elongating, respectively; Figure 1C), while Fs2 domain alone elicits only partial inhibition (66% of caps elongating).

In addition to phenotypic analysis of animal cap explants, semiquantitative RT-PCR was also performed to analyse levels of mesodermal gene expression in response to activin and follistatin. Upon treatment of animal caps with activin A, *Chordin* (*Chd*) and *Goosecoid* (*Gsc*) expression is induced relative to control animal caps (Figure 1D; Green *et al*, 1992; Sasai *et al*, 1994). Induction of these dorsal mesoderm markers is not perturbed by the addition of follistatin fragments Fs1, Fs3 or Fs23. Conversely, addition of Fs2, Fs12 or Fs123 results in the inhibition of activin-induced *Chd* and *Gsc* gene expression. Neither the phenotype of the animal caps nor the levels of marker gene expression are changed from that of the control caps when the animal caps are treated with any of the follistatin fragments in the absence of activin (data not shown).

Together, these functional analyses in the *Xenopus* animal cap system suggest that the follistatin constructs Fs12 and Fs123, and to a lesser extent Fs2, are sufficient for the inhibition of activin-mediated mesoderm induction, suggesting that Fs2 domain contains the main epitope for activin binding. The unique N-terminal Fs0 domain, as well as Fs3 domain, appears dispensable for activin inhibition in this analysis.

Formation of activin–follistatin complexes: analytical size exclusion chromatography

In order to confirm that the inhibitory action of these follistatin constructs on activin signalling is due to direct association of these proteins with the growth factor, we analysed their complex formation by analytical size exclusion chromatography. Activin A is poorly soluble in aqueous

buffers, and would not elute from a size exclusion column under conditions required for subsequent mass spectrometric analysis. However, when incubated with either Fs12 or Fs123 before loading into the column, a peak containing a complex of activin and the follistatin fragment was observed. None of the other follistatin fragments, including Fs2, were able to elute from the column in complex with activin A. The molecular weights estimated from the peak elution volumes indicate that most of the protein eluted in complex with expected 1:2 stoichiometry (one activin dimer to two follistatin fragments; Figure 2A and F).

Nondissociative mass spectrometry

The complexes isolated by size exclusion chromatography were analysed using nondissociative mass spectrometry. Both complexes gave rise to two major ion series (Figure 2B and G); a complex between an activin dimer and one chain of the follistatin construct (1:1 complex; charge states labelled with underlined text), and a higher intensity 1:2 complex. Each of these complexes was independently identified using tandem mass spectrometry.

The spectrum of the activin–Fs12 complex gives ion signals corresponding to 60613 ± 34 Da (1:2 complex, expected mass 58481 Da) and 43381 ± 38 Da (1:1 complex, expected mass 42207 Da; Figure 2B). Tandem mass spectra for the +16 charge state acquired at collision energy of 60 V reveal unbound Fs12 in the low mass region, and in the high mass region charge-stripped oligomers are observed corresponding to a 1:1 complex (Figure 2C). The tandem mass spectrum for the +13 charge state of the 1:2 complex acquired at collision energy of 50 V shows unbound Fs12 in the low mass region, and unbound activin in the high mass region (Figure 2D).

The spectra collected from the activin–Fs123 complex are similar. Figure 2G shows ion series for species of 76021 ± 92 Da (1:2 complex; expected mass 74433 Da) and 50889 ± 18 Da (1:1 complex, expected 50183 Da); tandem mass spectra for the +19 charge state of the 1:2 activin–Fs123 complex and the +15 charge state of the 1:1 complex are shown in Figure 2H and I, respectively. Both were acquired at collision energy of 70 V. In Figure 2H, unbound Fs123 is observed in the low mass region, and in the high mass region, charge-stripped oligomers are observed that correspond to a 1:1 complex.

Taken together, these spectra confirm that Fs12 and Fs123 form stable complexes with activin, and that the peak fractions from the size exclusion column are mostly composed of 1:2 complexes, with lesser amounts of 1:1 complexes.

Fs12 and Fs123 have similar affinities for activin A

We used isothermal titration calorimetry to measure the affinities of Fs12 and Fs123 fragments for activin A. Titration of the follistatin fragments into activin A indicated these two fragments had near-identical affinities with K_d of 430 nM for Fs12 and 420 nM for Fs123 (Figure 2E and J, respectively). These values are considerably higher than those reported in the literature for the interaction between full-length follistatin and activin A, as measured by surface plasmon resonance (280 pM; Glister *et al*, 2004). We have not been able to produce full-length follistatin in sufficient quantity for ITC measurements, and are unable to compare our affinities directly, given the differences in experimental conditions.

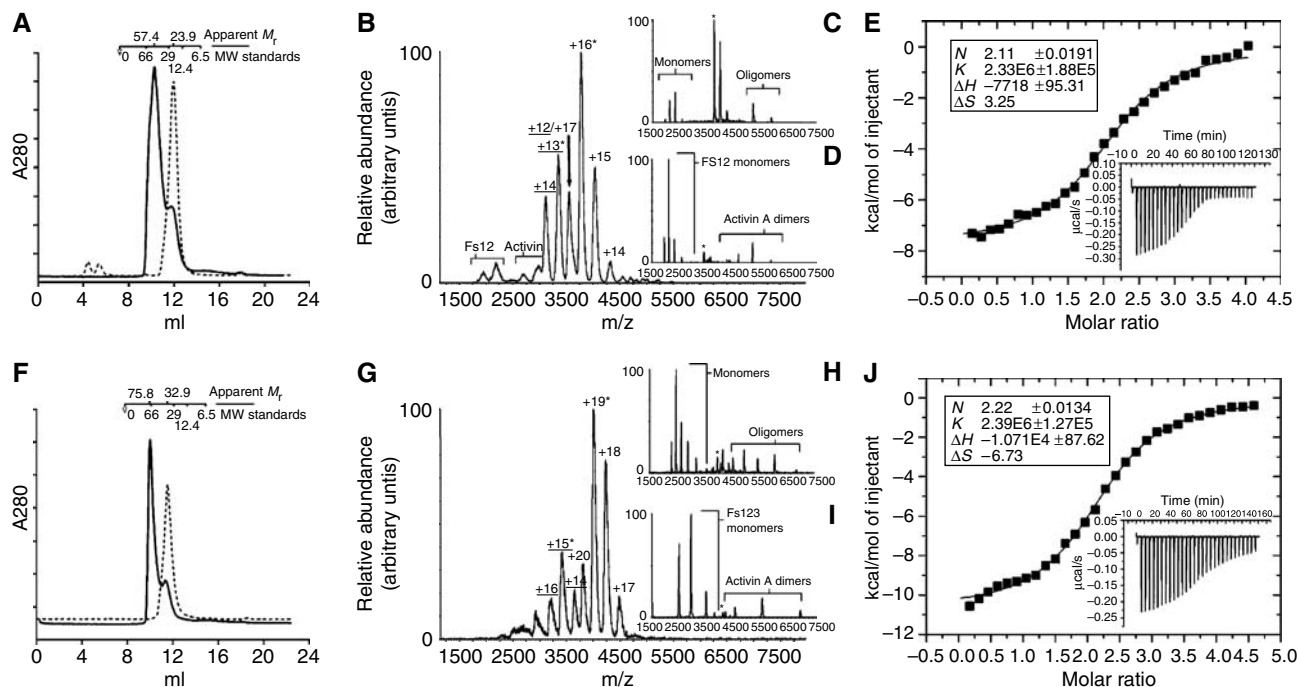


Figure 2 Preparation and analysis of activin–follistatin complexes. (A, F) Size exclusion chromatography of Fs12, Fs123 (dashed lines) and complexes with activin (solid lines). Elution volumes of calibration standards are illustrated along the profile along with calculated masses for the peaks. (B) Mass spectrum acquired for the activin–Fs12 complex. (C) Tandem mass spectrum for the +16 charge state of the 1:2 activin A–Fs12 complex (marked in B with an *) acquired at collision energy of 60 V. (D) Tandem mass spectrum for the +13 charge state of the 1:1 activin A–Fs12 complex (marked in B with an *) acquired at collision energy of 50 V. (G) Mass spectrum acquired for activin A–Fs123 complex. (H) Tandem MS acquired at collision energies of 70 V for ion species marked in (F) with asterisks, +19 and +15 charge states, respectively. (E, I) ITC data for affinity measurements for Fs12–activin (E) and Fs123–activin (I) interaction. Integrated heats and fitting to single binding site model is shown in the main figure with the raw ITC data shown in the inset of the corresponding graph. Stoichiometries, association constants and thermodynamic parameters derived from these experiments are listed in the figure.

Activin A and Activin A–Fs12 structures

Both activin–follistatin complexes described above, as well as free activin A were used for crystallisation trials. Diffraction-quality crystals were obtained with the free growth factor and the activin A–Fs12 complex, both structures solved by molecular replacement and refined to 2 Å resolution (Table I).

The activin A–Fs12 complex structure shows the expected 1:2 stoichiometry, with the follistatin fragments binding to the convex outside surfaces of the activin protomers, and flexibility in follistatin’s domain structure allows it to bend and follow the curvature of the activin protomer (Figure 3). Activin A dimer shows a more closed conformation compared to BMPs and TGF-βs, with the follistatins binding sideways-on in the complex (Figure 3B). Each follistatin fragment in the structure interacts with only one of the activin protomers and there are no contacts between the follistatin fragments. The Fs1 domain interacts with activin via its Kazal-like subdomain, while the heparan sulphate binding EGF-like N-terminal part points away from activin, and is poorly resolved in the structure. The Fs2 domain interacts with activin using both EGF- and Kazal-like subdomains and their relative orientation is very different from previously described Fs domains (Hohenester *et al*, 1997; Innis and Hyvönen, 2003). In comparison with the Fs1 domain, which is essentially identical to the structure seen earlier in the isolated Fs1 domain, the Fs2 shows a large difference in the relative orientation of the EGF- and Kazal-like subdomains, with the EGF subdomain rotated by approximately 180° and sandwiched between the two adjacent Kazal domains (Figure 4).

Table I Data collection and refinement statistics

	Activin A	Fs12–activin A
<i>Data collection and processing</i>		
Beamline	ESRF-BM14	ESRF-BM14
Wavelength (Å)	0.9788	0.97926
Resolution limit (Å)	2.0	2.0
Rmerge	0.065 (0.382) ^a	0.055 (0.427) ^a
Total number of observations	108 488	113 250
Number of unique reflections	24 709	23 201
Completeness (%)	92.5 (76.2) ^a	98.5 (98.1) ^a
I/σI	18.7 (2.0) ^a	24.0 (2.7) ^a
<i>Refinement (Refmac5)</i>		
R factor	0.216 (0.255) ^a	0.202 (0.238) ^a
R free	0.259 (0.342) ^a	0.254 (0.305) ^a
R.m.s.d. bonds	0.016	0.017
R.m.s.d. angles	1.381	1.710

^aValues in parentheses correspond to the highest resolution shell.

With very few contacts between the Fs2 EGF subdomain and the two Kazal subdomains, this conformation appears to be unique to the complex, with Fs2 domain in free follistatin acquiring a more elongated structure.

Fs12 blocks the type II receptor-binding site

The total interface area buried between the Fs12 and activin is 2040 Å², while each type II receptor ectodomain buries 1550 Å² when bound to activin (Greenwald *et al*, 2004). The binding site for Fs12 overlaps almost perfectly with the type II

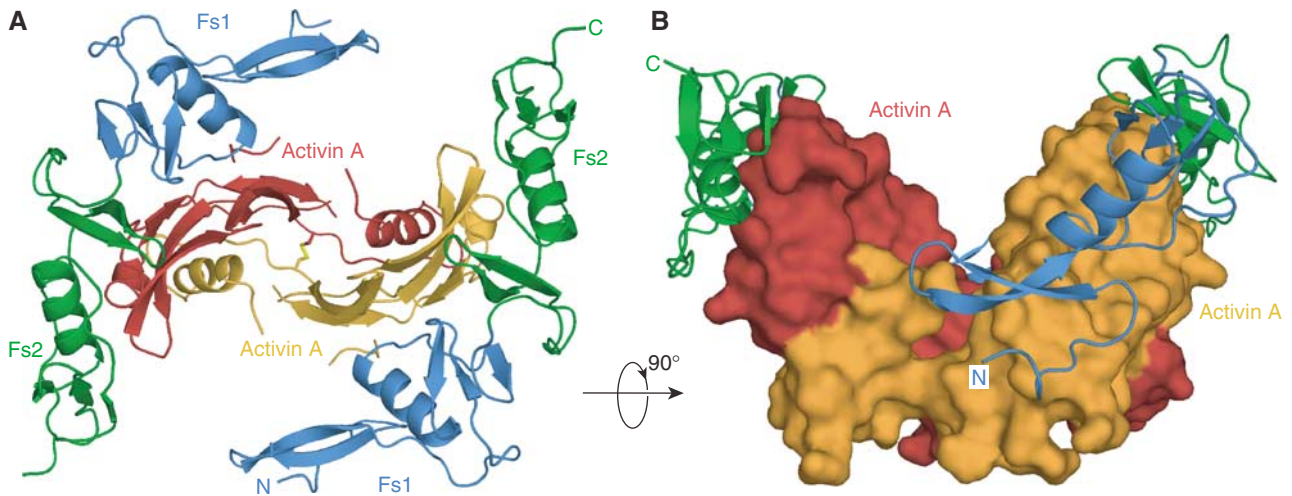


Figure 3 Overall architecture of the activin–Fol12 complex. (A) View down the two-fold axis of symmetry showing the two follistatin fragments binding to the back of the activin A fingers. Activin protomers are coloured red and orange, the interchain disulphide is shown in yellow. Follistatin domains Fs1 and Fs2 are coloured blue and green, respectively. (B) A perpendicular view of the complex showing the closed conformation of activin and Fs12 fragments wrapping along the activin A, shown as a surface model.

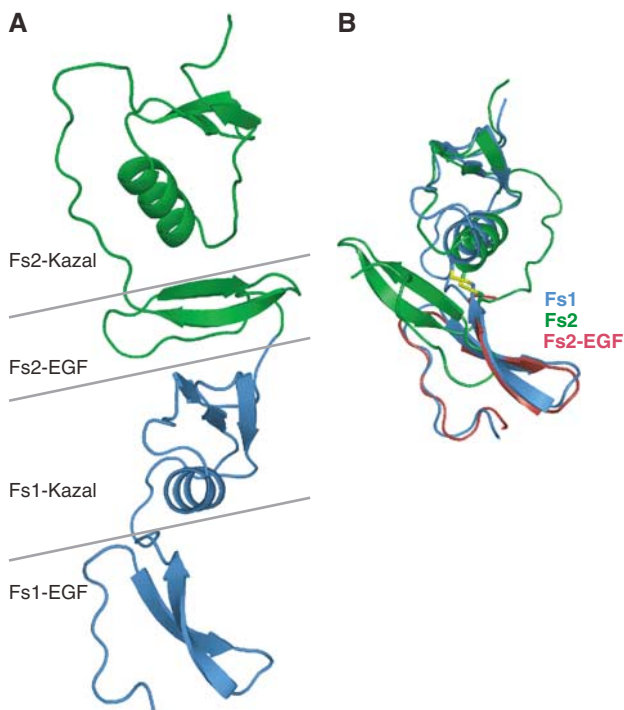


Figure 4 Structural flexibility in the Fs domains. (A) The structure of Fs12 fragment in the complex with Fs1 domain in blue and Fs2 in green. Horizontal lines mark the domain and subdomain boundaries highlighting the EGF subdomain of Fs2 sandwiched in between the two Kazal subdomains. (B) Superpositioning of Fs1 (blue) and Fs2 (green) domains using Kazal subdomains only, illustrating the EGF domains in opposite orientations. Disulphide bridge connecting the linker sequence from EGF subdomain to Kazal subdomain is shown for both Fs1 and Fs2. Similarity of the EGF domains is illustrated by the EGF domain of Fs2 alone in red, superimposed with equivalent part of Fs1 domain.

receptor-binding site as seen in previous structures. Fs1 domain interacts with the same epitope as loop 23 in ActRIIB, whereas Fs2 domain covers the large hydrophobic

surface in the knuckle epitope and also interacts with the activin fingertips (Figures 3 and 6).

The largely apolar knuckle epitope on activin A is covered by a hydrophobic patch on follistatin, comprising residues V151, Y159, V161 and C196, all from Fs2 domain. In the Kazal domain of Fs1, P125 is positioned above I109 of activin A, displacing the side chain of R87, which is held in place by an electrostatic interaction with E111 in the free and type II receptor-bound activin A. Y159 of follistatin occupies a similar position to that of Y38 from ActRIIB in its complex with activin A.

Key interactions at the activin A fingertips

Several specific polar contacts appear at the edges of the binding area. A key residue in follistatin is R192, located in the middle of the α -helix in the Kazal subdomain of Fs2. It is inserted between the fingertips of activin and lies above Y94 of activin (Figure 5A). The hydroxyl group of Y94 side chain is hydrogen-bonded to the main chain oxygen of R192 and the side chain of R192 is coordinated from both sides by polar residues in activin fingers, namely D27 and Q98. These residues in turn form part of a more elaborate hydrogen-bonding network that stabilises the fingertips. In the unliganded activin A, Q98 is poorly defined and points away from the binding site for R192. S201, immediately C-terminal to the α -helix of the Fs2 Kazal subdomain, is hydrogen-bonded to the main chain nitrogen of I100 of activin A.

R192 is fully conserved in follistatins and FSRP/FSL-3, and this C-terminal part of the Fs2 Kazal domain shows the highest degree of conservation between these proteins, further emphasising the critical role this region plays in activin binding.

K102 is part of a hydrogen-bonding network between the two proteins (Figure 5B). Its side chain is held in position by a salt bridge with D104, and it makes a further hydrogen bond to the main chain oxygen of D106 in Fs1. Q154 at the tip of the EGF subdomain of Fs2 hydrogen bonds in turn with the main chain amide of K102. On the other side of the interface,

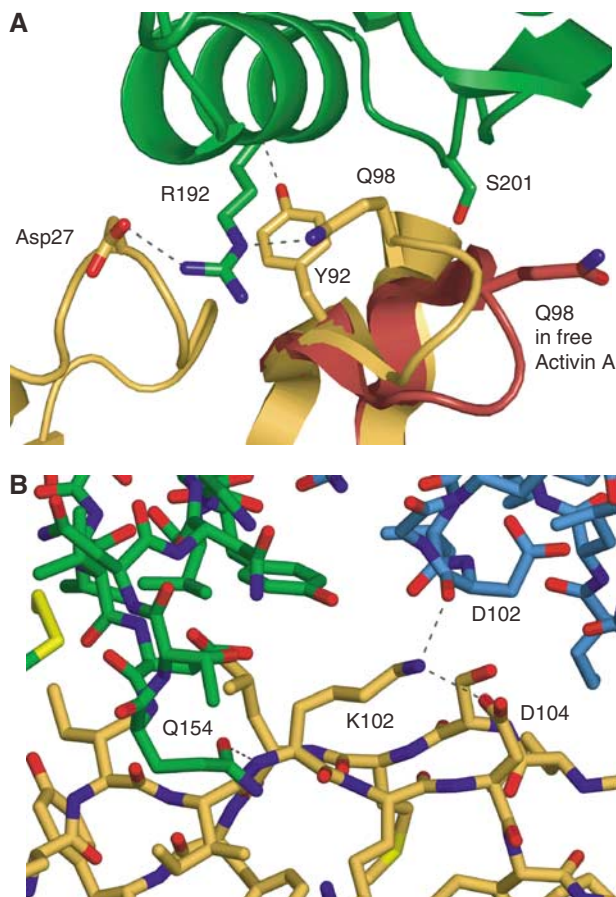


Figure 5 Details of activin–follistatin interactions. **(A)** Detailed view at the tip of the activin fingers with R192 of Fs12 inserting itself between the two β -hairpins and hydrogen bonded (shown as dashed lines) by Q98 and D27 of activin A. Y92 of activin and S201 of follistatin are shown hydrogen bonding to the main chain atoms of opposite molecules. Activin A is shown in orange and Fs2 domain in green. For comparison, the orientation of the Q98 in free activin A is shown in red. **(B)** View from the side of activin A showing hydrogen bonding network around K102 of activin.

next to P125, E126 of follistatin is at the centre of a large hydrogen-bonding network coordinating H45 of activin. A large number of ordered water molecules are also found in the interface region, in particular between the Fs1 domain and activin (Figure 6A).

Conservation of interacting residues in other follistatin ligands

Many of the BMPs show conservation of the residues surrounding the tip of the fingers in the growth factor, consistent with their ability to bind follistatin (Figure 7). The first fingertip is highly conserved containing two tryptophans that are only missing from anti-Müllerian hormone (AMH/MIS). TGF- β s themselves contain only a single lysine in between these tryptophans, whereas most other family members contain two residues. D27, which coordinates R192 in follistatin, is in this loop and is fully conserved in activins and most BMPs. In myostatin/GDF8, another high-affinity ligand for follistatin, only a single aspartic acid is found between the tryptophans, but analysis of the TGF- β 2 structure suggests that it could still be able to coordinate R192. The second fingertip, with Q98 in activin A, is less well con-

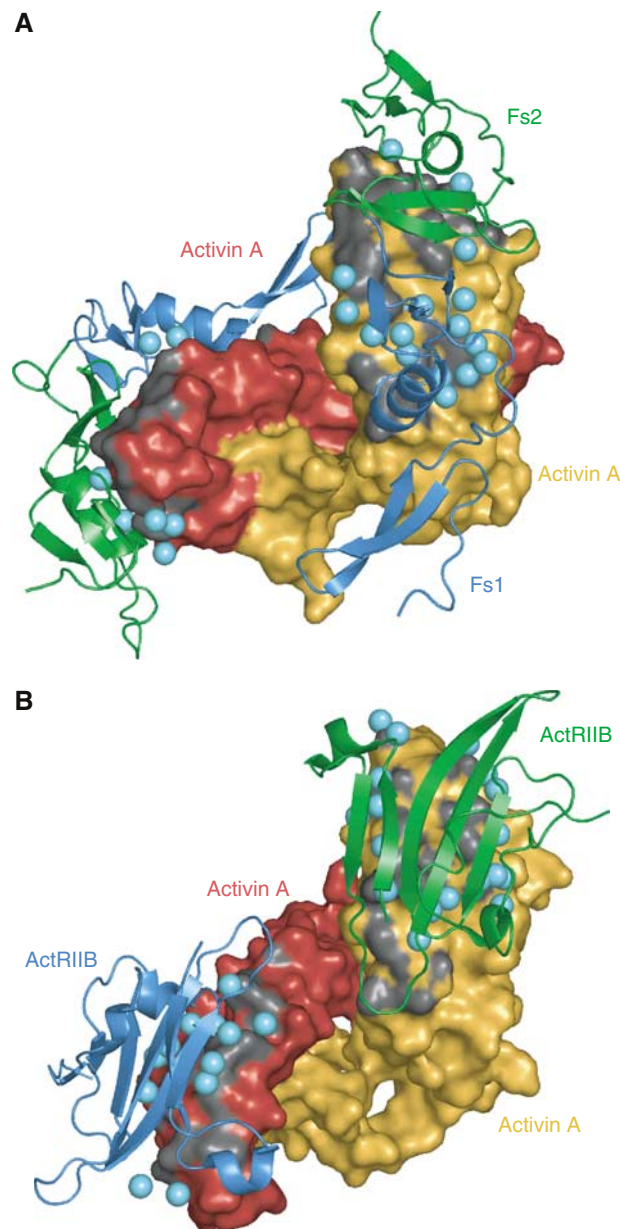


Figure 6 Interaction surface between activin and Fs12 and ActRIIB. Comparison of activin binding by Fs12 and the extracellular domain of the type II activin receptor (Greenwald *et al*, 2004; PDB:1s4y). Activin protomers are shown as molecular surfaces (orange and red), and the two Fs12 molecules **(A)**, blue Fs1 and green Fs2) and two type II receptor domains **(B)**, blue and green) are shown as ribbon diagrams. The activin surface is coloured dark grey over atoms that are closer than 4 Å from the interacting protein. Water molecules sandwiched between the two proteins are shown as light blue spheres. Both complexes are shown in the same orientation for the orange activin A protomer.

served. In TGF- β s, this region is shorter than in other family members and lacks the equivalent residue to Q98. Also, the orientation of this loop in TGF- β s differs from BMPs and activin A and would clash with follistatin. TGF- β s interact with type II receptors differently from activins and BMPs, and instead of the knuckle epitope they use the fingertips for this, explaining the diversity in their sequence and structure (Hart *et al*, 2002). BMP-9/GDF2, AMH/MIS and inhibin all have an extra residue in this loop, and the structure of

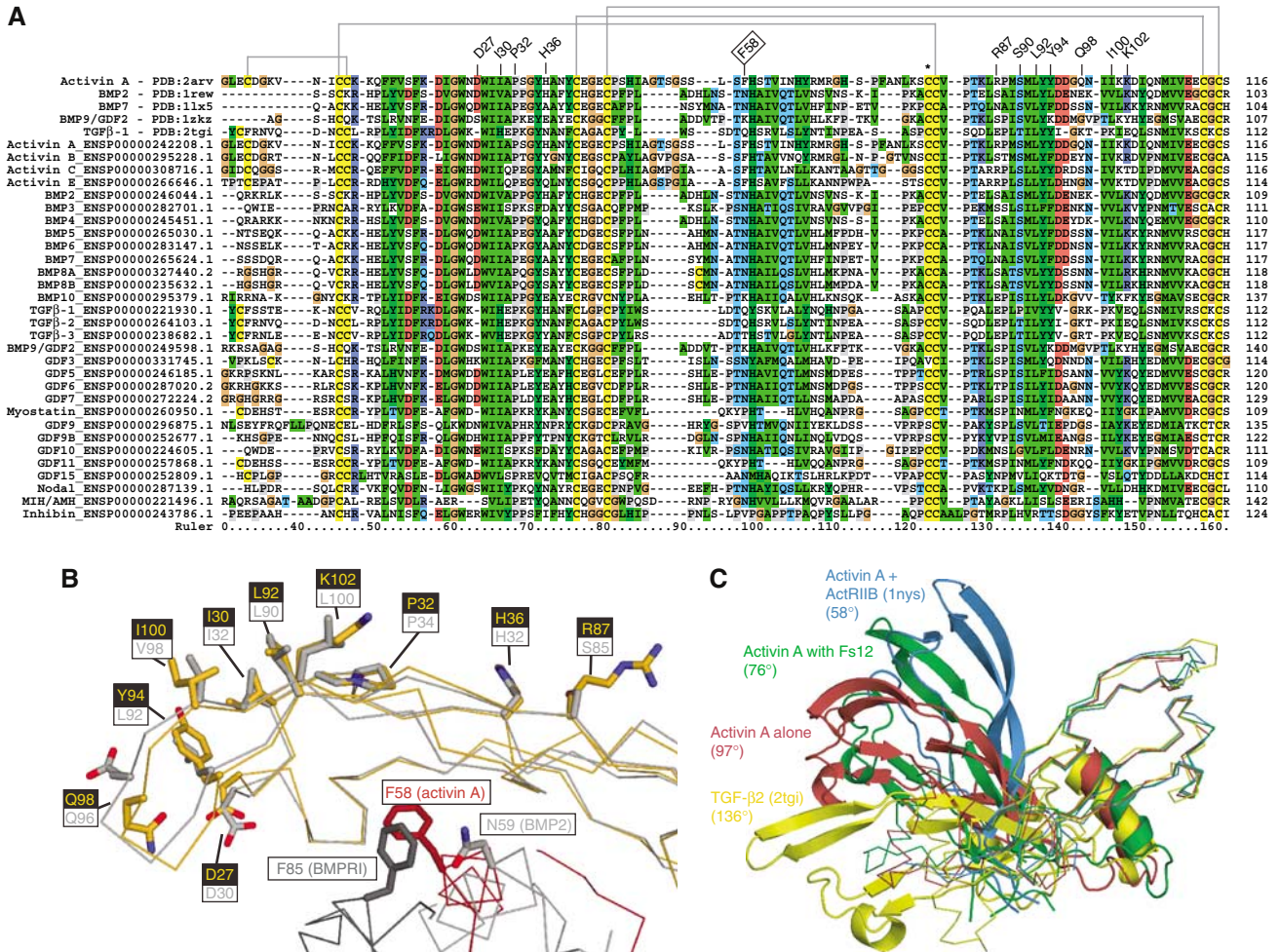


Figure 7 Follistatin-binding site conservation and structural flexibility among the TGFβ family members. (A) Protomers of activin A (PDB:2arv, this study), BMP2 (1rew), BMP7 (1lx5), BMP9 (1zlkz) and TGF-β2 (2tgi) were superimposed using SSM server (www.ebi.ac.uk/msd-srv/ssm) to obtain a structure-based sequence alignment. To this alignment, all members of the TGF-β family found in the human genome (www.ensembl.org) were aligned using ClustalX program, and coloured according to conservation (hydrophobics green, Cys yellow, Asp/Glu blue, Arg/Lys red, Gly brown, Pro grey, uncharged hydrophilic light blue). Activin A residues involved in follistatin binding are indicated above the alignment. F58 that occupies part of the type I receptor-binding site is labelled with a boxed text. Grey lines indicate disulphide connectivity in activin A, dimerisation disulphide is indicated by an asterisk. (B) Side view of activin A (in orange) with residues contacting F58 (labelled yellow on black background), as well as F58 at the interface of activin dimer are shown as stick models. Superimposed on the activin A is BMP-2 (light grey), another known ligand of follistatin, complexed with its type I receptor (dark grey; PDB:1rew). Equivalent BMP2 residues to those that interact with follistatin in activin A are shown as stick models. N59 of BMP2 is shown next to the F58 of activins, and F85 of the BMP type I receptor is shown next to F58 of activin A, highlighting the similar positions these residues occupy with respect to the dimeric growth factor as a whole. (C) Superpositioning of various activin structures and comparison with TGF-β2. Activin A alone (red), complexed with F58 (green) and ActRIIB (blue) as well as TGF-β2 (yellow) were superimposed on one protomer (Cα trace on the right side) to highlight the variation in the interprotomer angles between the proteins. The angle shown for each structure is measured between the Cα atom Y92 (or equivalent) of one protomer, the Cα atom of the dimerisation cysteine (C80 in activin A) and the Cα atom of Y92 in the other protomer.

BMP9 displays a very different conformation in this part of the molecule (Brown *et al*, 2005). Y94 that lies underneath R192 in the complex is followed in sequence by an aspartate that is well conserved, except in TGF-βs. This residue holds the fingertip loop in a conformation suitable for follistatin binding by coordinating the main chain of the next two residues. K102 is also highly conserved in activins A and B, and many BMPs, but replaced by threonine in activin C and E, and by glutamine in TGF-βs. In all, most BMPs and activins share good conservation of follistatin-binding residues around the knuckle epitopes and the fingertips, in line with their ability to bind follistatin. TGF-βs differ clearly in these parts, as do anti-Müllerian hormone, inhibin and nodal.

Mutation of arginine 192 abolishes F58 binding to activin A

To assess the role of R192 in the interaction between F58 and activin A, we created an R192A mutant of F58 and studied its interaction with activin A (See Supplementary data). The mutant protein fails to form a stable complex with activin A as studied by analytical size exclusion chromatography, in conditions where the wild type eluted in a 1:2 complex from the column. It is also unable to inhibit activin A-induced elongation of *Xenopus* animal caps and showed only weak inhibition of marker gene expression in comparison to the wild-type protein. Furthermore, affinity measurement using ITC failed to detect any binding between F58(R192A) and

activin A in the same conditions where the wild-type Fs12 binds its ligand with a K_d of 430 nM. Taken together, these results indicate that R192 is a key residue in activin A–Fs12 interaction, and we predict the equivalent residue will be similarly important in activin binding by FSL3, as well as in interactions between follistatin and its other ligands.

Conformational changes in activin

Previous structures of activin in complex with type II receptor domains showed the growth factor in two very different interprotomer conformations when compared to each other and to the canonical TGF- β family members (Thompson *et al*, 2003; Greenwald *et al*, 2004). The structures presented here further emphasise the flexibility of activin A (Figure 7C). While the uncomplexed activin A is very similar to the activin A in the type II receptor complex structure by Greenwald *et al* (2004), in the Fs12 complex, the growth factor exhibits a more closed structure. Here, the fingers rotate away from the other protomer, pulling with them the interfacial α -helix. β -strands 1 and 2, which show the largest displacement compared to free activin, move by more than 20 Å at the tip of the fingers.

With four independent crystal structures of activin now available, it is likely that the observed conformational divergence from the canonical TGF- β structures is a reflection of true structural plasticity in activins. There is evidence for this also from the comparison of both the structures and sequences of TGF- β -like growth factors. A unique feature in all activins is the presence of a phenylalanine at position 58 when most other superfamily members have a polar residue, typically an asparagine, in the same position. In BMPs, this asparagine hydrogen bonds to the main chain of β -strand 4 (Q104 in BMP-2, PDB code:1rew) stabilising the positioning of the interface α -helix. The phenylalanine in activin points in a different direction and inserts its side chain in the aromatic pocket of the other protomer, occupying a virtually identical position to that of F85 of the BMP type I receptor in its complex with BMP-2 (Kirsch *et al*, 2000; Figure 7B). At the same time, the phenylalanine pulls the interface helix up by half a turn. The shift of the α -helix is accompanied by bending of the activin A protomer at two hinges at either side of the helix. In comparison to TGF- β 2, the orientation of the interface α -helix in free activin differs by 35°. This correlates well with the interprotomer angle differences of TGF- β 2 (136°) and activin A (97°) (Figure 7C).

Given the fact that activin is the highest affinity ligand of follistatin, it is tempting to speculate that this unusual conformation of activin has evolved in order to maximise the affinity towards follistatin, but it cannot be ruled out that this is a mechanism by which activins have acquired specificity for their own type I receptor. While the type II receptor-binding sites are virtually the same for BMP-7 and activin A, the type I receptor-binding sites, as compared to that known for BMP-2, are clearly different. Given the low sequence conservation between the type I receptors, it is not impossible that activin A can still bind to its low-affinity type I receptor without structural rearrangements. Alternatively, F58 could move away from the opposite protomer to make room for a similar residue in its type I receptor, ALK4, and at the same time allow a structural change to occur in the activin dimer.

Discussion

The type II receptor is the primary high-affinity cell surface receptor for activins and it was expected that follistatin would block at least this interaction. The structure presented here confirms this hypothesis and our data from the *Xenopus* animal cap assay shows that neutralisation of the type II-binding site on activin A by Fs12 is sufficient for inhibition of activin signalling *in vivo*.

Although previous evidence shows that sequences from the unique N-terminal Fs0 domain can bind to activin, our data demonstrate clearly that it is not necessary for functional inhibition of activin. Our structure does suggest, however, that the Fs0 and Fs3 domains from different molecules would come into close proximity in a full-length activin–follistatin complex. While these domains could serve to increase the affinity of the activin–follistatin interaction, our data imply no direct role for them in the inhibition of activin A.

Our findings agree with previous work on the follistatin homologue FSRP/FSL3, in that the key residues for activin binding are found in the second Fs domain (Tsuchida *et al*, 2000). The key features identified in our complex structure are conserved in FSRP/FSL3, and we expect that the architecture of an activin–FSRP/FSL3 complex mirrors that described here. Our results also provide a framework for assessing the specificity of follistatin towards other TGF- β family members, and BMPs, which are also able to bind follistatin, show good conservation of the key interacting residues.

It is known that follistatin-bound BMP-4 can still interact with cell surface receptors (Iemura *et al*, 1998). In the activin–Fs12 structure, the type I receptor-binding site is unoccupied and this may explain how BMP-4 can interact simultaneously with follistatin and its high-affinity type I receptor, ALK2.

Implications for HS binding

Growth factors are not the only ligands for follistatin, and the short form (Fs288) of follistatin is known to associate with HS with high affinity. Whether binding to HS by follistatin would have significant effects on the structure of a complex with activin is debatable. It is likely that an HS-bound complex would have the EGF-like portion of the Fs1 domain closer to the activin dimer, and this might bring additional binding epitopes into contact with the growth factor. It is also feasible that an HS chain of sufficient length could bridge the two follistatin chains and an activin dimer by traversing the centre of the complex, perpendicular to the two-fold axis of symmetry (vertically in Figure 3A, along the groove in Figure 3B). This could explain the reported differences in activin binding by follistatin isoforms with differential affinities for HS (Sumitomo *et al*, 1995).

It is also not clear whether the activin–follistatin complex remains associated with HS. Many growth factors rely on HS for their signalling, for example, fibroblast growth factor (FGF) forms a heparin-mediated ternary complex with its cell surface receptor (Pellegrini *et al*, 2000). Dimerisation of follistatin on heparan sulphate in the absence of activin could facilitate binding of the two inhibitor molecules to a dimeric growth factor, but it is as yet not known if this happens *in vivo*.

Perhaps the most surprising finding from the structure of free activin A was to see that it acquires a similar architecture

to the liganded forms. As similar structures have now been observed for both free and receptor-bound activin A, it remains to be seen whether the binding of the type I receptor will cause further structural rearrangement in the ligand. This conformational flexibility could be assessed by solution methods, such as NMR, but this is likely to be hampered by poor solubility of these proteins.

Research must now proceed towards resolving the roles of domains Fs0 and Fs3 in activin binding and investigating what differences there might be between the complex reported here and follistatin bound to other ligands, such as activin B, myostatin and BMPs. Our structure suggests that interaction of FSRP/FSL-3 with activins will be very similar, but this too needs structural confirmation.

Materials and methods

Clones of human activin A (gi:4504699; Mason *et al*, 1986) and rat follistatin (gi:204173; Shimasaki *et al*, 1989) were kind gifts of Professor John Gurdon (Gurdon Institute, Cambridge, UK). PCR primers were synthesised by the Protein and Nucleic Acid Chemistry Facility (Department of Biochemistry, Cambridge, UK).

Recombinant protein expression and purification

The coding sequence of human activin A (residues 1–116 of the mature protein) was amplified by PCR and inserted into the T7-based expression vector pBAT4 (Peränen *et al*, 1996). Sequences encoding various follistatin fragments were amplified by PCR and ligated into similar vectors as *NcoI*–*HindIII* fragments. Fs1 and Fs3 were expressed from pBAT4, while the remaining follistatin constructs were expressed as TEV protease cleavable N-terminal hexahistidine fusions from pHAT4 vector. R192A mutant of Fs12 fragment was created by overlapping primer extension methods, cloned to pHAT4.

All proteins were expressed in *Escherichia coli* BL21 (DE3). For constructs with Fs2 domain, this strain was supplemented with the pUBS520 vector (Brinkmann *et al*, 1989). Fs1 and Fs3 were recovered from the soluble fraction after induction with 0.4 mM IPTG for 3 h at 37°C; all other constructs formed inclusion bodies in *E. coli*. Inclusion bodies were isolated from lysed cells, washed with detergents and high salt to remove lipid and nucleic acid contamination, solubilised, diluted rapidly into final refolding buffers and sealed for 1 week at 4°C.

Purification of Fs1 was as previously described (Innis and Hyvönen, 2003). Fs3 was purified by anion exchange, size exclusion and reversed phase liquid chromatography, and resuspended in water after lyophilisation. Refolded proteins were loaded directly onto Resource S or Resource RPC columns (GE Biosciences). Hexahistidine fusion constructs were treated with TEV protease overnight after the first purification step. Final purification steps included size exclusion and reversed phase chromatography. Masses of the purified proteins were in all cases measured by MALDI-MS at the Protein and Nucleic Acid Chemistry Facility (Department of Biochemistry, University of Cambridge, UK). Protein concentrations were determined spectrophotometrically by measuring absorbance at 280 nm and using calculated extinction coefficients for each construct (Gill and von Hippel, 1989).

Xenopus laevis embryos and animal cap assay

Xenopus embryos were obtained by *in vitro* fertilisation (Smith and Slack, 1983), dejellied with 2% cysteine pH 8.0, maintained in 0.1 × modified Barth's solution (MBS) and staged according to Nieuwkoop and Faber (1967). After fertilisation, embryos were maintained at 14°C and cultured until stage 8. Animal caps were dissected in 0.7 × MBS from stage 8/8.5 embryos; 20 caps per condition. They were incubated at room temperature in 1 × MBS containing 0.1% BSA in the presence or absence of activin ± follistatin until control embryos had reached the desired stage. For phenotypic analysis, caps were cultured until control embryos reached stage 25, and imaged. For RT-PCR analysis, caps were cultured until stage 10.5, and then snap-frozen prior to RNA isolation. A total of 30 units of activin were added (final concentration 150 pM), while follistatin fragments were used at a

concentration of 100 nM. Full-length follistatin used as a positive control was obtained from Peprotech (Rocky Hill, NJ, USA).

Semiquantitative reverse transcriptase PCR analysis

cDNAs were generated from the extracted mRNA according to the manufacturer's instructions (Applied Biosystems). All primers were used according to previous publications (Cho *et al*, 1991; Sasai *et al*, 1994). Quantitative ranges were determined before the final analysis. All reactions were normalised against the *ODC* gene product.

Size exclusion chromatography, mass spectrometry and isothermal titration calorimetry

Activin A in complex with Fs12 and Fs123 was analysed by size exclusion chromatography in a Superdex 75 10/30 HR column (GE Biosciences) equilibrated with 100 mM ammonium acetate. Activin A was coincubated with 1.1-fold excess of each of Fs12 and Fs123 for 1 h, injected onto the column and eluted at a flow rate of 0.7 ml/min. Peak fractions (concentration ~5 µM) were collected and analysed by nondissociating mass spectrometry in an instrument similar to that described previously (Sobott *et al*, 2002). ITC was performed in a Microcal VP-ITC instrument. Activin A was diluted to final concentration of 3.7 µM (dimer) in 100 mM Tris, 5 mM EDTA, pH 8.0, containing 3.2 µM BSA as carrier protein to prevent activin precipitation. Fs12 or Fs123 were dissolved to ~70 µM final concentration in the same buffer without BSA and titrated into activin. Data were processed using Origin 7.0 software package and integrated heats were fitted to single binding site model to obtain association constants and thermodynamic values for the interactions.

Crystallisation, structure determination and refinement

The activin A–Fs12 complex was eluted from a size exclusion column and concentrated to ~8 mg/ml for crystallisation trials. The best crystals grew at 18°C in 14–18% (w/v) PEG MME 2000, 3 mM nickel (II) sulphate, 100 mM Tris pH 8.0. These were cryoprotected in mother liquor supplemented with 20% (v/v) glycerol and frozen in liquid nitrogen for data collection at 100 K. Diffraction extended to 2.0 Å at beamline BM14, ESRF, Grenoble, France. Data were collected on a MAR CCD detector and processed using *DENZO/SCALEPACK* (HKL Research, Inc.). The crystals belong to space-group P2₁2₁2 with unit cell parameters $a = 79.297$ Å, $b = 94.502$ Å, $c = 44.873$ Å, $\alpha = \beta = \gamma = 90^\circ$. The positions of nickel ions in the crystals were independently confirmed by calculating anomalous difference maps using a data set collected at 1.4853 Å wavelength corresponding to the experimentally measured absorption peak for nickel.

Activin A (6 mg/ml in 20% acetonitrile) was crystallised in 1.2–1.5 M ammonium sulphate, 2–3% (w/v) PEG 300 and 100 mM Na-Hepes, pH 7.4–7.8 at 18°C. Needle-like crystals were soaked in mother liquor containing 20% (v/v) glycerol and frozen in liquid nitrogen. Crystals belong to space group I222 with unit cell dimensions $a = 63.57$ Å, $b = 96.25$ Å, $c = 118.04$ Å, $\alpha = \beta = \gamma = 90^\circ$.

Both structures were solved by molecular replacement with *PHASER* (Storoni *et al*, 2004), using activin protomer from activin A:ActRIIB complex as search model (Greenwald *et al*, 2004; PDB:1s4y). With the activin–Fs12 complex, the structure of Fs1 was used as a second search model once activin had been located in the first run of *PHASER* (Innis and Hyvönen, 2003; PDB:1lr9). *ARP/wARP* (Perrakis *et al*, 1997) was used for map improvement and iterative cycles of model building and refinement were carried out in *COOT* (Emsley and Cowtan, 2004) and *REFMAC5* (Murshidov *et al*, 1997).

In activin–Fs12 crystals, each asymmetric unit contains one activin protomer bound to one Fs12 molecule, and the dimer is formed by the unique two-fold symmetry along the *c*-axis. The final model contains an additional three nickel ions, three glycerol molecules, a fragment of polyethylene glycol and 174 water molecules.

Activin A crystals contain one dimer per asymmetric unit. Chain A is modelled in its entirety, but residues 45–55 in the loop before the single α -helix of the chain B were omitted as the electron density maps showed no clear density for these segments. In addition, the final model contains three sulphates, three glycerol molecules and 56 water molecules. Coordinates have been deposited in the Protein Data Bank under accession numbers 2ARP (activin A–Fs12) and 2ARV (activin A).

Supplementary data

Supplementary data are available at *The EMBO Journal* Online.

Acknowledgements

We are grateful to Professor John Gurdon for the follistatin and activin cDNA clones. We thank Drs Len Packman and Charles Hill from PNAC service for mass-spectrometric analysis and oligonucleotide synthesis, and for the DNA sequencing facility, Department of Biochemistry, Cambridge. We are grateful for the staff at beam-

References

- Amthor H, Christ B, Rashid-Doubell F, Kemp CF, Lang E, Patel K (2002) Follistatin regulates bone morphogenetic protein-7 (BMP-7) activity to stimulate embryonic muscle growth. *Dev Biol* **243**: 115–127
- Amthor H, Nicholas G, McKinnell I, Kemp CF, Sharma M, Kambadur R, Patel K (2004) Follistatin complexes myostatin and antagonises myostatin-mediated inhibition of myogenesis. *Dev Biol* **270**: 19–30
- Bachiller D, Klingensmith J, Kemp C, Belo JA, Anderson RM, May SR, McMahon JA, McMahon AP, Harland RM, Rossant J, De Robertis EM (2000) The organizer factors Chordin and Noggin are required for mouse forebrain development. *Nature* **403**: 658–661
- Beattie GM, Lopez AD, Bucay N, Hinton A, Firpo MT, King CC, Hayek A (2005) Activin A maintains pluripotency of human embryonic stem cells in the absence of feeder layers. *Stem Cells* **23**: 489–495
- Brinkmann U, Mattes RE, Buckel P (1989) High level expression of recombinant genes in *Escherichia coli* is dependent on the availability of the dnaY gene product. *Gene* **85**: 109–114
- Brown MA, Zhao Q, Baker KA, Naik C, Chen C, Pukac L, Singh M, Tsareva T, Parice Y, Mahoney A, Roschke V, Sanyal I, Choe S (2005) Crystal structure of BMP-9 and functional interactions with pro-region and receptors. *J Biol Chem* **280**: 25111–25118
- Cho KW, Blumberg B, Steinbeisser H, De Robertis EM (1991) Molecular nature of Spemann's organizer: the role of the *Xenopus* homeobox gene gooseoid. *Cell* **67**: 1111–1120
- Emsley P, Cowtan K (2004) Coot: model-building tools for molecular graphics. *Acta Cryst D* **60**: 2126–2132
- Esch FS, Shimasaki S, Mercado M, Cooksey K, Ling N, Ying S, Ueno N, Guillemain R (1987) Structural characterization of follistatin: a novel follicle-stimulating hormone release-inhibiting polypeptide from gonad. *Mol Endocrinol* **1**: 849–855
- Fainsod A, Deissler K, Yelin R, Marom K, Epstein M, Pillemer G, Steinbeisser H, Blum M (1997) The dorsalizing and neural inducing gene follistatin is an antagonist of BMP-4. *Mech Dev* **63**: 39–50
- Gill SC, von Hippel PH (1989) Calculation of protein extinction coefficients from amino acid sequence data. *Anal Biochem* **182**: 319–326
- Glister C, Kemp CF, Knight PG (2004) Bone morphogenetic protein (BMP) ligands and receptors in bovine ovarian follicle cells: actions of BMP-4, -6 and -7 on granulosa cells and differential modulation of Smad-1 phosphorylation by follistatin. *Reproduction* **127**: 239–254
- Green JB, New HC, Smith JC (1992) Responses of embryonic *Xenopus* cells to activin and FGF are separated by multiple dose thresholds and correspond to distinct axes of the mesoderm. *Cell* **71**: 731–739
- Greenwald J, Vega ME, Allendorph GP, Fischer WH, Vale W, Choe S (2004) A flexible activin explains the membrane-dependent cooperative assembly of TGF-beta family receptors. *Mol Cell* **15**: 485–489
- Groppe J, Greenwald J, Wiater E, Rodriguez-Leon J, Economides AN, Kwiatkowski W, Affolter M, Vale WW, Belmonte JCI, Choe S (2002) Structural basis of BMP signalling inhibition by the cystine knot protein Noggin. *Nature* **420**: 636–642
- Hart PJ, Deep S, Taylor AB, Shu Z, Hinck CS, Hinck AP (2002) Crystal structure of the human T β R2 ectodomain–TGF- β 3 complex. *Nat Struct Biol* **9**: 203–208
- Hemmati-Brivanlou A, Kelly OG, Melton DA (1994) Follistatin, an antagonist of activin, is expressed in the Spemann organizer and displays direct neuralizing activity. *Cell* **77**: 283–295
- Hohenester E, Maurer P, Timpl R (1997) Crystal structure of a pair of follistatin-like and EF-hand calcium-binding domains in BM-40. *EMBO J* **16**: 3778–3786
- Hsu DR, Economides AN, Wang X, Eimon PM, Harland RM (1998) The *Xenopus* dorsalizing factor Gremlin identifies a novel family of secreted proteins that antagonize BMP activities. *Mol Cell* **1**: 673–683
- Iemura S, Yamamoto TS, Takagi C, Uchiyama H, Natsume T, Shimasaki S, Sugino H, Ueno N (1998) Direct binding of follistatin to a complex of bone-morphogenetic protein and its receptor inhibits ventral and epidermal cell fates in early *Xenopus* embryo. *Proc Natl Acad Sci USA* **95**: 9337–9342
- Innis CA, Hyvönen M (2003) Crystal structures of the heparan sulphate-binding domain of follistatin. Insights into ligand binding. *J Biol Chem* **278**: 39969–39977
- Inouye S, Ling N, Shimasaki S (1992) Localization of the heparin binding site of follistatin. *Mol Cell Endocrinol* **90**: 1–6
- James D, Levine AJ, Besser D, Hemmati-Brivanlou A (2005) TGF- β /activin/nodal signaling is necessary for the maintenance of pluripotency in human embryonic stem cells. *Development* **132**: 1273–1282
- Keutmann HT, Schneyer AL, Sidis Y (2004) The role of follistatin domains in follistatin biological action. *Mol Endocrinol* **18**: 228–240
- Kirsch T, Sebald W, Dreyer MK (2000) Crystal structure of the BMP-2-BRIA ectodomain complex. *Nat Struct Biol* **7**: 492–496
- Mason AJ, Niall HD, Seeburg PH (1986) Structure of two human ovarian inhibins. *Biochem Biophys Res Commun* **135**: 957–964
- Massagué J (1998) TGF-beta signal transduction. *Annu Rev Biochem* **67**: 753–791
- Massagué J, Wotton D (2000) Transcriptional control by the TGF-beta/Smad signaling system. *EMBO J* **19**: 1745–1754
- Matzuk MM, Kumar TR, Vassalli A, Bickenbach JR, Roop DR, Jaenisch R, Bradley A (1995) Functional analysis of activins during mammalian development. *Nature* **374**: 354–356
- Murshidov G, Vagin A, Dodson E (1997) Refinement of macromolecular structures by the maximum-likelihood method. *Acta Cryst D* **53**: 240–255
- Nieuwkoop PD, Faber J (1967) *A Normal Table of Xenopus laevis (Daudin)*. Amsterdam: North Holland Publishing Co
- Pellegrini L, Burke DF, von Delft F, Mulloy B, Blundell TL (2000) Crystal structure of fibroblast growth factor receptor ectodomain bound to ligand and heparin. *Nature* **407**: 1029–1034
- Peränen J, Rikkonen M, Hyvönen M, Kääriäinen L (1996) T7 vectors with modified T7lac promoter for expression of proteins in *Escherichia coli*. *Anal Biochem* **236**: 371–373
- Perrakis A, Sixma TK, Wilson KS, Lamzin V (1997) wARP: improvement and extension of crystallographic phases by weighted averaging of multiple refined dummy atomic models. *Acta Crystallog D* **53**: 448–455
- Piccolo S, Sasai Y, Lu B, De Robertis EM (1996) Dorsoventral patterning in *Xenopus*: inhibition of ventral signals by direct binding of chordin to BMP-4. *Cell* **86**: 589–598
- Piepenburg O, Grimmer D, Williams PH, Smith JC (2004) Activin redux: specification of mesodermal pattern in *Xenopus* by graded concentrations of endogenous activin B. *Development* **131**: 4977–4986
- Sasai Y, Lu B, Steinbeisser H, Geissert D, Gont LK, De Robertis EM (1994) *Xenopus* chordin: a novel dorsalizing factor activated by organizer-specific homeobox genes. *Cell* **79**: 779–790
- Schneyer A, Tortoriello D, Sidis Y, Keutmann H, Matsuzaki T, Holmes W (2001) Follistatin-related protein (FSRP): a new mem-

- ber of the follistatin gene family. *Mol Cell Endocrinol* **180**: 33–38
- Schulte-Merker S, Smith JC, Dale L (1994) Effects of truncated activin and FGF receptors and of follistatin on the inducing activities of BVg1 and activin: does activin play a role in mesoderm induction? *EMBO J* **13**: 3533–3541
- Shi Y, Hou L, Tang F, Jiang W, Wang P, Ding M, Deng H (2005) Inducing embryonic stem cells to differentiate into pancreatic beta cells by a novel three-step approach with activin A and all-*trans* retinoic acid. *Stem Cells* **23**: 656–662
- Shimasaki S, Koga M, Buscaglia ML, Simmons DM, Bicsak TA, Ling N (1989) Follistatin gene expression in the ovary and extragonadal tissues. *Mol Endocrinol* **3**: 651–659
- Sidis Y, Schneyer AL, Keutmann HT (2004) Heparin and activin-binding determinants in follistatin and FSTL3. *Endocrinology* **146**: 130–136
- Sidis Y, Schneyer AL, Sluss PM, Johnson LN, Keutmann HT (2001) Follistatin: essential role for the N-terminal domain in activin binding and neutralization. *J Biol Chem* **276**: 17718–17726
- Smith JC, Slack JM (1983) Dorsalization and neural induction: properties of the organizer in *Xenopus laevis*. *J Embryol Exp Morphol* **78**: 299–317
- Sobott F, Hernandez H, McCammon MG, Tito MA, Robinson CV (2002) A tandem mass spectrometer for improved transmission and analysis of large macromolecular assemblies. *Anal Chem* **74**: 1402–1407
- Storoni LC, McCoy AJ, Read RJ (2004) Likelihood-enhanced fast rotation functions. *Acta Cryst D* **60**: 432–438
- Sugino K, Kurosawa N, Nakamura T, Takio K, Shimasaki S, Ling N, Titani K, Sugino H (1993) Molecular heterogeneity of follistatin, an activin-binding protein. Higher affinity of the carboxyl-terminal truncated forms for heparan sulphate proteoglycans on the ovarian granulosa cell. *J Biol Chem* **268**: 15579–15587
- Sumitomo S, Inouye S, Liu XJ, Ling N, Shimasaki S (1995) The heparin binding site of follistatin is involved in its interaction with activin. *Biochem Biophys Res Commun* **208**: 1–9
- Symes K, Smith JC (1987) Gastrulation movements provide an early marker of mesoderm induction in *Xenopus laevis*. *Development* **101**: 339–349
- Thompson TB, Woodruff TK, Jardetzky TS (2003) Structures of an ActRIIB:activin A complex reveal a novel binding mode for TGF- β ligand:receptor interactions. *EMBO J* **22**: 1555–1566
- Tsuchida K, Arai KY, Kuramoto Y, Yamakawa N, Hasegawa Y, Sugino H (2000) Identification and characterization of a novel follistatin-like protein as a binding protein for the TGF- β family. *J Biol Chem* **275**: 40788–40796
- Ullman CG, Perkins SJ (1997) The Factor I and follistatin domain families: the return of a prodigal son. *Biochem J* **326**: 939–941
- Vassalli A, Matzuk MM, Gardner HA, Lee KF, Jaenisch R (1994) Activin/inhibin beta B subunit gene disruption leads to defects in eyelid development and female reproduction. *Genes Dev* **8**: 414–427
- Wang Q, Keutmann HT, Schneyer AL, Sluss PM (2000) Analysis of human follistatin structure: identification of two discontinuous N-terminal sequences coding for activin A binding and structural consequences of activin binding to native proteins. *Endocrinology* **141**: 3183–3193
- Zimmerman LB, De Jesus-Escobar JM, Harland RM (1996) The Spemann organizer signal noggin binds and inactivates bone morphogenetic protein 4. *Cell* **86**: 599–606

Supplementary Material

Harrington AE et al.: Structural basis for the inhibition of activin signalling by follistatin

Figure 1. **Biochemical and biophysical analysis of R192A mutant of follistatin Fs12 fragment**

A) Analytical size exclusion chromatography on Superdex 75 10/30 column in 100 mM ammonium acetate, 5 mM EDTA, pH 7.0. 200 μ l of indicated proteins (activin A dimer concentration 50 μ M, Fs12 fragments 110 μ M) or protein mixtures were loaded onto the column and eluted at flow rate of 0.8 ml/min.

B) SDS-PAGE analysis of the size exclusion chromatography with Fs12(R192A) mutant and activin A. Activin A (lane 1) and mutant Fs12 protein (lane 2) were mixed together (lane 3), incubated for a few minutes and centrifuged at 15,000 rpm for three minutes to separate soluble protein (lane 4) from precipitated protein (lane 5, only activin A). The soluble fraction (lane 4) was loaded onto Superdex 75 10/30 column. 0.8 ml fractions (one fraction per minute) from 13 minutes onwards are shown in lanes 6-11. Lanes 7 and 8 show only Fs12(R192A) protein (elution peak at 14.8 min), whereas free activin A elutes as a much broader peak at 17.6 minutes, shown in lanes 9-11.

C) Isothermal titration calorimetric analysis of Fs12(R192A) interaction with activin A. 70 μ M Fs12(R192A) was titrated into 3.7 μ M activin A in 100 mM Tris-HCl, 5 mM EDTA, 3.2 μ M BSA, pH 8.0 at 25°C. Raw ITC data on the left panel shows only dilution heats, similar to Fs12 titration into the same buffer in the absence of activin A. Integrated heats after subtraction of dilution heats from control experiment are shown on the right panel. It is clear there is no binding of R192A mutant to activin A under these conditions.

